Passive Robotics for Accelerated Collaborative Therapy

Kazimierz Krzysztof Wojewoda

School of Mechanical Engineering

University of Leeds

PhD Thesis

Submitted in accordance with the requirements for the degree of Doctor of Philosophy

February 2018

The candidate confirms that the work submitted is his/her own, except where work which has formed part of jointly-authored publications has been included. The contribution of the candidate and the other authors to this work has been explicitly indicated below. The candidate confirms that appropriate credit has been given within the thesis where reference has been made to the work of others.

The work included in the papers below is partly used in Chapter 4.

- Wojewoda, K.K., Culmer, P.R., Jackson, A.E. and Levesley, M.C., 2016, June. Position tracking of a passive rehabilitation robot. In Cyber Technology in Automation, Control, and Intelligent Systems (CYBER), 2016 IEEE International Conference on (pp. 1-6). IEEE.
- Wojewoda, K.K., Culmer, P.R., Gallagher, J.F., Jackson, A.E. and Levesley, M.C., 2017, July. Hybrid position and orientation tracking for a passive rehabilitation table-top robot. In Rehabilitation Robotics (ICORR), 2017 International Conference on (pp. 702-707). IEEE.

Abstract

Each year 110,000 stroke cases are reported in the UK. 300,000 people are living with post-stroke complications, which for many include upper limb impairment. After-stroke therapy is most effective during the first 12 weeks, but improvement can continue for months or even years. To date, a number of devices prioritising early stroke rehabilitation have been developed, however most of these devices are active devices and cannot be used by patients without constant supervision due to safety concerns. In this work a low-cost, portable inherently safe rehabilitation robot is introduced. The robot is designed for use on existing table space in a home environment. Estimates of the robot's 2D position and orientation are computed by fusing data from two tracking systems, each utilizing a different sensor type: laser optical sensors and a webcam. Two laser optical sensors are mounted on the underside of the robot and track the relative motion of the robot with respect to the surface on which it is placed. The webcam is positioned directly above the workspace, mounted on a fixed stand, and tracks the robot's position with respect to a fixed coordinate system. The optical sensors sample the position data at a higher frequency than the webcam. A position and orientation fusion scheme is proposed to fuse the data from the two tracking systems. Active movements of a patient using the robot are assisted in real time by a custom-designed inherently safe guidance mechanism based on a COBOT unicycle architecture and capable of creating 2D virtual constraints. The guidance mechanism is mounted on the underside of the robot and in its centre, and is accompanied by four custom designed caster wheels with low rolling resistance. The guidance mechanism is actuated with a stepper motor, but no active force acting on the upper limb of the patient is generated. A prototype of the robot was manufactured and evaluated in a series of experiments including user testing with 38 healthy bodied adults. It was found that the robot is clearly capable

of applying a passive force of sufficient magnitude and in the right direction to increase the accuracy with which able bodied adults can perform reaching arm movements. The resistance to movement of the robot, both friction and inertia are sufficiently low that they do not appear to reduce the subjects' ability to move at normal reaching movement speeds.

Contents

List of Figures

List of Tables

Chapter 1

Introduction to Research

1.1 Background

Each year there are 110,000 cases of stroke reported in England. The estimated direct cost of strokes in 2008-2009 was at least £3 billion billion and the wider economical cost resulting from stroke cases was estimated to be £8 billion. Stroke is the single largest cause of adult disability in England and approximately 300,000 people are living with post–stroke complications. These numbers are likely to increase as the population ages (Morse & General, 2010).

Post–stroke disability is often associated with upper limb impairment affecting patients' functioning and quality of life (Lo *et al.*, 2010). The recovery process is the most effective during the first 12 weeks of rehabilitation. Therefore, to maximise the effects, intensive post-stroke rehabilitation should be started as quickly as possible (Kwakkel *et al.*, 1999).It was shown in previous research over a large number of trials that motor recovery can be enhanced by high-intensity, task-specific and repetitive exercises. Studies proved that increasing therapy intensity increases the rate of motor recovery. Despite being known to be necessary, the way traditional hands-on therapies are delivered has not been changed to become more frequent or intensive, usually due to labour limitations and costs. Moreover, physiotherapists themselves are subject to excessive fatigue and strain injuries during the rehabilitation training. In addition, hands-on therapy is affected by considerable variability caused by the human factors (Norouzi-Gheidari *et al.*, 2012).

One of the state–of–the–art and rapidly developing technologies in post-stroke recovery therapies is robotic rehabilitation. A robot-assisted therapy has many advantages

over hands–on, manual therapy. Robotic devices can monitor movements and measure motor skills and can deliver coherent training during each session (Dobkin, 2004; Norouzi-Gheidari *et al.*, 2012).

Robotic rehabilitation systems can be used to promote rehabilitation beyond hospital stay. Nowadays, despite an initial hospital based post-stroke rehabilitation being intensive, patients generally do not achieve full recovery potential. This occurs because patients do not receive proper rehab training after being discharged from hospital, which is mainly caused by economic pressure and lack of qualified human resources. Robotic technology advancements have resulted in the development of a few advanced robotic systems for upper limb post-stroke rehabilitation. However, most of these devices are not used on a mass scale due to cost, complexity and lack of comprehensive clinical trials (Loureiro *et al.*, 2011).

1.2 Problem Domain

The main area of expertise which is investigated in this thesis in order to identify the gap-in-the-knowledge in the current state-of-the-art post-stroke robotic rehabilitation advancements is the field of robotic rehabilitation. Covered robotic rehabilitation technology includes: review of developed devices for robot-assisted therapy, clinical outcomes of robot assisted therapy and advantages and disadvantages of robot-assisted therapy. In order to comprehensively understand the advantages and disadvantages of post-stroke robotic rehabilitation, literature on the problem of stroke, the limiting factors in conventional rehabilitation therapy and stroke rehabilitation is analysed.

1.3 Contributions to The Field of Robotic Rehabilitation

While a number of post-stroke robotic rehabilitation systems supporting upper-limb movements have been developed to date, they do not fully meet the above requirements or are unsuitable for unsupervised rehabilitation training after stroke. The work detailed within this thesis presents a novel type of a rehabilitation device developed for unsupervised upper-limb therapy after stroke. The developed robot utilises two novel features: a position and orientation-tracking system which fuses measurements from laser optical sensors and a webcam to obtain a higher accuracy of position and orientation data and a guidance

system of a type that has never before been implemented in an upper-limb rehabilitation device. The robot and the two novel features were experimentally evaluated to assess their potential for unsupervised robotic rehabilitation.

Two publications covering the developed tracking system were presented at IEEE international conferences in Chengdu and London:

- Wojewoda, K.K., Culmer, P.R., Jackson, A.E. and Levesley, M.C., 2016, June. Position tracking of a passive rehabilitation robot. In Cyber Technology in Automation, Control, and Intelligent Systems (CYBER), 2016 IEEE International Conference on (pp. 1-6). IEEE.

- Wojewoda, K.K., Culmer, P.R., Gallagher, J.F., Jackson, A.E. and Levesley, M.C., 2017, July. Hybrid position and orientation tracking for a passive rehabilitation table-top robot. In Rehabilitation Robotics (ICORR), 2017 International Conference on (pp. 702-707). IEEE.

1.4 Research Aims and Objectives

Research aim:
The aim of this study is to develop an inherently safe rehabilitation robot for upper-limb therapy of stroke survivors.

Research objectives:

1. Develop the mechanical design of an inherently safe upper-limb rehabilitation robot.

2. Develop a position tracking system for recording arm movements and rehabilitation progress monitoring.

3. Develop an inherently safe guidance system to guide patients' arm movements.

4. Test the performance of the developed rehabilitation system during training.

1.5 Thesis Overview

This thesis is composed of seven chapters. The chapters that follow this introduction (Chapter 1) are briefly introduced below:

Chapter 2: Literature Review
This chapter covers a review of literature around stroke and its complications, conventional after stroke therapy and state-of-the-art developments in the field of robotic rehabilitation. Limitations of the developed robots are identified and a gap in the knowledge is formulated.

Chapter 3: Design of an Inherently Safe Arm Rehabilitation Robot
This chapter presents technical requirements formulated on the basis of the gap in the knowledge identified in Chapter 2. The technical requirements are used to design four conceptual designs of a portable, table-top rehabilitation robot. One of these is selected to be developed into a final design. The final design and its mechanical design details are introduced.

Chapter 4: Position Tracking System
This chapter covers the development of a position and orientation tracking system for the table-top rehabilitation robot introduced in Chapter 3. Firstly, a proof of concept 2D position tracking system is introduced and evaluated in experiments. Secondly, a fully functional 2D position and orientation tracking system is introduced and experimentally evaluated.

Chapter 5: Inherently Safe Guidance System
This chapter presents an inherently safe guidance system developed for the rehabilitation robot prototype introduced in Chapter 3. Firstly, the design and working principles of the guidance system are explained. Secondly, the guidance system is evaluated in an experiment which tested its ability to constrain movements to a predefined trajectory.

Chapter 6: User testing
This chapter coves user testing conducted with 38 healthy participants using their non-dominant arms. The robot utilized in the testing was the prototype rehabilitation robot

introduced in Chapter 3. Firstly, the experimental scenario and goals are explained. Secondly, an experiment in which users were using the rehabilitation robot was conducted. Thirdly, data acquired during the experiments was analysed to evaluate the effect of the rehabilitation robot guidance system on the movements of participants.

Chapter 7: Discussion, Conclusions and Future Work

This is the final chapter of the thesis. Firstly, the performed research work is discussed and evaluated against the initial objectives. Secondly, the limitations of the work presented in this thesis are discussed. Thirdly, the main contributions to the body of knowledge are listed and discussed. Next, the research work presented in this thesis is concluded and recommendations are formulated. Finally, future research paths for building on the work presented in this thesis are suggested.

Chapter 2

Literature Review

2.1 Stroke

According to the World Health Organization, stroke is defined as: 'rapidly developing clinical signs of focal (or global) disturbance of cerebral function, lasting more than 24 hours or leading to death, with no apparent cause other than that of vascular origin' (Sacco *et al.*, 2013). In other words, stroke can be described as a cerebrovascular disease in which oxygen is not supplied to the brain tissue, which is most vulnerable to ischematic damage. The syndromes leading to stroke are divided into two categories: ischematic and hemorrhagic. Approximately 80% of all reported strokes are categorised as ischematic strokes, while the remaining 20% are categorised as hemorrhagic strokes. The ischematic stroke has numerous causes, however all of them result in the interruption of cerebral blood flow causing tissue anoxia. The hemorrhagic stroke has four most typical causes: intercerebral hemorrhages, ruptured saccular aneurysms, bleeding from an arteriovenous malformation and spontaneous lobar haemorrhages (Gillen, 2010).

2.2 Stroke Symptoms and Disabling Deficits

Common early stroke symptoms are: numbness of face, leg or arm on one side of the body; speech loss, sudden vision loss or dimness, unexplained dizziness and sudden headache (Rosamond *et al.*, 1998). The symptoms vary significantly in affected individuals and depend on the severity, location, and type of stroke. The human brain can be divided into several regions responsible for different functions such as speech, motor functions (voluntary movements), posture, balance and coordination. The region of the brain affected by

stroke and scale of damage to that region is linked directly to the stroke symptoms (Culmer, 2007). The most frequent disabling deficit observed in stroke survivors is hemiparesis (upper limb impairment). It affects 70% to 80% individuals after stroke and hemiparesis is often the deficit which needs rehabilitation therapy the most (Gladstone *et al.*, 2002). The other common disabling stroke symptoms are: incontinence (48% of the population); dysphagia (difficulty in swallowing, 45% of the population); and dysphasia (speech deficits, 23% of the population) (Lawrence *et al.*, 2001).

A significant percentage of the population has suffered a clinically undiagnosed stroke. Silent strokes were discovered with magnetic resonance imaging in 11% of adult population (aged from 55 to 64 years) in the Atherosclerosis Risk in Communities study (Fischer *et al.*, 2010). This number increased to 22% for the adult population aged 65 to 69 years and 43% for adults older than 85 years in the Cardiovascular Health Study. In each study, silent infarctions (tissue death due to insufficient blood supply) were detected using magnetic resonance imaging in individuals that could experience stroke symptoms which were not severe enough to be clinically diagnosed (Howard *et al.*, 2006). A case of mild stroke, where patients do not show disabling symptoms is called a "minor stroke" (Fischer *et al.*, 2010).

2.2.1 Upper Limb Impairment

Upper limb impairment is diagnosed in more than 70% of post-stroke survivors (Gladstone *et al.*, 2002). The upper limbs are crucial in our daily life activities and many tasks require simultaneous and cooperative use of both arms. Upper limb impairment might have a significant effect on post-stroke patients' ability to perform everyday functional tasks. Long-term disability in post-stroke survivors is frequently caused by chronic upper limb impairment 6 months or more after stroke (Lo *et al.*, 2010). The region of the brain controlling motor functions is separated into two parts controlling the right and left side of the body. Because the damage typically happens on only one side of the brain, upper limb impairment is usually observed on either left or right side of the body, which can be called the "affected side". The upper-limb impairment experienced after a stroke is a consequence of both physiological and neurological factors (Culmer, 2007).

2.2.2 Upper Motor Neurone Syndrome

Upper motor neurone (UMN) syndrome is a neurological factor causing upper limb impairment. The features of the UMN syndrome can be broadly categorised into two groups: negative and positive features. The typical positive features of the UMN syndrome are abnormal reflex activity or abnormal posture. The typical negative features of the UMN syndrome are muscle weakness, loss of dexterity and fatigability. Both negative and positive features of the UMN syndrome contribute to disability, but the negative features have a greater impact on impairment. Also, the negative futures are more difficult to alleviate through rehabilitation strategies (Barnes & Johnson, 2008).

Probably the most recognised positive feature of the UMN syndrome is a motor disorder called spasticity. Spasticity is characterised by increased muscle resistance to stretching which is more felt during faster muscle stretches. As spasticity resists muscle stretching, it causes two significant consequences. The first consequence is that the muscle tends to remain in a shortened state, which may initiate changes in soft tissue leading to contractures. Secondly, the spasticity constrains voluntary movements, which can, for example, reduce elbow extension and consequently reduce the arm range of motion (Barnes & Johnson, 2008).

Loss of dexterity and muscle weakness are the key negative features of the UMN syndrome. Dexterity is typically described as a skill in performing tasks, especially with hands. Loss of arm dexterity can cause difficulties with everyday functional tasks such as: writing, feeding and personal care. A simple task of lifting a cup which requires low force might be difficult for an individual with muscle weakness. Ultimately, poor arm dexterity and arm muscle weakness can gradually cause increased dependence on third parties and consequently decreased independence (Culmer, 2007) (Barnes & Johnson, 2008).

2.2.3 Contractures

Spasticity is not always responsible for decreased range of movement. Soft tissues surrounding joints, ligaments and tendons, can develop changes causing reduced compliance, which is called contracture. Contractures can result from the muscle remaining in a shortened state. It is likely, but not definitely demonstrated, that exercising the joint through a full range of movement might significantly reduce the risk of the development of soft tissue contractures (Barnes & Johnson, 2008).

2.2.4 Shoulder Complications

The shoulder is a complex joint system allowing for an extensive range of movements. Unfortunately, a typical hemiplegic arm is internally rotated and adducted at the shoulder along with the elbow being flexed, the forearm being pronated, and the wrist being flexed. Post-stroke shoulder complications are often very painful and are a consequence of shoulder spasticity. Shoulder complications can result in serious functional disability. If shoulder subluxation is detected, the shoulder joint must be supported during all movements to reduce the risk of further damage to the joint (Culmer, 2007) (Barnes & Johnson, 2008).

2.2.5 Sensory Loss

Neurological damage caused by stroke can cause impairment of sensory functions. Damage to brain regions responsible for processing of the senses leads to perception deficiencies. The crucial senses utilized in upper limb movement are sight and touch. Frequently observed sensory loss symptoms after stroke are the lack of skin touch sensation, problems with sensing the position of the body and decreased visual field. Commonly observed perception symptoms are not being aware of, or neglecting one side of the body and failure to identify the left and right sides of the body (Culmer, 2007).

2.3 Stroke Assesment

The severity of stroke can be objectively quantified by utilizing functional assessment scales, which allows for the implementation of treatment strategies tailored to a patient's needs (Cincura *et al.*, 2009). An example of such a scale is the National Institutes of Health Stroke Scale (NIHSS). This scale assesses 11 abilities and each ability can be graded from 0 to 4 (in increments of 1), where "0" indicates normal function and "4" indicates severe impairment (NINDS, 2018). Another example of a functional stroke assessment scale is the Barthel index with a maximal score of 100 points (Cabral *et al.*, 2003). The Barthel index (BI) assesses 10 activities of daily living (ADL) for a post-stroke patient. It was found to be consistent with inexperienced and experienced therapists (Shah *et al.*, 1989). The scores assigned to each task in the Barthel index are based on the level of physical assistance needed to perform the task. Nine of the eleven tasks are scored from 0 to 10 (0 points for inability to perform the task, 5 for if any level of assistance is required and 10 for tasks completed independently). Two of the eleven tasks are scored from 0 to 5, with

Table 2.1: The list of tasks and scores for the original Barthel Index (Shah *et al.*, 1989).

Items	Unable to perform task	Needs assistance	Fully independent
Personal hygiene	0	0	5
Bathing self	0	0	5
Feeding	0	5	10
Toilet	0	5	10
Stair climbing	0	5	10
Dressing	0	5	10
Bowel control	0	5	10
Bladder control	0	5	10
Ambulation	0	5–10	15
Wheelchair*	0	0	5
Chair/bed transfers	0	5–10	15
Range	0		100

0 points scored for both inability and assistance needed to complete the task, and 5 points scored for the task completed fully independently. Table 2.1 presents the tasks assessed to calculate a Barthel Index score. A Barthel Index score of 0-20 indicates the total dependence of a patient, 21-60 indicates severe dependence, 61-90 moderate dependence, and 91-99 slight dependence (Shah *et al.*, 1989).

Better sensitivity of the Barthel Index is necessary for subjects requiring some kind of assistance to perform the tasks. The original Barthel Index scale presented in Table 2.1 contains a three-level scale. In order to account for different levels of assistance, a modified Barthel Index scale presented in Table 2.2 was introduced.

The modified Barthel Index version utilizes a five-level scale and if a patient needs assistance, the level of assistance needed for a task can be classified as follows: "attempts task but unsafe" for subjects that are greatly dependent on assistance or are unsafe without assistance, "moderate help required" for subjects requiring moderate assistance to complete the task and "minimal help required" for subjects requiring minimal assistance or supervision. This modification of the Barthel Index scale was found to be more sensitive than the original Barthel Index scale (Shah *et al.*, 1989).

Another alternative for stroke assessment, considered by many stroke experts to be one of the most complete quantitative assessment methods of motor impairment resulting from stroke is Fugl-Meyer Assessment. It has been recommended for clinical trials measuring effectiveness of stroke rehabilitation. The Fugl-Meyer Assessment was developed specifically as an evaluative measure of recovery from hemiplegic stroke. It is a 226 items

Table 2.2: The modified Barthel Index scale accounting for three different levels of assistance needed (Shah *et al.*, 1989).

	Code				
Items	1 Unable to perform task	2 Attempts task but unsafe	3 Moderate help required	4 Minimal help required	5 Fully independent
Personal hygiene	0	1	3	4	5
Bathing self	0	1	3	4	5
Feeding	0	2	5	8	10
Toilet	0	2	5	8	10
Stair climbing	0	2	5	8	10
Dressing	0	2	5	8	10
Bowel control	0	2	5	8	10
Bladder control	0	2	5	8	10
Ambulation	0	3	8	12	15
Wheelchair*	0	1	3	4	5
Chair/bed transfers	0	3	8	12	15
Range	0				100

*Score only if Ambulation coded "1" and patient trained in wheelchair management.

scale divided into 5 categories (Gladstone *et al.*, 2002). These categories are: "motor function, sensory function, balance, joint range of motion, and joint pain" (Gladstone *et al.*, 2002). Each category contains multiple items and each is scored from 0 to 2, where 0 means cannot perform, 1 means performs partially, and 2 means performs fully. The motor category contains items assessing movement, reflex action and coordination about the ankle, knee, hip, shoulder, forearm, elbow, hand and wrist. The motor function score is from 0 (indicating hemiplegia) to 100 (indicating normal motor function). The maximum score of 100 is divided into 34 points for lower limb and 66 points for upper limb motor functions. The items scored in the motor function category are listed in Table 2.3. The other four categories can have the following maximum scores: 24 points for sensory function, 14 points for balance (sitting and standing), 44 point for joint range of motion and 44 points for joint pain. It is recommended that the Fugel-Mayer Assessment is conducted by a trained physical therapist, which should take approximately 30 minutes (Gladstone *et al.*, 2002).

The degree and rate of spontaneous recovery varies greatly among post-stroke individuals. As a result, the progress of stroke rehabilitation is very difficult to measure. Stroke can be classified as a heterogeneous disorder, therefore recovery is influenced by many factors such as: patient characteristics; the extent and location of lesion; stroke type;

Table 2.3: The motor category items of the Fugl-Meyer Assesment (Gladstone *et al.*, 2002).

Upper Extremity (66 points)	Lower Extremity (34 points)
Shoulder retraction	Hip flexion
Shoulder elevation	Hip extension (supine)
Shoulder abduction	Hip adduction (supine)
Shoulder abduction to 90 degrees	Knee flexion (supine)
Shoulder adduction/internal rotation	Knee flexion (sitting)
Shoulder external rotation	Knee flexion (standing)
Shoulder flexion 0–90 degrees	Knee extension (supine)
Shoulder flexion 90–180 degrees	Ankle dorsiflexion (supine)
Elbow flexion	Ankle dorsiflexion (sitting)
Elbow extension	Ankle dorsiflexion (standing)
Forearm supination	Ankle plantar flexion (supine)
Forearm pronation	Heel-shin speed
Forearm supination/pronation (elbow at 0 degrees)	Heel-shin tremor
Forearm supination/pronation (elbow at 90 degrees, shoulder at 0 degrees)	Heel-shin dysmetria
Hand to lumbar spine	Knee reflex
Wrist flexion/extension (elbow at 0 degrees)	Hamstring reflex
Wrist flexion/extension (elbow at 90 degrees)	Ankle reflex
Wrist extension against resistance (elbow at 0 degrees)	
Wrist extension against resistance (elbow at 90 degrees)	
Wrist circumduction	
Finger flexion	
Finger extension	
Extension of MCP joints, flexion of PIPs/DIPs	
Thumb adduction	
Thumb opposition	
Grasp cylinder	
Grasp tennis ball	
Finger-nose speed	
Finger-nose tremor	
Finger-nose dysmetria	
Finger flexion reflex	
Biceps reflex	
Triceps reflex	

severity, type and number of following neurological deficits; and stroke rehabilitation therapy. Stroke disability assessment scales, such as the National Institute of Health Stroke Scale and the Barthel Index are in common use but are inadequate for the measurement of the dynamic process of motor recovery and are therefore less likely to capture changes in response to different therapies. The lack of success of many clinical stroke trials might be caused more by the selection of therapy outcomes measure than the failure of the investigated agent (Gladstone *et al.*, 2002). Patients considered recovered neurologically, as defined by National Institute of Health Stroke Scale (score 0), might still have substantial weakness of the leg or arm that is not detected by the scale. The Fugl-Meyer scale might be a better tool to monitor hemiplegic stroke recovery and it has achieved international approval for assessment of motor recovery in post-stroke rehabilitation (Gladstone *et al.*, 2002).

2.4 Stroke Rehabilitation

The World Health Organization defines rehabilitation as "a set of measures that assist individuals who experience, or are likely to experience, disability to achieve and maintain optimal functioning in interaction with their environments" (Organization *et al.*, 2011). Generally, rehabilitation therapy is designed to improve an individual's functioning by, for example, improving the ability to drink or eat independently. The aim of rehabilitation is to reduce the impact of disabling health conditions. Usually, rehabilitation is delivered for a defined time period and can include multiple or single interventions delivered by rehabilitation therapists. Rehabilitation can be needed following the acute health condition phase (immediately following the detection of a health condition) through post-acute and chronic phases (Organization *et al.*, 2011). Rehabilitation is an iterative process which includes the assessment of the individual's requirements and problems, linking the problems to related personal and environmental factors, specifying rehabilitation targets, planning and delivering interventions and assessing the outcomes. Figure 2.1 presents the rehabilitation cycle diagram (Organization *et al.*, 2011).

2.4.1 Recovery Phases After Stroke

Recovery after stroke can be divided into three phases. The first one is the emergency care phase in a stroke unit. During this phase, a patient's outcome depends mainly on the

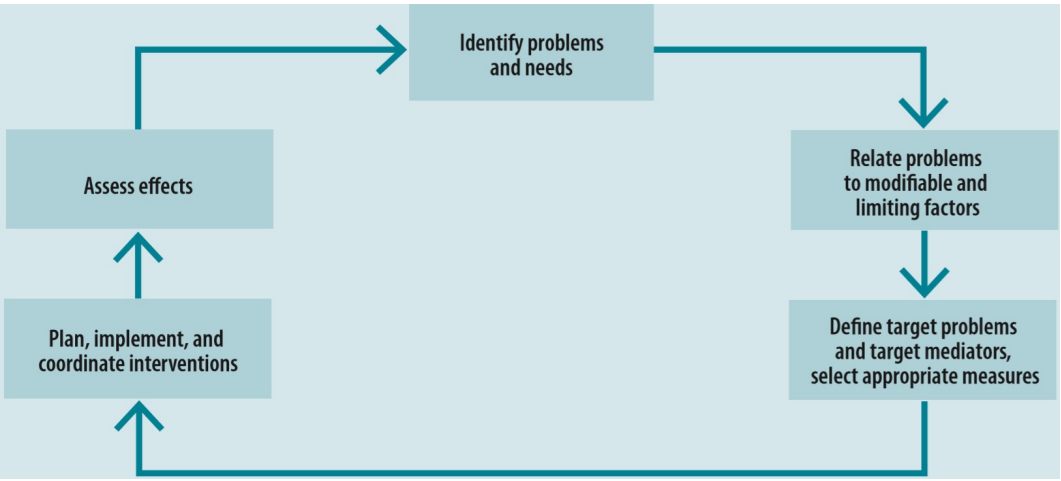

Figure 2.1: The rehabilitation cycle, source: (Organization *et al.*, 2011).

management and prevention of complications such as: recurrent stroke, impaired control of breathing, urinary tract infection, aspiration pneumonia and cardiac arrhythmia. The second phase of stroke recovery is early rehabilitation phase during which patients receive early rehabilitation and are in high demand for medical treatment or even intensive medical care. The third phase of after-stroke recovery is the rehabilitation phase. During this phase, patients are able to actively participate in rehabilitation therapy but they still may need therapists' assistance and medical treatment (Knecht *et al.*, 2011).

2.4.2 Upper-Limb Rehabilitation After Stroke

Impairment of upper extremities is a frequent ailment of post-stroke patients. Over 80% of stroke survivors develop chronic impairment in hand movement if they demonstrate significant weakness 6 weeks after stroke. It has been proven that intensive and frequent arm training is directly correlated with therapy results. Despite this, the amount of therapy delivered to a patient by a therapist is limited by cost considerations. Many scientists have argued that robotic rehabilitation might be a solution to this problem. Robotic rehabilitation can enable patients to train without the constant supervision of a qualified therapist. To date, data collected from medical trials suggests that robotic rehab devices are especially well suited for enhancing motor recovery and strength of upper extremities, enabling patients to achieve better outcomes than from traditional therapy

(Housman *et al.*, 2009).

It has been proven in several studies that task-oriented repetitive rehabilitation training of upper limbs in patients after stroke or spinal cord injury can enhance muscular strength and coordination of movements. Apart from restoring arm motor functions and coordination of movements, arm rehabilitation enables patients to learn alternative movement strategies to approach daily living activities in a new way. Arm movement rehabilitation also helps to avoid complications from stroke, including muscle atrophy, osteoporosis and spasticity (Nef & Riener, 2005).

There are no clearly-defined guideliens for optimal training intensity, however it is commonly accepted that intensive rehabilitation enhances recovery rate. It is also widely agreed that post-stroke rehabilitation should start as early as possible. After-stroke recovery can progress for months or even years, much longer than the duration of formal rehabilitation. It is very important for stroke survivors to support the recovery process after the formal rehabilitation ends (Langhorne *et al.*, 2011).

Increasing the intensity of arm rehabilitation therapy results in small but significant dexterity improvements. Generally, rehabilitation therapy induces improvements in the abilities for which the training is designed for. The experimental research has shown that the observed improvements in efficacy are correlated with greater intensity of arm rehabilitation. The differences in recovery are most significant during the first 12 weeks after stroke. After 12 weeks, the recovery process slows down, therefore intensive stroke rehabilitation should be started as quickly as possible. Figure 2.2 presents mean recovery patterns of Berthel index and it shows that the recovery process is the most intensive during the first 12 weeks of rehabilitation therapy (Kwakkel *et al.*, 1999).

2.4.3 Theoretical Basis for Stroke Rehabilitation - Motor learning

Motor learning can be defined as a "set of internal processes, involving both cognitive and motor processes, that is associated with practice or experience leading to a relatively permanent change in the capacity to respond" (Levin *et al.*, 2010). This definition emphasises the significance of achieving new motor skills, improving previously developed skills, or regaining skills that cannot be performed or are problematic to perform due to injury caused by, for example, stroke. Improvements that happen at performance or neurological levels because of motor learning and the elements impacting these improvements are of special interest for the rehabilitation of motor deficiencies. During rehabilitation therapy,

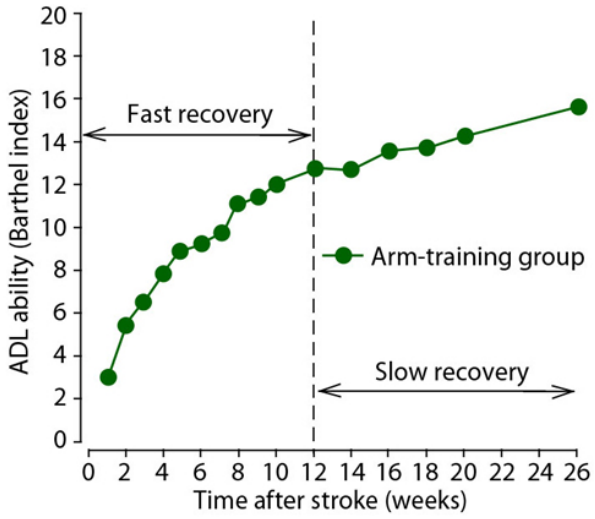

Figure 2.2: Recovery patterns of Activities of Daily Living (Barthel Index) in the first weeks after stroke. Adapted from: (Kwakkel *et al.*, 1999).

motor learning improvements at the movement outcome level can be measured in terms of movement variability, accuracy and speed. Motor learning improvements at kinematic or joint level can be defined as movement smoothness with suitable contributions of interjoint coordination, muscle activations patterns and joint ranges of motion (Levin *et al.*, 2010).

The principles of motor learning provide a base for rehabilitation. To maximise motor learning and, for example, post-stroke rehabilitation outcomes, three motor learning principles should be considered. Firstly, an individual must exercise the impaired limb as the repetition of action stimulates motor learning. Secondly, an individual must actively participate in therapy, as active involvement stimulates brain plasticity. Thirdly, the tasks performed by the individual should be realistic functional tasks enhancing motivation and engagement (Culmer, 2007). These motor learning principles and their positive influence during post-stroke rehabilitation are supported by a number of studies. The lasting benefits of therapy influenced by motor learning were presented in a study by (Feys *et al.*, 2004). A group of 62 of acute phase stroke patients was recruited. The aim of the study was to investigate the effect of repetitive sensorimotor training of the arm 5 years after stroke. Out of the 62 patients 33 patients (experimental group) were given additional sensorimotor treatment which followed the principles of the motor learning. The results showed significant functional improvement of the experimental group when compared to

the control group even 5 years after stroke. The effectiveness of task-oriented and repetitive motor learning therapy in the chronic stage of stroke (at least 6 months after stroke) in 21 patients was studied by (Byl *et al.*, 2003). The study outcomes showed significant functional improvement during the chronic phase of stroke.

2.4.4 Limitations of Current Stroke Rehabilitation Physiotherapy Practice

(Kwakkel *et al.*, 2008) reported that health professionals are experiencing increasing pressure to decrease healthcare costs. Moreover, the lack of time is reported to be the major factor preventing patients from complying with evidence-based procedures for upper-limb rehabilitation. Similarly, (Loureiro *et al.*, 2011) reported that patients generally do not achieve their full recovery potential after initial hospital-based rehabilitation because of lack of human resources and economic pressures.

There is evidence reporting that the stroke-damaged motor system is capable of reorganising itself because of motor practice. However, optimal therapies promoting such reorganisation are not clear (Loureiro *et al.*, 2011). Also, there is evidence that approximately 50% of patients after stroke continues to experience upper-limb disabilities after discharge from inpatient rehabilitation therapy. This causes a high risk of developing learned-non-use in the paretic upper limb which can be effectively prevented by organising rehabilitation programmes outside of the clinical environment. However, due to the unavailability of physiotherapists, the high cost of rehabilitation and problems with patients' motivation, learned-non-use is a common upper-limb disability (Loureiro *et al.*, 2011).

(Culmer, 2007) also reported that financial factors can have an impact on the effectiveness of conventional physiotherapy intervention after stroke. For example, the time a physiotherapist can spend with a patient can be inadequate. Additionally, the quality of treatment is further reduced by the increasing number of patients after stroke. There is growing evidence predicting that conventional stroke rehabilitation treatment will not provide sufficient treatment to the increasing number of stroke patients in the future (Culmer, 2007).

2.5 Robotic Stroke Rehabilitation

Robots are capable of delivering reliable and repeatable upper limb training. In contrast to human therapists, a robot does not get tired, can repeat exercises continuously preserving the same quality and intensity, and offers comprehensive feedback regarding performance and improvement (Kwakkel & Meskers, 2014). The development of rehabili- tation robots is supported by research evidence that intensive and repetitive paretic upper limb training enhances cortical organisation and brain plasticity resulting in increased use of the paretic upper limb (Loureiro *et al.*, 2011). Rehabilitation exercises performed by individuals in conventional therapy have a tendency to be monotonous. On the other hand, robotic rehabilitation, in order to maximise patients attention and therapy outcomes, in- troduces new therapy protocols incorporating interactive computer games (Kowalczewski *et al.*, 2011).

Physiotherapist-led rehabilitation training has various drawbacks. The major issues are intensity and duration of the training which are limited by the physiotherapist's availability and fatigue. These affect patients' recovery as the sessions are usually not long enough to achieve maximal rehabilitation results. Further, physiotherapist-led rehabilitation misses repeatability and verifiable recovery process monitoring. Conversely, robot-assisted upper-limb training is not limited in terms of duration, intensity and frequency of rehabilitation sessions, therefore the training can be adjusted to patients' needs. Introducing robot-assisted therapy in hospitals can reduce the number of physiotherapists necessary for one patient, which can result in reducing the cost of rehabilitation per each patient. Moreover, robotic rehabilitation systems enable detailed rehabilitation progress monitoring and assessment (Nef & Riener, 2005).

2.6 Classification of Rehabilitation Devices Based on Design and Training Mode

Rehabilitation robots can be grouped into two main categories based on their design: end-effectors and exoskeletons. The exoskeletons tend to be the most advanced and complex robots with several points of contact with the arm, and capable of controlling full arm movements. On the other hand, the end-effectors tend to be less complex in design, have one point of contact with the arm and are capable of guiding the arm only at the

point of contact. However, several more complex end-effector robots have been developed, having two points of contact with the arm and defined as multi-robot end effectors. Multi-robot end-effector devices are capable of supporting forearm and upper arm movements (Loureiro *et al.*, 2011).

Furthermore, the rehabilitation robots can be assigned to two categories based on the training modes supported: passive and active systems. Passive systems cannot help patients move their limbs as actuation systems for this are not incorporated in their design. They are not designed to actively assist movements, but can passively stabilise limbs, limit range of motion or provide gravity-compensating support. Many of the passive systems are based on stiff frames incorporating pulleys and cables connected to counter-weights. Active rehabilitation systems are usually based on electrical, pneumatic or hydraulic actuators and actively assist patients' limb movements. Many of these rehabilitation devices can be assigned to more than one category (Riener *et al.*, 2005).

2.7 Passive vs Active Stroke Rehabilitation Devices

Generally, active systems are more advanced than passive systems, at the cost of reduced safety, because they use actuators actively interacting with patients. Given these safety concerns, their use by patients must be limited to supervised sessions. Also, it has not been proven that actuators, which cause safety concerns and significantly increase device price, are needed to achieve treatment goals during robotic rehabilitation therapy. Assisting a patient's movements can in fact decrease their concentration and effort, particularly in cases where the robot is able to complete the movements without the patient's input. Generally, this has a negative effect on motor plasticity. On the other hand, passive devices are more likely to be safer, cheaper and suitable for unsupervised training. Passive rehabilitation devices (e.g. balanced forearm orthosis and mobile arm support) have been used in rehabilitation for many years. However, if a patient is not able to move his arm himself, an active or active assistive, actively supporting arm movements device might be the best approach for that patient (Housman *et al.*, 2009).

Table 2.4: Table-top portable end-effector arm rehabilitation devices

Table-top End-effector **Portable** Arm Rehabilitation Devices					
Device	Features	Feedback Provided	Position Tracking	Actuation	Workspace
ArmAssist	U, GS	A, V, F	HB, C, OS	OW, EM	2D
Arm Skate	U, GS	P, V, F	C	OW, MPB	2D
Arm Skate II	U, GS	A, P, V, F	OS	DCM	2D
Reha-Maus	U, GS	A, P, V	HB, O, C	OW, EM	2D
Features abbreviations: unilateral (U), bilateral (B), arm gravitational support (GS)					
Feedback provided abbr.: active force (A), passive force (P), haptic (H), Visual (V), free motion (F)					
Position tracking abbr.: hybrid (HB), camera (C), optical sensor (OS), odometry (O), encoders (E)					
Actuation abbr.: Omni wheel (OW), DC motor (DCM), magnetic particle brake (MPB)					

2.8 State-of-the-Art Arm Rehabilitation Devices

In this section current state-of-the-art rehabilitation devices for upper limb training are in- troduced. A number of passive rehabilitation systems are described in this chapter and they range from the simple antigravity support Armon to an advanced passive exoskeleton system Dampace, which offers passive guidance. Several active devices are mentioned as well, ranging from simple Bi-Manu-Track to very advanced semiexoskeleton ARMin. Apart from RUPERT and RHAROB, all of the listed active rehabilitation devices support some kind of passive (patient-active) training mode. In this work, the devices are grouped into four categories: table-top end-effector portable arm rehabilitation devices, table-top end-effector arm rehabilitation devices, end-effector arm rehabilitation devices, and ex- oskeleton arm rehabilitation devices.

2.8.1 Table-Top 2D Portable End-Effector Arm Rehabilitation Devices

his section focuses on table-top portable arm rehabilitation devices listed in Table 2.4, where their main features are compared. All of the analysed devices are portable (can be carried around by one person) and can be used on an existing table space in a home environment. Also, all of them can support one arm training at a time (unilateral) and incorporate omni wheels in their designs. Additionally, all of these devices support a 2D workspace.

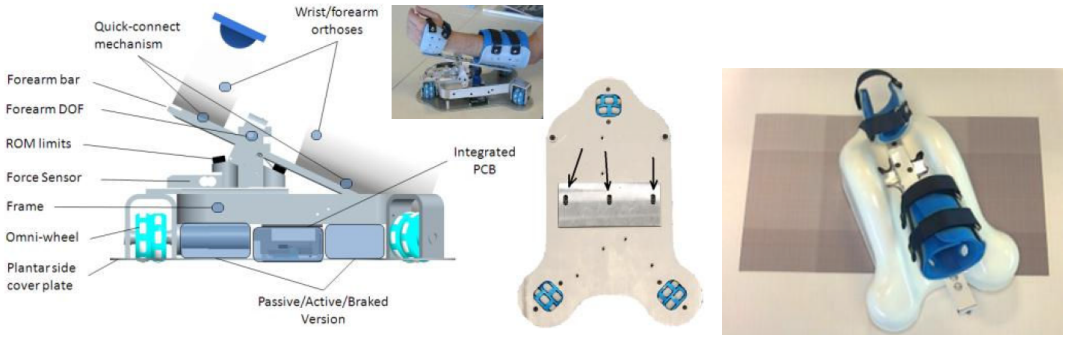

(a) (b)

Figure 2.3: ArmAssist CAD model (a) and ArmAssist prototype on a coded global position mat (b).

ArmAssist

ArmAssist, depicted in Figure 2.3, is a table-top, portable rehabilitation device developed for unilateral arm rehabilitation. The development of the device was motivated by rising numbers of stroke survivors living with arm motor deficiencies. The aim of the ArmAssist research was to develop a portable, uncomplex device that was easy to use, modular and including only necessary components that are essential for telerehabilitation. It was assumed that a low-cost, simple device that was easy to use, modular and included only the components that are essential for telerehabilitation. It was assumed that a low-cost, simple system would produce the maximum outcome regarding the total number of patients treated, while matching functional gains of more advanced systems (Perry *et al.*, 2012).

The ArmAssist system consists of a PC with a monitor, a coded global position-detection mat, telerehabilitation software and a wireless mobile base module. The device needs to be set up on a flat surface – a table at a patient's home should be sufficient. The system can be used by patients from remote locations while being remotely supervised by therapists if an internet connection is available. The structural frame of the wireless mobile base is made of aluminium. Three omni-directional wheels are attached to it. A vertical force sensor is

integrated in the design between the forearm support and the structural frame. The pur- pose of this sensor is to measure the vertical support provided by the device. ArmAssist utilizes three linearly arranged optical mouse sensors for position and orientation

measurements. The outer sensors detect relative position changes at 25 Hz, whereas the central sensor works as a camera taking pictures of the coded mat surface at 3.3 Hz. The orientation of the forearm is monitored by an analogue potentiometer. All of the measurements are wirelessly transferred to a computer via a Bluetooth module. The global position detection mat is laminated on a sheet of high density polyethylene. The sheet is 10 mm thick and can be placed on a table top. The sheet has 360 mm dimeter cutout that wraps around the patient and improves repeatability of a patient's position relative to the workspace. The size of the laminated coded print is 512x288 mm. This is also the size of the workspace. The accuracy of the position tracking is 6 +/- 3 mm and orientation 1.2 +/- 1.4 degrees. The forearm assembly of ArmAssist is attached to the base with brackets allowing one degree of freedom and with a quick-connect mechanism which enables changing forearm orthoses between sizes and left and right arm support. The forearm support design enables the user to perform natural forearm movements during 2d reach tasks. The forearm orthoses can be disconnected from the base unit by pressing a single button. The device is powered by 5000 mAh rechargeable battery which can continuously power the base unit for up to 20 hours. ArmAssist supports assessment and training games. The assessment games are short (1-2 min), and are designed to provide an assessment of the range of movements and point to point movements to the clinicians. The training games are longer (5-15 min) and provide more entertaining and challenging tasks. After every session and every game, performance assessment is computed and stored. For the assessment games, the stored information is more detailed and includes full trajectory recordings and force recordings for detailed analysis by the therapists. All games are displayed on a 21.6 inches screen placed in front of the patient. The ArmAssist system is portable when compared to most of the other systems, however the total weight of it is 15.4 kg which might be difficult to transport for some people (Perry *et al.*, 2012).

Arm Skate

Arm Skate, shown in Figure 2.4, is a table-top rehabilitation device for augmented reality therapy.It is designed to be suitable for home-based therapy. The device position is determined utilising only a webcam. Measurements from the webcam are used to control a resistive mechanism based on magnetic particle brakes connected to omni-directional wheels. The movement resistance can be automatically adjusted based on the position of the Arm Skate or set manually to a certain value in a range from 7 to 22.5 N, however

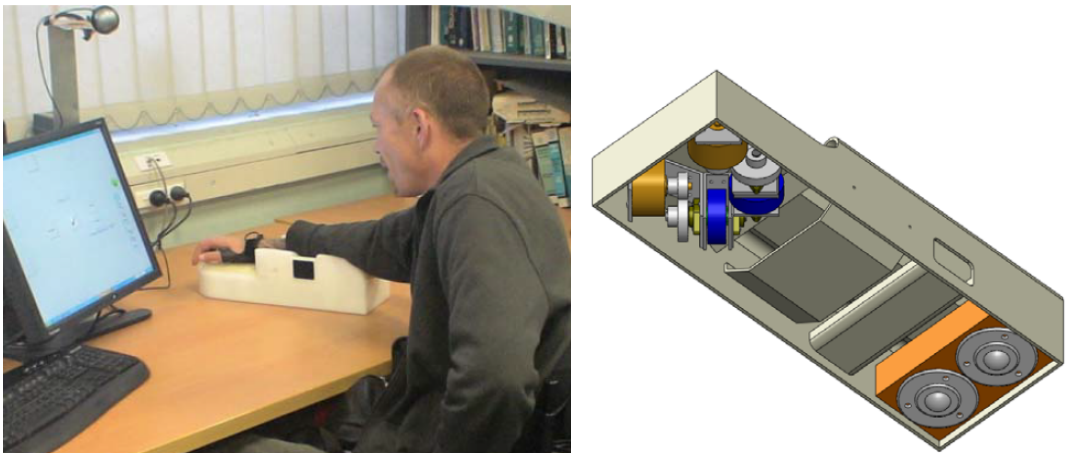

(a) (b)

Figure 2.4: A patient using the Arm Skate (a) and Arm Skate CAD model bottom view (b).

these numbers depend on the coefficient of friction between the wheels and the surface. Arm Assist communicates with a PC via a Bluetooth interface and the movable module is completely wireless. It employs an on-board battery allowing the device to be operated for 2 hours (Peattie *et al.*, 2009).

Arm Skate II

The aforementioned Arm Skate is a fully passive device requiring patients to actively perform arm movements. However, some patients have very weak arms and are not able to move it without assistance. In order to address the patients with significant arm weakness, the second version of the Arm Skate was developed. The Arm Skate II, presented in Figure 2.5,is a portable, table-top, arm rehabilitation device with forearm support. The device utilizes four DC motors, actuating four omnidirectional wheels. The position of the device is estimated based on measurements from two mouse optical sensors mounted on the underside of the device. The optical sensors act as a relative position and orientation tracking system, however the device does not use any absolute tracking system, therefore the position measurements are subject to accumulative error and the position has to be manually reset occasionally. In order to test the performance of the Arm Skate II a prototype PC graphical user interface was developed. During training sessions the progress

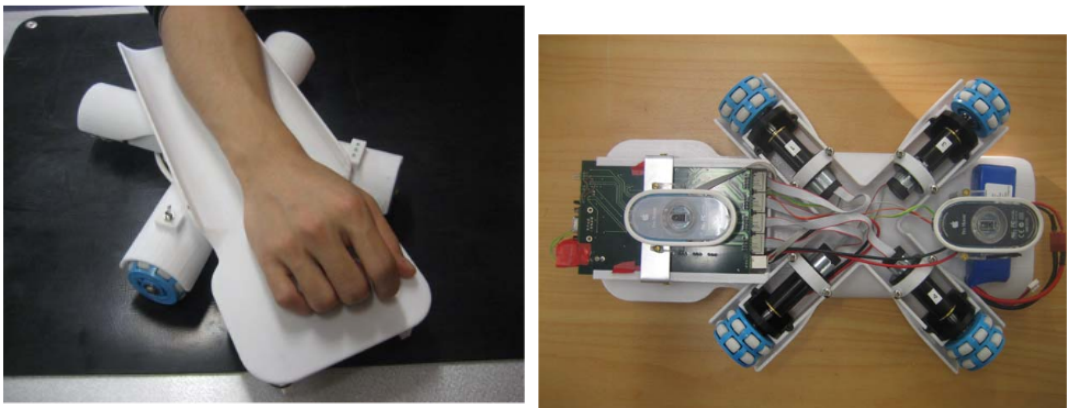

(a) (b)

Figure 2.5: A patient using the Arm Skate II (a) and Arm Skate II prototype underside view (b).

of a patient is monitored and if needed, assistive drive is automatically activated. As the game progresses and the patient improves, the level of assistance is reduced and level of resistance increases. The Arm Skate II prototype (similarly to ArmAssist and the Arm Skate I) has a wire-free design of the base module as it utilizes a 2500 mAh Lithium-ion battery and Bluetooth communication allowing the device to work continuously for 35 min (Wong *et al.*, 2011).

Reha Maus

Reha-Maus, shown in Figure 2.6 is an upper limb rehabilitation system pri- oritising portability. Similarly to the ArmAssist, Reha-Maus employs a sensor fusion to estimate the position and orientation of the base unit. The sensors utilized in this case are encoders measuring odometry of the three wheels, and an infrared camera (similar to Arm Skate) mounted above the robot. As illustrated in the Figure fig:rehamaus, Reha-Maus incorporates three DC motors actuating three omni-directional wheels and is capable of producing a force up to 51 N and torque up to 5 Nm. The maximum velocity and rotation are limited to 0.6 m/s and 9 rad/s respectively. The diameter of the robot is 300 mm, the weight is 2.8 kg, which is similar to the ArmAssist which has up to 3 kg weight require- ment for the base module. In the future development work, Reha-Maus is predicted to replace the

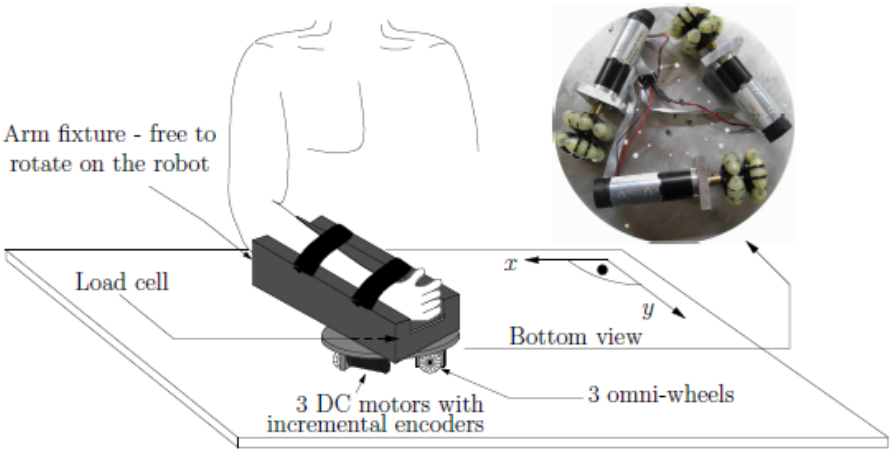

Figure 2.6: A possible application scenario of the Reha-Maus.

ceiling-mounted camera with an on-board camera looking down at a coded mat, a solution which was already presented in the ArmAssist (Luo *et al.*, 2012).

2.8.2 Table-top End-effector Arm Rehabilitation Devices

This section focuses on table-top end-effector arm rehabilitation devices listed in Table 2.5, where their main features are compared. All of these devices can be used on an existing table space.

Able-X

The Able-X, presented in Figure 2.7, is a device consisting of two main parts, a CyWee Z game controller attached to a handlebar. The CyWee Z is a motion sensing controller similar to the Nintendo Wii remote, however it is connected to a PC. Rotating the device in the sagittal plane controls vertical computer mouse cursor movements, whereas rotating it in the transverse plane controls horizontal mouse cursor movements. Using a single handle bar enables patients to support the more impaired hand with their healthier hand in a bilateral fashion and the bilateral training was reported to be effective for upper limb functional recovery. The Able-X supports self-assisted, highly repetitive and task oriented bilateral upper limb training (Bill *et al.*, 2011). In a pilot trial of the Able-X, fourteen individuals with chronic phase of stroke were selected to participate in a study. During

Table 2.5: Table-top end-effector arm rehabilitation devices

Table-top, end-effector, arm rehabilitation devices					
Device	Features	Feedback Provided	Position Tracking	Actuation	Workspace
Able-X	B	V	IMU	-	3D
APBT	B	A	-	-	Rotation only
BATRAC	B	V, F			1D
Bi-Manu-Track	B	A, P, V		EM	Rotation only
MIT Manus	U	A, P, V, F	E	EM	2D
Reha-Slide	B	P, F	-	-	1D
ReJoyce	B	P, V, F	E	-	3D
Tri-cable	U	A, V	E	EM	2D
Features abbreviations: unilateral (U), bilateral (B), arm gravitational support (GS)					
Feedback provided abbr.: active force (A), passive force (P), haptic (H), Visual (V), free motion (F)					
Position tracking abbr.: hybrid (HB), camera (C), optical sensor (OS), odometry (O), encoders (E), infrared arrays (IA), Inertial Measurement Unit (IMU)					
Actuation abbr.: DC motor (DCM), magnetic particle brake (MPB)					

the first stage of the training patients played simple mouse-based computer games, each session lasted between 45-60 minutes and was repeated 8-10 times over 2.5 weeks. This was followed by a 2 to 3-week washout period when no intervention was delivered. After the washout, patients were finally training with a custom-build handlebar with CYWee Z attached to it. The final stage of the intervention lasted for a period of 2.5 weeks and consisted of 8-10 sessions, 45-60 minutes each. It was estimated that number of repetitions done by each patient was in the range of 500 to 800, where one repetition is described as a left or right movement, up or down movement, or a combination of both. At the end, patients' scores on FMA had improved considerably, however the secondary scores (WMFT and DASH) had not improved (Bill *et al.*, 2011).

APBT The Rocker

The APBT was designed for active-passive bimanual wrist movement rehabilitation. The system consists of two manipulanda which are connected together via crankshafts and allow coordination of mirrored wrist movements in two horizontal directions. When training with the device, the patient actively moves their less impaired hand and this movement is transmited to the other, more impaired hand and causes it to move passively in a mirrored or 60 degrees phase lag mode. In a pilot trial with nine stroke patients, five of them had increased their FMA scores by at least 10%. In that study, patients took part in six, ten-

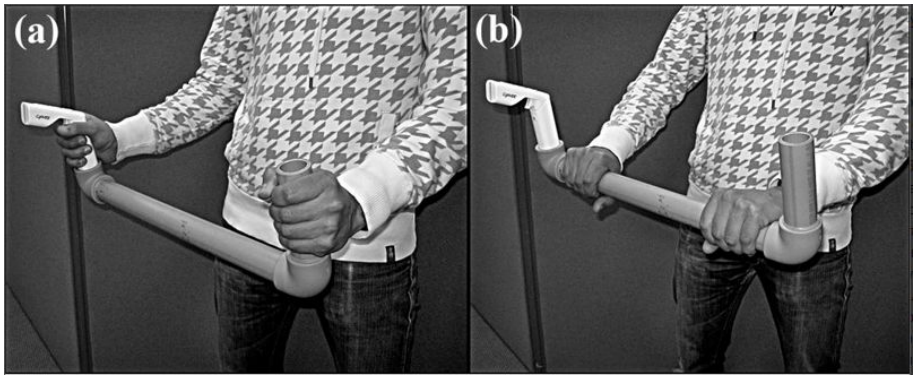

Figure 2.7: The Able-X device holded by a patient in two ways.

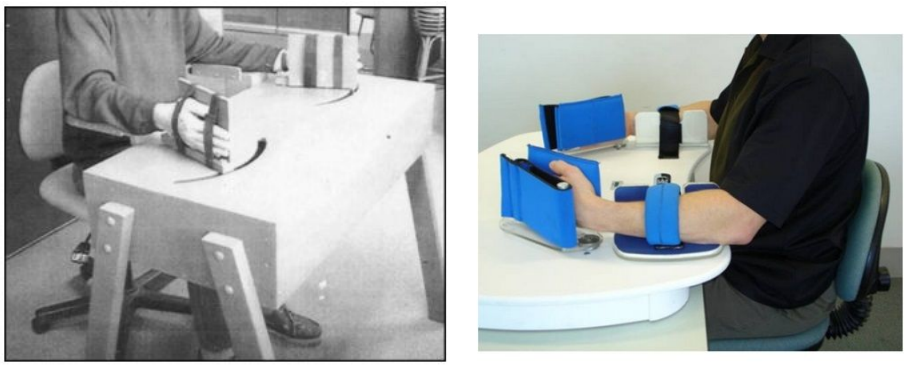

(a) (b)

Figure 2.8: The first APBT prototype (a) and improved APBT version (b).

minute long, daily training sessions with the rocker for a period of 4 weeks (van Delden *et al.*, 2012). The APBT Rocker device is shown in Figure 2.8 a and a leter version in Figure 2.8 b.

BATRAC (Tailwind)

BATRAC is an example of another passive device for bilateral upper limb training. A patient using the device has to grip two separate T-shaped handles which can be moved in a horizontal plane and are mounted on two independent low-friction tracks. The handles are supposed are supposed to be moved forward and backward with two hands simultaneously in either inphase or antiphase fashion at a frequency signalled by auditory signals. In a

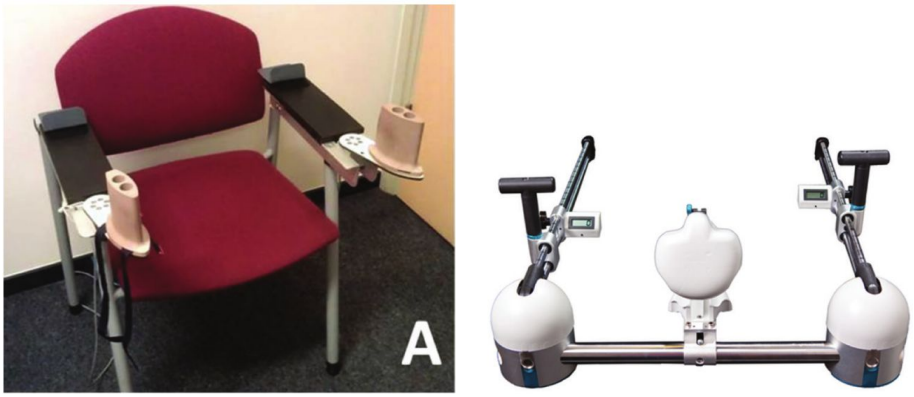

(a) (b)

Figure 2.9: The BATRAC with manipulanda attached to a chair's arm rests (a) and the Tailwind, a comercial version of BATRAC (b).

case where a patient with an impaired upper limb is not strong enough to grip the handle, the limb can be fastened onto the handle. The initial Tailwind protocol concentrates specially on elbow and shoulder training. A revised Tailwind protocol concentrates on distal movements of the hand (van Delden *et al.*, 2012). Figure 2.9 (a) shows a version of BATRAC where handles are attached to the arm rests of a chair. This version is especially designed for enhancing wrist and finger movements' range and control which, if affected, are the main cause of disability for a stroke patient (van Delden *et al.*, 2009). One iteration of BATRAC has been commercialised, it is called Tailwind (presented in Figure 2.9 b)and is intended for home-based rehabilitation therapy. It has some additional functionality, as in contrast to BATRAC, Tailwind functionality has been extended by outward and upward movements (van Delden *et al.*, 2012).

Bi-Manu-Track

The Bi-Manu-Track, presented in Figure 2.10, is a robotic rehabilitation system developed for bimanual wrist and forearm training. The device is aimed for hemiparetic patients and can be used in either active or passive mode. Prior to the design phase, the creators had decided that the device had to be suitable for autonomous, repetitive and standardized training and be available at low cost. The outcome of their work is a relatively simple rehabilitation system for bilateral forearm pronation and supination, along with wrist

dorsiflexion and volarflexion. The system can be fixed to any table, has two handles, both 30 mm in diameter, for the left and right hand. The handles are connected to electric motors via shafts. The two motors are able to provide a maximum of 5Nm torque each. A computer collects the data and controlling the positions of the handles and the motors' torques. There are two types of handles: with a horizontal axis of rotation for forearm training and with a vertical axis of rotation for wrist training. In order to swap the handles and change the training type, the device has to be tilted by 90 degrees as shown in Figure 2.10 a and b. The number of repetitions is displayed on an LCD screen and a digital control is used to switch between training modes. The device supports three different training modes which include: a passive mode with the possibility of changing settings for the range of motion and speed; an active mode in which a less impaired arm moves the paretic arm in a symmetrical pattern; and lastly an active mode which is similar to the previous active mode, however the difference is that the impaired arm had to overcome an initial adjustable isometric resistance to enable the bimanual movement. These three modes of training were based on several assumptions. The first one is that continuous, uninterrupted passive movements are approved neurodevelopmental treatment (NDT) mobilization approach increasing joint, muscle and tendon flexibility, while simultaneously decreasing muscle tone. The second assumption is that bilateral arm training helps the impaired arms' neural activity. Consensual movements of the unaffected arm were found to have a stimulating effect on ipsilateral corticospinal projections to the impaired arm. Respectively, functional imaging studies of motor recovery after a stroke reported that movements of the unaffected limb can increase blood flow in the impaired limb, and therefore accelerate motor recovery. The third assumption is that active, repetitive wrist movements can improve the arm's general motor functions. This has been confirmed in a study conducted by Butefish et al with 8.5-week post-stroke patients who had very limited finger function in the impaired hand. The study showed that an extra repetitive impaired wrist dorsiflexion can improve wrist extension acceleration and force, as well as handgrip strength, but apart from that it has a positive effect on the overall motor performance of the impaired arm. The last assumption is that repetitive movement training of the impaired arm can provide better results in curing a neglect syndrome than repetitive acoustic or visual stimulation enhancing using the affected side (Hesse *et al.*, 2003).

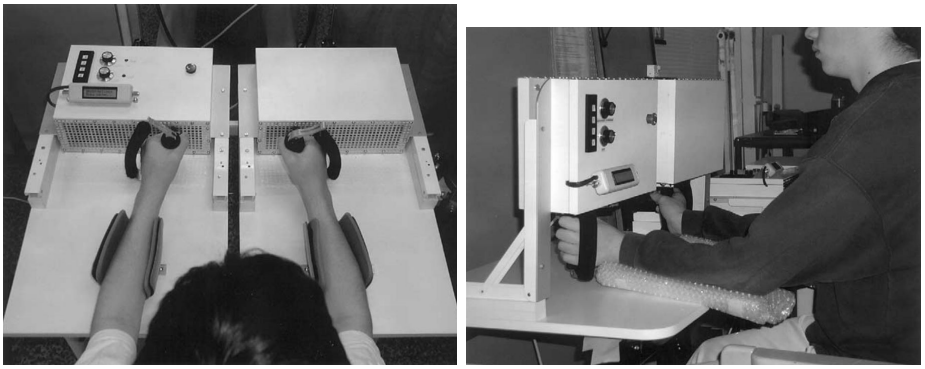

(a) (b)

Figure 2.10: A patient using the Bi-Manu-Track in a horizontal position for the bimanual forearm training(a) and a patient using the Bi-Manu-Track in a vertical position for the bimanual wrist training (b). Source: (Hesse *et al.*, 2003).

Reha-Slide Duo and Reha-Slide (Nudelholz)

The main part of the Reha-Slide Duo (shown in Figure 2.11 a) are two grips mounted on two parallel tracks fixed to a board. The grips are designed to be pushed forward and pulled back independently. The inclination angle between the board and the horizontal surface on which the device is placed can be set between 0 and 20 degrees. This makes forward moves more difficult and backward moves easier. Also, friction for movements in both directions can be set for both grips independently with two friction brakes. The breaking force can be adjusted to between 5 N and 80 N when the board inclination angle is 0 degrees. So far, no clinical results have been published for the Reha-Slide Duo, however the device was used for rehabilitation in an arm-studio (van Delden *et al.*, 2012). The Reha-Slide (presented in Figure 2.11 b)is a three degrees of freedom upper-limb trainer for stroke rehabilitation. It is very similar to the Reha Slide Duo, with the only difference being that the grips are connected with a rod. The angle between the base board and the surface can also be adjusted. The grips allow for bilateral forward and backward movements, side movements and rotations. The functionality of the device can be extended by attaching a computer mouse to the rod, allowing a patient to play computer games with biofeedback (Hesse *et al.*, 2007). During the first clinical trial, the Reha-Slide was used by two individuals, 5 and 6 weeks respectively, after stroke. Each training session

(a) (b)

Figure 2.11: The Reha-Slide Duo (a) and the Reha-Slide Nudelholtz (b).

was about 20-30 minutes long and it was repeated every work day for a period of 6 weeks. Patients were supposed to practicer forward and backward movements, draw a square in two directions (CW and CCW) while flexing their wrists. This treatment was conducted in parallel to a 10 week in-patient rehabilitation program including 45-minute sessions of physiotherapy four times per week and three 45-minute sessions of occupational training in accordance with neurodevelopmental therapy (NDT). At the end, both patients had improved their FMA (Fugl-Meyer) scores and muscle strength (van Delden *et al.*, 2012). Both the Reha-Slide Duo and the Reha-Slide are commercially available.

ReJoyce

ReJoyce is a passive rehabilitation workstation which has been designed for upper limb training for patients suffering from SCI and stroke. The device is also capable of assessing hand functions, which enables therapy progress monitoring. The main part of the equipment is a 4 DoF joystick, designed to be attached to a desk or table. A Passive force providing some elastic resistance to movements is generated by springs built into the joystick arm. When the joystick is released, it returns to its initial (neutral) position. The system provides feedback and monitors exercises using built-in sensors providing quantitative data on the grasping force and the displacement of the manipulated module. Signals from the sensors (rotational potentiometers) are fed into a computer and processed with dedicated software. ReJoyce enables patients to practice ADL in the form of interactive computer games and to perform the ReJoyce Automated Hand Function Test. Overall,

(a) (b)

Figure 2.12: ReJoyce joystick (a) and patient training with ReJoyce (b) .

the workstation consists of six manipulanda representing different tasks necessary in daily life. Figure 2.12 a shows the joystick with labels for the different tasks and Figure 2.12 b depicts a patient using the ReJoyce workstation (Dietz *et al.*, 2012; Kowalczewski *et al.*, 2011). The pair of horizontal handles can be rotated about the vertical axis, the peg can be pulled, the gripper (which has the diameter of a small jar) is designed to be squeezed and the door knob with the key element is designed to train opening doors. The ReJoyce can be used to perform the ReJoyce automated Hand Function Test (RAHFT) (Kowalczewski *et al.*, 2011).

Tri-cable

Tri-cable, shown in Figure 2.13 a, is a compact and inexpensive passive rehabilitation device for arm training. The passive resistive force is generated with three springs attached to the joystick at one end and to a table at the other end. In order to separate the patient's arm from the springs, a layer of glass is used, as shown in Figure 2.13 b. The upper part of the joystick is magnetically connected through the glass to the base. This solution increases the safety of the device, as the user is separated from the springs and if the interaction force is too large, the joystick's upper part will disconnect. This upper part is fitted with 16 evenly distributed LEDs to show movement directions to the user. The bottom base is fitted with a sensor used to track the position of the joystick. Three modes of operation are supported by the device: range of motion measurement, trajectory following and load application. In the range of motion mode, the springs are not connected and the patient can move the joystick enveloping as large an area as possible. The joystick's position is

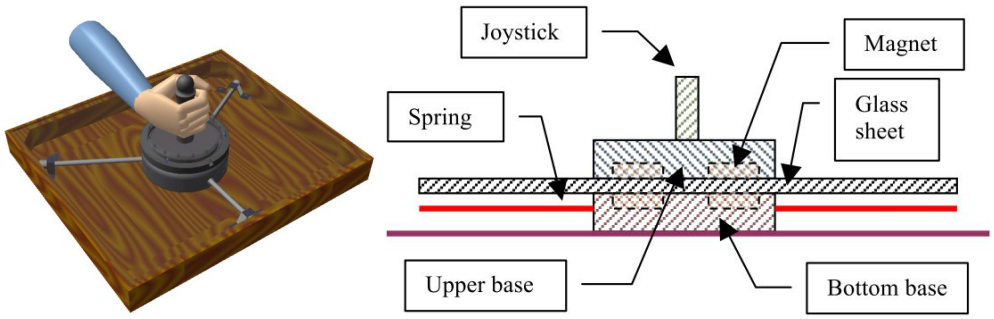

(a) (b)

Figure 2.13: The Passive Rehabilitation Joystick (a) and the side schematic view of the joystick (b).

recorded and sent to a computer. In the trajectory following mode patient moves the joystick following a predefined path. In this mode, the springs are not connected and the difference between the predefined and actual trajectories is recorded. Lastly, in load application mode the springs are connected and the patient has to apply a predefined force in a predefined direction(Masory & Sanroma, 2013).

2.8.3 End-effector Arm Rehabilitation Devices

This section focuses on end-effector arm rehabilitation devices listed in Table 2.6, where their main features are compared. These devices are bigger in terms of weight and size than the previously discussed devices. All of these devices are generally designed to be placed on a floor and require (or have included in their design) a chair.

ARM-Guide

The ARM Guide is an assistive and measurement rehabilitation system. It is able to mechanically assist arm reaching and retrieval movements and to measure range of motion, as well as constraint forces. Figure 2.14 presents schematic diagrams of the ARM Guide. While exercising, a patient using the system moves his arm along a linear path constrained by a three-splined steel shaft. The patient's hand is connected to the device with a custom splint that moves along the steel shaft on a spline nut incorporating low friction ball bearings. The custom splint can be rotated with respect to the three-splined steel shaft.

Table 2.6: End-effector arm rehabilitation devices

End-effector, arm rehabilitation devices					
Device	Features	Feedback Provided	Position Tracking	Actuation	Workspace
ARM-Guide	U	A, P, F	E	EM	2D
Armon	U, GS	-	-	-	3D
Braccio di Ferro	U	A, P, V, F	E	EM	2D
Driver's SEAT	B	A, P, V, F	E	EM	Rotation only
Freebal	U, GS	F	-	-	3D
Gentle/S	U, GS	A, P, V, F	E	EM	3D
Helparm	B, GS	F	-	-	3D
iPAM	U	A, P, V, F	E	P	3D
MIME	B	A, P, V	E	EM	3D
RHAROB	U, GS	A, V	E	EM	3D
Features abbreviations: unilateral (U), bilateral (B), arm gravitational support (GS)					
Feedback provided abbr.: active force (A), passive force (P), haptic (H), Visual (V), free motion (F)					
Position tracking abbr.: hybrid (HB), camera (C), optical sensor (OS), odometry (O), encoders (E), infrared arrays (IA), electromyography (EMG)					
Actuation abbr.: electric motor (EM), magnetic particle brake (MPB), pneumatic (P)					

The linear path angle is measured with an optical encoder and can be adjusted in a vertical plane referenced to the shoulder axis of rotation. The angle can be locked in the desired position with a magnetic particle brake. During each move, forces generated between the device and the arm are recorded with a six-axis force and torque sensor which is placed between the ball bearing spline nut and the shaft. The position of the patient's arm in respect to the splined-shaft is measured with a separate encoder attached to a sprocket in the centre of rotation in the adjustable stand which is further connected with a backlash chain to a second sprocket mounted on the distal end of the splined shaft. The ARM Guide was designed so that that a patient using it does not require any grasping skill. This was achieved by manufacturing a custom splint integrating a forearm brace and a wooden cone handle. The splint is positioned to support the forearm at 30 degrees of pronation, so that patients with restricted supination skill can exercise. In cases where the patient is not able to grasp the handle, the supervisor wraps their palm around the handle. The forearm is fastened in the brace with two straps immobilizing the wrist. The system can be used for both left and right arms (Reinkensmeyer *et al.*, 1999).

The described version of the ARM guide is a passive system, as no actuators have been incorporated in the design. However, in a later development of the ARM Guide an electric motor has been added to assist arm movements. Since the motor has been included the

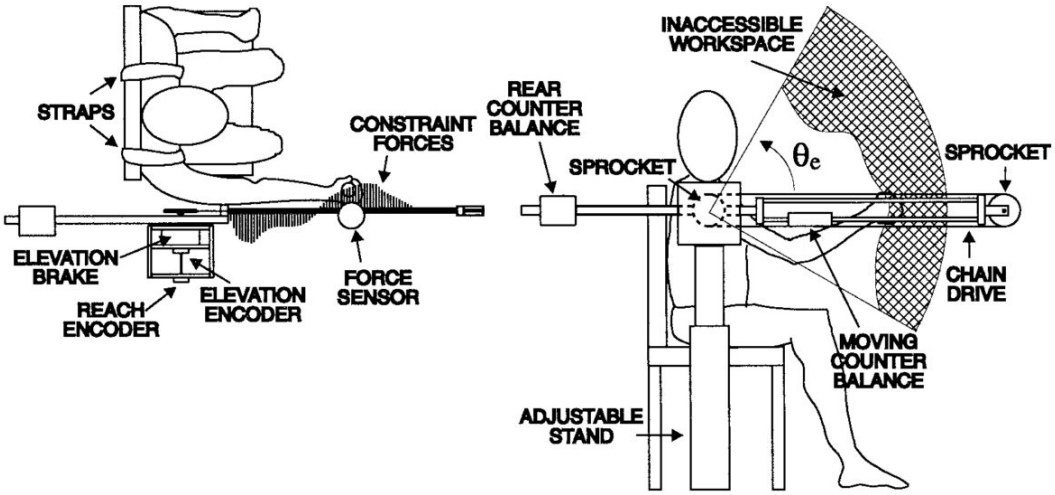

Figure 2.14: The ARM Guide side left) and top (right) view schematic diagram. Source: (Reinkensmeyer *et al.*, 1999).

system has been classified as an active rehabilitation device, which also supports passive training (Reinkensmeyer *et al.*, 2000).

Armon

The Armon, presented in Figure 2.15 a, is an upper limb passive support based on a statically balanced, spring loaded mechanism with an electric motor employed to regulate the supportive force produced by the mechanism, Figure 2.15b presents the Armon linkage design. As an electric motor is used, the individual using the device can quickly change the support level to account for lifting a heavy object or wearing heavy clothing. The device is designed so that the entire mass of an upper limb is not carried. The mass is partially supported by the shoulder. This approach reduces the number of supporting cuffs to one. The Armon is designed to be attached to a wheelchair as shown in Figure 2.15 c. A person using the device is able to reach his or her face and laps or each point on the wheelchair Table (Herder, 2005; Herder *et al.*, 2006).

Braccio di Ferro

The Braccio di Ferro is a robotic workstation for neurological rehabilitation. The mechanical structure of the robot is presented in Figure 2.16. Before the design stage, the Braccio

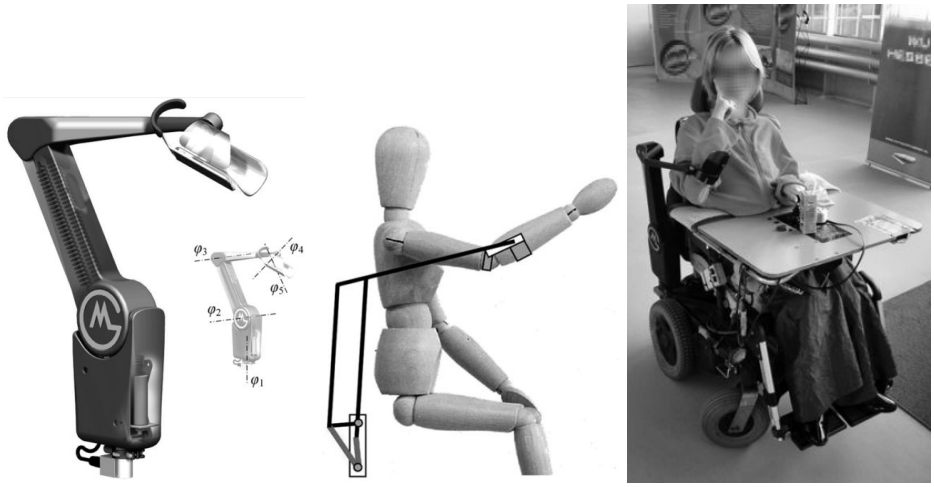

(a) (b) (c)

Figure 2.15: The Armon's 3D CAD model (a), the Armon's linkage design (b) and a wheelchair user using the Armon.

di Ferro team had set several goals which included:

'1) an extended range of forces, in order to match the natural capabilities of the human motor system; 2) backdriveability of the system, in order to have natural haptic interaction; 3) very low friction and inertia in order to enable experiments near proprioceptive thresholds; 4) mechanical robustness, taking into account the intended clinical usage of the device; 5) the possibility to operate in different planes; 6) an open programming environment, which could allow the user to add new functionalities and design personalized rehabilitation protocols.' (Casadio *et al.*, 2006).

The Braccio di Ferro is an open source system aiming to popularize robotic rehabilitation. The creators of the device are willing to share their experience about the system development. This device also intends to give users an opportunity to modify the software and therefore anyone can implement modifications and add personalized rehabil- itation protocols. The system was required to have backdriveability in order to perform similarly to the human motor system. For this reason, the creators avoided solutions based on motors using non-reversible gears, such as DC motors with harmonic gears used in typical robotic designs. The mechanical linkage of the device is based on a parallelogram and is directly driven by the motors as shown in Figure 2.16 a. This solution is characterised

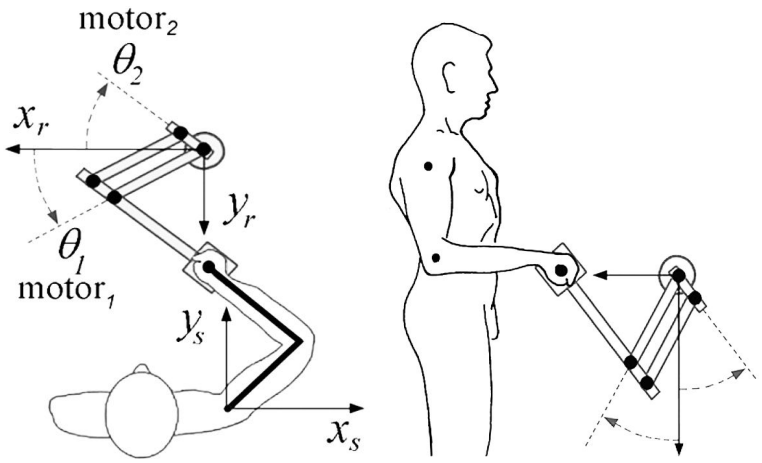

Figure 2.16: Mechanical structure of the Braccio di Ferro and a user position when the device is oriented horizontally (a) and vertically (b). Source: (Casadio *et al.*, 2006).

by satisfactory structural rigidity, lack of force and motion transmission backlash and low inertia, as most of the mass is located near the rotation axis or is immovable. The mechanical design of the manipulanda had to compromise three fundamental requirements which included: spacious workspace, large force produced at the handle and a high level of manipulability. These requirements were partly contradictory, e.g. the size of the device increases with the workspace, but the force generated per unit of the motor torque (force to torque ratio) at the handle decreases. The high level of manipulability improves the backdriveability of the manipulanda, therefore its control can be simplified. Other technical requirements were: an elliptical workspace with a major diameter of 800 mm (parallel to the user chest) and minor diameter of 400 mm and a minimum force to torque ratio at the handle of 2 N/Nm (Casadio *et al.*, 2006).

Driver's SEAT

The Driver's SEAT (Simulation Environment for ARM Therapy), shown in Figure 2.17, is a one degree of freedom robotic system simulating a car steering wheel designed for upper limb rehabilitation training. This device was designed to help post-stroke patients with impaired upper limbs in general, however more specifically, the device was designed for restoring driving skills.

Upper limb impairment is a common symptom after a stroke. If it is present, it can affect driving abilities and even make driving a car impossible. Being unable to drive a car can increase the chances of depression and social isolation in stroke patients. Therefore, regaining driving abilities after a stroke can increase a person's independence and overall rehabilitation prospects. The creators of the Driver's seat think that the motivation of stroke patients to use the system should be strong, especially if they are not able to drive and want to regain this ability.

The complete Driver's SEAT system is presented in Figure 2.17. In the photo on the left in Figure 2.17, the user interacting with the device is seating on a chair and holding a steering wheel. The steering wheel is connected as shown on the diagram in Figure 2.17 on the right. It is attached to the shaft with four flexible spokes and incorporates two independent force sensors which measure forces generated by each hand independently. The system supports three steering modes which include: passive movement, active steering and normal steering. In the passive movement mode a patient holds both hands on the steering wheel and the active steering movement is performed with the patients less impaired hand which moves the impaired hand passively. This mode was designed for patients whose paretic arms are not strong enough to perform exercises without support. On the other hand, the active mode is intended for patients whose impaired arm has some strength allowing independent movements. In this mode, patient's paretic arm is actively stimulated to perform movements, while at the same time the healthy or less impaired arm is actively impeded from performing movements. A servo-mechanism is used to oppose forces generated by the healthy arm. The third mode of steering is called normal steering and it was designed to evaluate the performance of the paretic limb. This mode should be the first mode patients use as the data regarding the paretic limbs performance can be used to choose the first (Passive Movement) or the second (Active Steering) mode as well as training intensity (Johnson *et al.*, 1999).

Freebal

The Freebal, shown in Figure 2.18 a, is a passive rehabilitation system designed to compensate the gravity force acting on the patient's arm. The counterbalancing force is generated with a nearly inertia-free spring mechanism, presented in Figure 2.18 b (Stienen *et al.*, 2007b).

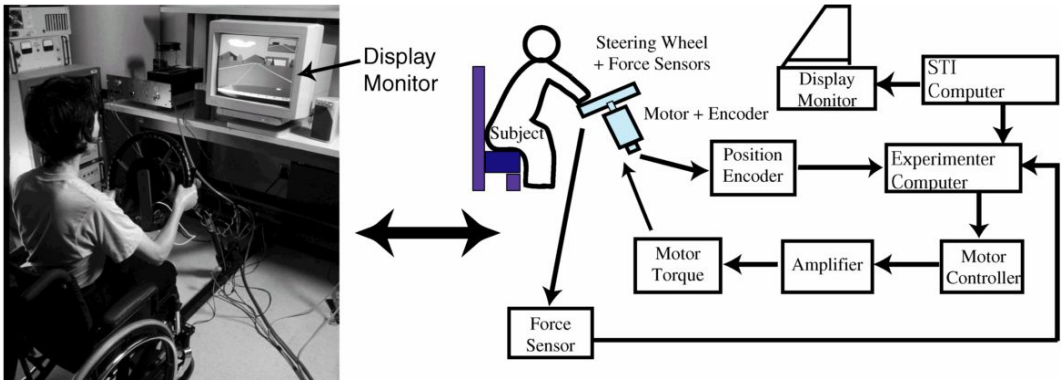

Figure 2.17: A patient using the Driver's SEAT rehabilitation device and a schematic diagram of the Driver's SEAT system (right). Source: (Johnson *et al.*, 1999).

The compensation force produced by the Freebals spring mechanism can be smoothly adjusted and provides support for the full range of motion. The arm is supported at two points, the elbow and the wrist. It could also be connected at the centre of mass of the upper and lower arm, but patients find the first option more comfortable. The device is easy to maintain and transport and can be used both standing up and sitting down (Stienen *et al.*, 2007b).

To investigate how the Freebal affects patients a pilot study was conducted with eight stroke survivors and ten healthy elderly subjects. Patients were asked to perform two exercises: linear maximal reaching movements and maximal circular range of motion movements. Each exercise was performed twice, once with full anti-gravity support and once without any support. The pilot studies' results showed that healthy elderly subjects were able to achieve the same range of motion with and without support. In the case of post-stroke patients the results were different and their range of motion increased by 7% when the arm was supported (Stienen *et al.*, 2009b).

Act 3D, ADLER and Gentle/S

The Gentle/S project was initially funded by the EU Framework 5 to research arm robot mediated stroke therapy. During the project, a computer assisted visual-sensorimotor rehabilitation system was developed, as depicted in Figure 2.19 a. The main focus of the Gentle/S project was robot-based neurorehabilitation therapies for stroke survivors. The initial aims of the project were to lower the cost of rehabilitation and increase effectiveness.

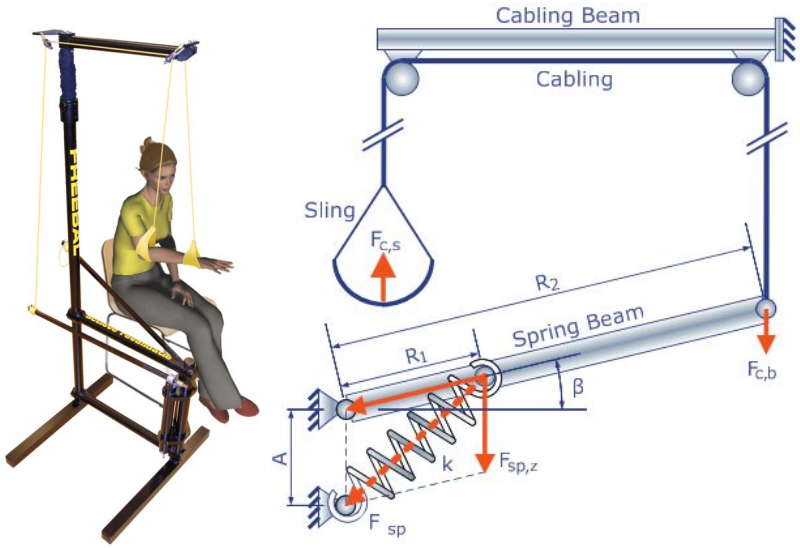

(a) (b)

Figure 2.18: The Freebal Anti-gravity rehabilitation device (a) and the Freebal's spring mechanism generating anti-gravity support (b).

The Gentle/S system delivers reach to touch training to the individuals upper limb and movements are initiated from the shoulder. While training with the Gen- tle/S, the patient sits on a chair in front of a table. The patient's arm is located inside an orthosis providing anti-gravitational support and suspended from a frame positioned above the patient's head. The orthosis supports the arm at two points, one in the forearm and the other in the upper arm. Although both are located close to the elbow, the patient is still able to flex it. The patient's wrist is attached to a wrist orthosis which is connected to a HapticMaster robot. The control software developed for the system to control upper limb movements is based on minimum jerk and errorless learning theory. The Gentle/S can be used in one of three modes: patient passive, patient active assisted and patient active. In each mode, neural activity is stimulated by repetitive movements performed to complete virtual tasks. The patient active mode was designed for patients who have satisfactory muscle motor strength to move their hand. In this mode, the robot involvement in the exercise is passive and it only produces resistive force in order to guide active hand movements. When the movement is off the predefined trajectory, the robot is pulls the hand back to the correct position by applying a virtual spring-damper system. The force of interaction

between the user and the robot is measured with a force sensor located at the end-effector (Amirabdollahian *et al.*, 2007).

The Act 3D (Arm Coordination Training) and ADLER (Activities of Daily Living Exercise Robot) are based on the Gentle/S system. Each of these three devices shares a modified HapticMaster robot developed by FCS Control Systems in the Netherlands. The Act 3D only uses the same robot platform, whereas the ADLER also uses identical wrist splint attachments and identical gimbals. The main purpose of developing the Act 3D system was to investigate how the gravity effect influences the impaired upper limb muscle synergies. The ADLER and Gentle/S are designed for robot-mediated rehabilitation therapies, however their functionality in ADL trainings is constrained by an insufficient range of motion (Loureiro *et al.*, 2011; Sukal *et al.*, 2005).

The main difference between the Gentle/S and ADLER is that the first one was designed for 3D point- to-point movements in a physical world or in virtual reality. On the other hand, the ADLER was designed for practising ADL tasks in both 2D and 3D planes. This was motivated by previous studies' results which showed that the presence of a real target (e.g. a bottle) enhances reaching movement smoothness and peak velocity for both stroke impaired patients and healthy individuals. Figure 2.19 b presents patient practising grabbing a bottle with the ADLER system (Johnson *et al.*, 2006). The effectiveness of the Gentle/S robot-mediated therapy on arm function after stroke was investigated in a study with 20 participants. All of them suffered from residual arm dysfunction and had only had one stroke. During the robotic therapy, participants were asked to practice three functional exercises with visual and haptic feedback from the Gentle/S. Apart from the robotic therapy they also participated in three single-plane exercises. Overall, the intervention was delivered over six weeks, where the robotic therapy lasted for three weeks and the single-plane exercises also lasted for three weeks. The study findings suggested that the robotic rehabilitation therapy can have better outcomes than non-functional training of the same duration (Coote *et al.*, 2008).

Swedish Helparm

The Swedish Helparm, presented in Figure 2.20, is a passive rehabilitation device based on a system of weights and pulleys connected with ropes to the patient's arm. The device can be easily adjusted to different arm weights and motor skills. The level of support can be increased and decreased in steps, changing the amounts of assistance or resistance.

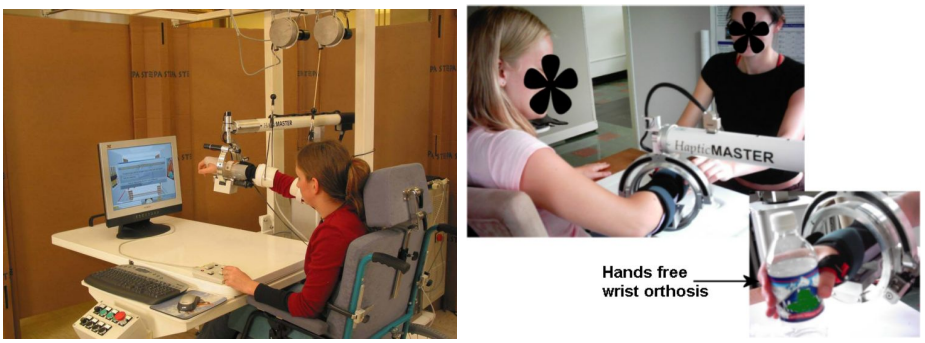

(a) (b)

Figure 2.19: A patient training with the Gentle/S (a) and a patient training with ADLER (b)

The Swedish Helparm is suitable for patients with shoulder muscle impairment or paresis, cervical spine injury, shoulder nerves injuries, hemiplegia and multiple sclerosis. It provides constant assistance and can be used to practice ADL at a hospital or at home (Riener *et al.*, 2005). There are some issues with patient comfort while using the Swedish Helparm. It has been reported that the device can cause shoulder pain. A speculative explanation for this might be the fact that the Helparm lacks independent support for the elbow and the wrist. While a patient is exercising with the device, their arm is supported only at a single point close to the wrist. This makes the shoulder joint bear most of the arm weight (Stienen, 2009).

Other End-effector Rehabilitaton Devices

Not all of the available end-effector based robotic rehabilitation devices are covered in this report. This subsection will briefly introduce and comment on other end-effector based devices, which are not suitable for home based rehabilitation or which are analogues to devices described in previous sections.

A type of rehabilitation robot which has not been previously mentioned is a device based on an industrial robot, such as MIME and REHAROB. MIME, presented in Figure 2.21 a, is based on an industrial robot which is attached to a patient's forearm. It supports both unilateral training in three modes: passive mode, assistive mode and constrained mode. The device also supports bilateral training with a joystick connected to the healthy

Figure 2.20: The Swedish Helparm.

arm. In the bilateral mode, the healthy arm is used to move the paretic arm in a mirrored fashion while it is connected to the robot (Lum *et al.*, 2005). REHAROB, presented in Figure 2.21 b, is also based on industrial robot actuation, but in this case two industrial robots supporting the upper arm and the forearm are employed. The industrial robots used were not modified and are supposed to work simultaneously. Reharob can be used for left and right arm therapy and is intended for passive movement therapy in which the patient is passive and the robot actively guides movements (Toth *et al.*, 2005).

Another example of a dual robot system is iPAM, presented in Figure 2.22.iPAMs robots are pneumatically actuated and support upper limb movements by providing controlled assistance. As in the case of RHAROB, the patient's arm is supported at two points (forearm and upper arm) mimicking the way physiotherapists hold the arm. iPAM is capable of sensing voluntary movements made by the patient's arm and guides the paretic arm to provide coordinated motion (Jackson *et al.*, 2013).

The first planar robot designed and manufactured in 1991 for rehabilitation was MIT-MANUS. This device is very similar to Bracio di Ferro, described earlier in this chapter. MIT-Manus is intended for arm and wrist rehabilitation (Krebs *et al.*, 2007).

(a) (b)

Figure 2.21: (a) MIME rehabilitation system during bilateral training and (b) a patient exercising left arm with REHAROB. Source: (Lum *et al.*, 2005; Toth *et al.*, 2005).

Figure 2.22: The iPAM pneumatically actuated dual robot rehabilitation system. Source: (Jackson *et al.*, 2013).

Table 2.7: End-effector arm rehabilitation devices

Exoskeleton, arm rehabilitation devices					
Device	Features	Feedback Provided	Position Tracking	Actuation/ Guidance	Workspace
ARMin	U, GS	A, P, V, F	E	EM	3D
Dampace	U, GS	P, V, F	E	DB	3D
L-Exos	U, GS	A, P, V, H, F		EM	3D
Pneu-WREX	U, GS	A, P, V, F	PM	P	3D
RUPERT	U, GS	A		P	3D
T-Wrex	U, GS	V, F	PM	-	3D
Features abbreviations: unilateral (U), bilateral (B), arm gravitational support (GS)					
Feedback provided abbr.: active force (A), passive force (P), haptic (H), Visual (V), free motion (F)					
Position tracking abbr.: hybrid (HB), camera (C), optical sensor (OS), odometry (O), encoders (E), infrared arrays (IA), electromyography (EMG), disk brakes (DB), potentiometer (PM)					
Actuation abbr.: electric motor (EM), magnetic particle brake (MPB), pneumatic (P)					

2.8.4 Exoskeleton Arm Rehabilitation Devices

Exoskeleton-based robotic rehabilitation devices are considered to be the most ad- vanced rehabilitation systems, however they are also the most expensive ones. Taking this into consideration, it is reasonable to assume that they are more suitable for hospital-based use than for home-based rehabilitation. The exoskeleton devices considered in this section are listed in Table 2.7, where their main features are compared.

When compared to end-effector systems, the exoskeleton systems can control arm movements better as they are connected to the arm at several points and allow control of the position of the arm, as the joint axes of the arm are completely determined. Therefore, the exoskeleton robot supports whole arm movements, which eliminates unexpected arm and elbow rotations and reduces the possibility of joint injuries which might occur if 3D spatial movements are not supported. Full arm control also enhances the relearn process of correct upper limb orientation patterns. The drawback of exoskeleton rehab devices is the possibility of misalignment of the arm's anatomical axes with the robots axes, which can lead to injures (Loureiro *et al.*, 2011).

The list of product requirements is longer for active exoskeleton-based rehabilitation robots than for other rehabilitation devices. It is essential that ex- oskeleton robots are adjustable or fitted for a patients arm, which means that the range of motion, length of links and number and location of the degrees of freedom has to match the patient's arm. This results in a large number of degrees of freedom enabling patients to practise activities of daily living, (ADL) as it was proven that ADL-focused reha- bilitation is more effective

than single-joint movements. A robotic device is capable of assisting in ADL training if it is able to move the patient's arm to every point in the range of motion space, and if it is capable of moving the arm in all of the arm's degrees of freedom. The ADL training can be delivered by an exoskeleton or end-effector robot. It is necessary that the robot has at least four degrees of freedom in order to control the arm's orientation and position in space (Nef & Riener, 2005).

To date, several exoskeleton-based rehabilitation devices have been developed. All of the devices mentioned in this section, excluding Dampace and T-Wrex, are active rehabilitation systems, however, apart from RUPERT, they support a passive mode of practice as well. These systems are usually quite complex and therefore expensive and are generally not safe enough for home–based unsupervised training.

Dampace

The Dampace, presented in Figure 2.23a , is a dynamic force coordination system in which hydraulically controlled disk brakes can generate controlled torques which resist arm movements. They are mounted on the shoulder and elbow rotational axes, as shown in Figure 2.23 b. The hydraulic disk brakes are only capable of applying resistive torques and therefore, according to control engineering terms the device is passive. The drawback of the passiveness of the system is the lack of ability to actively aid a patient's movements, but as compared to active systems the Dampace is much safer. The orthosis does not have to be aligned with the patient's elbow and shoulder axes, as the orthosis has extra degrees of freedom (DOF) for both joints. The Dampace functionality is increased by a spring-based gravity compensation mechanism generating a constant vertical force pulling the arm up via two cables attached to the patient's wrist and elbow. The gravity compensation force can be linearly adjusted with a worm-wheel slider in the spring mechanism (Stienen *et al.*, 2007a).In order to enhance patients' motivation during training, the Dampace can be used to control computer games. So far, the device was used as a controller in a car racing game. The car's gas pedal was controlled with isotone rotations or isometric thoracohumeral elevation torques and the steering wheel was controlled with isotone rotations or humeroulnar isometric torques (Stienen *et al.*, 2009a).

Another exoskeleton device which also uses controlled brakes to generate controlled torques resisting arm movements is the Force Reflected Exoskeleton-Type Masterarm, depicted in Figure 2.24, developed at the Korean Institute of Science and Technology

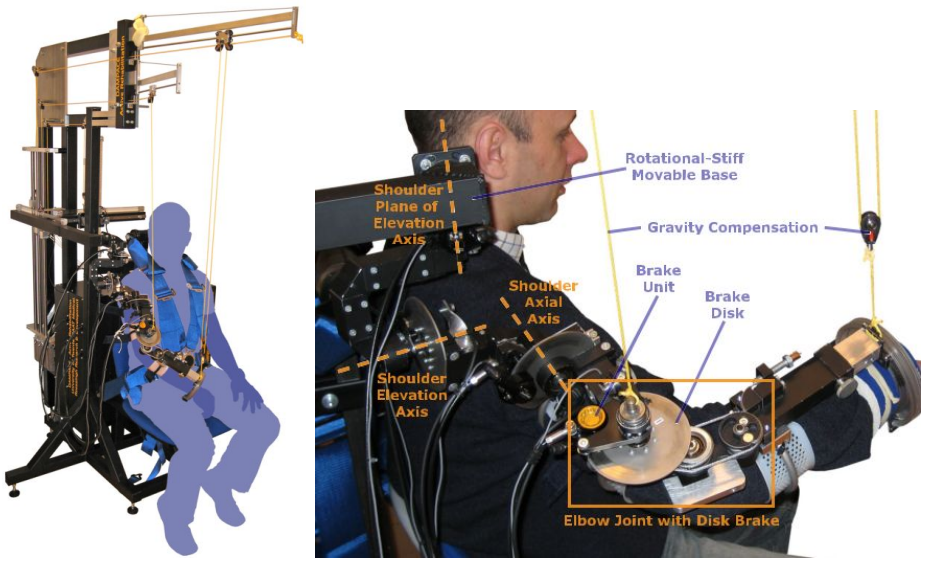

(a) (b)

Figure 2.23: The Dampace passive rehabilitation system (a) and the Dampace's orthosis (b).

(KIST). This semi-exoskeleton was developed for human-robot interactions, which include haptic interaction and teleoperated interaction. In contrast to the Dampace, this device does not use hydraulically controlled brakes, but electrical brakes connected with torque sensors to enable force haptic feedback. In the first mode of operation (haptic interaction), the exoskeleton Masterarm is worn by the user and operated as a haptic feedback device. The device is capable of creating virtual obstacles, such as surfaces, characterised by different stiffness values. In the teleoperated mode, the exoskeleton works as a motion controller for the upper body of the humanoid robot CENTAUR, also developed at KIST. The exoskeleton master arm built by KIST showed that using electric brakes for force feedback enables designers to build compact and light devices when compared to exoskeletons based on electric motors used for force feedback. The main drawback of electric brakes is that they are not capable of generating an active force, only a resistive (braking) force(Kim *et al.*, 2005).

Figure 2.24: The exoskeleton-type master arm developed at KIST worn by a user (Kim *et al.*, 2005).

T-Wrex

T-WREX is a passive semi-exoskeleton rehabilitation device aimed at individuals with chronic upper limb impairment (hemiparesis) to enable them to exercise the affected arm outside the hospital without constant supervision from a physiotherapist. The main part of the device is an orthosis with a grip sensor reading grip pressure, and computer software designed to virtually simulate functional activities. The orthosis has 4 degrees of freedom and the weight of the patient's arm is passively counterbalanced to counteract the effect of gravity (Dietz *et al.*, 2012) (Housman *et al.*, 2007). The device monitors hand movements while the user plays computer games and it enables patients to start using their impaired arms in a purposeful way as soon as they regain minimum movement ability. Patients with moderate to severe impairments using T-WREX can extend the range of motion (ROM) of hand movements (when compared to the hand's ROM without T-WREX), because of the arm support. As the T-WREX is a passive workstation, it is considerably safer than active robotic systems. The user himself has to start each movement, therefore he has to be active all the time. The device is also easily adjustable, the levels of gravity support can be quickly changed and it can fit different hand sizes. The first medical trial conducted at the University of California at Irvin showed that 8 weeks of therapy with T-WREX can considerably enhance arm movement performance in patients with moderate to severe hemiparesis(Housman *et al.*, 2009). Figure 2.25 a and b show a patient training with the

(a) (b)

Figure 2.25: A patient training with the T-Wrex. Source:

T-WREX workstation.

Other Exoskeleton Devices

An example of an active rehabilitation system based on a semi-exoskeleton frame is ARMin, presented in Figure 2.26 a. This robot is intended for clinical training of activities of daily living for patients with upper limb impairement. The ARMin's orthosis is fitted with force and position sensors and it is actuated with DC brushed motors. It has been optimized for patient-cooperative control strategies based on admittance and impedance control schemes. ARMin is capable of moving the shoulder joint in three degrees of freedom and the elbow joint in one degree of freedom. The robot's range of motion (ROM) matches the arm's ROM. Also ARMin is characterised by low friction and inertia, as well as a lack of backlash to ensure satisfactory performance of the patient–cooperative control schemes. Moreover, the robot is backdrivable, which means that the physiotherapist can manually move the orthosis to further assist the patient. ARMin was designed to support hand movements with an acceleration of 10 m/s2 and a velocity of 1 m/s. While a patient trains with the ARMin, a physiotherapist supervises the session and holds a dead-man's button, which stops the robot instantly when released. ARMin is fitted with passive anti-gravity support, therefore the robot is not going to suddenly fall down if the power is disconnected (Nef & Riener, 2005).

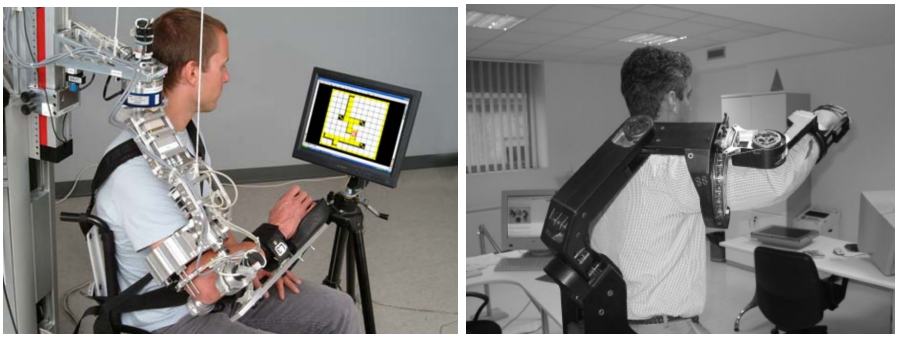

(a) (b)

Figure 2.26: A patient training with the ARMin semi-exoskeleton rehabilitation robot (Nef *et al.*, 2007) (a) and a patient training with the L-Exos (Montagner *et al.*, 2007) (b).

In one of three therapy modes supported by ARMin (game therapy) the robot assists the patient's arm movements only if the patient is not capable of performing tasks independently. In cases where the patient is able to move his arm without assistance, the robot does not provide any support apart from compensating for the orthosis weight (Nef *et al.*, 2006). A commercialised version of ARMin has seven actuated axes which make it the most advanced commercially available robot. It also offers antigravity support for the paretic arm. The position and interaction force between the patient and the robot is controlled by the combination of sensors and efficient gears. This enables patients with significant impairment to play games and exercise daily tasks in a virtual environment (Kwakkel & Meskers, 2014).

Another exoskeleton rehabilitation system which operates in a similar way to ARMin is L-Exos, presented in Figure 2.26 b. This robotic orthosis is also attached to a stand on the ground and a patient's arm is placed in the orthosis, which has five degrees of freedom. L-Exos supports a training mode in which the arm has to be actively moved to complete a task while the robot provides passive guidance if the patient has a problem with completing the task. L-Exos supports virtual reality-based training scenarios with haptic feedback, which enhances the patient's motivation and therefore improves therapy outcomes (Montagner *et al.*, 2007).

As mentioned before, the actuators used in the ARMin are DC brushed motors. Electrical motors are not the only type of actuators used in rehabilitation exoskeletons. For ex-

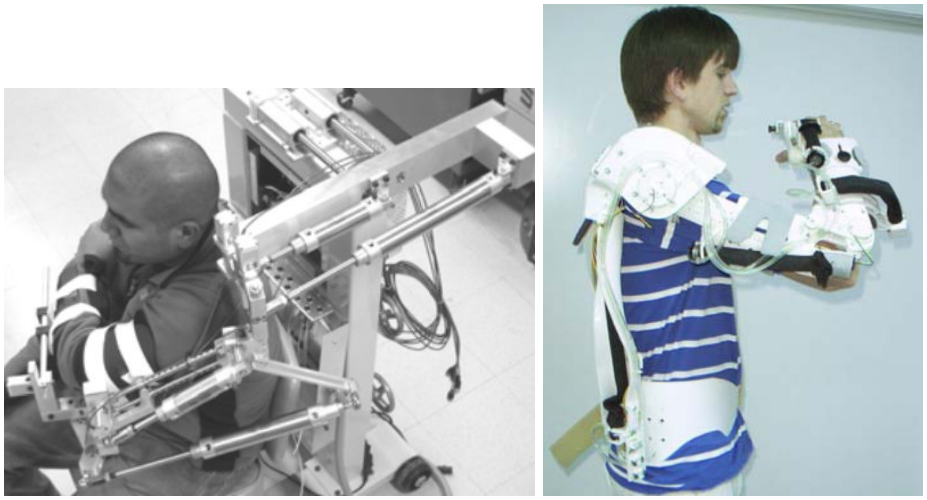

(a) (b)

Figure 2.27: A patient training with the Pneu-WREX semi-exoskeleton rehabilitation robot (Sanchez Jr *et al.*, 2005) (a) and a patient training with the RUPERT (He *et al.*, 2005) (b).

ample, Pneu-Wrex and RUPERT are fitted with pneumatic actuators. The Pneu-WREX, shown in Figure 2.27 a, is an actuated version (using cylinders and pistons) of the passive T-WREX described in the Exoskeleton Based Passive Systems For Upper Limb Rehabilitation. In this case, pneumatic actuators were chosen, as they are capable of generating large forces while being compact. In contrast to the Pneu-WREX, RUPERT, depicted in Figure 2.27 b, is actuated with pneumatic muscles mimicking human muscles' work. They generate a pulling force when pressurized. In order to enable joint flexion and extension, a spring was incorporated into the pneumatic muscle. RUPERT was developed for clinical and home–based training and as shown in Figure 2.27 b, tthe exoskeleton is only attached to the patient's body. The mechanical design of the device is compact and very portable when compared to the other exoskeleton systems (He *et al.*, 2005; Sanchez Jr *et al.*, 2005).

2.9 Advantages and Disadvantages of Robot-Assisted Upper-Limb Stroke Therapy

Rehabilitation robots enable patients to improve their upper-limb functional level through exercise independently of therapists. It was noted that robots can optimize the required upper limb movement pattern by applying custom constraints. As a result, the complexity of the motor task to be practised can be managed far more precisely in robot-assisted therapy than in conventional therapy methods. Many studies suggest that highly repetitive movement training results in improved upper-limb recovery and robot-assisted therapy allows patients to exercise intensively with their impaired upper limb (Kwakkel *et al.*, 2008). The number of movements performed by a patient in robot-assisted therapy is significantly greater than in other forms of therapy. It is assumed that high intensity repetitive movements have a great positive effect on the effectiveness of robotic rehabilitation (Kwakkel *et al.*, 2008). Robot-assisted therapy might be used to decrease the cost of after-stroke upper-limb rehabilitation or to provide more effective intervention at a similar cost (Kwakkel *et al.*, 2008). Additionally, robot-assisted therapy can be used to transform repetitive movement practice into interactive games by displaying visual cues on a computer monitor to increase the patients' motivation (Loureiro *et al.*, 2011).

There is evidence confirming that robot-assisted upper-limb therapy started 3 months after stroke provides more favourable outcomes than conventional therapy. However, evidence confirming more favourable outcomes of robot-assisted therapy during the first 3 months after stroke is lacking (Veerbeek *et al.*, 2017).

2.10 Clinical Outcomes of Robotic Rehabilitation after Stroke

A number of studies investigating the effects of robot-assisted therapies on upper limb impairment have been conducted. (Kwakkel *et al.*, 2008) prepared a systematic review of studies investigating the effects of robot-assisted therapy on upper-limb recovery after stroke. The review covered studies published up to October 2006 meeting the following selection criteria: "(1) patients were diagnosed with cerebral vascular accident; (2) effects of robot-assisted therapy for the upper limb were investigated; (3) the outcome was measured in terms of motor and/or functional recovery of the upper paretic limb; and (4) the study was a randomized clinical trial (RCT)" (Kwakkel *et al.*, 2008). In total, 10 randomized

trials involving 218 patients with stroke were analysed in the review. The rehabilitation robots used in the reviewed studies were: MIT-MANUS, Arm Guide, MIME, InMotion (commercial version of MIT-MANUS (Daly *et al.*, 2005) and Bi-Manu-Track. Performed sensitivity analysis of trials including only elbow-shoulder robotics showed a significant improvement in paretic upper-limb motor function. Five of the random controlled trials reported statistically significant motor recovery results in favour of robot-assisted therapy and four of the trials did not report statistically significant differences (Kwakkel *et al.*, 2008). The review by (Kwakkel *et al.*, 2008) confirmed the potential of robot-assisted therapies in improving proximal upper limb function.

Later review of the state-of-the-art rehabilitation technology was published by (Loureiro *et al.*, 2011). The review focused on upper limb rehabilitation devices promoting reach-to-touch, fine motor control, whole-arm movements and devices enabling rehabilitation beyond hospital stay. Several rehabilitation robots (Gentel/S, T-WREX, ARMin) that were not included in the review by (Kwakkel *et al.*, 2008) were discussed and their clinical trials outcomes reported. A randomised clinical trial of the Gentle/S system involving 31 chronic stroke patients reported an increase in arm function similar to MIME and MIT-MANUS trials. A trial was conducted to compare Gentle/S therapy effectiveness with a sling suspension. The outcomes analysis did not show significant difference between the Gentle/S and sling suspension therapies, which suggest that passive gravity-compensated therapies can have a positive impact on the recovery of chronic stroke patients (Loureiro *et al.*, 2011). A pilot study of the ARMin, advanced exoskeleton robotic device reported Fugel-Meyer assessment gains in chronic stroke patients. Moreover, a clinical trial of T-WREX comparing outcomes of T-WREX supplemented upper-limb rehabilitation therapy with conventional therapy showed significant difference favouring T-WREX (Loureiro *et al.*, 2011). (Loureiro *et al.*, 2011) stated that the most comprehensive multicentred randomized clinical trial investigating the effectiveness of robot-assisted therapy at the time of writing the review was the study published by (Lo *et al.*, 2010). The trial involved 127 patients with severe to moderate upper-limb impairment at least 6 months after stroke (chronic stage). A group of 49 patients was assigned to receive intensive robot-assisted therapy, 50 patients were assigned to receive intensive comparison therapy, and 28 patients received conventional therapy. Therapy included 36 one-hour long sessions over 12 weeks. The robot used in therapy was InMotion. The result showed that the robot-assisted group had modest functional improvements but did not improve significantly more than

the intensive or conventional therapy group. Moreover, the cost of the non-robot and robot therapies was similar. Although the results of the trial by (Lo *et al.*, 2010) did not show the significant advantage of the robot-assisted therapy over non-robotic therapies, (Loureiro *et al.*, 2011) suggests that robotics research should be continued. Using robots as assessment tools of motor recovery during therapy is important and it is not present in non-robotic therapies (Loureiro *et al.*, 2011).

A recent systematic review of the effects of robot-assisted therapy for upper-limb rehabilitation after stroke was conducted by (Veerbeek *et al.*, 2017). This review is a continuation of work presented in the 2008 review by (Kwakkel *et al.*, 2008). Nine years later (Veerbeek *et al.*, 2017) found that the field of robot-assisted upper-limb rehabilitation was flourishing and a total of 341 unique randomised control trials were screened in the review. The main aim of the review was to determine the effects of robot-assisted therapy of the paretic upper limb after stroke on activities of daily living, upper-limb capacity, and outcomes of motor control on the paretic upper limb. Secondary outcomes considered were muscle tone and muscle strength. The studies which were included in the systematic review met the following conditions: (a) patients had been diagnosed with stroke, (b) effects of robot-assisted therapy for upper-limb (RT-UL) were investigated, (c) outcomes were assessed in terms of motor recovery and/or upper limb capacity and/or basic activities of daily living (ADL) and/or muscle strength and tone postintervention, (d) the study used a randomised controlled trial (RCT) design. Additionally, all the studies which did not compare the outcomes of robot-assisted therapy with conventional therapy were excluded. A total of 38 (involving 1206 patients) out of 341 screened trials were selected for quantitative analysis. The most commonly used robots in the trials were MIME, BiManuTrack, MIT MANUS and InMotion Shoulder Elbow robot. The review confirmed that robot-assisted therapy for upper-limb rehabilitation after stroke for the wrist-hand and the shoulder-elbow robots improves motor control of the arm. However, it was reported that the overall effects are small, smaller than the minimum clinical importance difference on the Fugl-Meyer assessment for arm scores (Veerbeek *et al.*, 2017). The findings in the (Veerbeek *et al.*, 2017) review are similar to the findings presented in (Kwakkel *et al.*, 2008) review. The review concluded that translational research in the field of robotic rehabilitation is still in the infancy stage and more interdisciplinary research findings are expected to be published in the future.

Table-top portable rehabilitation robots were also proved to be more effective than conventional arm training. The ArmAssist (a low-cost active robotic system for upper limb motor training designed to be less dependent on therapist assistance) was utilized in a randomized clinical trial comparing the efficacy of the ArmAssist-delivered training with conventional rehabilitation training. 26 patients with moderate to severe upper-limb impairment within 3 months after stroke were recruited and randomly allocated into two groups: the ArmAssit training group and the conventional training group. Each group trained for three weeks, five days a week. The outcome of the study was that the ArmAssist group showed a significantly higher Fugl-Meyer Assessment Upper Extremity increase than the conventional training group (Tomić *et al.*, 2017).

2.11 Colaborative Robot Architecture (COBOT)

The COBOT architecture introduced in this section may be used to design an inherently safe braking and guiding mechanism for a rehabilitation device. COBOTs are inherently safe devices and safety is a key feature of their design (Gillespie *et al.*, 2001).

"COBOT" is a general term describing mechanically passive robots designed to be operated directly by human operators. COBOTs are capable of simulating haptic effects such as sturdy virtual surfaces, but all the motive power is provided by the operator. COBOTs do not generate any forces assisting the operator, they just provide virtual guiding and the operator feels as though walls constraining their movement are present. Their kinematic design is significantly different than other robots' kinematic design. The crucial difference is the number of degrees of freedom (DOF), COBOTs only have one mechanical DOF, but their task space can have any number of dimensions (Peshkin *et al.*, 2001; Wannasuphoprasit *et al.*, 1997)

The main purpose of COBOT is to recreate a programmed virtual environment in the physical world. The virtual environment (VE) can restrict the regions which can be penetrated with the payload and regions in which the payload cannot be moved. The functionality of the VE can be likened to a ruler. Drawing a straight line with a ruler can be performed quicker and better than completing the same task without the ruler. The ruler constraints the movements to a straight line, but the human can still control speed and power of motion. In the case of a cobot's VE, task control is divided between the operator and the computer, however the constraints do not have to be physically present.

The number of possible haptic effects which can be generated in the VE is unlimited. A good example explaining the functionality of the VE is a virtual surface (VS). The VS can be contained in any task space e.g. a 2D task space can contain a one-dimensional constraint. If a task space has three dimensions, a 2D VS can be contained in it. The virtual surface can itself contain lower-dimension constraints (Peshkin *et al.*, 2001).

The virtual surface (VS) can be implemented into the physical world in several ways. One way is to use powered actuators to generate forces to prevent the penetration of the virtual surface. However, the use of e.g. electric motors can cause safety hazards. The VS can be created in a safer way by employing brakes instead of actuators. The brakes cannot generate movements, therefore the robot can be inherently safe. It is also possible to use actuators together with brakes to achieve the desired VC effect. However, COBOTs are inherently safe devices and they do not use actuators to generate active force (Peshkin & Colgate, 1999; Peshkin *et al.*, 2001; Wannasuphoprasit, 1999)

The simplest example of a COBOT is a rolling wheel on a planar surface. This cobot, shown in Figure 2.28 a, is called the unicycle and is designed to implement 2D virtual constraints in the 2D task space. Even though the task space is 2D, the unicycle has one degree of freedom. Figure 2.28 b shows how a virtual wall constraint is created along the direction of rotation of the wheel. As the user applies a force on the unicycle cobot, the constraint is implemented with a friction force generated between the wheel and the surface acting in the opposite direction to the force applied by the user (Chua, 2006; Peshkin *et al.*, 2001).

The task space dimensionality can be extended by adding a second wheel, which would allow for control of rotational motion, as presented in Figure 2.29 a. However, if two wheels are positioned so that their centres of rotation are coaxial, also shown in Figure 2.29 a, the system has two degrees of freedom. In order to avoid the case where the two wheels are in singular configuration, a third wheel can be added, as shown in Figure 2.29 b. The advantage of the three wheel cobot (called "scooter") is that it is capable of standing on its own without additional support. In a free mode where the scooter's three wheels are free to rotate, the cobot behaves similarly to a shopping trolley on casters. For all of the three wheel based cobots, movement direction is constrained by the wheels' orientation and the friction generated between the wheels and the surface. The wheels tend to allow movements only in their rolling direction (Chua, 2006; Peshkin *et al.*, 2001).

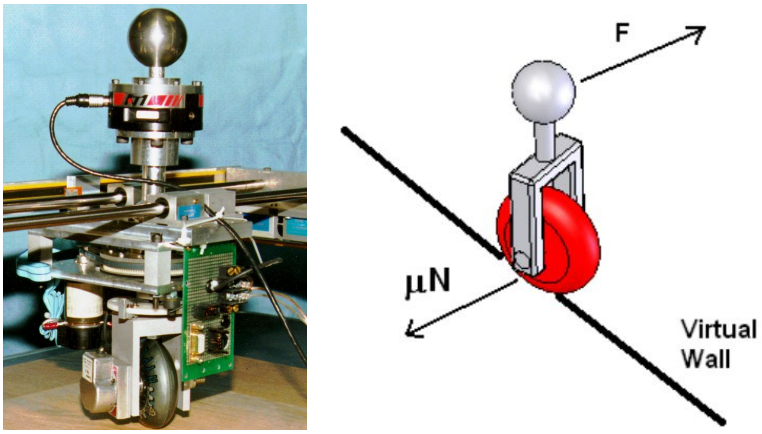

(a) (b)

Figure 2.28: The unicycle cobot (a) and virtual wall constraint created with the unicycle cobot (b). Source: (Chua, 2006)

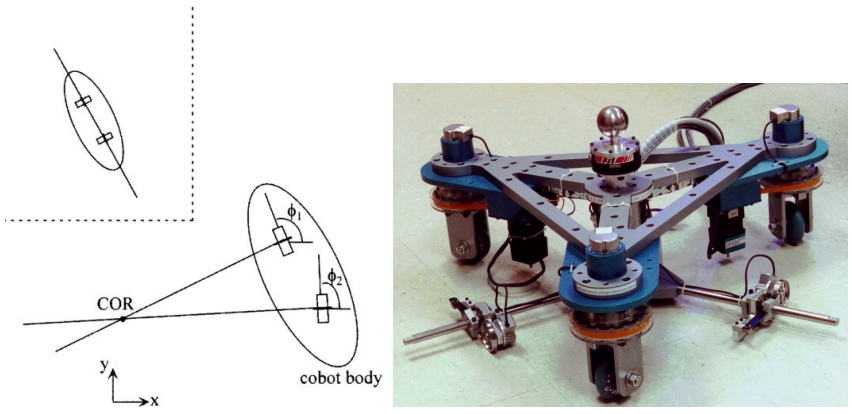

(a) (b)

Figure 2.29: The two wheel cobot experience singularity if the wheels are coaxial (a) and the Scooter three wheel cobot prortotype (b). Source: (Peshkin *et al.*, 2001)

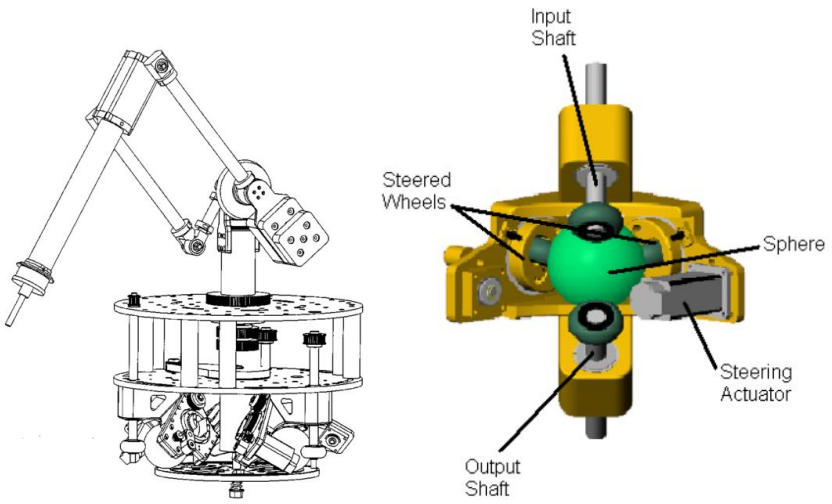

(a) (b)

Figure 2.30: The arm cobot (a) and the continous variable transmission (CVT) (b). Source: (Chua, 2006; Peshkin *et al.*, 2001)

The previously mentioned COBOT are wheel-based and their task space is two dimensional. However, a COBOT arm, presented in Figure 2.30a, is capable of creating three-dimensional virtual surfaces in the Cartesian x, y and z coordinate system. This COBOT has been designed for industrial research and e.g. constraints generated by the arm's end effec- tor can simulate pressing a door handle. The arm cobot enables the user to feel the path and height of the door handle without the need for making a physical prototype. The revolute joints of the arm cobot are coupled with spherical continuous variable transmissions (CVTs). The CVTs, illustrated in Figure 2.30 b, enable the COBOT to create 3D virtual surfaces. The input shafts of the CVTs are connected to revolute joints and the output shafts are connected to other output shafts, mechanically connecting the CVTs. The main purpose of the CVT is to create a ratio between the input and output shaft speeds us- ing a transmission sphere actuated with steering wheels controlling the rotational axis of the sphere. The actuated steering wheels can be related to the unicycle COBOT's steering wheel. The steering actuator coupled with the CVT cannot generate any motion of the arm COBOT's end point. The way the actuator in the CVT works is analogous to a driver turning a steering wheel in a parked car. In both cases the motive force generated by the driver does not move the end point or the car (Chua, 2006).

2.12 Workspace Dimensions

Dimensions and proportions of human bodies vary, therefore it is impossible to provide the exact dimensions of an ideal desk workspace area. However, arm range of motion for a person sitting in front of a desk can be analysed for a large population and dimensions of a workspace fitting most of the population (between the 5th and 95th percentile) can be defined.

While designing a rehabilitation device intended for use by a patient sitting in front of a desk it is important to take into consideration the workspace dimensions which the device is going to offer. For example, the minimum workspace requirement of the Braccio di Ferro system described in this chapter was an ellipse with a major diameter of 800 mm and minor diameter of 400 mm for single arm training (Casadio *et al.*, 2006).

According to the Canadian Center for Occupational Health and Safety (CCOHS) the max- imum desk workspace dimensions fit into a 500 mm by 1600 mm rectangle and the usual workspace fits into a 250 mm by 1000 mm rectangle, as depicted in Figure 2.31 a. Alternative workspace dimensions have been proposed by the Engineering and Production Plans (EPP) Industrial group from Ontario, as shown in Figure 2.31 b. The workspace dimensions presented by CCOHS vary from the dimensions presented by (EPP). Maximum lengths of workspaces are similar for both (around 50 cm), but there is a 10 cm difference between maximum widths. It is also noticeable that there is a difference in the sizes of usual (normal) work areas. The normal work area proposed by LPP is larger than the equivalent proposed by (CCOHS) (CCOHS, 2008; EPP, 2006).

Rehabilitation devices with larger workspace areas can be utlised better during training, especially if the patient using it is large. Larger workspace size should not make a noticeable difference to a small person. It is important to mention that workspace dimensions in Figure 2.31 are for two arms and that dimensions for one arm workspaces can be inferred from them.

2.13 Directive Concerning Medical Devices

Medical devices introduced on the EU market have to be CE certified. Therefore, during the development phase the COUNCIL DIRECTIVE 93/42/EEC of 14 June 1993 concerning medical devices was considered. This directive applies to medical devices and their

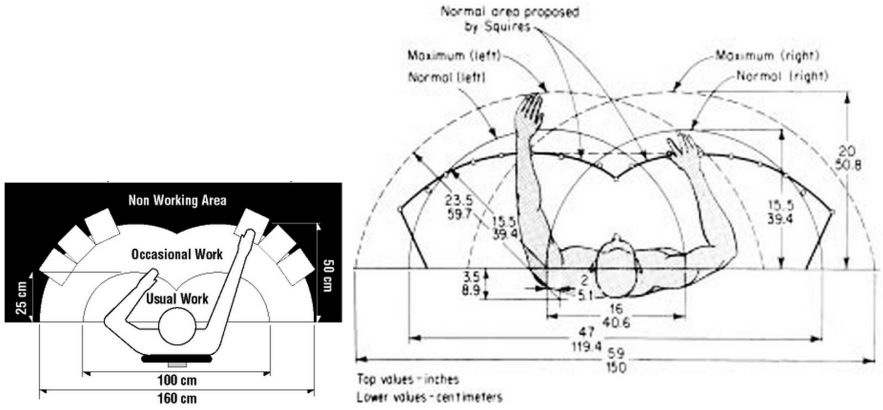

(a) (b)

Figure 2.31: Desk workspace dimensions according to CCOSH (CCOHS, 2008) (a) and desk workspace dimensions according to LPP(EPP, 2006) (b).

accessories. The accessories should also be treated as medical devices. A medical device is defined in the directive as any apparatus, instrument, appliance, material or software utilized alone or in combination for diagnosis, monitoring, treatment, alleviation of or compensation for an injury or handicap, and which does not achieve its main intended action in or on the human body by metabolic, immunological or pharmacological means (Directive, 1993).

The directive requires every medical device to comply with the general requirements defined in it. The most important are requirements regarding patient safety such as: the design of a device should be optimised for patient safety, and if possible, the design of the device shall be inherently safe. It is absolutely crucial that mechanical, electrical and thermal risks are avoided as much as possible (Directive, 1993).

The device developed in this project incorporates a power supply (or will support an on-board power source), therefore it has to comply with (Directive, 1993) regulations for medical devices connected to or with a power source. The most important regulations concerning the developed device are: designing the device to guarantee intended performance, as well as reliability and repeatability, and if a device incorporates software, the software shall be validated utilizing state of the art methods, taking into consideration life cycle, risk management, validation and verification (Directive, 1993).

According to the medical classification criteria covered in the (Directive, 1993), any

medical device whose operation depends on any source of power and conversion of this power, excluding power directly generated by the human or by gravity, is considered to be an active medical device. Also, any active medical device utilized to restore, modify or support biological structures or functions with the purpose of treating or alleviating an injury, illness or handicap is considered an active therapeutic device. Furthermore, any active medical device utilized for collecting information for monitoring, diagnosing, treating or detecting states of health or illness is considered to be an active device for diagnosis (Directive, 1993).

Medical devices can be grouped in three classes; I, IIa, IIb and III. Software which impacts the use of a device automatically falls in the same class as the device. Any active therapeutic device designed to exchange or administer energy to or from the human body is classified as Class IIa (Directive, 1993). The device developed in this project would probably have to be classified as a Class IIa medical device before commercialization.

2.14 Rationale for the Robot Developed in the Thesis

A number of robots have been developed for robot-assisted therapy to date. However, (Veerbeek *et al.*, 2017) suggested, after reviewing 38 robot-assisted therapy trials, that the translational research in rehabilitation robotics after stroke is still in the early stage. There is no evidence in dose-matched trials, in which control and experimental groups of stroke patients spend equal time exercising, that robot-assisted therapy is a meaningful factor in the outcome. This suggests that robot-assisted therapy with costly robots that control many degrees of freedom is not guaranteed to be more effective than robot-assisted therapy with cheaper devices controlling fewer degrees of freedom. This unexpected finding might be a result of a fact that change in degrees of freedom is mainly happening during the first 3 months after stroke. (Not sure what you mean here)

(Veerbeek *et al.*, 2017) reported that robot-assisted therapy trials were neglecting the combination of robot-assisted and conventional rehabilitation therapy. (Veerbeek *et al.*, 2017) suggested that robot-assisted therapy should not be utilized as standalone therapy but should be part of a comprehensive therapy package to increase paretic arm motor function. This view is shared by (Loureiro *et al.*, 2011) who suggested that robots can be used as new tools for physiotherapists to automate labour-intensive exercises and increase

patient access to therapy. This suggest that physiotherapists would be making all the decisions and when appropriate, would decide to use a robot.

(Loureiro *et al.*, 2011) reported no significant outcome differences between intervention delivered with passive gravity-based sling suspension devices and treatment delivered with the Gentle/S robot. This suggest that passive gravity-compensated therapies positively influence the recovery of chronic stroke patients. Active assisted movement is beneficial when patients are not able to move their upper limb independently. However, for improving patients who are able to move their affected arm independently, exercising without active assistance could be better (Kwakkel & Meskers, 2014).

The rehabilitation robotics concept was identified as the right approach for expanding rehabilitation therapy to a home environment. However, to enable the use of robotic systems in a home environment the robots must be affordable, which might mean developing inexpensive robots which support less degrees of freedom but use simple interactive games enhancing motivation to practise (Loureiro *et al.*, 2011). Surprisingly, sensitivity analysis comparing 38 trials performed by (Veerbeek *et al.*, 2017) presented a trend favouring the use of end-effector robots instead of exoskeletons.

The literature review conducted in this thesis suggest that there is a group of patients neglected by most of the state-of-the-art rehabilitations robots. This group are post-stroke patients with mild upper-limb hemiparesis who despite suffering decreased movement coordination and clumsiness might have normal Fugl-Meyer scores and neurological examinations. Their deficits might be diagnosed only with more sensitive kinematic testing (Krakauer, 2006). These patients are likely to return to work after stroke and their deficits, despite being mild, can have a destructive effect on their performance at work. This is especially problematic for post-stroke patients working as, for example, car mechanics, electricians and hairdressers (Krakauer, 2006).

The literature review suggests that there is a need for a portable, low-cost, safe to use at home, end-effector rehabilitation device developed for patients suffering mild stroke deficiencies, such as mild upper-limb hemiparesis. The device should target upper-limb functional reach movements training during the chronic phase of stroke in order to improve the speed, precision and range of movement. Moreover, such a device could be used by patients which improved during the initial phase of rehabilitation enough to move their impaired upper limb independently but have not fully recovered their arm function. It is very important that the new rehabilitation robot is safe to use without professional

supervision to enable patients to train independently at home or at a rehabilitation centre. Actively actuated rehabilitation robots are not suitable for unsupervised training, therefore the new robot should not generate active forces on the upper limb.

2.15 Summary of the Literature Review - Gap in the Knowledge

The Problem of Stroke in the Future

Stroke is a significant problem in the UK as well as worldwide. According to recent data, the number of stroke cases is going to increase as the population ages. Moreover, it was reported that 80% of all stroke patients develop chronic upper limb impairment. In order to maximise outcome, rehabilitation therapy should be started as soon as possible, as the recovery rate is the highest during the first 12 weeks after stroke. After 12 weeks, the recovery progress slows down, but it can last for months or even years, therefore it is important to continue rehabilitation training.

Challenges in Rehabilitation Healthcare Provision

Several studies have confirmed that intensive and frequent rehabilitation training can significantly improve therapy outcomes. Moreover, it has been noticed that interactive therapy (e.g. involving computer games) enhances patient motivation to practice and also results in better therapy results. Currently provided post–stroke rehabilitation therapies are constrained by the availability and cost of physiotherapists. The rehab training quality can also be affected by physiotherapists' physical strength and fatigue over time. In order to overcome the limitations of the current rehabilitation approach, several robotic rehabilitation devices were built and in many cases tested with patients. Robots have advantages over physiotherapists. Most importantly, they can provide high quality repetitive training, in which each repetition is exactly the same and do not fatigue. The rehabilitation robotics could be an effective addition used together with conventional rehabilitation therapy to maximise therapy outcomes.

Current Robotic Rehabilitation Devices

The current rehabilitation devices can be classified in two main categories; end-effector and exoskeleton systems. Exoskeleton-based devices are considered to be more advanced, complex and expensive, but they can control arm movements better, because they are connected to the arm at several points (e.g. ARMin, L-Exos, Pneu-WREX). End-effectors, on the other hand, focus on movements of the end of the arm (fist) and they support the arm at one point only (e.g. Braccio di Ferro, ARM-Guide, ReJoce) or in some cases at two points: forearm and upper arm (e.g. iPAM, REHAROB, Freebal). The recent state-of-the-art development in robotic rehabilitation are table-top portable end-effector devices designed for home-based independent therapy. This category is represented by devices such as: ArmAssist, Arm Skate, Arm Skate II and Reha-Maus, which share many similarities in their designs .

Limitations of the Current Robotic Rehabilitation Devices

Frequent and intensive training over a long period of time can be exhausting for a patient as it often requires them to travel to a hospital rehabilitation clinic. Also, most of the developed rehabilitation systems are not suitable for home–based unsupervised use. Actuated systems cannot generally be used unsupervised. In a situation in which the patient experiences pain, someone has to interrupt the exercise. Another factor preventing many systems from home use is the cost of equipment. For example passive exoskeleton based systems such as Dampace and T-Wrex are safe, but their cost and portability limit the possibility of home-based training. These devices are more suitable for unsupervised (at least a physiotherapist does not have to be present all the time) hospital–based training. Devices such as Able-X, ReJoyce and Reha-Slide are suitable for unsupervised training, but they do not have any inherently safe guidance mechanisms which could constrain the patients' arm movements. ArmAssist, Arm Skate II and Reha-Maus robots utilise existing table space and are actuated with electric motors which might make them difficult to use in passive mode (patient active mode) as the patient using the device has to overcome electric motors' internal resistance. These robots provide active arm movement support, which prioritises patients with severe arm impairment, and it seems that there is room for a new arm rehabilitation device developed for helping patients 12 weeks after stroke

and later by providing movement guidance and very low resistance in the patient's active exercise mode.

Home–Based Rehabilitation

Stroke survivors, after finishing formal clinical based rehabilitation, generally stop training and do not achieve full recovery goals. To address this problem, some of the robotic rehabilitation systems are designed for home training. In order to use a rehabilitation device at home it has to be safe. However, it is also desirable that the device can provide some guidance. Generally, it is agreed that brakes are safer than actuators, and robotic devices offering active arm movement assistance are not suitable for home-based rehabilitation. This implies that a device for home–based use can provide only inherently safe guidance, which means that the guiding mechanism can resist movements performed in a wrong direction, but it cannot actively assist the movement by applying force. Brakes, such as magnetic particle or friction brakes, can be the solution to this problem, but they have some limitations. The main drawback of using brakes is an issue with simulating smooth constraints, especially if several brakes are used and they have to be synchronised. This limitation can be overcome by designing a passive guiding mechanism based on a COBOT (Collaborative Robot) mechanism, which will allow for implementing smooth virtual constraints and is inherently safe by design. Moreover, the unicycle COBOT mechanism can be coupled with a brake. A COBOT unicycle-based rehabilitation robot has not been developed to date.

User Interface and Rehabilitation Games

Using a rehabilitation device instead of a computer mouse for using a computer is not a common option for rehabilitation robots. A computer mouse can be used together with the Reha-Slide device, but the mouse has to be attached separately and there is a problem with accessing mouse buttons. None of the previously mentioned devices are intended to be used as a replacement for a computer mouse. In the majority of cases, if a given device was intended to be used as an input device for rehabilitation games and if it has an interactive user interface and games, these were custom-developed for that particular device. It has been proven that utilizing rehabilitation games is beneficial for patient concentration, which results in better therapy outcomes.

Need for a New Type of Rehabilitation Robot

The conducted literature review has shown that there is a research/market gap for a new type of a rehabilitation table-top device providing low movement resistance and guidance for training after stroke for patients suffering mild upper-limb hemiparesis. In order to be unique, the new device can be based on one of the inherently safe COBOT mechanism variations and it can bring together features such as low cost, portability and interactive user interface with games design for training 2D reaching tasks and point-to-point movement. The system must be safe and suitable for home-based unsupervised training. The main arm functional outcomes targeted by the system should be the speed, precision and range of arm movements.

Chapter 3

Design of an Inherently Safe Rehabilitation Robot

In this chapter the developed design of an inherently safe upper-limb rehabilitation device is presented. First, a list of product requirements is derived. Secondly, four conceptual designs are presented. Next, one of the conceptual designs is selected to be developed into a final design. Lastly, the final design is presented and a prototype is manufactured.

3.1 Main Product Requirements

The literature review highlighted several state-of-the-art robotic rehabilitation devices and the limitations of current rehabilitation therapy delivered to stroke survivors. It has been found that a rehabilitation device utilizing the COBOT (covered in the literature review) guidance mechanism has not been developed to date. The list of product requirements for the inherently safe rehabilitation system presented in this project was developed based on the literature review performed in Chapter 2, putting extra focus on the defined gap in the knowledge. The key words used to indicate requirements levels are defined below and were adapted from (Bradner, 1997):

1. SHALL This word indicates that the definition is an absolute requirement of the specification.

2. SHALL NOT This phrase indicates that the definition is an absolute prohibition of the specification.

3. RECOMMENDED This word indicates that there might exist valid reasons in specific circumstances to ignore a specific requirement.

4. NOT RECOMMENDED This phrase indicates that there might exist valid reasons in specific circumstances when the specific requirement is acceptable or even useful.

5. MAY This word indicates that a requirement is truly optional.

For clarity, the list of product requirements was grouped into three categories; safety, usability and functionality.

Safety requirements were mainly derived from the European Council directive concerning medical devices as well as standard safety concerns. Additionally, to ensure the safety of the shoulder joint, an additional requirement concerning the arm support was included. Post- stroke patients have a tendency for shoulder injuries as a result of muscle atrophy after a stroke. To prevent the shoulder from injuries caused by the gravitational pull acting on it, a therapeutic robotic device developed for upper limb stroke rehabilitation should provide adequate hand and forearm support to reduce the gravitational pull on the shoulder (Perry *et al.*, 2012).

1. Safety Requirements:

   (a) The device SHALL comply with the legal regulations concerning Class IIa medical devices defined in (Directive, 1993).

   (b) The device SHALL be inherently safe, all active forces SHALL be generated only by the patient.

   (c) The device SHALL provide adequate resistance to overturning torques during normal operation.

   (d) The device SHALL provide optional vertical forearm support to minimise the effect of gravitational pull on the shoulder and therefore prevent shoulder injuries.

   (e) The device SHALL incorporate a solution preventing it from falling of a table edge during training while attached to a patient's arm.

   (f) The device construction SHALL be inherently safe.

(g) The device SHALL NOT have any sharp or pointy edges that can come into contact with a patient using the device.

(h) The device is RECOMMENDED to be designed so that all of the on-board systems operate at a voltage lower than 24 V.

(i) The state of an on-board battery is RECOMMENDED to be monitored.

The usability requirements for the developed rehabilitation device are derived for a scenario where the device is primarily used by a patient at home or in a rehabilitation centre without constant professional supervision.

2. Usability requirements:

   (a) The device SHALL fit existing table space so that it can be easily set up in the home environment.

   (b) The device SHALL be light and compact. The size of the base of the device is RECOMMENDED to fit a square of size 30 by 30 centimetres. The weight of the movable module is RECOMMENDED to be less than 2.5 kg.

   (c) The device setup and takedown time SHALL be less than 2 minutes.

3. Functionality requirements:

   (a) The device SHALL support an inherently safe guidance system which can constrain the motion of a patient's upper limb on a planar surface.

   (b) The device MAY provide variable resistance (braking).

   (c) The device SHALL support a large planar workspace, at least 50 by 30 centimetres.

   (d) The device SHALL support low rolling resistance, less than 2.5 N static and less than 2 N rolling.

   (e) The device position and orientation SHALL be measured at least up to +/- 10 mm and +/- 10 degrees.

   (f) The device SHALL monitor patients' therapy progress.

   (g) The device is RECOMMENDED to have an on-board rechargeable battery enabling 10 hours of continuous use.

(h) The device SHALL support a virtual user interface with interactive games.

(i) The device is RECOMMENDED to support wireless connectivity to avoid wires that could potentially interrupt training.

(j) The device SHALL be designed to ensure the repeatability and reliability of arm rehabilitation training.

(k) The device SHALL be designed to account for different arm sizes.

4. Clinical requirements:

(a) The device SHALL be suitable for functional reach movement training of patients after stroke who are suffering from mild upper-limb hemiparesis.

(b) The device SHALL be suitable for functional upper-limb reach movement training of patients after stroke who are able to move their upper limbs independently.

(c) The device SHALL focus on rehabilitation training targeting upper-limb deficiencies after stroke such as: reduced range of movement, reduced movement speed and reduced movement precision.

Among the above four groups of requirements, the requirements concerning safety are the most important. Ideally, all of the requirements would be fulfilled by the initial design of the rehabilitation robot, however it is more realistic that some of the requirements will not be met in the first iteration of the design and that only later design iterations will meet all of the requirements.

3.2 Initial Designs

Four initial conceptual designs based on the developed product requirements are presented in this section. All of them aim to utilize existing table space in a home environment. Also, all the designs incorporate a 2D planar movement joystick which is very straight forward to use as a computer input device for interactive gaming. Additionally, if the joystick is combined with an inherently safe guidance mechanism, it can be an effective end-effector, inherently safe, rehabilitation device.

The *initial design 1* is presented in Figure 3.1. The main part of the design is a 2 DoF (degrees of freedom) joystick moving on a planar surface in X and Y directions on two

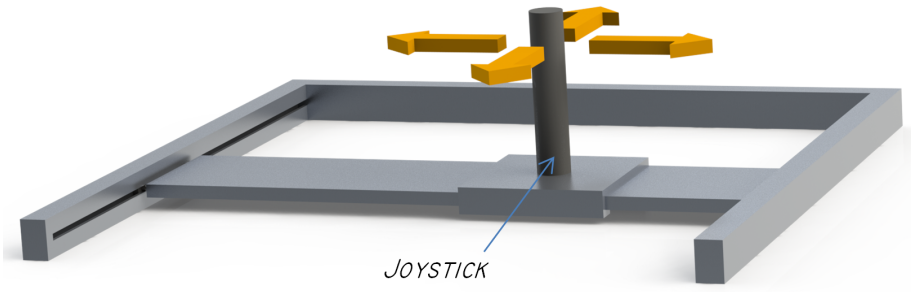

Figure 3.1: *Initial design 1*, a 2 DoF (degrees of freedom) joystick moving in X and Y direction on two rails.

rails. The position of the joystick can be determined very accurately by employing two optical encoders in X and Y directions. An inherently safe guidance mechanism can be implemented in this design by using two magnetic particle brakes creating resistance in X and Y directions. The limitation of such a mechanism can be a difficulty of simulating smooth 2D constraints. Another drawback of this design is the large size of the device, which must be larger than the desired workspace. This design can be used on a table top, but the table top has to be larger than the device to guarantee stable support.

The *initial design 2*, illustrated in Figure 3.2, is also based on the joystick concept and it is also intended to be used with a magnetic particle based guidance mechanism. The guidance mechanism in this case uses four magnetic particle brakes positioned in the corners of the workspace. The brakes are connected to the joystick with four retractable cables. Two optical encoders measuring the retraction of the cables can be employed to measure position and control brakes and guide the patient's hand based on this information. This braking mechanism might not be appropriate for simulating smooth 2D constraints. As in the case of the initial design 1, the size of this device might be problematic as it must be larger than the desired workspace. The portability of this design might also be an issue.

The *initial design 3*, depicted in Figure 3.3, is also based on a joystick and can utilize existing table space in a home environment, but a different solution for position tracking is used.The workspace is covered with a reed switch grid in which corresponding switches close in the presence of a magnetic field from a magnet attached underneath the joystick. The main drawback of the reed switch positioning system is the low resolution of the grid,

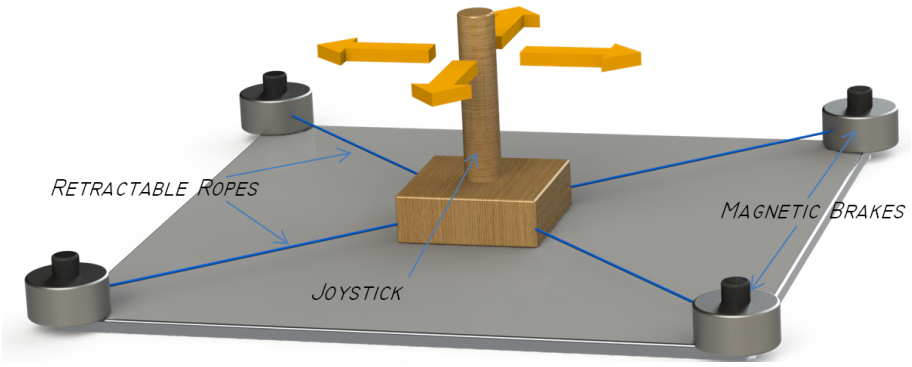

Figure 3.2: *Initial design 2*, a 2 DoF (degrees of freedom) joystick connected to magnetic particle brakes with ropes.

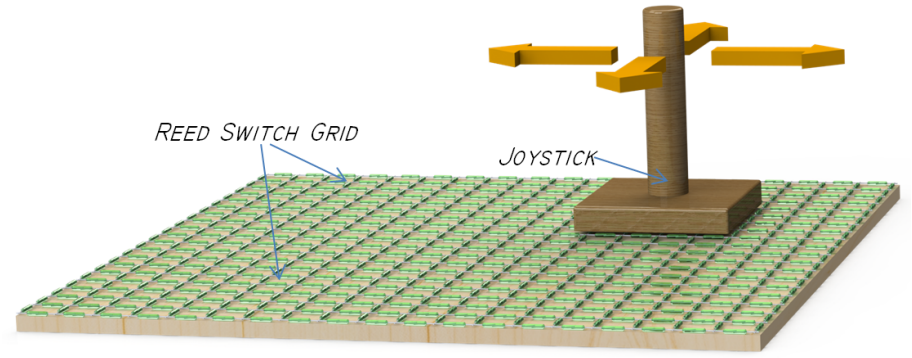

Figure 3.3: *Initial Design 3*, a 3 DoF joystick with a magnet attached beneath and moved on a reed switch greed used for position tracking.

which is limited by the size of the reed switches. This design can be very large, as the size of the device has to be bigger than the size of the desired workspace. Also, the complexity of manufacturing a large mat implementing hundreds of reed switches can adversely affect the cost of the device. This device can accommodate a novel COBOT-based guidance module, which is an advantage.

The *initial design 4*, presented in Figure 3.4,is also based on a joystick which is intended to be moved by a patient on an existing table workspace. This design can accomodate a novel COBOT inherently safe guidance module underneath the joystick. A standard webcam is utilized for tracking the position of the joystick. In order to determine X and Y

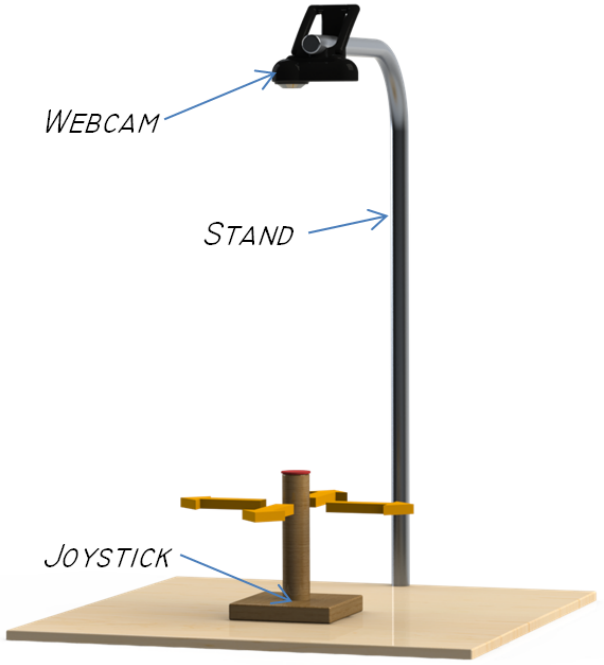

Figure 3.4: *Initial design 4*, a 3 DoF joystick with a webcam tracking system.

coordinates, the webcam is positioned above the work surface and a red marker is attached to the top of the joystick for tracking. This design can accommodate large workspaces and at the same time have compact dimensions.

3.3 Conceptual Design

The *conceptual design* is based on one of the initial designs, which was evaluated to have the best potential to meet the product requirements list. The best initial design was chosen using a multiple criteria decision making approach based on a decision matrix presented in Table 3.1, where A_1, A_2,...,A_m are alternatives from which we choose, C_1, C_2,...,C_n are criteria used to measure performance of alternatives, x_{mn} is the rating of alternative A_m for critertion C_n, w_1, w_2,...,w_n are weights for criteria C_1, C_2,...,C_n(Jahanshahloo *et al.*, 2006).

The most suitable initial design was chosen using the decision matrix presented in Table 3.2. The four designs were rated against four key criteria based on the product requirements list including: safety, usability, functionality and complexity. As the designs were

Table 3.1: Multiple criteria decision making problem expressed in matrix format. Source: (Jahanshahloo *et al.*, 2006)

	C_1	C_2	...	C_n
A_1	x_{11}	x_{12}	...	x_{1n}
A_2	x_{21}	x_{22}	...	x_{2n}
A_m	x_{m1}	x_{m2}	...	x_{mn}

$$W = [w_1, w_2, \ldots, w_n]$$

not manufactured and experimentally evaluated, the assigned marks take in the consideration the predicted performance of the initial designs. The highest weight was assigned to the safety criterion and the least significant was complexity. For each criterion a mark in a scale from 1 (worst) to 10 (best) was given. The final (total) score for each design was calculated by multiplying individual criteria scores with weights and summing them together. For each category each design started with 10 points and for each design flaw one point was subtracted.

The safety criterion is crucial and any major safety concern would disqualify the design without considering the other three criteria. No major safety concerns were found and removing the indicated safety concerns would be possible with designs modifications. The initial design 1 lost 2 points because of the risk of trapping one's fingers between the frame elements and the risk of pinching the skin by the frame elements. The initial design 2 lost 1 point for the risk of the user's arm getting tangled in the ropes. Finally, the designs 3 and 4 lost 1 point because of the risk of the robot being moved off the edge of a table and falling off.

The usability criterion is very important as the device must be comfortable and easy to use. The initial design 1 lost 1 point for portability, as it is predicted to be larger than the work surface, and 1 point for its weight which is predicted to be significantly heavier than 2.5 kg. The initial design 2 also lost 1 point for portability and 1 point for weight for the same reasons. The initial design 3 lost also 2 points, for the same reasons as the initial designs 1 and 2. The initial 4 design is predicted to weigh less than 2.5 kg and be the most portable rehabilitation system among the four initial designs.

The functionality criterion is also very important as the device must provide functionality which is important for patient active (robot passive) upper limb rehabilitation

training. The initial designs 1 and 2 lost 1 point each as they would utilise magnetic particle brakes for guidance, and a COBOT guidance mechanism, which has not been utilised in a rehabilitation device to date is desired. Additionally, initial designs 1 and 2 lost 1 point each for the possibility of exceeding the maximum desirable movement resistance, due to the need for overcoming the magnetic particle brakes' internal resistance to move the robot. Initial designs 3 and 4 did not lose points for the functionality criterion.

The complexity criterion is very important as complex designs require more components as well as difficult manufacturing, contributing to excessive cost. An inherently safe rehabilitation robot must be affordable so that it can be used by patients in a home environment. The most difficult, time consuming and expensive design to manufacture would be initial design 3 as it would require the manufacturing of a custom mat with hundreds of reed switches. A 50 cm by 30 cm mat would require more than 700 reed switches which would cost over 1000 GBP for the reed switches alone. Additionally, the initial design 3 requires a custom-designed COBOT guidance mechanism. The initial design 3 lost 4 points for the complexity criterion. The second most complex design is the initial design 2, which requires four magnetic particle brakes (increasing the cost of the device) and four cable retraction mechanisms, therefore initial design 2 lost 3 points for the complexity criterion. The initial design 1 requires two magnetic particle brakes for an inherently safe guidance mechanism, and a large sturdy frame, therefore it lost 2 points for the complexity criterion. Similarly to the initial design 1, the initial design 4 lost 2 points, as it requires a hybrid position tracking (e.g. webcam and mouse optical sensors) and a custom designed COBOT guidance mechanism.

According to the decision matrix 3.2, all of the four initial designs scores are high, yet the *initial design 4* has the highest score.

Table 3.2: Decision matrix evaluating the most suitable initial design.

Criteria (Weight%)	Design 1	Design 2	Design 3	Design 4
Safety (30%)	8	9	9	9
Usability (25%)	8	8	8	10
Functionality (25%)	8	8	10	10
Complexity (20%)	8	7	6	8
Total (10 max)	8	8.1	8.4	9.3

As the *initial design 4* was evaluated as the best initial design, the *conceptual design*

is based on it. A 3D CAD design of the *conceptual design* is presented in Figure 3.5. As in the case of the initial design 4, the joystick is positioned under the HD webcam, which is mounted on a stand placed on the table. When a patient moves the joystick the webcam tracking system tracks the position. The guiding mechanism is mounted beneath the joystick and it can be based on one of the cobot architecture variations.

Figure 3.5: Conceptual design of a table-top rehabilitation robot based on a webcam tracking system.

3.4 Final Design

In this section, the final design of an inherently safe rehabilitation robot is presented and its opera- tion is explained. A guidance mechanism and navigation system are introduced, however their operation details are explained in Chapters 4 and 5 respectively. The presented design was developed prioritising robustness and a fast manufacturing process rather than style.

3.4.1 The Final Design

To date, a COBOT unicycle mechanism, which is covered in Chapter 2, has not been utilized in a table-top rehabilitation robot. All of the previously developed devices, (Perry *et al.*, 2012), (Peattie *et al.*, 2009), (Wong *et al.*, 2011), (Luo *et al.*, 2012),utilizing existing table space use omni-directional wheels for actuation or for creating resistive force, and to move over a table. The COBOT unicycle mechanism can be used to create virtual constrains. In this section, a unicycle COBOT inherently safe (patient active) guidance mechanism-based arm rehabilitation robot is introduced. The proposed design is shown in Figure 3.6.The final design was developed to accommodate position tracking and inherently safe guidance systems, which are introduced in detail in chapters 4 and 5 respectively.

The COBOT inherently safe guidance module, shown in Figure 3.7, was designed to fit in between the underside of the robot and the surface of a table which measures 40 mm.The shaft on which two wheels are mounted is free to rotate to equally distribute pressure between two wheels and to account for an uneven surface. A spring-based suspension is fitted into the design to ensure constant and equal friction force between the COBOT wheels and the surface of a table. Single-wheel and dual-wheel COBOT designs were considered for the final design of the robot, but the dual-wheel design was chosen for two main reasons. First, the two of the COBOT mechanism wheels are mounted on one axis and can rotate independently, and as a result avoid dry steering when the robot is stationary which would be a problem in a unicycle COBOT design. Secondly, utilizing the COBOT dual-wheel design allows for larger diameter wheels in the design. A single-wheel COBOT design could have wheels that are at most 10 mm in diameter and the utilized COBOT dual wheels are 25 mm in diameter. Larger diameter wheels are easier to manufacture. The dual wheel COBOT mechanism is not stable alone, therefore four custom designed casters are employed. The design of the casters is presented in Figure

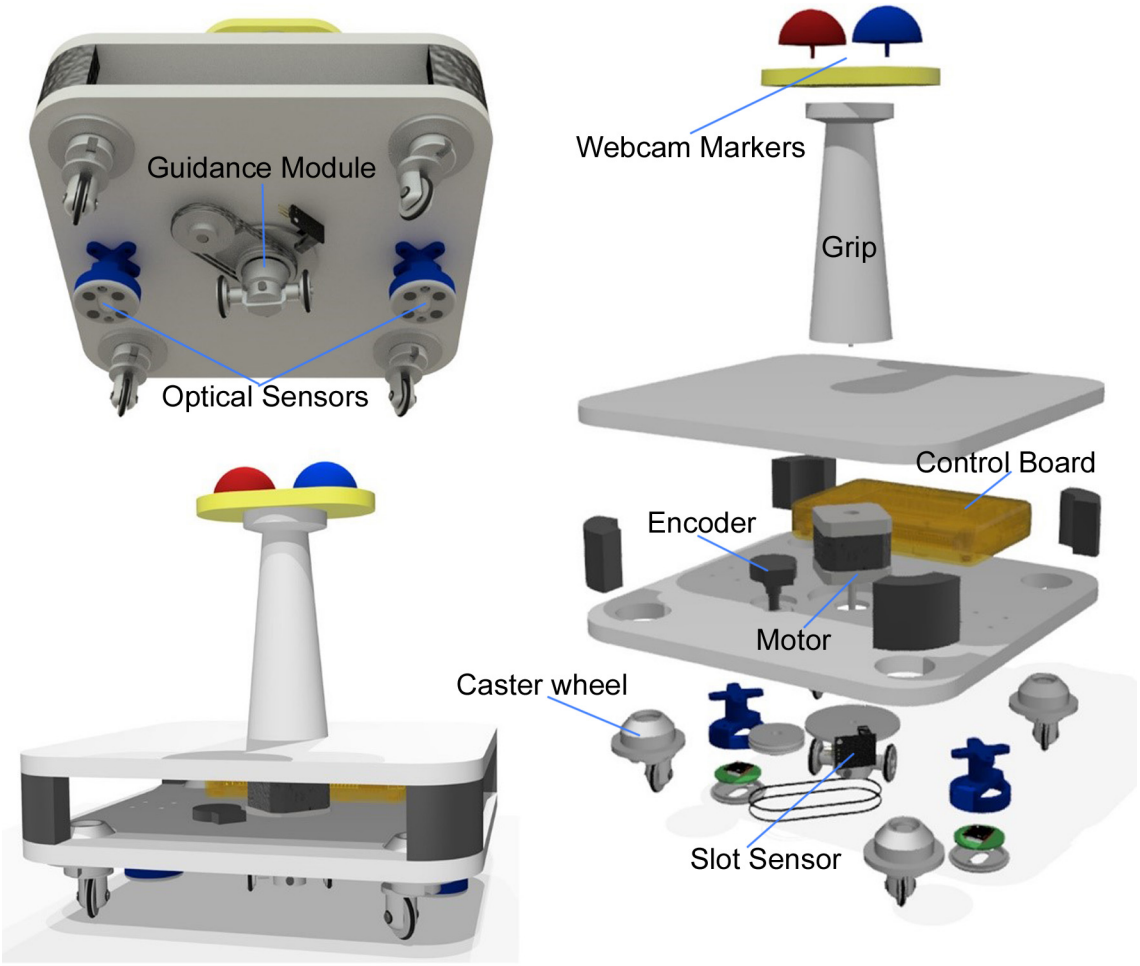

Figure 3.6: The final design of the rehabilitation robot.

3.8. The casters have adjustable offset feature which can be set to any distance from 0 to12 mm. Three bearings are used in the caster design to ensure low rolling resistance. The grip of the robot has a conical shape, because it was reported that the use of a conical shape grip with the larger diameter end positioned in the ulnar side of the hand can reduce hand and wrist spasticity (Fess *et al.*, 2005).

3.4.2 Manufactured Prototype

The final design was manufactured. The guidance module was manufactured out of aluminium. The caster wheels were also manufactured out of aluminium. The body of the robot was manufactured out of polyethylene plastic. The brackets for optical sensors were 3D-printed in ABS. Pictures presenting the manufactured prototype are shown in Figure 3.9.

The quality and functionality of the manufactured prototype was evaluated. It was found in hands-on testing that to minimize the rolling resistance, the offset of the caster has to be set to 12 mm, which is the maximum possible offset setting. At the 12 mm caster offset the rolling resistance of the robot is low and movements are smooth. The device was also tested at the 6 mm caster offset and it was found that in this setting the device was not usable, the rolling resistance significantly affected movements. It is predicted that the device would benefit from an even larger offset. The spring employed in the guidance mechanism suspension is pressing the wheels with a force equivalent to approximately 10 N. All the wheels utilise rubber tires to increase the friction force in the case of COBOT wheels and to protect the surface from scratching in the case of casters. Additionally, thanks to the rubber tyres the noise created during robot movement is reduced.The quality of the prototype was deemed to meet all the design tolerances and it predicted that the quality of the prototype and all manufactured components should not have a negative influence on experimental testing, which will be conducted using the prototype. During the design phase, no computational stress analysis of the components was performed, however the manufactured prototype is deemed to be very robust and computational stress analysis could be used later for design optimization.

Manufactured Prototype and the Product Requirements

The list of the product requirements was divided into three groups: safety, usability and functionality requirements. In this section the manufactured prototype is evaluated against

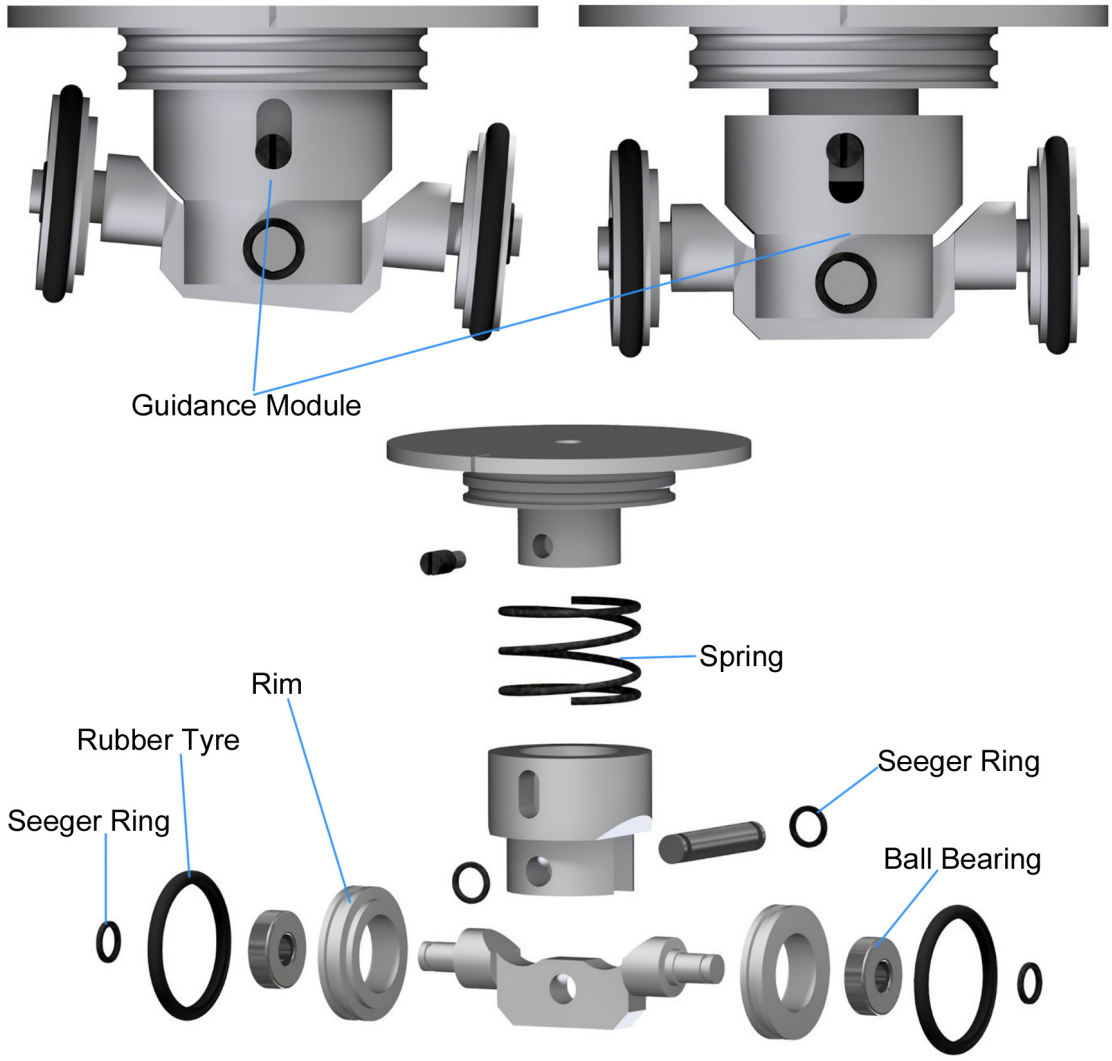

Figure 3.7: A custom designed dual-wheel COBOT inherently safe guidance mechanism.

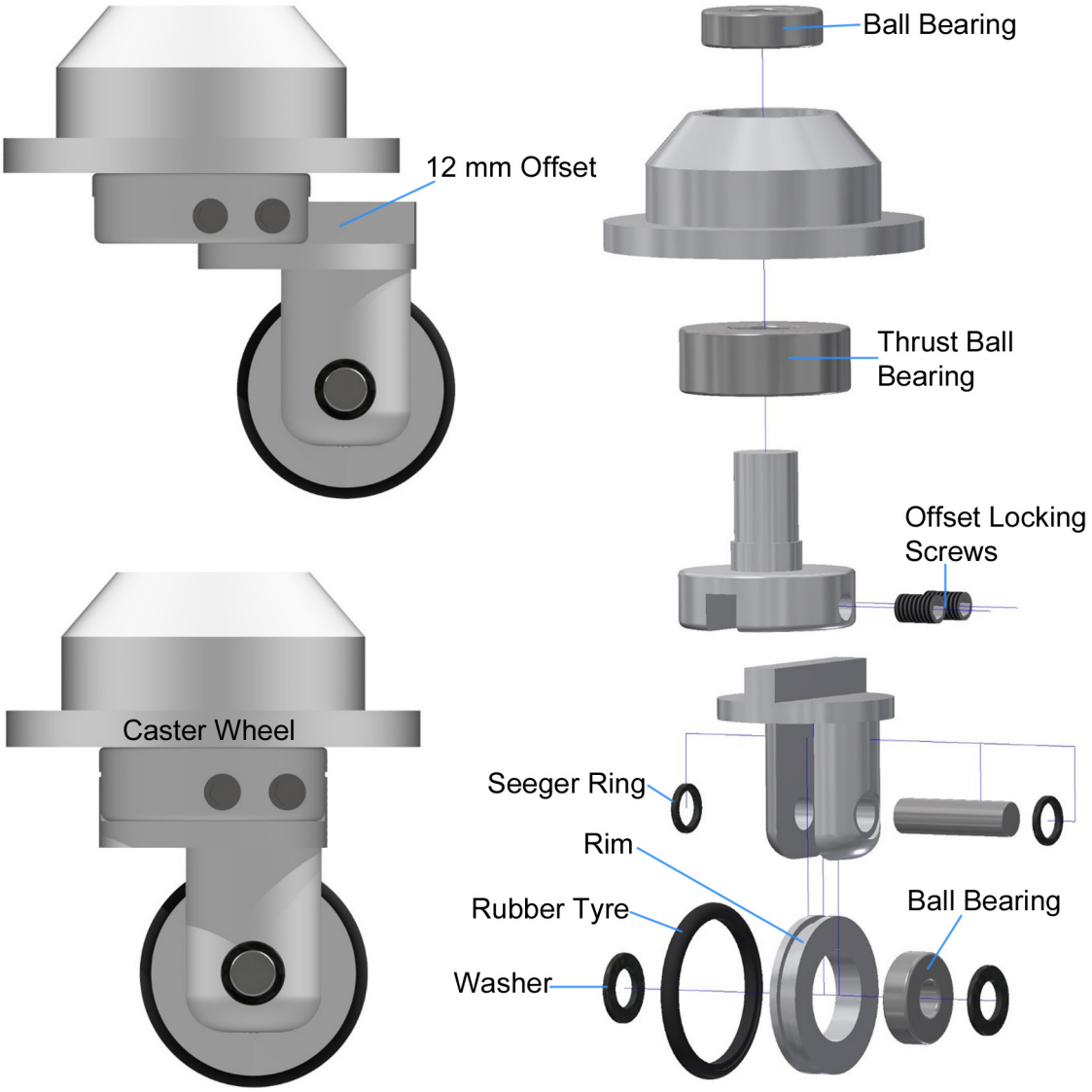

Figure 3.8: A custom designed caster which is utilized in the final design.

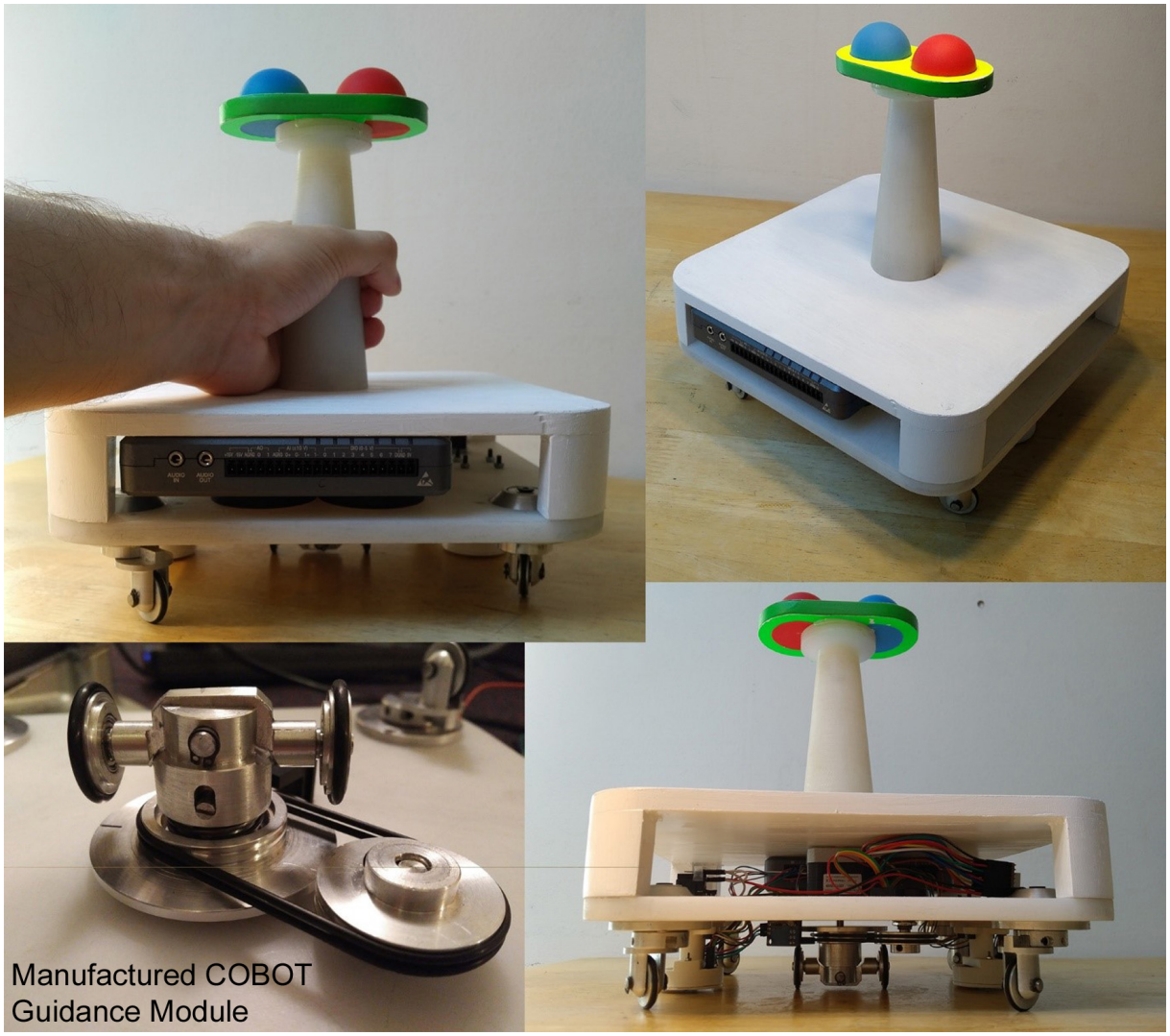

Figure 3.9: Pictures of the manufactured prototype.

the products requirements list:

1. Safety Requirements:

   (a) The prototype can be classified as a medical Class IIa device as it is designed to administer energy from the human body. It can be said that the prototype complies with the legal regulations concerning Class IIa medical devices concerning safety. The design of the robot is inherently safe even though it utilizes an electric motor in the guidance module. The current version of the prototype is powered with a DC charger (12V) connected to a 230V socket. All the onboard electrical and electronic components operate at 12 V or below, therefore the risk of electrical shock is minimized. As user testing has not been conducted yet, it will be necessary to come back to this requirement after the user testing is completed. At the moment, no safety concerns that could affects users using the device are known (apart from table fall prevention feature, which will be discussed later in this section).

   (b) The porotype operation is inherently safe. The design ensures that the guidance module motor cannot generate any active force acting on the user's arm.

   (c) The prototype provides adequate resistance to overturning torques during normal operation. Short hands-on testing indicates that overturning the robot during normal operation is highly unlikely. Chapter 6 presents user testing with the prototype and any issues with the device overturning will be reported.

   (d) The optional vertical forearm support is not included in the current version of the prototype. However, the design provides vertical support for a part of the palm and a part of the forearm close to the palm. .

   (e) A system preventing the device from falling of a table edge is not present in the current version, therefore the device cannot be safely operated if a user's arm is fastened to the prototype. However, the device can still be safely operated if the user's arm is not fastened to the prototype.

   (f) The device construction is inherently safe.

   (g) The device does not have any sharp or pointy edges that could contact a user while using the prototype.

(h) All the onboard electronic and electrical components operate at 12V or lower voltage, which is significantly lower than the maximum acceptable voltage (24V).

(i) The current prototype does not include a battery in the design. However, if a battery will be added in the future, its state will be monitored.

2. Usability requirements:

(a) The developed prototype can be easily used on any existing table surface. The setup of the device is very easy. It has to be placed on a table, cables have to be connected and it is then ready to use.

(b) The prototype satisfies the weight and size requirements. The measured weight of the robot movable unit was measured to be 2.2 kg, and as it is below the maximum weight specified in the product requirements list there is no need to reduce the weight of the prototype. The product requirements specified the maximum size of the base unit to be small enough to fit on a square 30 by 30 cm and the actual prototype would fit on a square 24.5 by 24.5 cm, therefore there are no issues with the compactness of the design.

(c) The setup and take down of the prototype takes less than 2 minutes. However, the prototype must be connected to the computer in order to operate and if the time needed to switch on the computer and load the necessary software is added, the setup time will take longer than 2 minutes.

(d) The prototype is not powered from an on-board battery. This functionality will be added in the future. Future iterations of the prototype are planned to include wireless communication and an on-board battery, which will make the robot completely wireless.

3. Functionality requirements:

(a) The prototype includes an on-board guidance system which can create virtual constrains on a planar surface, forcing the user's arm to move in the desired direction.

(b) The prototype does not include variable resistance braking. This feature might be included in the future.

(c) The prototype supports a large planar workspace. The position tracking system, which is covered in Chapter 4 is designed so that the area covered by the system can be easily increased, however this results in a loss of accuracy. A square 50 by 30 cm workspace can be easily covered by the prototype.

(d) The rolling resistance of the prototype was experimentally evaluated in a quick test with a digital scale which indicated that the rolling resistance of the prototype is 1 N and static resistance is 1.5 N. However, this test should be repeated with e.g. a load cell connected to a data acquisition system.

(e) The requirement regarding position tracking accuracy will be evaluated later in Chapter 4.

(f) The current prototype is not capable of monitoring the progress of a patient's therapy. However, it is capable of recording patients' movements, which can be used for developing therapy progress monitoring algorithms in the future.

(g) A battery is not included in the current prototype, however in the next iteration of the prototype it is planned to be included. It is desired that the battery would be able to power the prototype for 10 hours of continuous use.

(h) The current prototype is connected to a PC via a USB cable. In the next iteration of the design thi will be replaced with wireless communication to make the prototype completely wireless. The cable connection used in the prototype does not have a significant effect on the prototype's performance, it is comparable to the operation of a wired computer mouse.

(i) The prototype is designed to ensure repeatability and reliability during training. At this stage, commenting on the performance of the prototype regarding repeatability and reliability is not possible. It will be possible after the position and orientation tracking, guidance system and user testing experiments are completed.

(j) The current prototype is designed to fit most hand sizes. The prototype can be comfortably used by people with a palm width of up to 12.5 cm. However, the grip can easily be replaced with a larger sized one if necessary.

3.5 Summary – The Final Design

The product requirements for the developed rehabilitation device are derived for a scenario where the device is primarily used by a stroke patient at home or in a rehabilitation centre without constant professional supervision. However, the presented prototype is planned to be evaluated with healthy participants only. A decision on conducting experiments with post-stroke survivors will be made after finishing user testing, which is presented in Chap ter 6.

The safety requirements concerning the prototype, which are not met or partially met are: arm support and fall prevention. The arm support requirement is partially met, as the weight of the palm and part of the forearm is supported in the proposed design. This could be improved by redesigning the handlebar design to accommodate the full length of a forearm. At the current stage of the project full forearm support is not necessary as only tests with healthy participants are planned. In the future, if tests with healthy participants are completed successfully, a full forearm support can be added before performing clinical trials. The fall off a table edge prevention was not implemented in the design. This feature is very important if a patient's arm is fastened to the robot during use. However, at the current stage of the project only healthy participants will be recruited for trials and their arms will not be fastened to the robot. The fall off table prevention feature in the design is not crucial for the planned testing. Also, it is predicted that it is unlikely that a person moving the robot will move it off a table, however this will be monitored during the planned user testing in Chapter 6.

The usability requirements concerning the prototype, which are not satisfied are: implementation of an onboard battery and setup time. The battery, which is not included now, will be included in the next iteration of the design. The setup time is satisfied if it does not include switching on a PC. The PC used for testing uses a spinning disk hard drive (HDD). However, it is predicted that if a modern PC with a fast solid state hard drive (SSD) would be used, then the boot up time is likely to drop below 2 min.

The functionality requirements concerning the prototype have mostly been satisfied. One of the crucial functionality requirements is the requirement to include a guidance system capable of creating 2D virtual constrains, and this is satisfied by the prototype. However, at the moment it can only be said that the guidance system is implemented in the prototype and a statement regarding the guidance system performance can be

formulated after completing the guidance system testing, which is presented in Chapter 5. Also, the requirement regarding the position tracking accuracy cannot be commented on until Chapter 4. The requirement regarding repeatability and reliability also cannot be evaluated now, but it will be possible to comment on it after user testing (Chapter6) is completed.

The final design was presented and a prototype based on it was manufactured. No significant problems which would prevent the prototype from full experimental evaluation with healthy participants were found. The prototype utilizes a COBOT inherently safe guidance mechanism, which (to the author's knowledge) was not implemented in a table-top reha- bilitation robot before. The prototype's crucial subsystems, the position and orientation tracking, and the guidance system are evaluated in the next two chapters.

Chapter 4

Position Tracking System

The work presented in this chapter has been published in two jointly-authored publications:

- Wojewoda, K.K., Culmer, P.R., Jackson, A.E. and Levesley, M.C., 2016, June. Position tracking of a passive rehabilitation robot. In Cyber Technology in Automation, Control, and Intelligent Systems (CYBER), 2016 IEEE International Conference on (pp. 1-6). IEEE.

- Wojewoda, K.K., Culmer, P.R., Gallagher, J.F., Jackson, A.E. and Levesley, M.C., 2017, July. Hybrid position and orientation tracking for a passive rehabilitation table-top robot. In Rehabilitation Robotics (ICORR), 2017 International Conference on (pp. 702-707). IEEE.

Data for Figure 4.15 was processed by Gallagher, J.F. The author confirms that the rest of the work presented in these publications is his own work and that the co-authors were responsible for reviewing the publications.

4.1 Introduction

The design of the rehabilitation robot presented in the previous chapter constrains the type of tracking system which can be implemented. The robot presented in Figure 3.9 9 is a table-top portable device which is supposed to utilize existing table space in a home environment as the workspace. To date, only a few rehabilitation devices of this type were developed and they are described in Table 2.4. These devices are ArmAssist, Arm Skate,

Arm Skate II and the Reha-Maus. Each of these devices is designed to work on existing table space and each of them has a different position tracking system.

The ArmAssist utilizes two independent position and orientation tracking systems, a relative tracking system based on two mouse optical sensors and an absolute tracking system based on one mouse optical sensor (Perry *et al.*, 2012). The two relative position tracking optical mouse sensors operate as a typical computer mouse providing 2D incremental position measurements. They are positioned in parallel to each other and the distance separating them is known. The relative position measurements from the two optical sensors are taken at 125 Hz. The normal speed to be measured during operation is assumed to be 0.1 m/s and the position and angle estimations are updated at 25 Hz. Absolute position measurements are taken by one optical mouse sensor positioned in the centre of the ArmAssist base unit, between the two mouse sensors used for incremental position measurements. This sensor is a camera taking pictures of a surface which is coded with unique landmarks. An optical symbol recognition algorithm was used to compute the position based on the image of the coded surface taken. In order to fuse the relative and absolute position measurements the ArmAssist utilizes non-systematic odometry error correction approach. The algorithm is stopped when surface quality (SQUAL) measurements detected by optical sensors indicate a lack of surface underneath. During the initial development of the ArmAssist it was reported that the accuracy of position tracking was 36.7 +/- 22.5 mm and orientation was 2.81 +/- 1.57 degrees (Zabaleta *et al.*, 2011). However, during later development higher accuracy was reported, 6 +/- 3 mm and 1.2 +/- 1.4 degrees for position and orientation respectively (Perry *et al.*, 2012).

The Arm Skate employs a simpler solution. There is one webcam tracking the movements of a patient's arm. The webcam is mounted overhead and tracks a colour marker attached to the Arm Skate base unit. Peattie (Peattie *et al.*, 2009) described the performance of the position tracking of the Arm Skate as behaving as a normal PC mouse, but without position drift (Peattie *et al.*, 2009). Arm Skate II is the second iteration of Arm Skate and the position and orientation tracking system was completely redeveloped. It utilizes two optical mouse sensors instead of the webcam. As the robot only uses the relative position tracking system, the position measurements are subject to drift. It was reported that the Arm Skate II accumulative error was on average 11.5 mm for the X coordinate and 12.5 mm for the Y coordinate after every 1 m travelled. Its orientation

can be measured up to +/- 5 degrees in a range from -40 to 40 degrees and is subject to large error, and fails outside this range (Wong *et al.*, 2011).

Reha-Maus has a position tracking system which similarly to ArmAssist employs two independent position and orientation tracking systems: an absolute tracking system based on an infrared camera and a relative tracking system based on wheel odometry. The infrared camera absolute position and orientation measurements are subject to noise and a low-frequency update rate (20 Hz). The wheel odometry (encoders) can provide significantly higher frequency (1000 Hz, compared to infrared camera) position and orientation measurements. The robot utilizes the Kalman filter in order to combine relative and absolute position measurements, resulting in high-frequency position and orientation measurements without the accumulative error inherent in odometry measurements. The accuracy of the Reha- Maus tracking system was reported to be in the range of millimetres for position and within 5 degrees for orientation (Luo *et al.*, 2012).

Gap in the Knowledge – Position and orientation Tracking

Among the analysed table-top portable rehabilitation devices, ArmAssist has the most precise and repeatable position and orientation tracking. To function properly, ArmAssist requires a coded mat made of a 10 mm thick polyethylene sheet. The usable workspace of the mat is 512 x 288 mm, but the actual dimensions are larger. The weight of the mat is 6.5 kg, making it heavier than the ArmAssist robot unit (less than 3 kg). The large dimensions and weight (compared to the base robot unit) significantly affect the portability of the whole ArmAssisit system (Perry *et al.*, 2012). The first Arm Skate used camera-based colour detection position tracking which was reported to be complicated to set up. Arm Skate II abandoned the camera and used two optical mouse sensors which are subject to accumulating measurement error (drift). Reha-Maus uses an effective sensor fusion algorithm (relative and absolute systems work better together), but its position tracking accuracy was not precisely reported. Based on the provided information, the ArmAssist is more precise than the Reha-Maus position and orientation tracking. Performed analysis showed limitations in the present state-of-the-art tracking systems employed in table-top portable rehabilitation robots utilizing existing table space. ArmAssist and Reha-Maus show the benefits of sensor fusion while Arm Skate and Arm Skate II rely on a single tracking system. It seems that fusing together measurements from the Arm Skate and

and Arm Assist II camera and mouse optical sensors respectively could give better results than if the systems are used alone.

4.2 Requriements of The Position Tracking System

The position and orientation tracking system has two main requirements regarding its functionality, which are: tracking the 2D position of the rehabilitation robot presented in Figure 3.9, and to track the orientation of the robot. While tracking the position and orientation of the robot, the tracking performance of the system must be reliable and repeatable and offer sufficient accuracy to allow arm movement tracking and monitoring the patient's recovery. It was specified in the product requirements in Chapter 3 that the tracking system shall measure position and orientation at least up to +/- 10 mm and +/- 10 degrees respectively, which is a minimum requirement for the system to be usable. However, in order to provide high accuracy in rehabilitation progress monitoring and to pro- vide more challenging exercises for patients who improve, the tracking performance of the Arm Assist must be matched or exceeded.

The second crucial requirement a position tracking system has to meet is the capability of tracking the speed of movement which is typical for post-stroke rehabilitation training. In a study conducted by B. Rohrer at MIT, a planar robotic rehabilitation device (MIT Manus) was used to analyse the movement smoothness of the hemiparetic arm in 31 subjects. Twelve of the subjects were acute-stage stroke survivors and 19 were chronic-stage stroke survivors. The task all of the subjects had to perform were 14 cm point-to-point movements in different directions. Each of the analysed subjects performed at least 100 movements and each trial was conducted with the MIT Manus working in a passive (solely patient active) mode. In the performed anal- ysis the mean and peak speeds were calculated. The maximum recorded peak speed was less than 0.12 m/s and the maximum average speed was less than 0.07 m/s (Rohrer *et al.*, 2002). Therefore, a position tracking system for a rehabilitation robot shall accurately and reliably track 0.12 m/s movements.

4.3 Position Tracking Utilizing Webcam and Mouse Optical Sensor

In this section, the concept of a position tracking system fusing position data from a webcam and an optical mouse sensor is presented and experimentally evaluated. The aim of the presented concept is to evaluate how the webcam and mouse optical sensor position tracking performance compares when they are used alone and when their measurements are fused.

4.3.1 Position Tracking Utilizing Webcam and Mouse Optical Sensor - Fusion Algorithm

The presented concept of a position tracking system consists of two independent subsystems whose measurements are fused together. This tracking system is designed prioritising low cost and robustness. These two subsystems are: an absolute position tracking system, and a relative position tracking system, the main components of which are a webcam and an optical sensor respectively. The absolute position tracking system is based on a webcam mounted on a fixed stand and tracking a marker moving underneath it. The webcam detects the motion of the moving marker relatively to a fixed coordinate system. The relative position tracking system is based on a mouse laser optical sensor which is attached to the tracked object. The laser optical sensor detects motion relatively to the surface on which it is being used. A suggested fusion scheme, described later, combines position data acquired from the webcam and the optical sensor in order to obtain higher precision position estimates than would be possible if the systems were used on their own. Data sampling time is different and unsteady for both the webcam and the optical sensor. The optical sensor sampling frequency is assumed to always be faster than the sampling frequency of the webcam. A fusion trajectory is based on optical sensor measurements and the webcam measurements are utilized to correct the drift inherent to the optical sensor. A schematic diagram of a proposed fusion scheme is presented in Figure 4.1. The webcam acquires low-update-rate absolute position measurements which are subject to noise corruption. The optical sensor acquires fast-update-rate position measurements which are subject to drift affecting tracking accuracy. Position measurements acquired from the webcam and optical sensor are fused together utilizing the fusion scheme presented in this

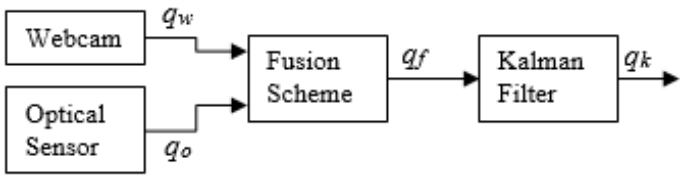

Figure 4.1: Schematic diagram of the fusion scheme fusing position data acquired from a webcam and an optical sensor in order to obtain higher precision position estimates.

section. In the last step fused data which is partially noise-corrupted is filtered using a discrete Kalman filter.

Fusion scheme: A case when webcam data is not available

If the webcam data is not available the following equation was used to calculate the position:

$$q_f(t) = q_f(t-1) + \Delta q_o(t) \tag{4.1}$$

where q_f is the fused position, Δq_o is an optical sensor-measured position increment from the most recent position measurement and t is the time when the measurement was taken.

Fusion scheme: A case when webcam data is available.

When webcam position measurements q_w are present the position is calculated as follows:

$$q_f(t) = q_f(t-1) + \Delta q_o(t) + w \times C(t_w) \tag{4.2}$$

where w is a weight, C is a position correction term and t_w is a time when webcam measurements are available. The correction term C is calculated according to:

$$C(t_w) = q_w(t_w) - q_f(t_w) \tag{4.3}$$

where q_w is a position measurement from the webcam. q_f was interpolated at t_w, for each iteration t_w satisfies:

$$t\text{–}1 < t_w \leq t \tag{4.4}$$

Instead of adding the correction term C in one time step to compute position results, it is divided by eight and added eight times. This approach minimises sudden sharp changes on a trajectory graph. Implementing the correction C over eight steps is done as the minimum measured number of measurements acquired by the optical sensor between two webcam position measurements was eight.

The gain w is calculated based on an average strength (AS) parameter measured by the webcam. Average strength is the gradient magnitude of the detected edge (of the tracked marker) and it was measured on a scale from 0 to 1. The gain w was calculated using the following experimentall derived formula:

$$w(t_w) = \begin{cases} 0 & \text{if } AS(t_w) < 0.9 \\ 6.25 \times AS(t_w) - 5.125 & \text{if } 0.90 \leq AS(t_w) < 0.98 \\ 1 & \text{if } 0.98 \leq AS(t_w) \end{cases} \tag{4.5}$$

Fusion scheme: Kalman Filter

The type of the Kalman filter used is a discrete Kalman filter (Welch & Bishop, 1995) which was applied to the fused position data. The Kalman filter was designed to estimate the state of a discrete-time controlled process that can be described by the use of a stochastic difference equation:

$$q_k = Aq_{k-1} + Bu_k + w_{k-1} \tag{4.6}$$

with a stochastic output equation:

$$z_k = Hx_k + v_{k-1} \tag{4.7}$$

where x_k is the process state and z_k is the process measurement at the step k. The variable w_k is the process noise and the variable v_k is the measurement noise. H is a matrix of compatible dimension that relates the state to the output. uk is the optional control input. A and B are matrices that govern the dynamic behavior of the system.

Assuming that Q and R are the process noise covariance and the measurement covariance, the recursive discrete Kalman filter algorithm can be written with the following five equations:

1. Time update equations:

(a) A state prediction:

$$\hat{q}_k^- = A\hat{q}_{k-1} + Bu_k \tag{4.8}$$

(b) Prediction of the error covarience::

$$P_k^- = AP_{k-1}A^T + Q \tag{4.9}$$

2. Measurement update equations:

(a) Computing the Kalman filter gain:

$$K_k = P_k^- H^T (HP_k^- H^T + R)^- 1 \tag{4.10}$$

(b) Correct the state prediction (1a) with updated measurement:

$$\hat{q}_k = \hat{q}_k^- + K_k(z_k - H\hat{q}_k^-) \tag{4.11}$$

(c) Update error covariance:

$$P_k = (I - K_k H)P_k^- \tag{4.12}$$

The position of the marker tracked in the experiment can be written in a matrix form as follows:

$$q_k = \begin{bmatrix} x_t \\ y_t \end{bmatrix} = \begin{bmatrix} 1 & \Delta t \\ 1 & \Delta t \end{bmatrix} \begin{bmatrix} x_{t-1} \\ y_{t-1} \end{bmatrix} + \begin{bmatrix} (\Delta t)^2 \\ (\Delta t)^2 \end{bmatrix} \begin{bmatrix} \ddot{x}_t \\ \ddot{y}_t \end{bmatrix} \tag{4.13}$$

Where x and y are the position coordinates of the tracked marker at a time step t. The Kalman filter was applied separately to X and Y fused coordinates considering them to be one-dimensional problems.

4.3.2 Position Tracking Utilizing Webcam and Mouse Optical Sensor - Experimental Methodology

The sensor fusion scheme has been validated in experiments. Figure 4.2 shows a diagram of how the experimental apparatus was utilized. During the experiments, a robotic arm (Denso VS-068) was used to perform 2D movements which were tracked by the webcam and the optical sensor attached to a fixed stand. In order to evaluate the tracking performance, a reference (benchmark) trajectory was acquired using an Optotrak motion capture system

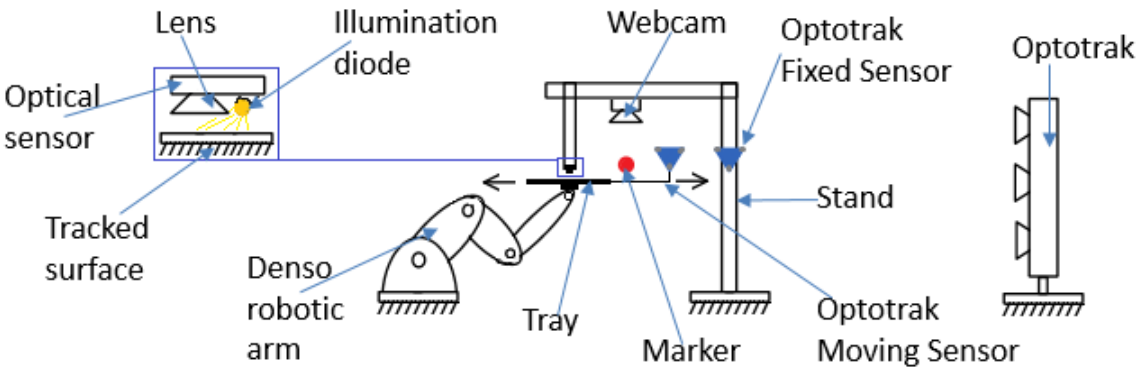

Figure 4.2: Schematic diagram of the experimental apparatus utilized to test the sensor fusion scheme.

with two infrared sensors. Data acquired by the Optotrak was sampled at 400 Hz with two infrared sensors: a moving body sensor (moving) and a lab frame sensor (stationary). According to the data acquired with the Optotrak, the measurement error was 0.17 (0.02) mm for the moving body sensor and 0.25 (0.001) mm for the lab frame stationary sensor.

During experiments, two different trajectories were tracked: a circular trajectory and a pentagram star trajectory. During each experiment, each trajectory was repeated continuously ten times at three different velocities V1 (40 mm/s), V2 (55 mm/s) and V3 (70 mm/s). For reference, the maximum average velocity in an experiment with 31 post-stroke survivors subjects using hemiparetic arm conducted at MIT using MIT Manus robot was less than 0.07 m/s Position data acquired from the webcam and the optical sensor was fused and filtered using the Kalman filter after the experiments.

hemiparetic arm in 31 subjects. Twelve of the subjects were acute-stage stroke survivors and 19 were chronic-stage stroke survivors. The task all of the subjects had to perform were 14 cm point-to-point movements in different directions. Each of the analysed subjects performed at least 100 movements and each trial was conducted with the MIT Manus working in a passive (solely patient active) mode. In the performed analysis the mean and peak speeds were calculated. The maximum recorded peak speed was less than 0.12 m/s and the maximum average speed was less than 0.07 m/s (Rohrer *et al.*, 2002).

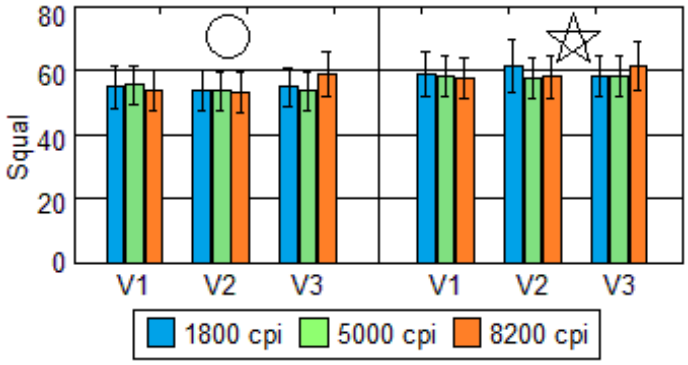

Figure 4.3: Mean optical sensor surface quality (Squal) for circular and pentagram trajectories for three movement velocities and three resolution settings of the optical sensor. Confidence intervals represent standard deviation.

4.3.3 Position Tracking Utilizing Webcam and Mouse Optical Sensor - Experimental Results

The results presented in this section are for the optical sensor tracking system, the webcam tracking system, and the fusion scheme.

Result for optical sensor tracking

During experiments, a laser diode-illuminated optical sensor (ADNS-9800) was utilized. The mean measured sampling frequency of the optical sensor was 108.4 (21.9) Hz. During experiments three different optical sensor resolutions settings and three different surfaces above which the sensor was used were investigated.

The optical sensor was measuring surface quality (Squal) at each time step. Sqaul is a number from 0 to 169 representing the number of valid features visible by the sensor at the current time step. The higher is the Squal, the more accurate the tracking results. Figure 4.3 presents mean Squal results for three movement velocities and three resolutions of the optical sensor.

The data presented in Figure 4.3 shows that there is no clear dependence between the movement velocity and the Squal value. There is also no significant variation between optical sensor resolutions and Squal values. However, it can be noticed that mean Squal values for each optical sensor resolution are higher for the pentagram trajectory movement

Table 4.1: Mean optical sensor surface quality (SQUAL) for circular (c) and pentagram (p) trajectories and three surfaces (standard deviation in brackets) at V3 velocity and 5000 cpi.

Surface type	Gaming mat (c)	Gaming mat (p)	MDF board (c)	MDF board (p)	White paper (c)	White paper (p)
Squal	53.20 (6.38)	57.90 (6.48)	37.81 (4.30)	39.55 (6.94)	36.58 (4.36)	39.24 (6.01)

Table 4.2: Optical sensor drift (mm) per 100 mm distance travelled for circular (c) and pentagram (p) trajectories and three optical sensor resolutions at V3 velocity and 5000 cpi.

Resolution [cpi]	1800 (c)	1800 (p)	5000 (c)	5000 (p)	8200 (c)	8200 (p)
Drift [mm]	0.30	0.15	0.33	0.16	0.32	0.13

than for the circular trajectory movement. Table 4.1 shows mean Squal values for the three different surfaces types.

The results in Table 4.1 indicate that mean Squal values are higher for the pentagram trajectory movement tracking than for the circular trajectory movement tracking for each of the three surfaces. The mean Squal value is the highest for the gaming mat surface – it is more than 40% higher than the mean Squal values for the MDF board. The lowest Squal values were observed for the white paper. Based on the results presented in Table I, the best tracking performance of the optical sensor can be achieved with the gaming mat surface. Table 4.2 shows the dependence between optical sensor drift values per 100 mm travelled and the resolution of the optical sensor. The total drift was calculated as a distance between the start and the end point of the trajectory tracked by the optical sensor. The drift per 100 mm traveled was calculated by multiplying the total drift with 100 mm and dividing by the total distance traveled. The data in Table 4.2 indicate that the drift per 100 mm traveled values do not vary significantly with different optical sensor resolutions. However, it can be noticed that the drift values for circular trajectory tracking are double those of pentagram trajectory tracking.

Table 4.3 shows the relation between surface type and drift values. As expected, for the pentagram trajectory tracking the lowest drift value (0.16 mm) was recorded for the gaming mat. However, for the circular trajectory tracking the lowest drift value was

Table 4.3: Optical sensor drift in mm per 100 mm distance travelled for circular (c) and pentagram (p) trajectories for three surface types at V3 velocity and 5000 cpi.

Surface type	Gaming mat (c)	Gaming mat (p)	MDF board (c)	MDF board (p)	White paper (c)	White paper (p)
Drift [mm]	0.33	0.16	0.07	0.75	2.25	1.88

recorded for MDF board (0.07 mm), whereas a corresponding value for the gaming mat was 0.33 mm. It is difficult to explain the unexpectedly low drift value for the MDF board during circular trajectory tracking. Squal values presented in Table 4.2 are lower for the MDF wood than for the gaming mat, therefore it was expected that the drift value for the gaming mat would be the lowest while tracking a circular trajectory. The very low drift value (circular trajectory) for the MDF board can be explained by the fact that the direction of the optical sensor drift changes during movement and in this special case the drift was effectively being cancelled out.

Result for webcamr tracking

During the experiments, a standard webcam (Logitech Pro 9000) capable of recording at 30 fps maximum was used. The webcam was mounted on a stand above the tracked object and covering an area 448 by 336 mm, larger than an A3 sheet of paper. The selected resolution was 640 by 480 pixels, therefore 1 pixel was equivalent to 0.7 mm. In order to neutralize the effect of lens distortion, a division calibration method was applied, which reduced the maximum sampling frequency. The mean measured sampling frequency for the webcam was 10 (0.05) Hz. The diameter of the tracked marker (matte red painted ball) was 40 mm. In order to monitor the quality of the recorded data (with the webcam) two parameters were recorded at each time step: average strength (AS) (gradient magnitude of the edge) and radius of the tracked marker. Table 4.4 shows the relation between mean AS values, marker radius and the three velocities. No significant dependence between AS and experimental velocities was observed. The AS values are similar for the circular and pentagram path tracking. However, it can be noticed that the marker radius measurements are more accurate for the circular movement tracking than for the pentagram movement tracking. This suggests that there is an image calibration accuracy problem, which can

Table 4.4: Mean webcam average strength and mean measured radius of the marker for circular (c) and pentagram (p) trajectories for three velocities (standard deviation in brackets).

	V1	V2	V3
Average Strength (c)	0.985 (0.010)	0.985 (0.010)	0.986 (0.010)
Average Strength (p)	0.985 (0.008)	0.987 (0.009)	0.987 (0.009)
Radius mm (c)	19.94 (0.47)	19.94 (0.48)	19.92 (0.49)
Radius mm (p)	19.68 (0.44)	19.67 (0.48)	19.59 (0.51)

be solved using a more efficient image calibration method. However, this can lead to an increase in the computational cost of the position calculations.

Results for the fusion of webcam and optical sensor data

The performance of the fusion tracking scheme was experimentally evaluated. To compute the results trajectories tracked with the Optotrak were used as a benchmark to evaluate the performance of the other tracking systems. Figure 4.4 presents a comparison between root mean squared errors (RMSE) of the tracking systems at three velocities. Fusion trajectory is based on combined webcam and optical sensor tracked position results, therefore it is significantly dependent on the performance of these two systems. The RMSE values in Figure 4.4 show that the fusion scheme is benefiting from both the webcam and optical sensor tracking systems. At each velocity, the RMSE value is lower for the fusion scheme when compared to RMSE values for the webcam and the optical sensor. Utilizing the Kalman filter to filter the fused position data did not improve the accuracy of the fusion scheme. It can be noticed in Figure 4.4 that RMSE values for the Kalman filter are slightly lower for the circular movement tracking than the corresponding values for the fusion. However, for the pentagram point-to-point movement tracking, the RMSE values for the Kalman filter are higher than the corresponding RMSE values for the fusion. It seems that using the Kalman filter was not significantly beneficial, as the fused tracking data was not very noisy. Utilizing the Kalman filter may be beneficial for tracking movements at velocities higher than the velocities used during the testing or tracking movements with changing acceleration.

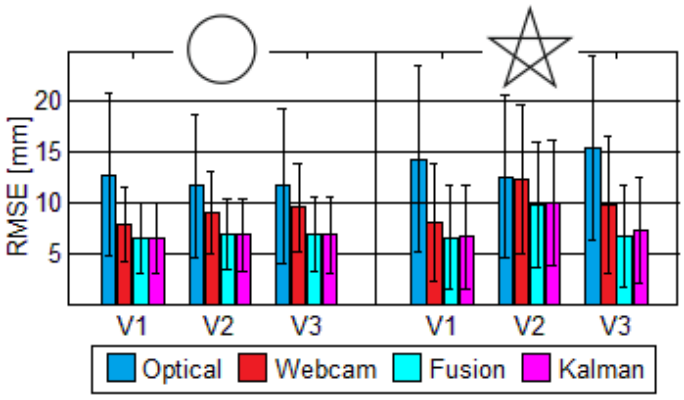

Figure 4.4: Root mean squared error (RMSE) for optical sensor, webcam, fusion scheme and Kalman filter, for circular and pentagram trajectories for three velocities (V1 (40 mm/s), V2 (55 mm/s) and V3 (70 mm/s). Confidence intervals represent standard deviation.

Figure 4.5 presents a sample plot of root mean squared tracking error vs. time for the tracking of a pentagram movement repeated seven times at V3 velocity. It can be observed that the tracking error value for the optical sensor was diverging with time. No significant divergence was observed for the webcam, fusion and Kalman filtered fusion.

Figure 4.6 (a) presents the circular movement tracking results for one full movement repetition (revolution). It grants a closer look at sample plots of X and Y coordinates, surface quality (Squal) measured with the optical sensor, and average strength (AS) together with the marker radius (R) measured with the webcam plotted against the same time scale. It can be seen that the optical sensor measurements diverge and that the trajectory of the fusion scheme is similar to the Optotrak reference trajectory.

Similarly, Figure 4.7 (a) presents the pentagram movement tracking results for one full movement repetition. It grants a closer look at sample plots of X and Y coordinates, Squal, AS and R plotted against the same time scale. In this case, optical sensor measurement divergence is more noticeable than during the circular trajectory tracking. However, once again the trajectory of the fusion scheme is similar to reference trajectory recorded with the Optotrak.

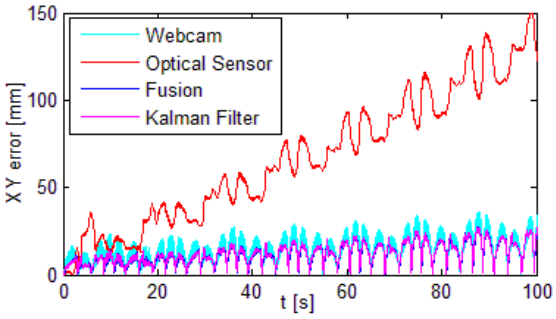

Figure 4.5: Tracking root mean squared error vs time for the pentagram movement tracking at V3 (70 mm/s) velocity, on a white paper surface.

4.3.4 Position Tracking Utilizing Webcam and Mouse Optical Sensor - Discussion

According to the results, fused data from the webcam and the optical sensor can be successfully utilized for position tracking of an inherently safe rehabilitation robot resulting in more accurate position estimates than would be possible if the systems were used on their own. Interestingly, in this case it has been shown that using the Kalman filter did not improve the tracking performance as the tracking trajectory was not very noisy. Instead, a simpler approach using a fusion algorithm with an eight-step correction reduced sudden position data changes during trajectory corrections and provided an effective strategy for position tracking. There are many forms of the Kalman filter which can be implemented, and only the simple discrete Kalman filter was investigated in this work. However, different types of the Kalman filter will be considered in future work if this become necessary. Nonetheless, as long as it performs well, the fusion algorithm will be kept as simple as possible in order to increase computational efficiency. It has been noticed that the accuracy of position estimations calculated with the fusion algorithm is limited by the quality of absolute and relative position measurements from the webcam and the optical sensor respectively. The accuracy of the webcam positioning is highly dependent on the implementation of a calibration method, whereas the accuracy of the optical sensor positioning varies with different surface types. The methods employed in this work can be adapted

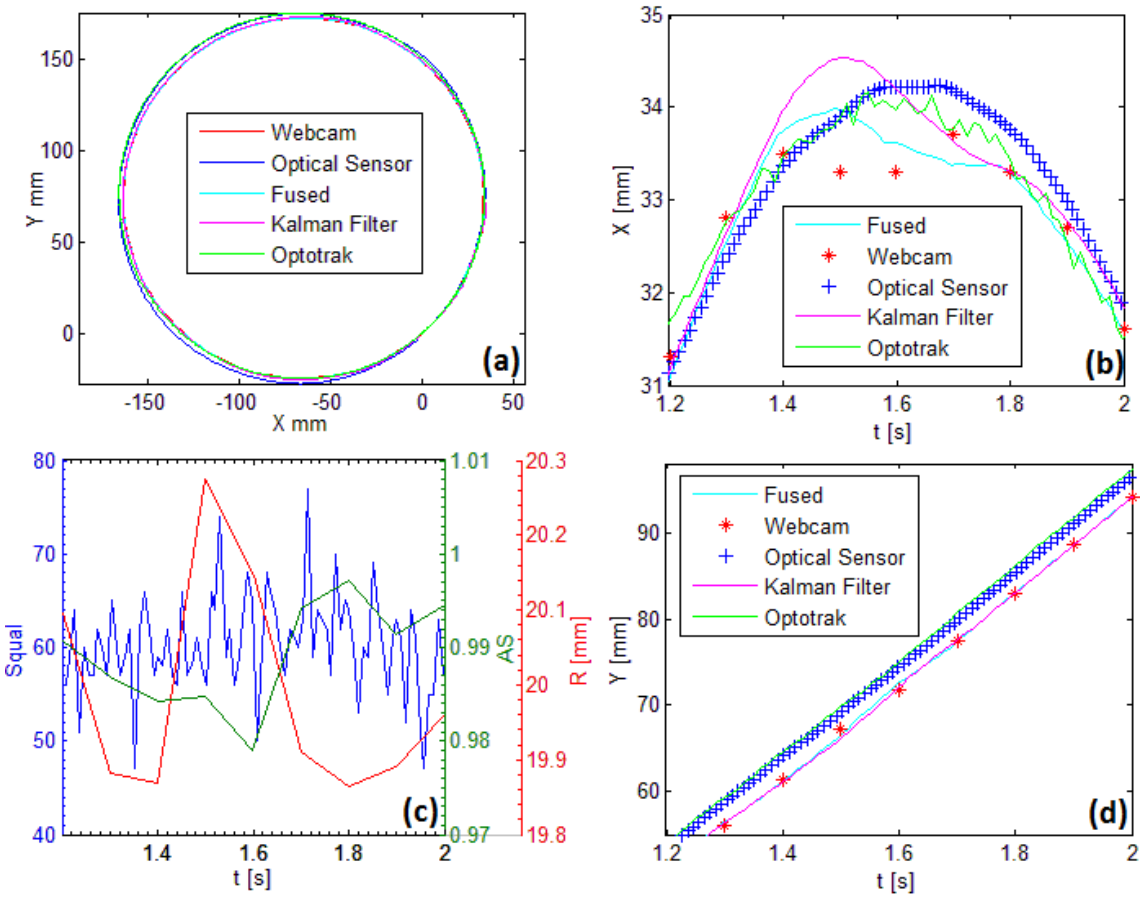

Figure 4.6: Results for the circular movement tracking: one full revolution (a), sample plot of X coordinate vs time (b), sample plot for Squal (optical sensor) and AS and R plots vs time and sample plot of Y coordinate vs time (d).

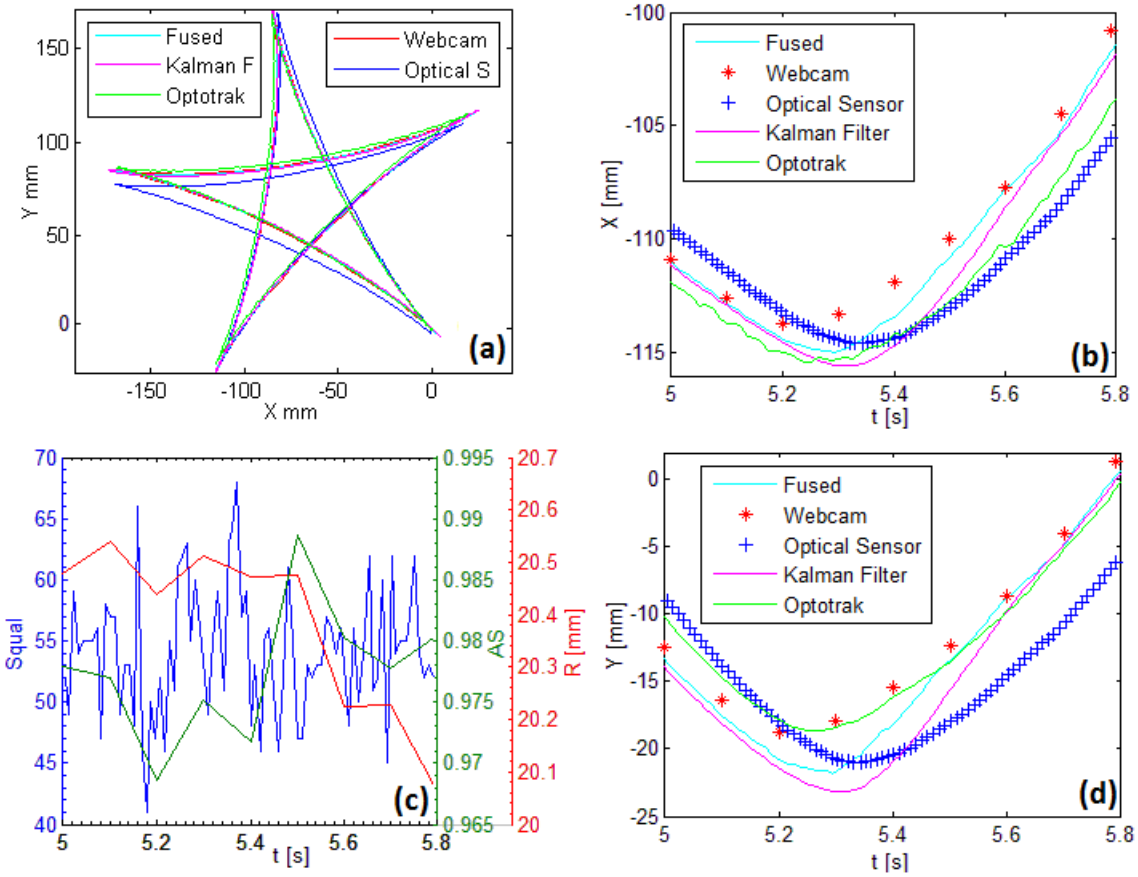

Figure 4.7: Results for the pentagram movement tracking: one full repetition (a), sample plot of X coordinate vs time (b), sample plot for Squal (optical sensor) and AS and R plots vs time and sample plot of Y coordinate vs time (d).

to include the tracking of orientation in addition to linear position. This requires one additional optical sensor and an extension of the fusion algorithm. In its current form, the algorithm cannot be used to track simultaneous changes in an object's position and orientation. The focus of the work reported here was to evaluate the feasibility and performance of the above techniques under controlled conditions. The trajectories used were representative of human movement in terms of their speed and range of motion. However, to ensure this work is appropriate for use in the design of home rehabilitation equipment, a key requirement to evaluate these techniques using human participants must be fulfilled. Testing with human participants will reveal the effects of different features of movement such as jerk and spasm on the tracking performance of the system.

4.3.5 Position Tracking Utilizing Webcam and Mouse Optical Sensor - Conclusion

A novel type of a position tracking system fusing data from a webcam and an optical sensor was proposed and experimentally evaluated, demonstrating appropriate performance (both temporally and spatially) for use in rehabilitation. The accuracy of the fusion tracking system can be further improved by improving the calibration of the webcam. The proposed fusion tracking system is simple and has the potential to be easily be implemented in a table-top robot designed for home-based upper limb rehabilitation.

4.4 Hybrid Position and Orientation Tracking

The work presented in this section is a continuation of the work previously shown in section 4.3, which proved that the 2D hybrid position tracking system fusing position estimates from two sensors, an optical mouse sensor and a webcam, can estimate the position with greater accuracy than would be possible using each sensor alone. In this section, the functionality of the tracking system is extended by including orientation tracking. The tracking system introduced in section 4.3 could not track rotation and could not function properly if rotation of the tracked object occurred.

4.4.1 Hybrid position and Orientation Tracking - Introduction

An innovative 2D hybrid position and orientation tracking system is presented and experimentally evaluated. It is validated through an experimental set-up whereby the re-

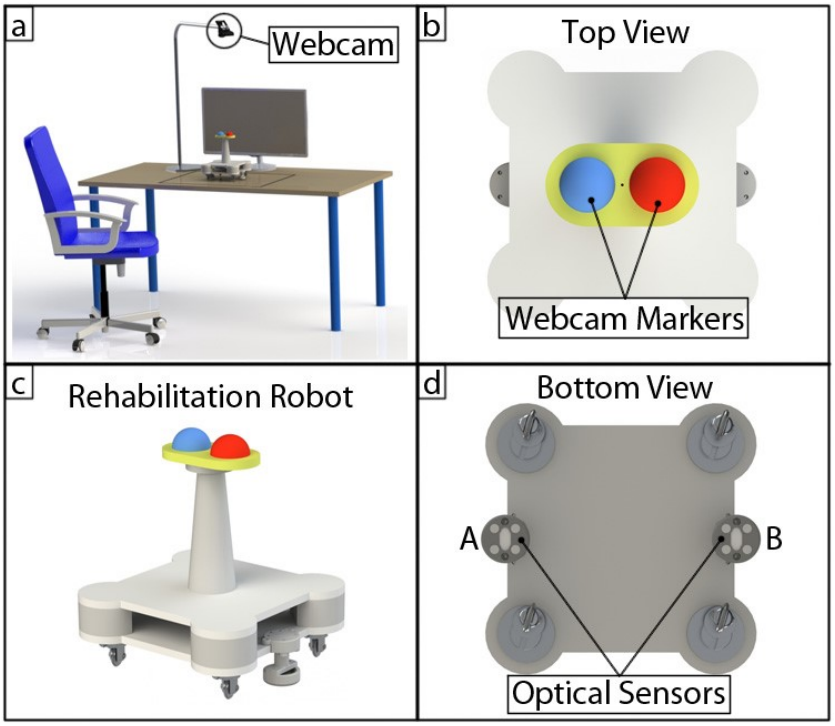

Figure 4.8: a) Conceptual setup of an inherently safe table-top rehabilitation system, b) Top view of the robot presenting blue and red webcam markers, c) The rehabilitation robot, d) Bottom view of the robot presenting A and B mouse optical sensors. The actuated module of the robot is not presented here.

habilitation robot is moved by a humanoid robotic arm replicating previously recorded movements of a stroke patient. The system is designed to monitor movements of an inherently safe rehabilitation robot, which is presented in Figure 4.8 (a and c). The system fuses position data from a webcam and two optical mouse sensors. The webcam is positioned directly above the workspace, mounted on a fixed stand, and tracks the robot's absolute position by detecting two markers fixed on top of the robot (Figure 4.8 b). Two laser optical sensors are mounted on the underside of the robot (Figure 4.8 d) and track the relative motion of the robot with respect to the surface on which it is placed. Utilizing the webcam enables the tracking system to record videos of rehabilitation exercises performed by a patient' which can be beneficial for medical evaluation, especially during home based rehabilitation therapy.

4.4.2 Hybrid position and Orientation Tracking - Fusion Alghorithm

Sensor fusion models greatly depend on the application, thus there is no general solution of sensor fusion (Elmenreich, 2007). A sensor fusion can by performed at multiple levels of fusion, depending on the number and types of sensors (Nicosevici *et al.*, 2004). In this work, the fusion algorithm performs a two-level fusion. First, data from two optical sensors is integrated together and secondly the data from the optical sensors and the webcam is fused.

Webcam based absolute position and orientation tracking

The absolute position tracking subsystem is based on a standard off-the-shelf Logitech Pro 9000 webcam. The webcam is attached to a fixed stand (Figure 4.8 a) and detects the motion of the robot (Figure 4.8 c) by detecting two markers, blue and red (Figure 4.8 b), which are 40 mm in diameter. The webcam absolute tracking algorithm works in 5 main steps:

1. Acquire a frame.
2. Apply a calibration filter.
3. Detect the blue marker centre coordinates.
4. Detect the red marker centre coordinates.
5. Calculate the robot's position and orientation.

The robot's 2D position and orientation are calculated based on the centre coordinates of the blue and red markers.

Optical sensors based relative position and orientation tracking

The relative position tracking is based on two ADNS-9800 laser optical mouse sensors, which are used in many computer mice designs. The optical sensors, labelled A and B, are mounted on the underside of the robot, as shown in Figure 4.8 d. The optical sensors hover around 2.4 mm above the surface and track the position changes relative to the starting position. The operation of the relative tracking system can be summarised in 3 steps:

1. Read A sensor coordinates increments.

2. Read B sensor coordinates increments.

3. Calculate robot's position and orientation increments.

Fusion Alghorithm

The data sample rate is different for both the webcam and the optical sensors. The webcam sampling frequency, which is inherently slower than the optical sensor sampling frequency, is assumed to always be slower than the sampling frequency of the optical sensors. The fused trajectory is based on optical sensors measurements with the webcam measurements being used to correct the accumulative error (drift) inherent in the optical sensor.

When the fusion algorithm is running, two different cases are utilized based on the availability of the webcam data, a case when webcam data is available and a case when it is not. This approach is related to the fusion strategy presented in (Luo *et al.*, 2012), but in the presented fusion scheme a Kalman filter is not implemented to fuse data and correct accumulative odometry errors.

The operation of the proposed tracking system can be described in 3 steps:

1. Reading measurements from the sensors.

   The generalized position vectors can be written as:

$$q_w = \begin{bmatrix} x_w \\ y_w \\ \alpha_w \end{bmatrix} \qquad \Delta q_o = \begin{bmatrix} \Delta x_o \\ \Delta y_o \\ \Delta \alpha_o \end{bmatrix} \tag{4.14}$$

   Where q_w contains the webcam absolute coordinates readings, x_w and y_w, and the absolute orientation α_w. Δq_o includes the optical sensors relative coordinates readings from the most recent position measurement, Δx_o and Δy_o, and the relative orientation $\Delta \alpha_o$.

2. Checking if the new webcam data q_w is available.

3. Calculate fused data.

(a) A case when the next q_w is not available:

$$q_f(t) = q_f(t-1) + \Delta q_o(t) \tag{4.15}$$

Where q_f is the fused position and orientation vector and t is the time step when the measurement was taken.

(b) A case when the next q_w is available:

When the new q_w is present the fused position and orientation is calculated as follows:

$$q_f(t) = q_f(t-1) + \Delta q_o(t) + w_k \times C(t_w) \tag{4.16}$$

where w is a gain and C is a position correction term. The correction term C is calculated as follows:

$$C(t_w) = q_w(t_w) - q_f(t_w - t_d) \tag{4.17}$$

where t_w is the time when webcam measurements are available, t_d is a webcam data processing delay updated during each t_w time step, and q_f was interpolated at $t_w - t_d$. To interpolate $q_f(t_w - t_d)$ 20 past measurements of q_f were stored in memory. For each iteration $t_w - t_d$ satisfies:

$$t(n-1) < t_w(n) - t_d(n) \leq t_n \tag{4.18}$$

To minimize sudden sharp changes on a trajectory graph, rather than adding the correction term C in one t time step to correct the fused position and orientation (q_f), C was divided by 10 and added during 10 time steps t. The correction C divided by 10 was implemented over 10 steps because the minimum number of optical sensors measurements between two webcam position measurements was always greater than 10 during experimental testing.

The gain w is computed based on average strength AS parameters acquired by the webcam in each frame. The AS is a gradient magnitude of the tracked marker's detected edge measured from 0 to 1. The gain w_k was computed by multiplying together gains w_b and w_r, where w_b and w_r were separately

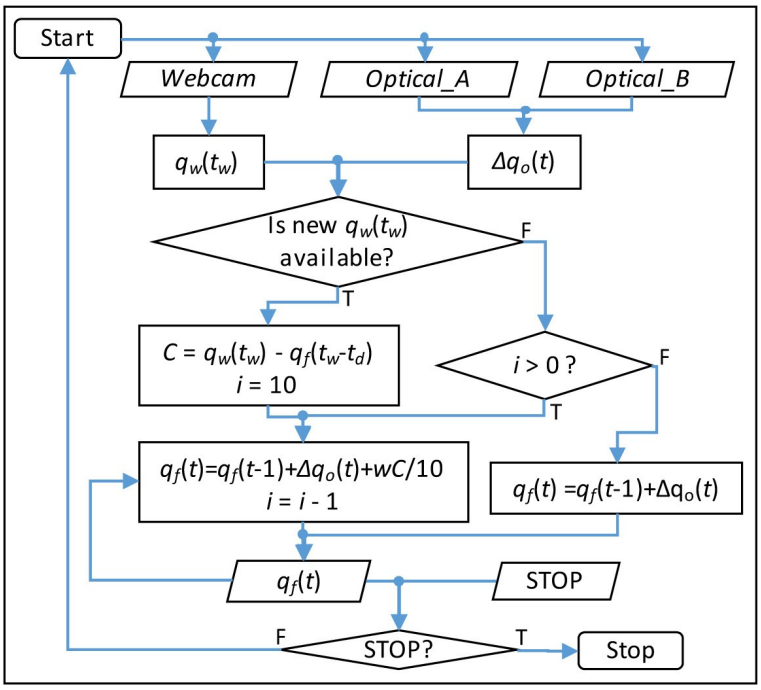

Figure 4.9: Simplified schematic diagram of the fusion scheme used to fuse position data from a webcam and two optical mouse sensors. .

determined for the blue and red markers respectively (Figure 4.8b) using the following formula:

$$w_k(t_w) = \begin{cases} 0 & \text{if } AS(t_w) < 0.9 \\ 6.25 \times AS(t_w) - 5.125 & \text{if } 0.90 \leq AS(t_w) < 0.98 \\ 1 & \text{if } 0.98 \leq AS(t_w) \end{cases} \tag{4.19}$$

which was determined experimentally to filter out the noise-corrupted webcam measurements.

The simplified diagram of the proposed fusion scheme is presented in Figure 4.9, i is the number of correction steps.

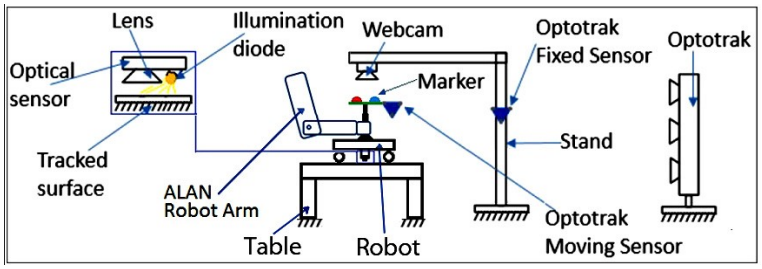

Figure 4.10: Schematic diagram of the experimental apparatus utilized to validate the performance of the hybrid position and orientation tracking system.

4.4.3 Hybrid position and Orientation Tracking - Experimental Methodology

The accuracy of the tracking system was experimentally evaluated against a reference trajectory captured at 100 Hz with Optotrak Certus motion capture system which can measure position up to +/-0.1mm. Figure 4.10 presents a diagram of the experimental apparatus utilized to collect the results. During the testing, a humanoid robotic arm, ALAN (Brookes *et al.*, 2017), developed at the University of Leeds, was used to replicate the recorded arm movements of a representative stroke patient playing a rehabilitation game. The patient trajectory data utilized was collected during a trial of the MyPAM system, an active home-based rehabilitation robot also developed at the University of Leeds (Gallagher *et al.*, 2015). A sample data set was chosen belonging to an 81 year old female who was 132 days post-stroke at the time of recruitment to the aforementioned trial. She was right arm impaired, which was also her dominant side, and she had a baseline Fugl-Meyer upper-limb assessment score of 32. The data represents the patient performing a repeated pentagram task (trying to follow a pentagram shaped trajectory for 60 seconds). In this study, 18 of the recorded 2D trajectories were tracked with the developed hybrid tracking system. As the tracked trajectories had been recorded while the patient was performing the pentagram task, the speed and range of motion was typical for rehabilitation therapy. An additional reason for selecting this patient is that she had shown clear improvement during her rehabilitation, and the question of whether the presented hybrid tracking system is accurate enough to show her therapy progress was investigated in this work.

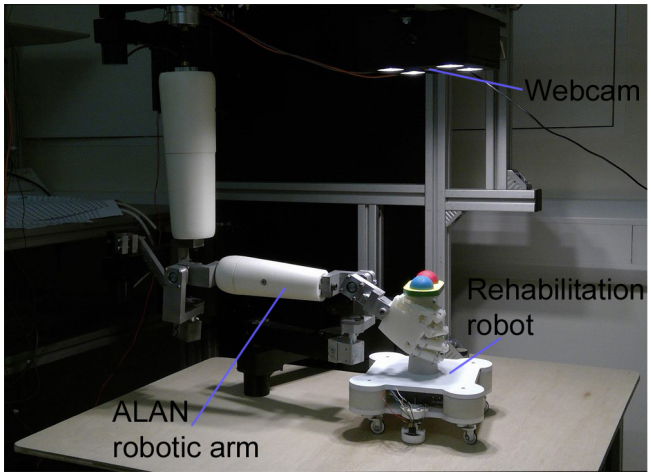

Figure 4.11: A photo taken during one of the experiments investigating the performance of the hybrid position and orientation tracking system.

Figure 4.11 presents a photo taken during one of the experiments. The photo shows the ALAN robot arm moving the rehabilitation robot, which is tracked by the developed hybrid tracking system.

During the experiments the webcam was attached to a stand and positioned over the tracked robot covering an area of 336 by 448 mm. The resolution was set to 640 by 480 pixels, which resulted in 0.7 mm to pixel ratio. To minimize tracking errors caused by the webcam's lens distortion, a calibration algorithm utilizing a polynomial distortion model and a grid of dots was employed. To check the quality of acquired webcam data, three parameters were measured at each time step: blue and red marker radius (real radius is 20 mm), distance between the centers of the markers (real value is 50 mm), and AS.

4.4.4 Hybrid position and Orientation Tracking - Experimental Results

Results for the webcam tracking subsystem

The average recorded frequency of the webcam was 5 Hz. Table 4.5 summarizes the quality measurements recorded while tracking the first pentagram assessment recreated by the ALAN robot arm. It can be noted that the detected radii for the markers by the webcam were less than the actual radii (20 mm) and are more accurate for the red maker than for the blue marker. The measurements of the distance between the markers are

Table 4.5: Summary of the webcam measurements. Mean radius of the red marker (R_r), mean radius of the blue marker(R_b), mean distance between the red and blue markers centres(d_{rb}), mean Average Strength of the red marker(AS_r) and the mean Average Strength of the blue marker(AS_b), (standard deviation in brackets)

R_r (mm)	R_b (mm)	d_{rb} (mm)	AS_r	AS_b
19.4 (±0.2)	18.8 (±0.2)	50.4 (±0.2)	0.996(±0.01)	0.98(±0.01)

accurate, 50.4mm on average, which is close to the 50mm reference value. Average strength measurements indicate (similar to the marker's radii measurements) that the quality of the red marker detection was better, however all the average strength measurements are close to the 1 reference value with the minimum detected AS value equal to 0.95 and 0.97 for the blue and red markers respectively.

Results for the optical sensors tracking subsystem

The average measured sampling frequency of the two optical sensors used was 97.2 +/- 17.6 Hz. To evaluate the quality of the measurements acquired by the optical sensors, surface quality measurements (Squal, measured from 0 to 169) were recorded during each t time step by the optical sensor itself. While tracking the first pentagram assesment recreated by the ALAN robot arm, the Squal measurements were 38.5 +/- 5.3 for the optical sensor A and 35.4 +/-5.3 for the optical sensor B. These values indicate correct operation of the sensors and are similar to Squal values recorded for the smooth MDF surface presented in (Wojewoda *et al.*, 2016). A smooth Plywood surface was utilized in this instance.

Sample results for the fusion tracking system

Figure 4.12 presents the XY recorded trajectories for the assessment 1 (out of 18) played by the patient.

Figure 4.13 presents sample X, Y coordinate, and angle of rotation plotted versus time for the XY trajectory plot shown in Figure 4.12.

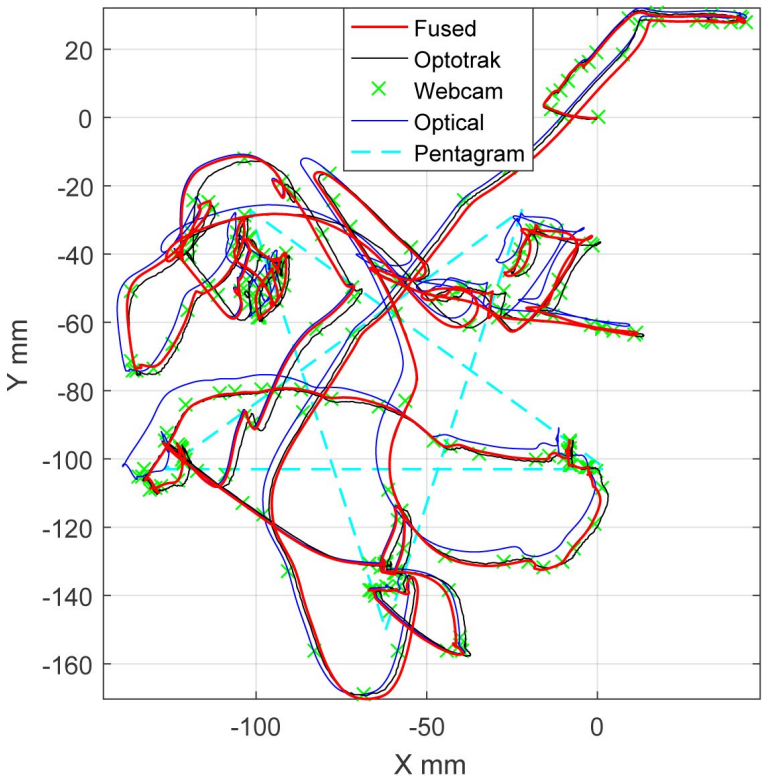

Figure 4.12: XY trajectory graph for Fusion, Optotrak, Webcam and Optical sensor-recorded trajectories for the pentagram assesment 1 performed by the patient.

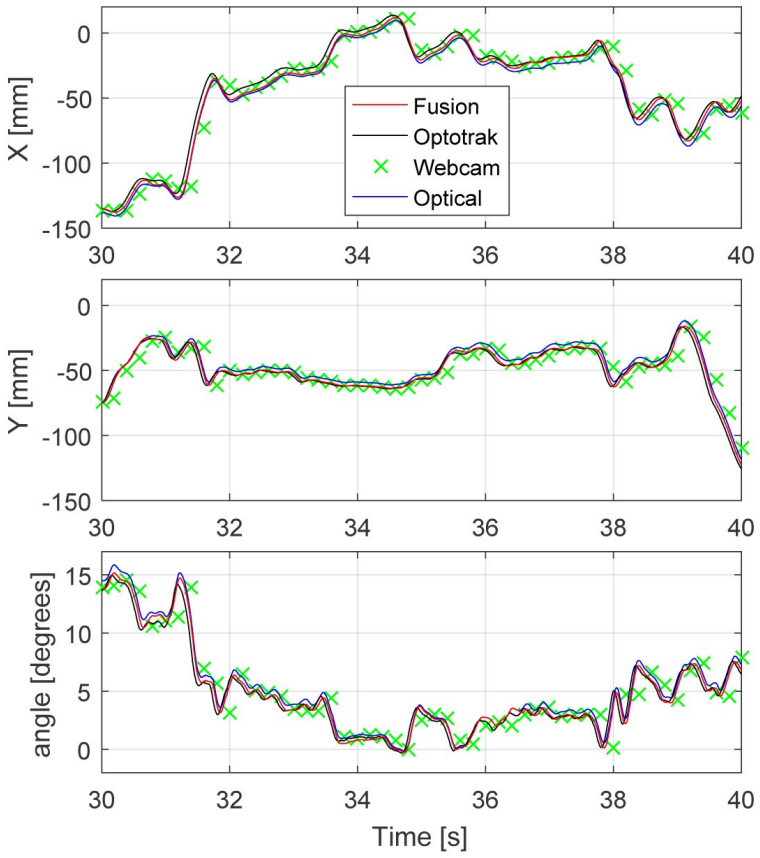

Figure 4.13: X, Y coordinates, and angle of rotation plots vs time (10s of 60s) for the pentagram assesment 1 performed by the patient.

Summary of fusion tracking results

Figure 4.14 summarizes the average 2D tracking and orientation accuracy of the hybrid tracking system. In both the position and orientation tracking, the calculated average RMSEs confirm that the fusion algorithm improves the accuracy by fusing data from the optical sensors and the webcam.

Suitability for use in post-stroke rehabilitation therapy

To investigate the suitability of the developed tracking system for an application in upper-limb robotic rehabilitation, recovery trends for path length, path length time and normalized jerk were compared between the fusion and Optotrak recorded trajectories as presented in Figure 4.15. The path length is the sum of all of the component movement lengths between each point to point movement on the pentagram assessment. For each of the 18 assessments, an average length of the trajectory the patient needed to connect the vertices of the pentagram was calculated (Culmer *et al.*, 2009). Path length time is the time the patient took to move between pentagram vertices, averaged for each of the 18 assessments. The normalized jerk is the derivative of acceleration and measures jerkiness. Jerk is used to describe smoothness of movement (it is minimized in a smooth movement) and is normalized with respect to distance and time, therefore it is unit less, so the trajectories of different lengths and durations can be compared (Culmer *et al.*, 2009).

The recovery trends for PL, PLT and NJ for fusion and Optotrak data plotted in Figure 4.15 were compared by calculating an average percentage difference for all assessment as it is presented in Figure 4.16. The ideal average percentage values for the fusion would be equal to Optotrak reference values if they perfectly matched the recovery trends recorded by the Optotrak. Average PL, PLT and NJ data for the optical sensors and the webcam is plotted for comparison.

4.4.5 Hybrid position and Orientation Tracking - Discussion

Similarly to the results shown in (Wojewoda *et al.*, 2016), which is coverd in section 4.3, the results comparing the RMSE (Figure 4.14) have confirmed that utilizing the proposed fusion scheme gives more accurate results than if the webcam and optical sensors were used alone. In this work, the functionality of the hybrid position tracking system was

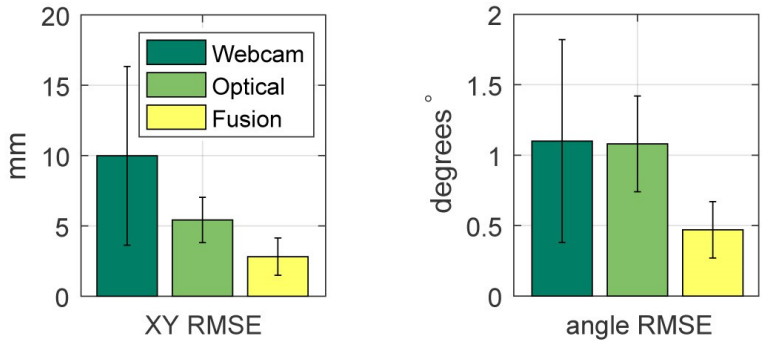

Figure 4.14: Average root mean square error calculated for 18 data sets for 2D XY coordinates and orientation (confidence intervals represent standard deviation).

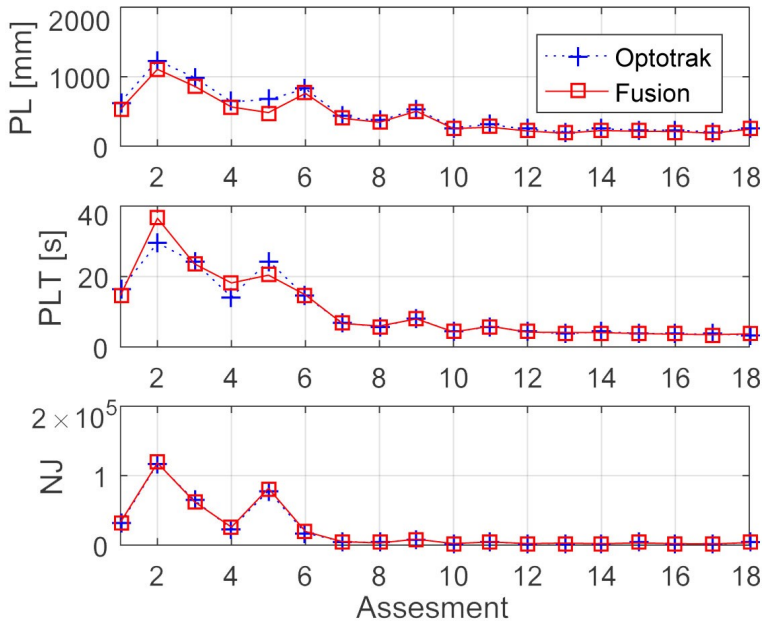

Figure 4.15: Average root mean square error calculated for 18 data sets for 2D XY coordinates and orientation.

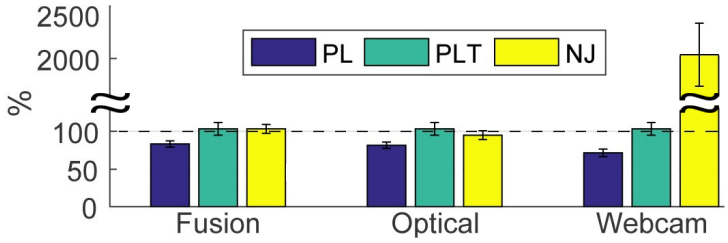

Figure 4.16: Path length(PL), path length time (PLT), and normalized jerk (NJ) average percentage values calculated for the fusion tracking system, the optical sensors and the webcam for all 18 assesments compared to 100% Optotrak average reference values (confidence intervals represent standard deviation).

extended to orientation tracking and likewise in the case of the position, the orientation tracking also benefits from the fusion scheme providing more accurate orientation results.

Also, compared to the results in (Wojewoda *et al.*, 2016), the fusion trajectory RMS error average has improved from 6.8 +/- 3.4mm to 2.8 +/- 2.6mm, even though the webcam frame rate was lowered from 10 Hz to 5 Hz. This is due to a new calibration method being employed. The webcam tracking presented in (Wojewoda *et al.*, 2016) used a division distortion algorithm and in this case a polynomial distortion model was used. It can also be noted that the average RMS error for the optical sensors-tracked trajectory has decreased compared to the optical tracked trajectory average RMS error in (Wojewoda *et al.*, 2016). It might be caused the fact that in this study two optical sensors separated by a distance of 180mm were used together, compared to only one sensor used in (Wojewoda *et al.*, 2016). As presented in (Wojewoda *et al.*, 2016), it has been shown that utilizing the average strength as the quality indicator of the webcam position measurements can be an effective approach to minimize the effect of noise in webcam measurements on the final fused trajectory. In future work, to minimize the changes of AS with the changes of light intensity of the scene, the markers (red and blue) can be illuminated from the inside to improve their visibility in low-light conditions.

Apart from AS, three more quality measurements from the webcam were recorded: the distance between the markers and the radii length of the markers (4.5). It can be noted that the measurement of the distance between the markers, 50.4 +/- 0.2mm (where 50mm is the real world measure), and the radii measurements 18.8 +/- 0.2mm (blue) and 19.4 +/- 0.2mm (red) (where 20mm is the real world measure) are feasible considering the

pixel to millimeter ratio (1pix = 0.7mm). In the future, improvements could be achieved by adjusting the settings of the color filters. However, if higher precision is needed then the best option might be increasing the resolution of the webcam.

The main requirement of the presented hybrid position and orientation tracking system is tracking the motion of the inherently safe rehabilitation robot shown in Figure 4.8c. (Perry *et al.*, 2012) has specified the global position and orientation accuracy requirements for the desktop rehab robot ArmAssist to be within +/- 10 mm and +/- 5 deg. Their tested ArmAssist can track absolute position up to 6 +/- 3 mm and orientation up to 1.2 +/- 1.4 degrees. In comparison with the ArmAssist's, the proposed absolute position and orientation tracking system is more accurate, tracking 2D position up to 2.8 +/- 2.6mm and orientation up to 0.5 +/- 0.4 degrees. In the next stage of this project, an inherently safe guiding system for the rehab robot (Figure 4.8b) will be developed and tested with the presented tracking system.

The feasibility of the proposed tracking system for detecting improvements during rehabilitation therapy was evaluated. The results shown in Figures 4.15 and 4.16 indicate that the hybrid system can be useful in tracking the recovery trends for the path length, path length time and normalized jerk. The percentage difference results (Figure 4.16) indicate that there are some inaccuracies in measuring the PL, PLT and NJ, (for fusion 90 +/- 5%, 102 +/- 10% and 102 +/- 7% respectively) but these should not affect the general recovery trends (Figure 8). The results in Figure 4.16 indicate that the webcam is not capable of tracking NJ, the average calculated value for NJ is 20 times greater than the reference value. The results in Figure 4.16 also indicate that the optical sensors can detect recovery trends with similar accuracy to the hybrid system. However, as the optical sensors are measuring relative position changes, they cannot be used alone.

During the experimental evaluation of the proposed hybrid position and orientation tracking system, the ALAN robot arm was used to replicate the recorded arm movements of a representative stroke patient completing assessment tasks during a rehabilitation program. Therefore, the tracked trajectories were representative of upper limb rehabilitation training in terms of their speed and range of motion.

4.4.6 Hybrid position and Orientation Tracking - Conclusions

A hybrid position and orientation tracking system utilizing a proposed fusion algorithm was presented and experimentally evaluated. The performance was deemed to be feasible

for consideration for tracking recovery trends in upper-limb rehabilitation. The system is designed to be implemented on a low-cost inherently safe rehabilitation table-top robot suitable for therapist-independent home-based rehabilitation therapy, which prototype was presented in Chapter 3.

4.5 Summary of The Position Tracking System

The work presented in this chapter introduces the hybrid position and orientation tracking system based on a webcam and two optical sensors and investigates its performance. First, it was investigated whether fusing webcam and optical sensor position measurements can provide more accurate position estimates than a webcam or a mouse optical sensor used alone. The presented results confirmed that the fusion of the webcam and optical sensor is beneficial and that it has the potential to be used as a 2D position tracking system for a rehabilitation robot. Secondly, a fully functional hybrid position and orientation tracking system was introduced and experimentally investigated. The hybrid tracking system was investigated in an experiment where the system was used to track the position of a rehabilitation robot which was moved by an ALAN robotic arm recreating previously recorded movements of a stroke survivor using a rehabilitation robot. The outcome of the research was that the developed hybrid position and orientation tracking system could be recommended for tracking the position of the rehabilitation robot prototype introduced in Chapter 3.

Finally, the developed hybrid position and orientation tracking system satisfies the specified product requirement regarding accuracy and monitoring patient movements during upper limb rehabilitation therapy.

Chapter 5

Inherently Safe Guidance System

5.1 Introduction

In this chapter an inherently safe guidance mechanism based on the COBOT unicycle design covered in Chapter 2 is presented and experimentally evaluated. The guidance system is designed for the table-top rehabilitation robot presented in Chapter 3. The mechanical design of the guidance module is presented in Figure 3.9, (Chapter 3). This chapter focuses on explaining the working principles and testing the performance of the inherently safe guidance system.

5.2 Recent Developments in Guidance Systems for Table-top Portable Rehabilitation Robots

To date, only a few portable rehabilitation robots able to utilize existing table space were developed. Those devices, ArmAssist (Perry *et al.*, 2012), Arm Skate (Peattie *et al.*, 2009), Arm Skate II (Wong *et al.*, 2011) and Reha-Maus (Luo *et al.*, 2012) were introduced in Table 2.4 (Chapter 2). These devices utilize omni-directional wheels. The omni-directional wheels enable these robots to move over a surface and can generate resistive force or active force, thus actively assisting arm movements. The active actuation is achieved by mounting the omni-directional wheels on electric motor shafts (Arm Assist, Arm Skate II, Reha-Maus) or electro-magnetic particle brakes (Arm Skate I). The team developing ArmAssist reported that even small misalignments of less than 0.5 degrees between a table and the omni-directional wheel axis causes noticeable vibrations during movement (Perry

et al., 2012). ArmAssit and Reha-Maus use three motors each, whereas Arm Skate II uses four motors. On the other hand, the Arm Skate I uses two electro-magnetic particle brakes.

5.3 Gap in the Knowledge – Guidance Systems for Table-top Portable Rehabilitation Robots

The state of the art table-top portable rehabilitation robots (ArmAssist, Arm Skate II, Reha-Maus) are designed for exercising upper limbs with various levels of assistance provided by the robots. Active assisted movement is beneficial when patients are not able to move their upper limbs independently. However, for improving patients who are able to move their affected arm independently, exercising without active assistance could be better (Kwakkel & Meskers, 2014). The aforementioned state-of-the-art robots might not be optimal for patient-active (robot-passive) training, as the patient must overcome the resistance of electric motors to move the robot. A solution which might be more suitable for patient-active (robot-passive) training is the unicycle COBOT mechanism which was mentioned in Chapter 2. The unicycle COBOT mechanism can generate virtual constrains, but does not create additional resistance in the movement direction.

5.4 Requirements of the Guidance System

Most of the requirements concerning the guidance mechanism are covered in Chapter 3 product requirements. The most important requirements concerning the guidance mechanism for the developed rehabilitation robot are:

1. Constraining patients' movements by creating virtual constrains.
2. Inherently safe design.
3. Accurate movement guidance up to 150 mm/s.
4. Must fit into the prototype presented in Chapter 3.

5.5 Guidance System

The mechanical design part of the guidance system was presented in Figure 3.7 in Chapter 3. The design utilizes the COBOT unicycle design instead of omni-directional wheels, a solution which was not investigated in any table-top rehabilitation robot to date (according to the author's knowledge). The COBOT guidance mechanism is employed together with casters to create an inherently safe (patient-active) 2D movement guidance system. The custom designed COBOT guidance system and all its elements are shown in Figure 5.1. At this stage of the project a stepper motor (Nema 17) was selected for the design as it provides high torque and the COBOT guidance mechanism can be mounted directly on the motor shaft. Predicting the exact torque specification for the motor is very difficult as it can be affected by several factors such as generated friction and movement of the robot. The selected stepper motor offers holding torque of 4.4 kg*cm which is deemed to be more than sufficient for its application. The exact torque generated by the motor can be calculated based on the current drawn by the motor during movements with the guidance system working. A stepper motor is also relatively easy to control and holds the desired wheel angle well. The rotation of the guidance module wheels is measured with two sensors: a relative encoder and a slot sensor. The slot sensor combined with the relative encoder creates an absolute encoder. When the guidance system is powered, the stepper motor rotates until the slot sensor detects the slot. There is only one slot. Once the slot is detected, the absolute encoder is initialized and the stepper motor can rotate the wheels to the desired absolute angle. The stepper motor is controlled with a stepper motor driver connected to a control board and it is set to perform half-steps (0.9 deg) at a time. The stepper motor used was spinning at 1.1 rev/s which was deemed to be satisfactory based on simulation plots presented in Figure 5.9 which are presented later in this Chapter.

5.5.1 Controller Design

In this research a simple closed loop controller for a stepper motor was designed. The schematic diagram of the utilized control scheme is presented in Figure 5.2 and the simplified schematic diagram of the controller algorithm is presented in Figure 5.3. The main purpose of the controller is to change the rotation of the COBOT wheels to the desired angle which is calculated based on the position of the robot and the position of a target

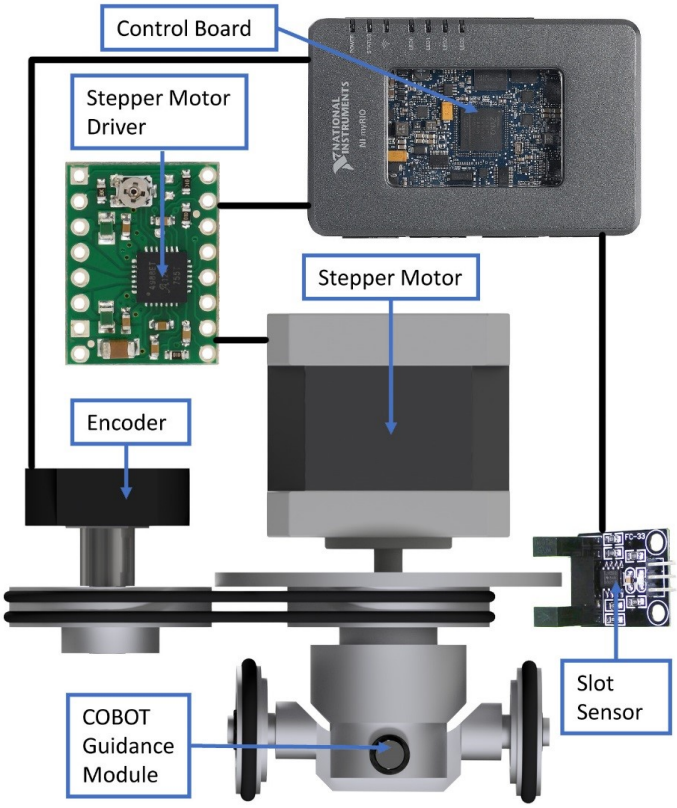

Figure 5.1: The developed COBOT dual wheel guidance system with all major components.

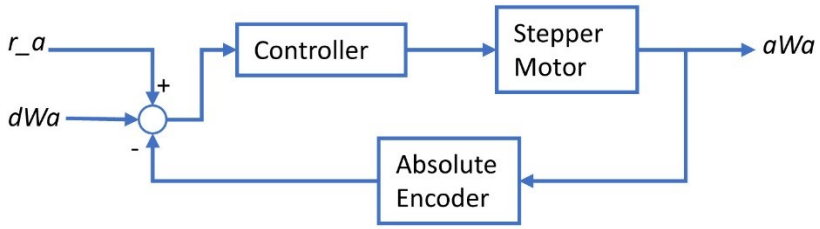

Figure 5.2: The simplified diagram of the guidance system control scheme. The inputs to the system are the desired wheel angle (dWa) and robot rotation angle (r_a), while the output is the actual wheel angle (aWa).

point. The controller checks the difference between the actual (aWa) and desired COBOT wheel angles (dWa) during each iteration, accounting for the rotation of the robot (r_a). If the difference between the desired wheel angle and the actual wheel angle is greater than 1 degree, the stepper motor performs 0.9-degree steps until the difference is less than 1 degree. The control algorithm was realized using the LabVIEW programming language running in a real-time NI myRIO control board. The presented controller is completely dependent on the developed position tracking system presented in Chapter 4. The tracking system provides real-time information regarding the position and rotation of the robot, which are crucial in computing the desired real-time rotation of the COBOT wheels.

5.5.2 Point-to-Point Movement and Point Hit-and-Miss

The developed COBOT guidance system can follow (while a force is applied) predefined 2D virtual constrains. As the position of the robot changes, the absolute angle of the COBOT wheels changes to follow a programmed path. The programmed path is defined with a sequence of 2D points. When a point is reached, the guidance system guides the robot to the next point in the sequence and after reaching the next point this process is repeated. Each point is in the centre of a 6 by 6 mm square and a point is reached if the position of the robot is detected to be anywhere in the square. In addition to the 6 by 6 mm square there is a larger 12 by 12 mm square with the same centre point, which is utilized to detect a situation when the robot passes close to the small square but misses it. In this case if the robot enters the big square and leaves it without entering the small

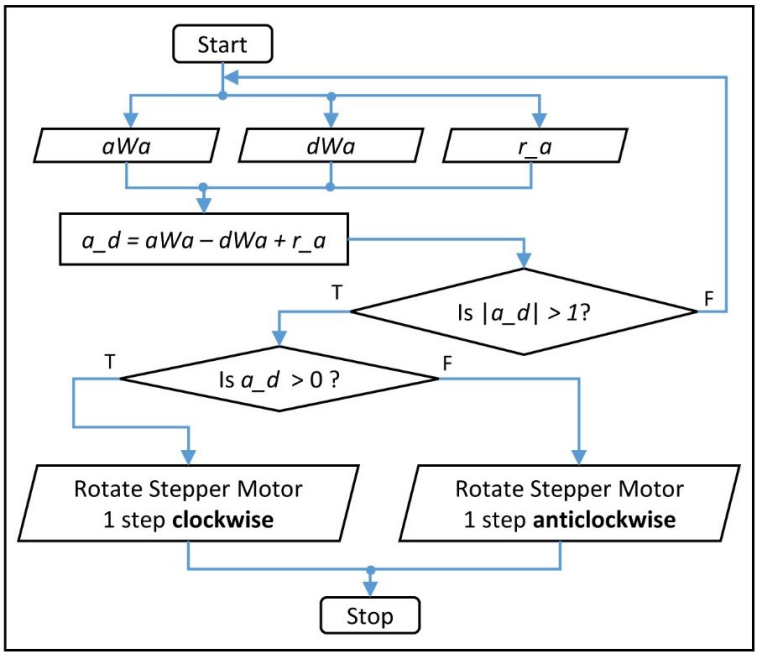

Figure 5.3: The simplified algorithm flowchart of the controller utilized for control of the stepper motor.

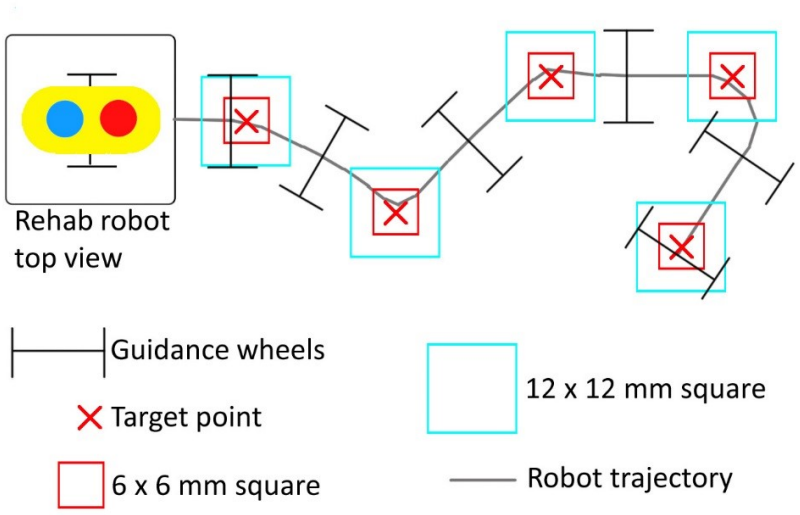

Figure 5.4: The ideal performance of the guidance system while following a trajectory defined with 5 points.

square, the point is marked as hit and the robot is guided to the next point. An example of the robot ideally following a path consisting of 5 points is shown in Figure 5.4.

Figure 5.5 presents an example of a scenario where the robot moves at a higher velocity and misses the target, but enters the large hit-and-miss large square zone and the square is counted as hit. This solution was introduced as some problems with the guidance system accuracy where expected during the experimental testing.

5.6 Guidance System Experiment

The guidance system was tested in an experiment investigating its ability to stay on a trajectory defined with a sequence of points. The system is inherently safe and in order to move an external force had to be applied to move the robot. The main focus of the experiment was the repeatability and performance of the system at different trajectory shapes and velocities. The response of the designed guidance mechanism to disturbances was not investigated experimentally. However, the static friction force required to overcome in order to push (slip) the robot in an undesired direction (the direction which is different to the direction in which the COBOT wheels are constraining the movement) was measured to be approximately 7 N. This suggests that any disturbances which are

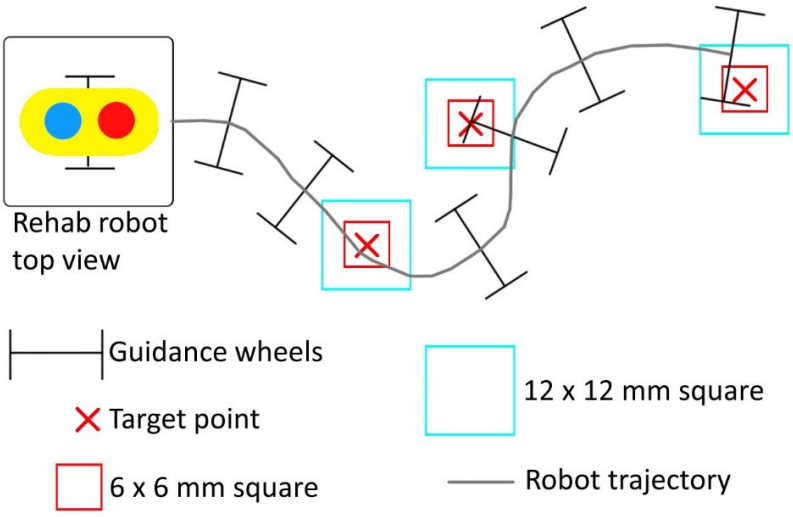

Figure 5.5: The performance of the guidance system while following a trajectory defined with 3 points at high velocity where the robot misses the target but goes through the large hit-and-miss square.

less than 7 N in magnitude should not affect the position of the robot. In the case where the disturbing force would be greater than 7 N the robot would be pushed away from the desired trajectory. However, this should not have any significant effect on the performance of the COBOT controller as it would detect the slip and try to guide the robot to the correct target point even if some of disturbances acting on the robot are greater than 7 N.

5.6.1 Experimental Procedure

The following experimental questions were formulated:

1. Is the developed guidance system able to follow a predefined trajectory when a force is applied to the robot?
2. How accurate is the guidance system?
3. How does the velocity of movement affect the performance of the guidance system?
4. How does the shape and number of points affect the performance of the guidance system?

5. Is the performance of the guidance system stable during 30 min operation?

6. Is the robot ready for testing with healthy human participants?

To answer the experimental questions, the following experimental variables were formulated:

1. Two different sine wave trajectories:
   (a) The length of a sine wave is 600 mm.
   (b) The first trajectory defined with 4 points.
   (c) The second trajectory defined with 16 points.
2. Four different amplitudes of the sine wave trajectories:
   (a) 0 mm
   (b) 50 mm
   (c) 100 mm
   (d) 150 mm
3. Three different robot movement velocities:
   (a) 50 mm/s
   (b) 100 mm/s
   (c) 150 mm/s
4. The number of repetitions:
   (a) 5 repetitions of trajectory test (less than 3 minutes).
   (b) 30 minutes long stability test.

Figure 5.6 presents the shapes of trajectories used during the experiment.

To answer all of the experimental questions 14 experiments were performed. The settings used during each of the 14 experiments are presented in Table 5.1.

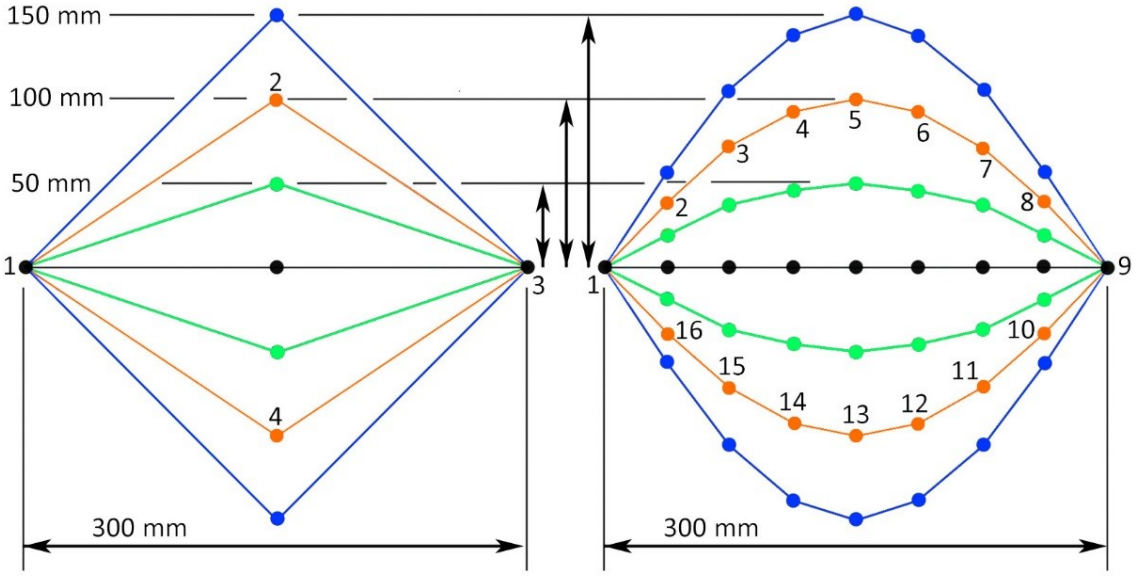

Figure 5.6: Eight trajectories used during experiments. The trajectories on the left are defined with 4 points, whereas the trajectories on the right are defined with 16 points. Points on the two of the trajectories are numbered in order in which they are in the sequence.

Table 5.1: A list of the performed experiments.

Experiment number	Trajectory Points	Repetitions	Velocity mm/s	Amplitude
1	4	5	100	50
2	4	5	100	100
3	4	5	100	150
4	4	5	100	0
5	4	5	50	100
6	4	5	150	100
7	16	5	100	50
8	16	5	100	100
9	16	5	100	150
10	16	5	100	0
11	16	5	50	100
12	16	5	150	100
13	4	30 minutes	100	100
14	16	30 minutes	100	100

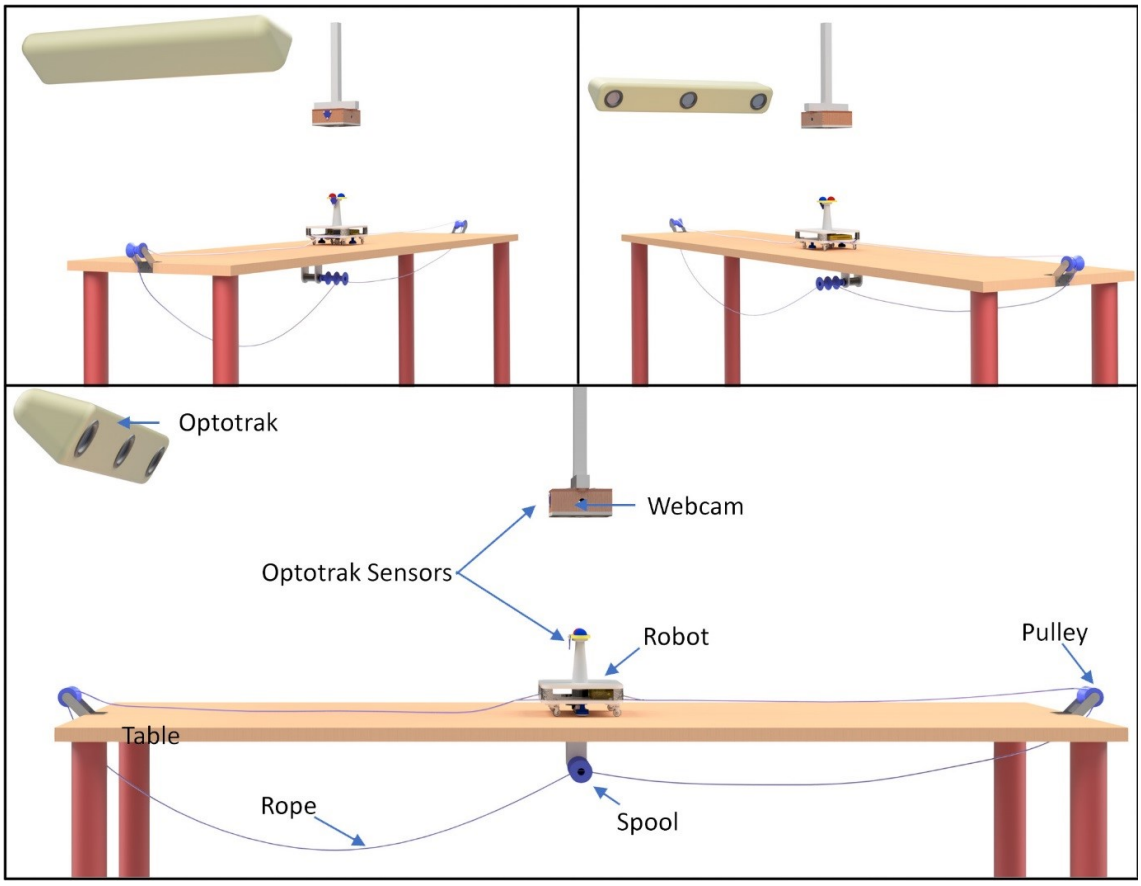

Figure 5.7: The experimental apparatus used during the guidance system testing. The webcam and the Optotrak are mounted to the celling.

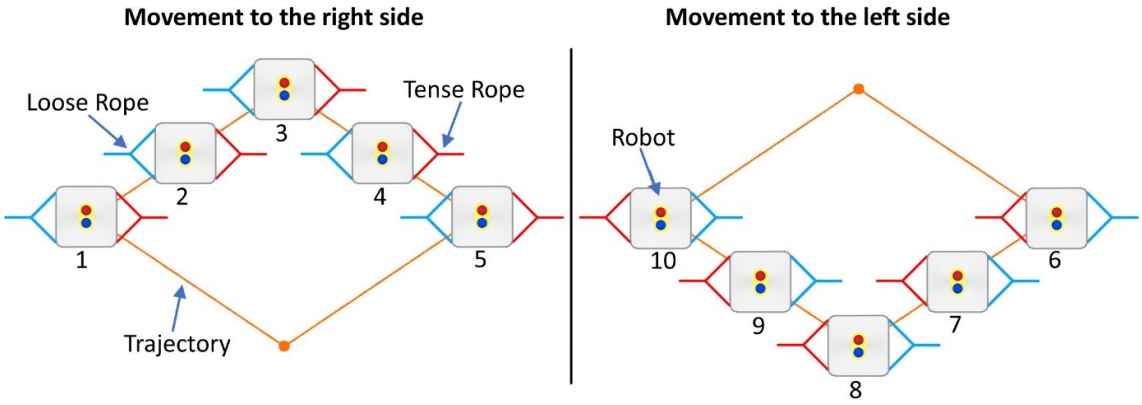

Figure 5.8: The visualization of the robot (top view) ideal performance while the guidance system is guiding it along a trajectory defined with 4 points (100 mm amplitude). The position of the robot depends only on the tension of the rope and the performance of the guidance system.

5.6.2 Experimental Apparatus

The experimental apparatus used during the guidance system testing is presented in Figure 5.7.

The experimental apparatus was set up to pull the rehabilitation robot left and right at the distance of 300 mm. A rope was attached to the robot at both ends and it was wound on a spool attached to a motor shaft. To allow the guidance system to guide the robot, the rope was loose on one side. While the robot was pulled to the left side of the desk, the rope on the right side was loose. On the other hand, when the robot was pulled to the right side of the desk, the rope to the left of the robot was loose. Figure 5.8 presents a visualisation of the robot ideal performance while the robot moves from the left to the right and back to the left (one trajectory repetition).

The guidance system is designed for point to point movement, which could be made by moving on a straight line connecting two points. However, due to the design characteristics the guidance system is not capable of staying exactly on the ideal (straight line between two points) path. After reaching a target point, the COBOT guidance wheels must rotate to guide to the next point. The faster the rotation of the COBOT guidance wheels, the smaller the difference between the actual path travelled by the robot and the actual path.

Figure 5.9 presents simulations of the robot ideal performance in experiments 3, 6, 9 and 12. The simulations consider ideal performance of the guidance system and maximum rolling friction (no slip) between the COBOT guidance wheels and the surface of a table. Robot inertia and friction forces are also neglected. Each plot in Figure 5.9 presents one repetition of the trajectory at a constant velocity, 1.1 rev/s motor rotation and 0.01 seconds time interval. The starting angle of the COBOT guidance wheels is 0 degrees (positive X axis direction). The simulations results predict that the designed COBOT guidance mechanism should be able to successfully complete all the experiments (hitting all of the target points).

The minimum velocity at which the COBOT guidance system cannot hit all the target points on a trajectory was investigated for the trajectories from experiments 6 and 12 and the simulation results are presented in Figure 5.10. According to the simulation results presented in Figure 5.10 the guidance mechanism is more effective (the robot can move faster) when the distance between target points is larger. The velocity of movement was increased in 10 mm/s increments and it was found that the guidance system is not able to hit all the target points at 650 mm/s and 190 mm/s, for the 4 point and 16 point trajectories (100 mm amplitude each) respectively.

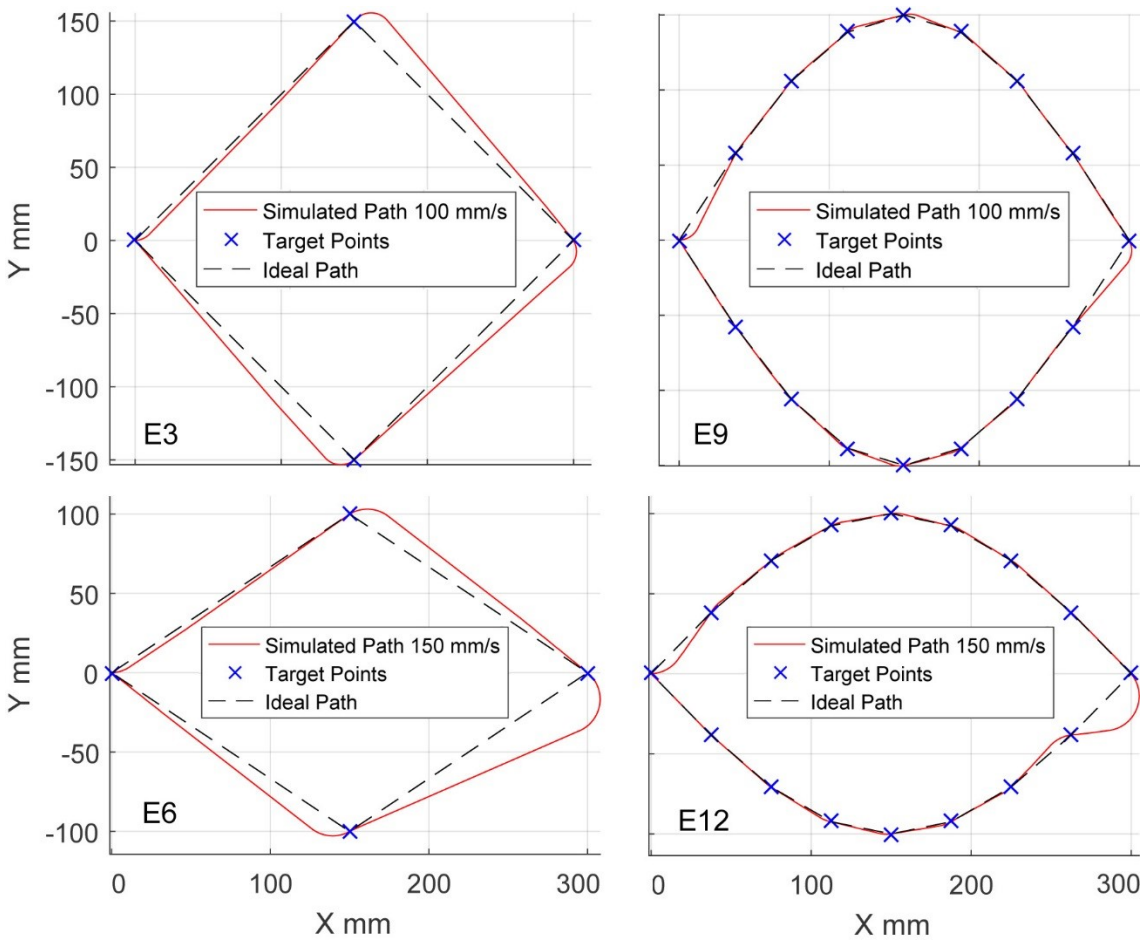

Figure 5.9: Simulations of the COBOT guidance system performance in experiments 3, 6, 9 and 12 for one repetition of the trajectory at constant velocities, 1.1 rev/s stepper motor rotation and 0.01 s time interval.

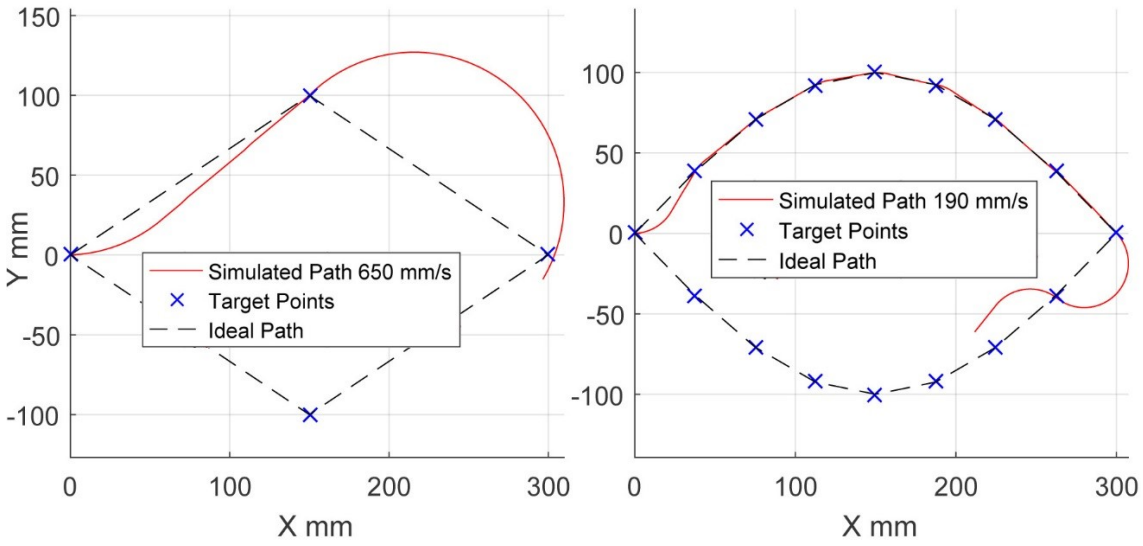

Figure 5.10: Plots presenting simulations of minimum velocities (10 mm/s intervals) at which the guidance system cannot hit all the points on the trajectories.

5.6.3 Modifications of the Position Tracking System

The developed guidance system is dependent on measurements from the position and orientation tracking system which was introduced in Chapter 4. The orientation of the guidance COBOT wheels is changed based on the most recent position and orientation of the robot and the position of a target point. The aforementioned position and orientation tracking system was slightly modified before the guidance system testing started to maximise its performance. Two significant changes were made. First, the frequency of the webcam acquisition was increased to 10 Hz, the maximum possible FPS for the webcam with the webcam calibration applied. Secondly, the method for calculating the error term was modified (equation 4.17). Previously, the error term was calculated by interpolating q_f (fused position and orientation) at t_w (time when webcam data is available), which is working well when the time measurements are precise. However, to reduce the reliance of the position and orientation tracking system on precise time measurements, the error term was calculated in a different way. Instead of finding one q_f interpolated at t_w, a sequence of q_f points is selected for a time threshold (less than 0.1 s) during which the latest webcam measurement is taken. The elements in the sequence (q_f) are compared

with the webcam measurement (q_w) by calculating a distance separating the q_w with each of theq_f points. The error term is calculated based on the q_f point which is the closest to the q_w. The rest of the algorithm is the same as it is presented in the Chapter 4.

The main motivation for the modification was the stability and repeatability of the tracking system performance. The previous method of fusing webcam and optical sensors measurements was highly dependent on precise time measurements and calculation of the webcam measurements delay. The experiments validating the performance of the hybrid position and orientation tracking system in Chapter 4 proofed the accuracy while tracking 18 pentagram tasks recreated by ALAN robotic arm and originally performed by a stroke survivor, each task was approximately 1 min long. However, this testing was not long enough to investigate the stability of the system, which was only done during the guidance system presented in this chapter. Longer pre-experimental tests with the developed robot with the guidance system employed revealed some stability problems caused by the performance of the hybrid tracking system. These did not affect the overall accuracy of position estimations, but occasionally occurring errors were disturbing the performance of the guidance system. This was predicted to affect the guidance system results presented in this chapter.

5.6.4 Experimental Results

All the 14 planned experiments were conducted. Photos taken during the experiments are presented in Figure 5.11. The spool utilized during the experiments has a 'dual spool' design. The reason for this is that the first design of the spool used had both ends of the rope on one spool and the rope was tangling when the motor was spinning. It was found that tangling of the rope can be avoided by using the current design.

Figure5.12 presents results for experiments 1 to 6 (trajectories defined with 4 points).

Figure 5.13 presents results for experiments 7 to 12 (trajectories defined with 16 points).

Figure 5.14 and Figure 5.15 present results for experiments 13 and 14 respectively, the 30 minutes endurance tests.

During all the 14 experiments several measurements were acquired, such as X and Y coordinates and the orientation of the robot.

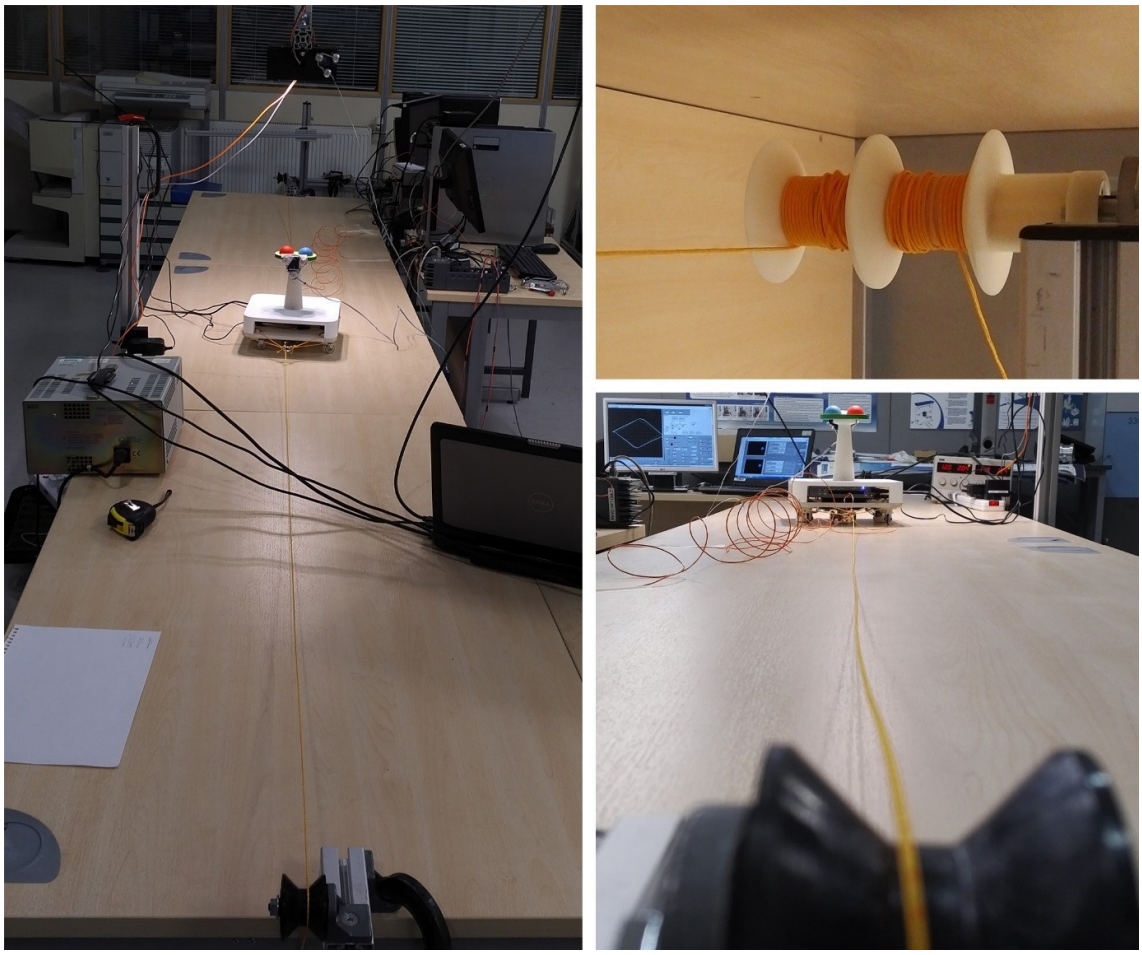

Figure 5.11: Photos taken during the guidance system experiments.

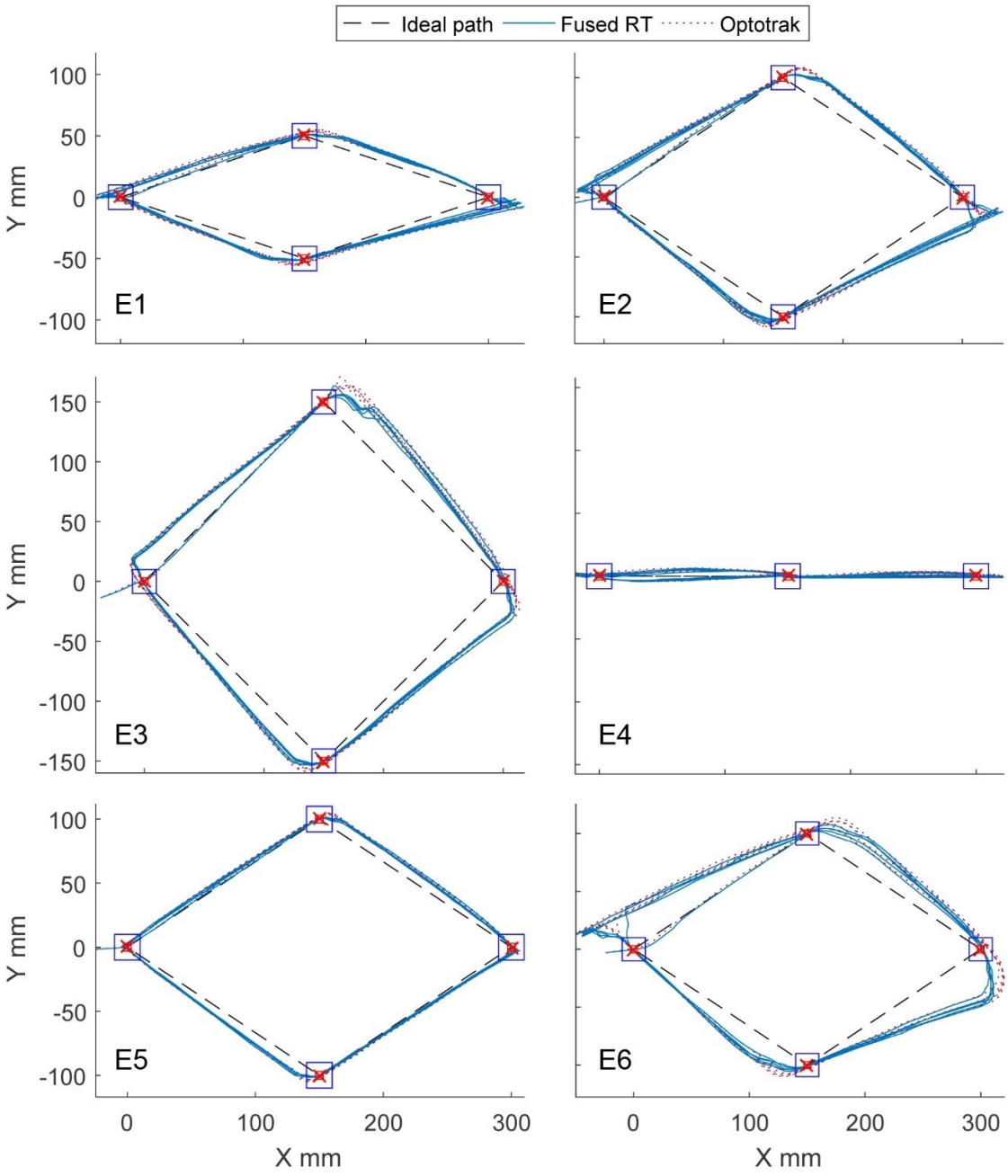

Figure 5.12: Results for experiments 1 to 6. All the paths are defined with four points and present 5 repetitions.

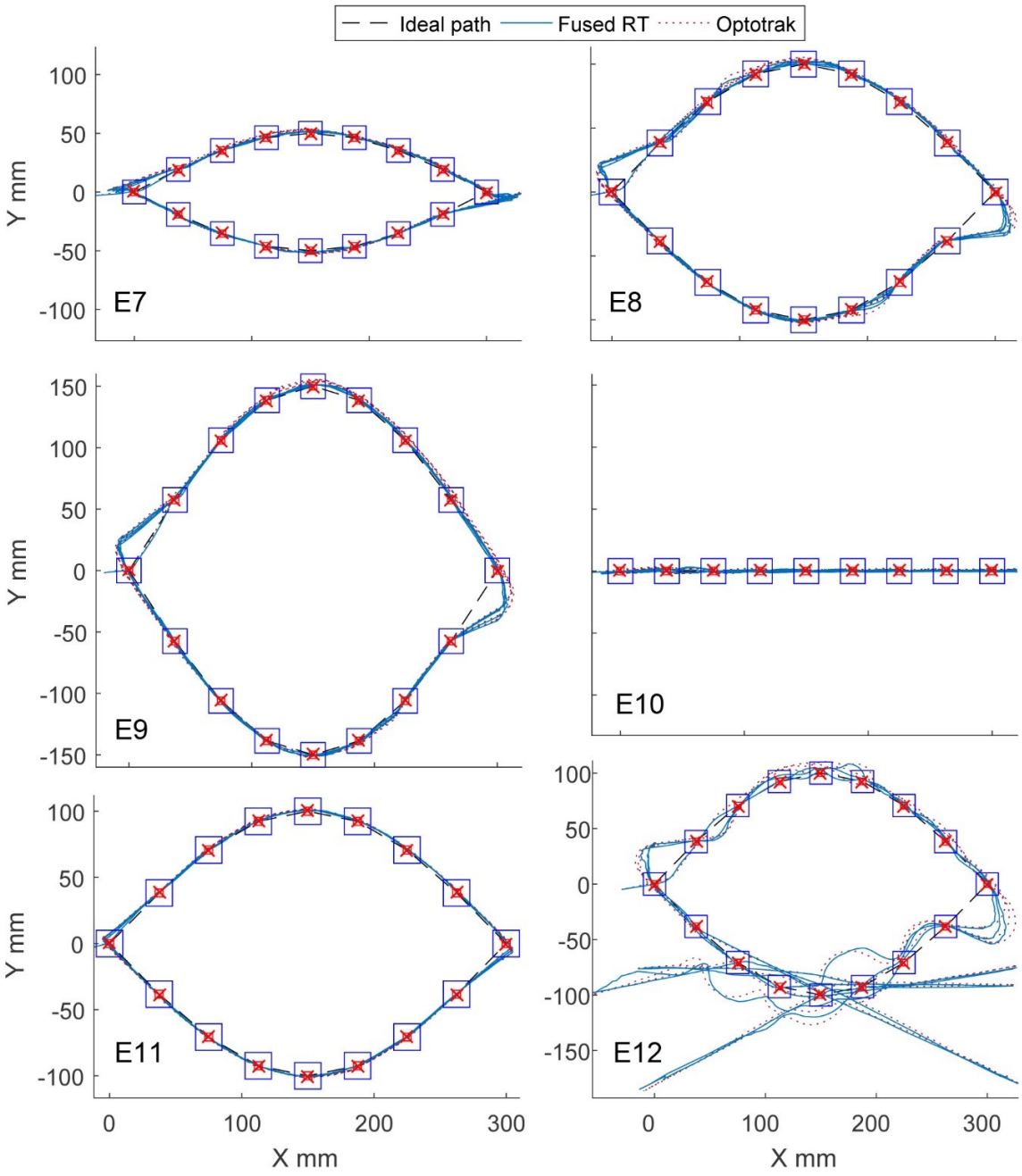

Figure 5.13: Results for experiments 7 to 12. All the paths are defined with 16 points and present 5 repetitions.

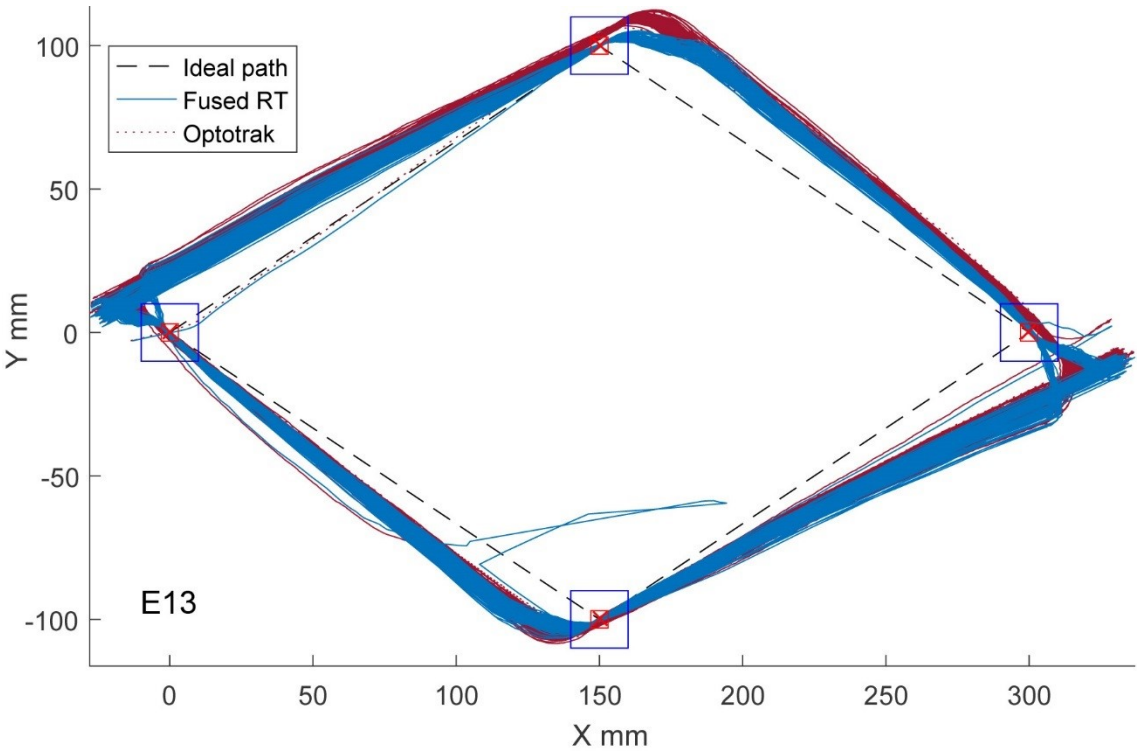

Figure 5.14: Results for the 30 minutes test of the robot continuously following the 100 mm amplitude trajectory (4 points) at 100 mm/s.

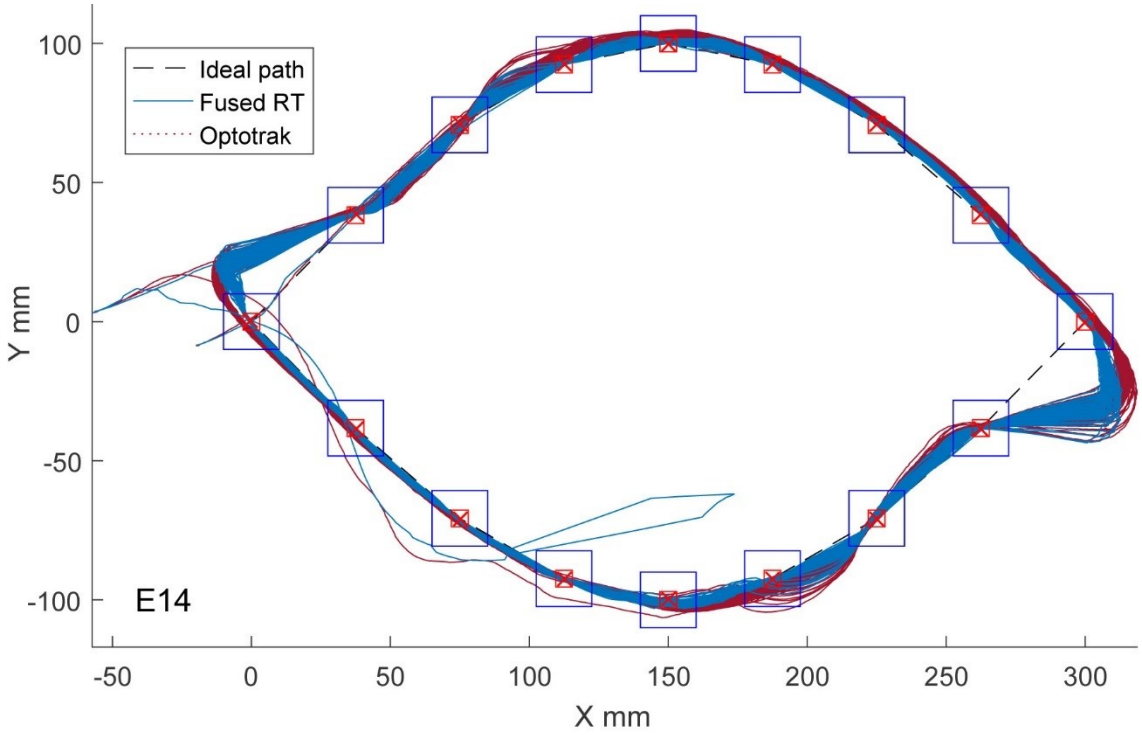

Figure 5.15: Results for the 30 minutes test of the robot continuously following the 100 mm amplitude trajectory (16 points) at 100 mm/s.

5.6.5 Results Analysis

As the position and orientation tracking algorithm was modified (webcam FPS increased to 10, and modification of the error term calculation method), the results analysis covers both the guidance system evaluation and the position and orientation tracking system evaluation.

Position Tracking Performance

The performance of the position and orientation tracking system was investigated by comparing trajectories recorded with the developed position tracking system and trajectories recorded with a commercially available motion tracking system Optotrak, which was introduced in Chapter 4.

The Optotrak was recording position data at 100 Hz, while the developed tracking system was recording at 93 (8) Hz. The subsystems of the position and orientation tracking system, the webcam and optical sensors, were recording at 10 (0.02) Hz and 93 (8) Hz respectively.

As the performance of the position and orientation tracking was investigated in details in Chapter 4, the analysed results presented in this section compare only Optotrak recorded data with real time fused data. Although the webcam and optical sensors recorded results are not presented, it was noticed that similarly to the results presented in Chapter 4, the fused position and orientation data is again combining the benefits of the webcam and optical sensors providing more accurate position and orientation tracking.

Figure 5.16 presents real time root mean square error results (RT RMSE) results for the experiments 1, 2, 3, 4 (4 points trajectories) and experiments 7, 8, 9, 10 (16 points trajectories) during which the velocity of movement was 100 mm/s. The RT RMSE takes time into consideration, which means that for Optotrak data available at a point in time, the RT RMSE is calculated using only the fused position and orientation data available before that point in time.

Figure 5.17 presents real time root mean square error results for experiments 2, 5, 6, 8, 11, 12 conducted at three different velocities and 100 mm trajectory amplitude.

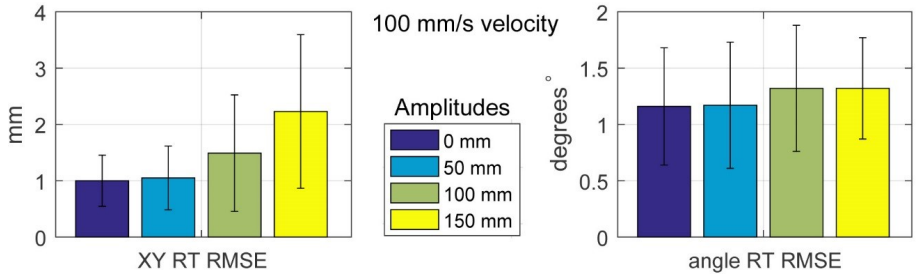

Figure 5.16: Real Time Root Mean Square Error calculated for experiments 1, 2, 3, 4, 7, 8, 9, 10, where the robot was moving at 100 mm/s. The RT RMSE is calculated for fused position data (recorded with the developed position tracking system) using as a reference Optotrak recorded position data. The analysed experiments cover four different trajectories amplitudes and both 4 and 16 points trajectories.

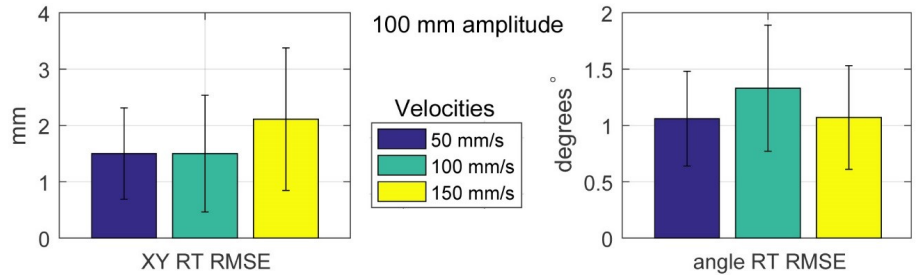

Figure 5.17: Real Time Root Mean Square results for experiments 2, 5, 6, 8, 11, 12, where the trajectory amplitude was 100 mm. RT RMSE is calculated for fused position data (recorded with the developed position tracking system) using as a reference Optotrak recorded position data. The analysed experiments cover three different movement velocities and both 4 and 16 points trajectories. Confidence intervals represent standard deviation.

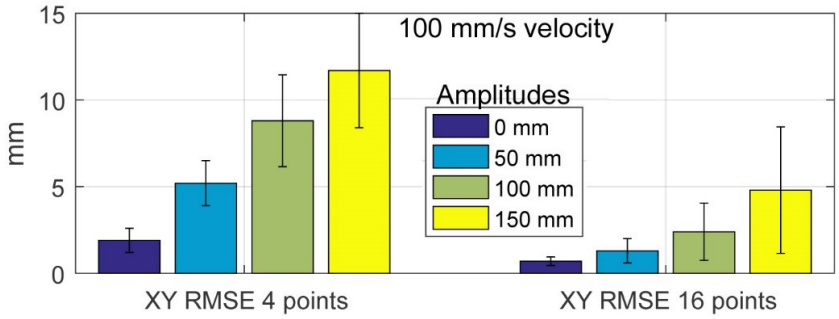

Figure 5.18: Average root mean square error (RMSE) for the experiments 1, 2, 3, 4 (4 targets trajectories) and the experiments 7, 8, 9, 10 (16 targets trajectories). Confidence intervals represent standard deviation.

Guidance System Performance

The performance of the guidance system was investigated by comparing together the actual trajectory (Fused RT) of the robot with the desired trajectory. Ideally, the actual trajectory would have the same shape as the desired trajectory, but the experiments (Figure 5.12 and 5.12) have shown noticeable differences. To quantify the differences between the actual and ideal paths the root mean square error (RMSE) was calculated. In this case the RMSE is not time dependent (not RT RMSE) and it is calculated each point of the actual path as a minimum distance to the desired path.

Figure 5.18 presents the average root mean square error summarizing the difference between the ideal and actual robot path followed at 100 mm/s separately for the 4 points (experiments 1, 2, 3, 4) and 16 points trajectories (experiments 7, 8, 9, 10) and 4 different trajectory amplitudes each.

Figure 5.19 presents the average root mean square results summarizing the difference between the ideal and actual path followed by the robot at three velocities (50, 100 and 150 mm/s) and 100 mm amplitude 4 (experiments 2, 5, 6) and 16 (experiments 8, 11, 12) point target trajectories.

5.7 Discussion - Guidance System

First, the guidance system, which design was presented in Chapter 3, was successfully assembled and implemented in the inherently safe rehabilitation robot. It seems that

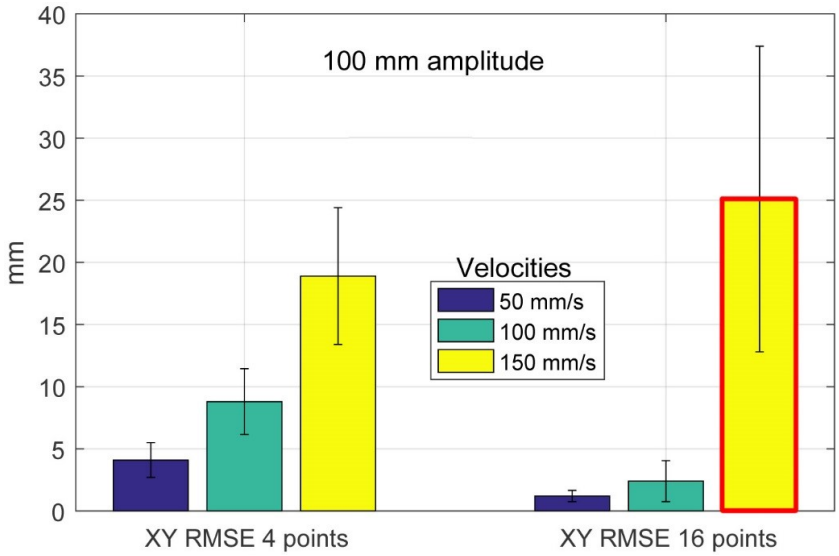

Figure 5.19: Average root mean square error (RMSE) for the experiments 2, 5, 6 (4 targets trajectories) and the experiments 8, 11, 12 (16 targets trajectories). Confidence intervals represent standard deviation.

there is no need for significant changes in the design. However, some optimisation solutions could make the guidance design more compact and robust. The relative encoder, which is connected to the motor shaft with a pulley and two rubber belts, could be mounted directly on the motor shaft. To make this possible the motor shaft would have to be longer and sticking out of the motor on both ends.

The experimental setup with the rope attached to the spool on the DC motor and to the robot pulling it right and left was successfully implemented and was very robust. If modifications are made to the guidance system, the setup can be highly recommended for future experiments. However, the choice of possible trajectories is limited. When the robot is pulled to the left, no movement to the right is possible. Similarly, when the robot is pulled to the right, no movement to the left is possible.

In total, 14 experiments were performed and 13 out of 14 are considered to be fully successful. The only experiment which cannot be considered fully successful is the experiment 12. Figure 5.13 E12 shows that during the experiment 12 the robot was able to follow the targets on the first part of the trajectory (movement from the left to the right) but failed to follow the targets on the second part of the trajectory (movement from

the right to the left). Simulation for the experiment 12 performed before the experiment presented in Figure 5.9 shows that the guidance system should be able to guide the robot to all the targets on the trajectory. However, the simulation neglects the inertia of the robot and considers that there is no slippage between the table surface and the COBOT guidance wheels and it seems that some slippage has occurred. To minimise the possibility of slippage, the friction between the COBOT wheels and the surface should be increased. In this case, the friction can be increased by changing the rubber tyres to ones made out of rubber material which offers better grip or by mounting thicker tyres.

The simulations in Figure 5.10 indicated that when the spacing between the points is larger the robot can move faster and the experiments 11 and 12 proved this, as experiment 11 was successful and the experiment 12 failed while the robot velocity was the same in both experiments. Excluding experiment 12, in experiments 1 to 11, during which trajectories were repeated 5 times, the performance of the guidance system was as desired and the robot reached all the targets points. The guidance system has satisfied the requirement of creating 2D virtual constrains. The 30 min stability experiments presented in Figures 5.14 and 5.15 prove stability of the guidance system. All the target points were reached, apart from one recorded exemption in Figure 5.15 when the robot did not reach the 6 by 6 mm target but went through the large 12 by 12 mm square and the current target was changed to the next point in the sequence. If the large hit and miss prevention was not implemented (small 6 x 6 mm target and large 12 x 12 mm square which marks target as reached if the robot goes in and out the square without reaching the target) the experiment 14 would have failed. In both experiment 13 and 14 a flaw in the position recording is seen. It happened once in each of the 30-minute-long tests. It can be explained by webcam noise-corrupted measurements being used for position estimation, which should not have happened as the average strength (AS) filter in the tracking system should prevent this.

The modifications of the position and orientation tracking were generally successful, the overall accuracy of the position tracking has been maintained, however, a small drop in orientation tracking was observed. The reason for the orientation tracking precision decrease can be a problem with webcam marker detection due to light conditions. A solution to this is discussed in Chapter 4. However, the orientation tracking precision could also benefit from fusion algorithm optimisation.

The developed guidance system incorporates a power supply, therefore if it was to be commercialised, it would have to comply with (Directive, 1993) regulations (covered in Chapter 2) for medical devices connected to or with a power source. Any active therapeutic device designed to exchange or administer energy to or from the human body is classified as Class IIa device (Directive, 1993). The device developed in this project would have to be classified as a Class IIa medical device before commercialisation.

5.8 Summary – Guidance System

The guidance system for the developed robot was introduced and experimentally evaluated. The presented results show that in the majority of the investigated scenarios the guidance system works as intended. Stability of the system was confirmed in two 30-minute experiments. Some problems were reported, but it is recommended that the robot is tested in a user testing experiment in order to evaluate the performance of the system in a real-life scenario.

Chapter 6

User Testing

6.1 Introduction

In this chapter user testing of the developed inherently safe rehabilitation device is presented. The previous chapter (Chapter 5) showed how the robot performs when a force is applied to it. Some problems with moving to targets at higher velocities (150 mm/s) were detected. Before implementing any changes in the design, a decision was made to test the device in a real-life scenario, which in the case of this robot is to be used by people with arm movement deficiencies, especially stroke survivors. The working hypothesis was that the robot should improve point to point movement of users while the guidance module is employed. For safety and ethical reasons, the system was tested with healthy participants. 38 healthy participants were recruited for experiments where they had to reach a series of targets on predefined paths. The effect of the robot guidance on the movements of participants was investigated. Data regarding the velocity of movement and precision of movement was recorded for future development of the device.

6.2 Rationale for User Testing

The main goal of user testing was to show the repeatability and validity of the developed inherently safe device during training. Also, it was investigated whether the guidance system can improve the speed and precision of arm movements. The presented user testing is a pilot study. If it is successful, a future study with post-stroke patients could be instigated.

6.3 Participants

Thirty-eight healthy adult participants were randomly recruited for user testing between November and December 2017. Twenty-four participants were males and fifteen were females. For the purpose of analysis, each subject was numbered from 1 to 38. During the screening process all participants were interviewed by the principal investigator (the author of the thesis). The inclusion criteria were a lack of vision impairment or colour blindness that would affect participants' performance in the testing. The exclusion criterion was an inability to provide informed consent. All participants were asked to perform the experiment with their non-dominant arm. Out of the 38 subjects, 37 were right handed and one subject (subject 35) was left handed. Left or right handedness of subjects was determined by asking them which hand they use for the following tasks and for holding objects: writing, drawing, scissors, toothbrush, knife (without fork). As the performed user testing was a pilot study of the novel device that had not been investigated in a real-life scenario before, the statistical power of the experiment was calculated after the testing.

6.4 Experimental Questions

This chapter presents a study which aims to address the hypothesis that the developed robot improves the precision and speed of participants' point-to-point movements when the guidance module is employed. This relates to the following experimental questions:

1. What is the difference of participants' point-to-point movement accuracy when the guidance module is used and when it is not?
2. What is the movement velocity when the guidance module is used and when it is not used?
3. Does the guidance module make it easier to move the rehab robot to targets?
4. How does the user testing compare to the experiment presented in Chapter 5?
5. Is the robot safe to use?
6. Is the performance of the robot repeatable?
7. What are the recommendations for future development of the robot?

6.5 Experimental Setup

During the experiments, 38 participants performed point-to-point movements using the rehabilitation robot prototype which was presented in Chapter 3. Figure 6.1 presents the experimental setup during user testing and Figure 6.2 presents two of the subjects using the robot during the testing. The robot was placed on a table and the subjects were seated on a chair in front of it. A computer screen was placed in front of the subjects, leaving enough free table space to complete the experiment. The screen displayed the current position of the robot represented by a red triangle and the position of the next target as a green square. While the subjects were moving the robot, the red triangular cursor was moving on the computer screen. Only one target point (green square) was displayed on the screen at a time. When the target was reached, it disappeared and the green square was displayed in a new position. The shape of the trajectory on which the targets were appearing was outlined on the screen with a solid blue line.

In total, five various trajectories defined by a sequence of target points were utilized. The details of the used trajectories are presented in Table 6.1. Figure 6.3 presents the shapes of the five trajectories: sin4, sin16, pentagram, square and circle, with the target points numbered in the order in which they appeared on the screen during the experiments. Trajectories sin4 and sin16 (based on a sine wave) are the same as the sin4 and sin 16 trajectories utilized for the guidance system experiment in Chapter 5 and are used again so the results from the user testing can be compared with the results from the guidance experiment presented in Chapter 5. The pentagram and square trajectories were chosen to investigate the effect of the robot guidance when the subjects have to perform 36 and 90 degrees turns respectively. The last trajectory, a circle, was the only trajectory which was used in two visual feedback modes: with visual feedback on (computer screen switched on) and visual feedback off (computer screen switched off). All the other trajectories were used only with the screen switched on.

The robot was used in the experiments in two guidance modes: guidance off and guidance on. In the guidance on mode the guidance module, as it is described in Chapter 5, was used to safely guide subjects' hand movements by constraining movement direction in real-time. In the guidance off mode the guidance module was dismounted from the robot and subjects could freely move the robot in any direction. Each subject repeated movements connecting targets on each trajectory with the robot in both guidance off and

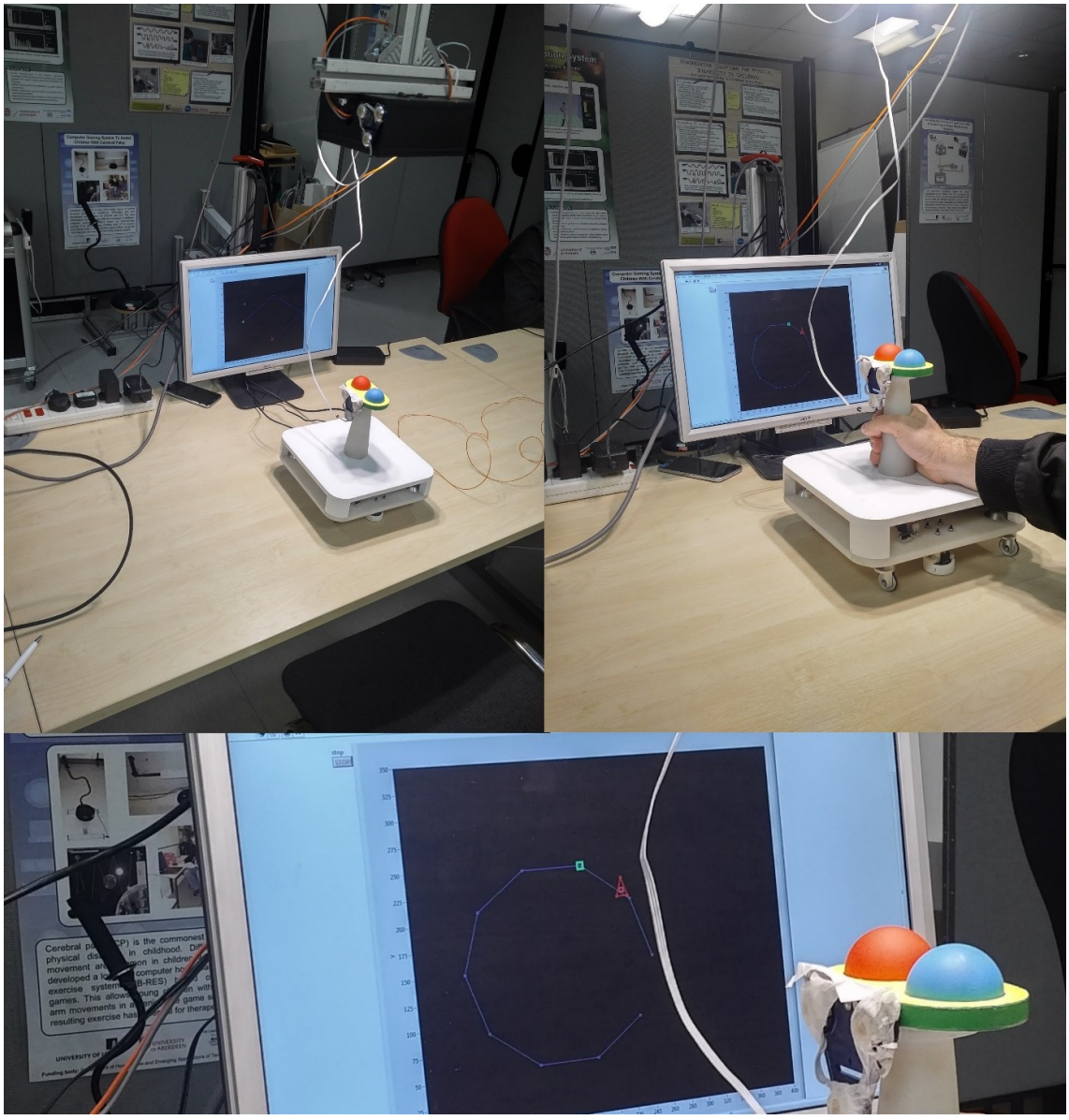

Figure 6.1: Photos showing the experimental setup used during the user testing.

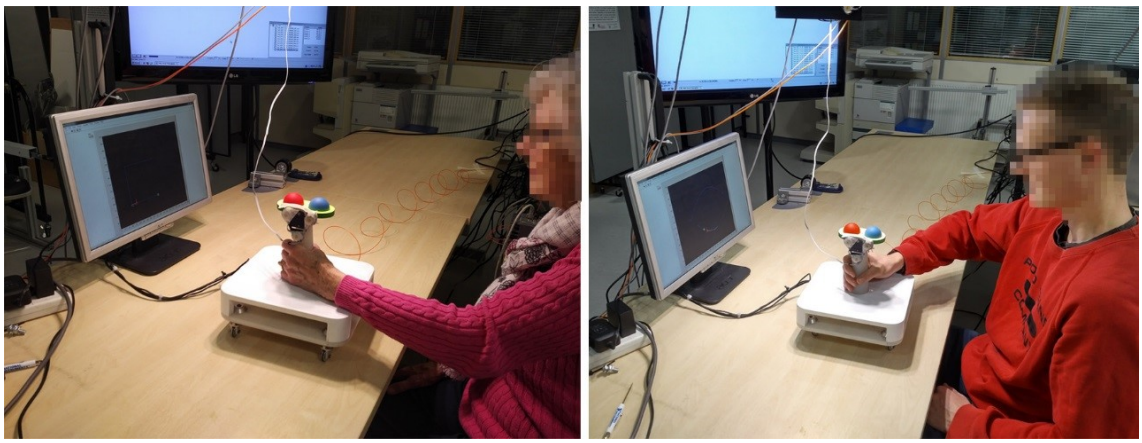

Figure 6.2: Two of the subjects using the rehabilitation robot during the experiments.

Table 6.1: 5 of the trajectories utilized during the user testing.

Trajectory name	sin4	sin16	pentagram	square	circle
Number of targets	4	16	5	4	10
Distance between targets [mm]	180	38 (min) 54 (max)	190	150	62

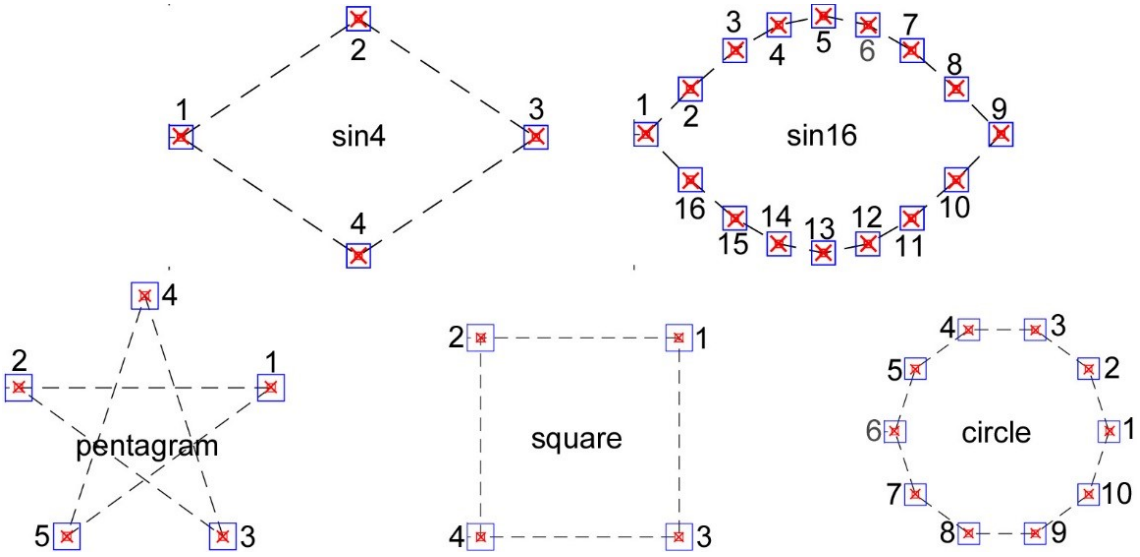

Figure 6.3: Trajectories utilized during user testing with the positions of the target points. The target points are numbered in the sequence in which they appeared on the screen during experiments.

on modes five times. Also, the recruited group of 38 subjects was divided in two subgroups of 19 subjects each. The first subgroup, consisting of subjects number 1 to 19, started the experiment in guidance off mode, performed movements reaching targets on each of the five trajectories and then repeated the task for all trajectories with the guidance module mounted under the robot in the guidance on mode. The second subgroup, subjects 20 to 38, performed the experiment in the reverse order, first with the guidance on and then with the guidance off.

The ethical approval (PSC-144) for the experiment was granted by the School of Psychology Research Ethics Committee, University of Leeds.

6.6 Experimental Procedure

Each experiment was completed by one subject at a time. Subjects did not see other subjects performing the experiment, only one subject and one investigator were present in the room during the experiment at a time. Each experiment lasted approximately 20 minutes and all subjects were paid 5 GBP for their participation.

The following experimental procedure was followed:

1. A subject was welcomed into the room and asked to sit on a chair in front of the table with the rehabilitation robot.

2. The details of the experiment were explained to the subject, the subject was asked to sign a consent form and was paid 5 GBP.

3. It was determined whether the subject was right or left handed. The subject was asked to move the rehabilitation robot with their non-dominant hand.

4. Before the actual experiment begun, all subjects had a chance to practise with the robot until they informed the investigator that they are ready to start the experiment. Subjects 1 to 19 performed the experiment with the robot in the guidance off mode first and subjects 20 to 38 performed the experiment in the guidance on mode first.

5. The first part of the experiment began (guidance off subjects 1 - 18, guidance on subjects 20 – 38).

6. The subject was asked to repeat the trajectories 5 times in the following order: sin4, sin16, pentagram, square and circle (visual feedback, circle_v_f) with the computer screen switched on.

7. The subject was asked to repeat movement along the circle trajectory 5 times for the second time with the screen switched off (no visual feedback, circle_n_v_f).

8. he first part of the experiment was completed, the subject was asked to rest for 1min. During this time the guidance module was attached to the robot (subjects 1-19) or disconnected from the robot (subjects 20-38).

9. Before the second part of the experiment started, the subject was asked to practise with the robot in the new guidance setup, guidance on (subjects 1-19) or guidance off (subjects 20-38).

10. The experiment was resumed in the new guidance mode when the subject confirmed that they are ready.

11. Points 6 and 7 were repeated, but this time the subject was using the robot in the guidance on mode (subjects 1-19) or guidance off mode (subjects 20-38).

12. The experiment was completed.

6.7 Experimental Results

The experimental results presented in this section cover results for all the trajectories 6.1, sin4, sin16, pentagram, square and circle for visual feedback and no visual feedback repetition (circle_v_f, circle_n_v_f). For each trajectory two XY plots showing the XY position measurements and positions of all targets are presented. For presentation purposes, subjects are divided into two groups based on the order of the guidance mode during the experiment, guidance off in the first part of the experiment group (subjects 1-19) and guidance on in the second part of the experiment group (subjects 20-38). Results covering the RMSE (root mean square error) and the mean and maximum recorded velocity are presented in this sections for all subjects and all trajectories. The RMSE was calculated against an ideal trajectory connecting the target points.

6.7.1 Results for the Sin4 Trajectory

The sin4 trajectory was utilized previously in the guidance system experiment in Chapter 5. The results presented here allow to compare with the results presented for sin4 trajectory in Chapter 5. Figure 6.4 presents sample XY plots of subject 9 (guidance off first) and subject 28 (guidance on first) results for 5 repetitions of the sin4 trajectory. The difference between the guidance off and on mode is visible in the plots. Figure 6.5 presents results for RMSE, mean velocity and maximum velocity for sin4 trajectory for subjects 1 to 19 for both guidance off and on modes. It can be seen that the RMSE for the guidance on mode part of the experiment is lower than the RMSE for the guidance off part for most of the subjects, apart from subjects 3, 4, 12, 13 and 19 which showed lower RMSE for the guidance off mode when compared to guidance on mode. However, it was recorded that for the subjects 3, 4, 12, 13 and 19 the mean recorded velocity of movement was higher in the guidance on mode when compared to the guidance off mode, which could cause the higher RMSEs values. In the case of the majority of the subjects the recorded mean velocity was higher for the guidance on mode, however subjects 6, 7, 8,

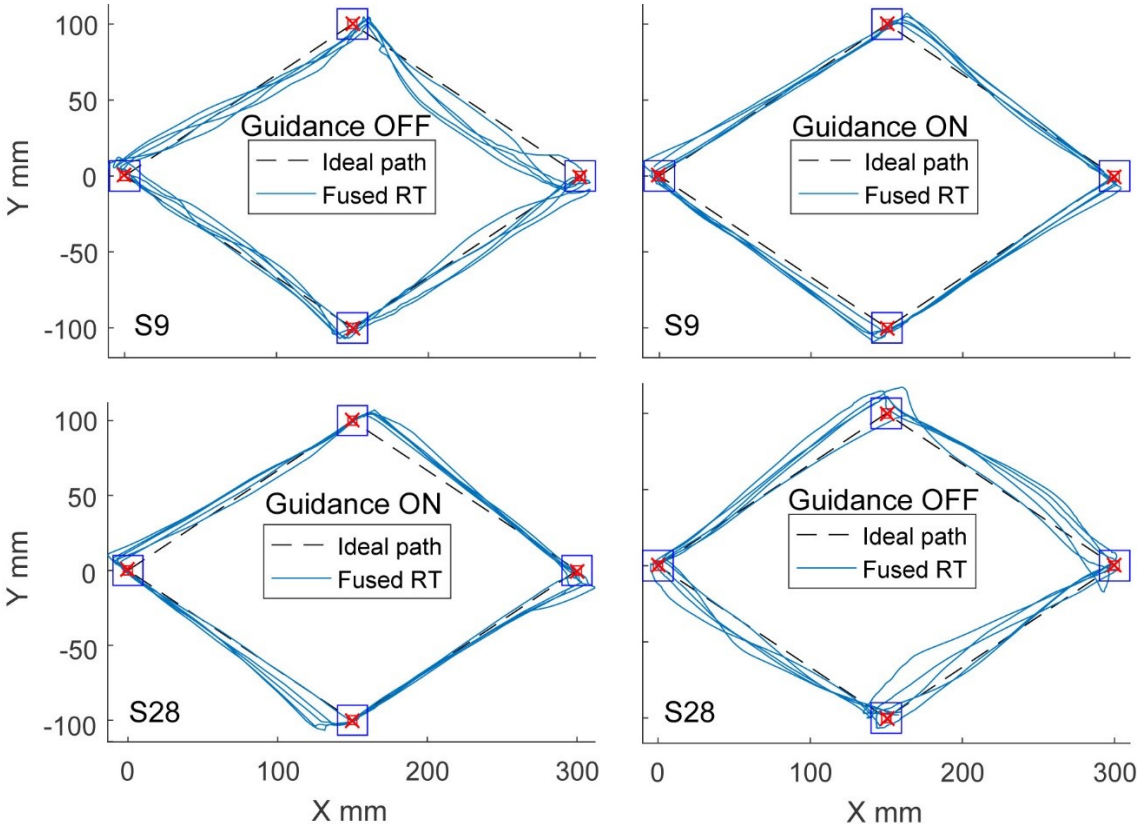

Figure 6.4: Results for 5 repetitions of the sin4 trajectory in guidance off and on modes for subject 9 and guidance on and off modes for subject 28.

10, 11, 16 and 18 showed a different trend, in their case mean velocities for the guidance off mode movement were higher than the mean velocities for the guidance on mode part of the experiment. However, for all the 6, 7, 8, 10, 11, 16 and 18 subjects the RMSEs recorded for the guidance on mode were lower when compared to the guidance off mode. It was recorded that the maximum measured velocity of movement for both guidance off and on mode could reach over 300 mm/s. The RMSE and velocity results for the sin4 trajectory and subjects 1-19 indicate that the subjects using the robot in the guidance on mode could achieve higher movement speed and accuracy (subjects 1, 2, 5, 9, 14, 15, 17), or just higher accuracy (subjects 1, 2, 5-11, 14-18).

Figure 6.6 presents results for RMSE, mean velocity and maximum velocity for sin4

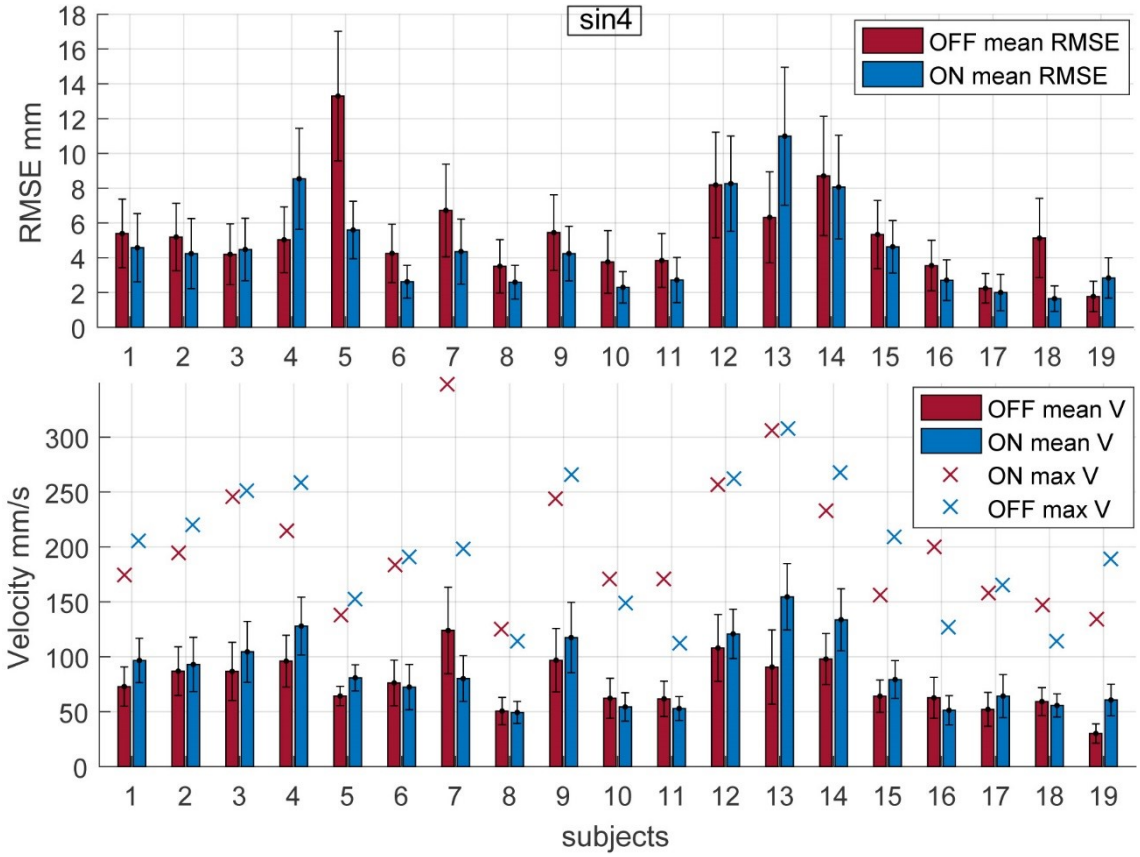

Figure 6.5: Mean root mean square error, mean velocity and maximum velocity results for 5 repetitions of the sin4 trajectory by subjects 1-19 in guidance off and on mode. The guidance off mode was utilized first. The variability of the mean RMSE and mean velocity is shown as standard deviation.

trajectory for subjects 20 to 38 for both guidance off and on modes. It can be seen that the RMSE for the guidance on mode part of the experiment is lower than the RMSE for the guidance off part for most of the subjects, apart from subjects 22, 24, 26 and 27 which showed lower RMSE for the guidance off mode when compared to guidance on mode. However, it was recorded that for the subjects 22, 26 and 27 the mean recorded velocity of movement was higher in the guidance on mode when compared to the guidance off mode, which could cause the higher RMSEs values. In the case of the majority of the subjects the recorded mean velocity was higher for the guidance on mode, however subjects 23, 24, 25, 30, 33, 34, 35 and 36 showed a different trend, in their case mean velocities for the guidance off mode movement were higher than the mean velocities for the guidance on mode part of the experiment. However, for the subjects 23, 25, 30, 33, 34, 35 and 36 the RMSEs recorded for the guidance on mode were lower when compared to the guidance off mode. It was recorded that the maximum measured velocity of movement for both guidance off and on mode could reach over 250 mm/s. The RMSE and velocity results for the sin4 trajectory and subjects 20-38 indicate that the subjects using the robot in the guidance on mode could achieve higher movement speed and accuracy (subjects 20, 21, 28, 29, 31, 32, 37, 38), or just higher accuracy (subjects 20, 21, 23, 25, 28-38). It seems that subject 24 performed better in the guidance off mode than guidance on.

subsectionResults for Sin16 Trajectory

The sin16 trajectory was utilized previously in the guidance system experiment in Chapter 5. The results presented here allow to compare with the results presented for sin16 trajectory in Chapter 5. Figure 6.7 presents sample XY plots of subject 7 (guidance off first) and subject 29 (guidance on first) results for 5 repetitions of the sin16 trajectory. The difference between the guidance off and on mode is visible in the plots.

Figure 6.8 presents results for RMSE, mean velocity and maximum velocity for sin16 trajectory for subjects 1 to 19 for both guidance off and on modes. It can be seen that the RMSE for the guidance on mode part of the experiment is lower than the RMSE for the guidance off part for most of the subjects, apart from subject 19 which showed lower RMSE for the guidance off mode when compared to guidance on mode. However, it was recorded that for the 19 the mean velocity of movement was higher in the guidance on mode when compared to the guidance off mode, which could cause the higher RMSE value. In the case of the majority of the subjects the recorded mean velocity was higher for the guidance on mode, however subjects 16 and 19 showed a different trend, in their case

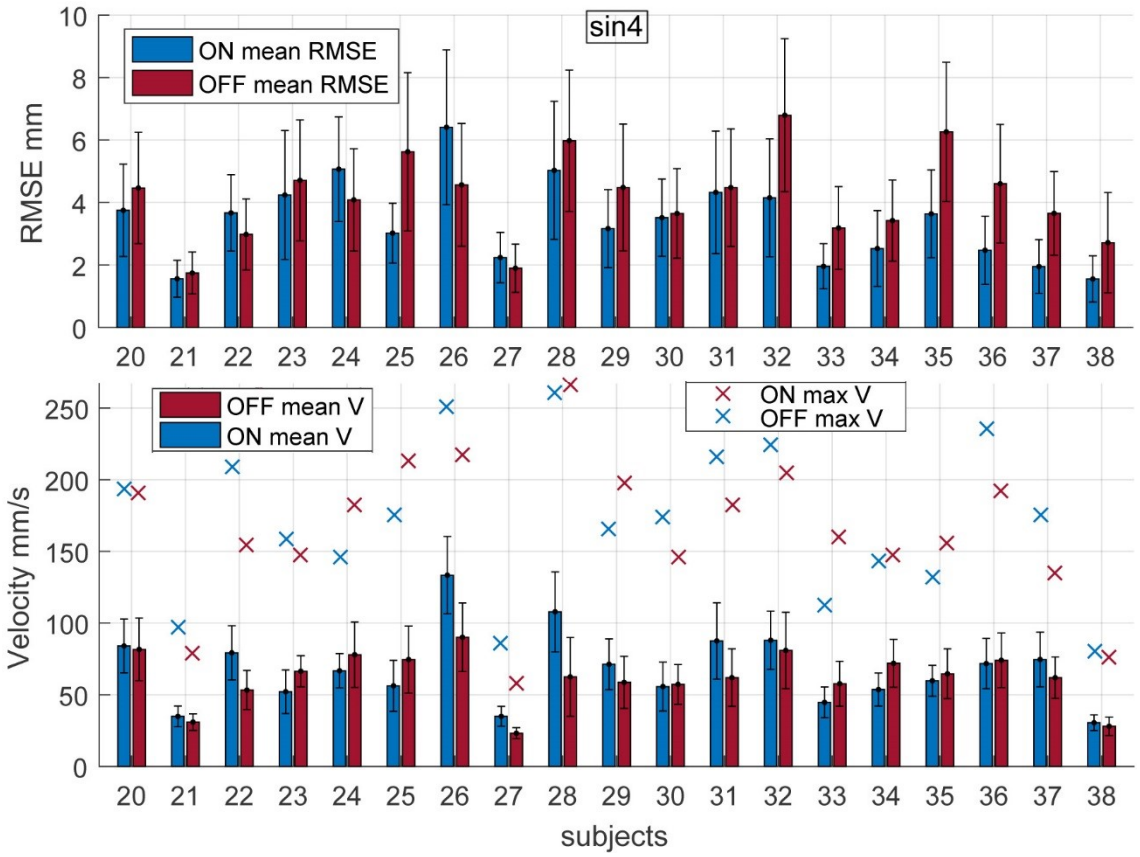

Figure 6.6: Mean root mean square error, mean velocity and maximum velocity results for 5 repetitions of the sin4 trajectory by subjects 20-38 in guidance on and off mode. The guidance on mode was utilized first. The variability of the mean RMSE and mean velocity is shown as standard deviation.

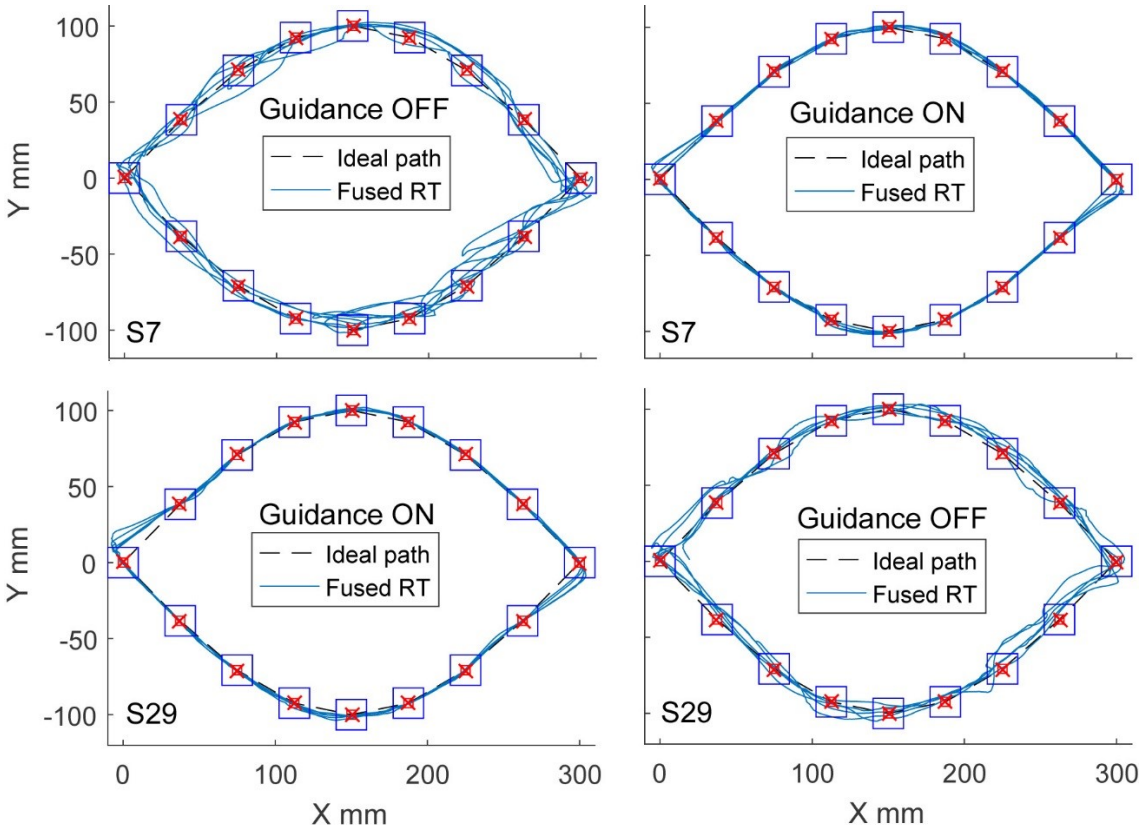

Figure 6.7: Results for 5 repetitions of the sin16 trajectory in guidance off and on modes for subject 7 and guidance on and off modes for subject 29.

mean velocities for the guidance off mode movement were higher than the mean velocities for the guidance on mode part of the experiment. However, for the subject 16 the RMSE recorded for the guidance on mode were lower when compared to the guidance off mode. It was recorded that the maximum measured velocity of movement for both guidance off and on mode could reach over 200 mm/s for the guidance on mode and over 150 mm/s for the guidance off mode. The RMSE and velocity results for the sin16 trajectory and subjects 1-19 indicate that the subjects using the robot in the guidance on mode could achieve higher movement speed and accuracy (subjects 1-15, 17-18), or just higher accuracy (all subjects excluding subject 19).

Figure 6.9 presents results for RMSE, mean velocity and maximum velocity for sin16 trajectory for subjects 20 to 38 for both guidance on and off modes. It can be seen that the RMSE for the guidance on mode part of the experiment is lower than the RMSE for the guidance off part for most of the subjects, apart from subject 27 which showed lower RMSE for the guidance off mode when compared to guidance on mode. However, it was recorded that for the subject 27 the mean recorded velocity of movement was higher in the guidance on mode when compared to the guidance off mode, which could cause the higher RMSE value. In the case of the majority of the subjects the recorded mean velocity was higher for the guidance on mode, however subjects 23, 25 and 35 showed a different trend, in their case mean velocities for the guidance off mode movement were higher than the mean velocities for the guidance on mode part of the experiment. However, for the subjects 23, 25 and 35 the RMSEs recorded for the guidance on mode were lower when compared to the guidance off mode. It was recorded that the maximum measured velocity of movement for both guidance off and on mode could reach over 250 mm/s. The RMSE and velocity results for the sin16 trajectory and subjects 20-38 indicate that the subjects using the robot in the guidance on mode could achieve higher movement speed and accuracy (subjects 20, 21, 24, 26, 28-34 and 36), or just higher accuracy (subjects 20-26, 28-38).

6.7.2 Results for Pentagram Trajectory

Figure 6.10 presents sample XY plots of subject 12 (guidance off first) and subject 30 (guidance on first) results for 5 repetitions of the pentagram trajectory. The difference between the guidance off and on mode is visible in the plots.

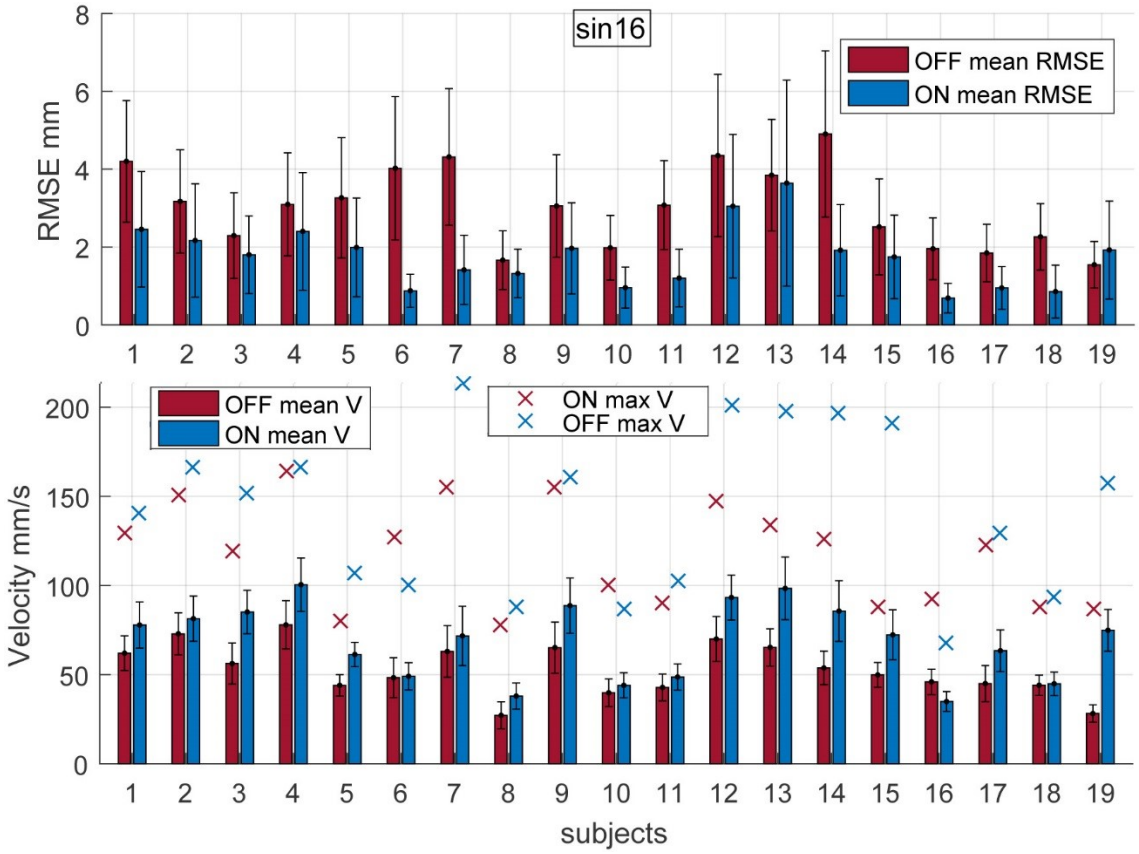

Figure 6.8: Mean root mean square error, mean velocity and maximum velocity results for 5 repetitions of the sin16 trajectory by subjects 1-19 in guidance off and on mode. The guidance off mode was utilized first. The variability of the mean RMSE and mean velocity is shown as standard deviation.

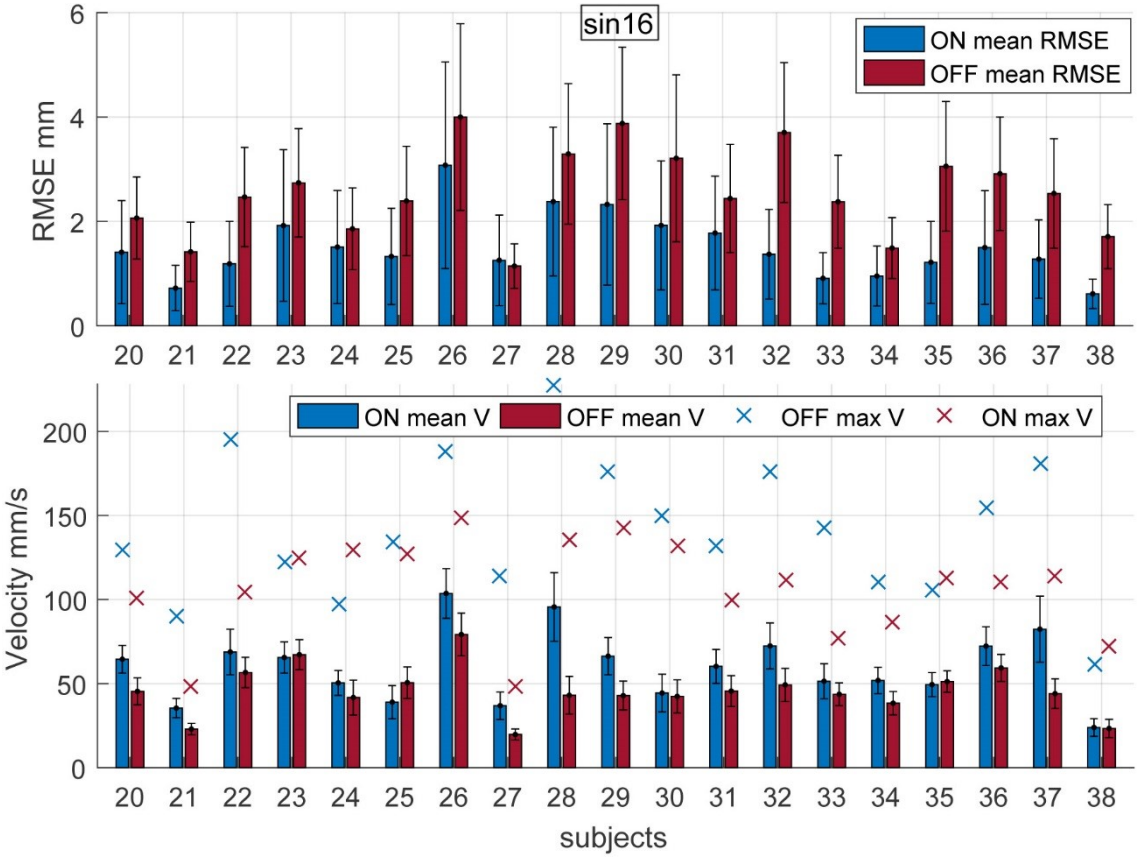

Figure 6.9: Mean root mean square error, mean velocity and maximum velocity results for 5 repetitions of the sin16 trajectory by subjects 20-38 in guidance on and off mode. The guidance on mode was utilized first. The variability of the mean RMSE and mean velocity is shown as standard deviation.

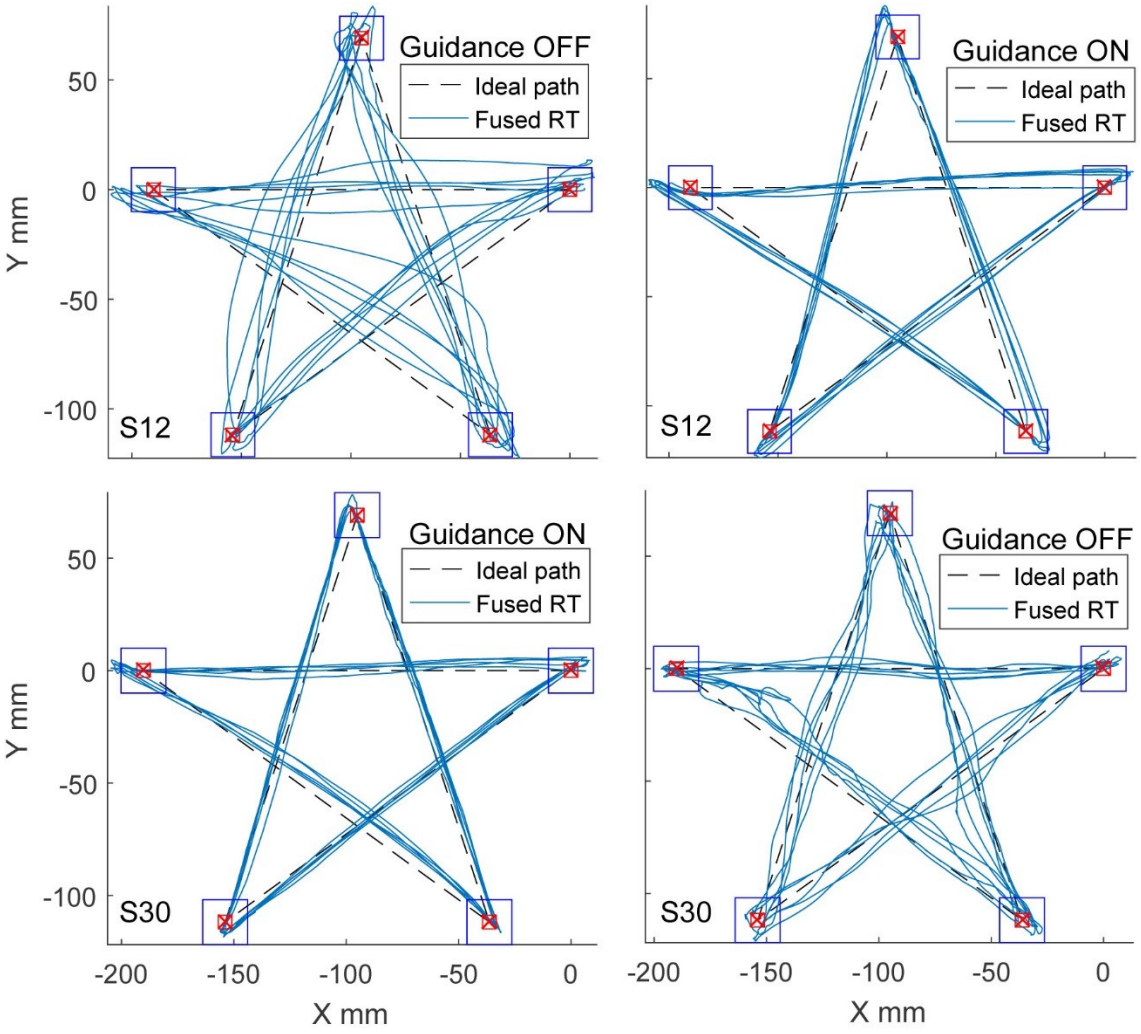

Figure 6.10: Results for 5 repetitions of the pentagram trajectory in guidance off and on modes for subject 12 and guidance on and off modes for subject 30.

Figure 6.11 presents results for RMSE, mean velocity and maximum velocity for pentagram trajectory for subjects 1 to 19 for both guidance off and on modes. It can be seen that the RMSE for the guidance on mode part of the experiment is lower than the RMSE for the guidance off part for most of the subjects, apart from the subjects 1, 14 and 19 which showed lower RMSE for the guidance off mode when compared to guidance on mode. However, it was recorded that for the subjects 1, 14 and 19 the mean velocity of movement was higher in the guidance on mode when compared to the guidance off mode, which could cause the higher RMSE value. In the case of the majority of the subjects the recorded mean velocity was higher for the guidance on mode, however subjects 6, 7, 11, 16, and 18 showed a different trend, in their case mean velocities for the guidance off mode movement were higher than the mean velocities for the guidance on mode part of the experiment. But, for the subjects 6, 7, 11, 16, and 18 the RMSE recorded for the guidance on mode were lower when compared to the guidance off mode. It was recorded that the maximum measured velocity of movement for both guidance off and on mode could reach approximately 400 mm/s. The RMSE and velocity results for the pentagram trajectory and subjects 1-19 indicate that the subjects using the robot in the guidance on mode could achieve higher movement speed and accuracy (subjects 2-5, 8-10, 12-13, 15, 17), or just higher accuracy (all subjects, excluding subject 27).

Figure 6.12 presents results for RMSE, mean velocity and maximum velocity for pentagram trajectory for subjects 20 to 38 for both guidance on and off modes. It can be seen that the RMSE for the guidance on mode part of the experiment is lower than the RMSE for the guidance off part for most of the subjects, apart from subject 27 which showed lower RMSE for the guidance off mode when compared to guidance on mode. However, it was recorded that for the subject 27 the mean recorded velocity of movement was higher in the guidance on mode when compared to the guidance off mode, which could cause the higher RMSE value. In the case of the majority of the subjects the recorded mean velocity was higher for the guidance on mode, though subjects 23, 25 and 38 showed a different trend, in their case mean velocities for the guidance off mode movement were higher than the mean velocities for the guidance on mode part of the experiment. However, for the subjects 23, 25 and 38 the RMSEs recorded for the guidance on mode were lower when compared to the guidance off mode. It was recorded that the maximum measured velocity of movement for guidance off mode could reach close to 250 mm/s and for the guidance on mode 270 mm/s. The RMSE and velocity results for the pentagram trajectory and

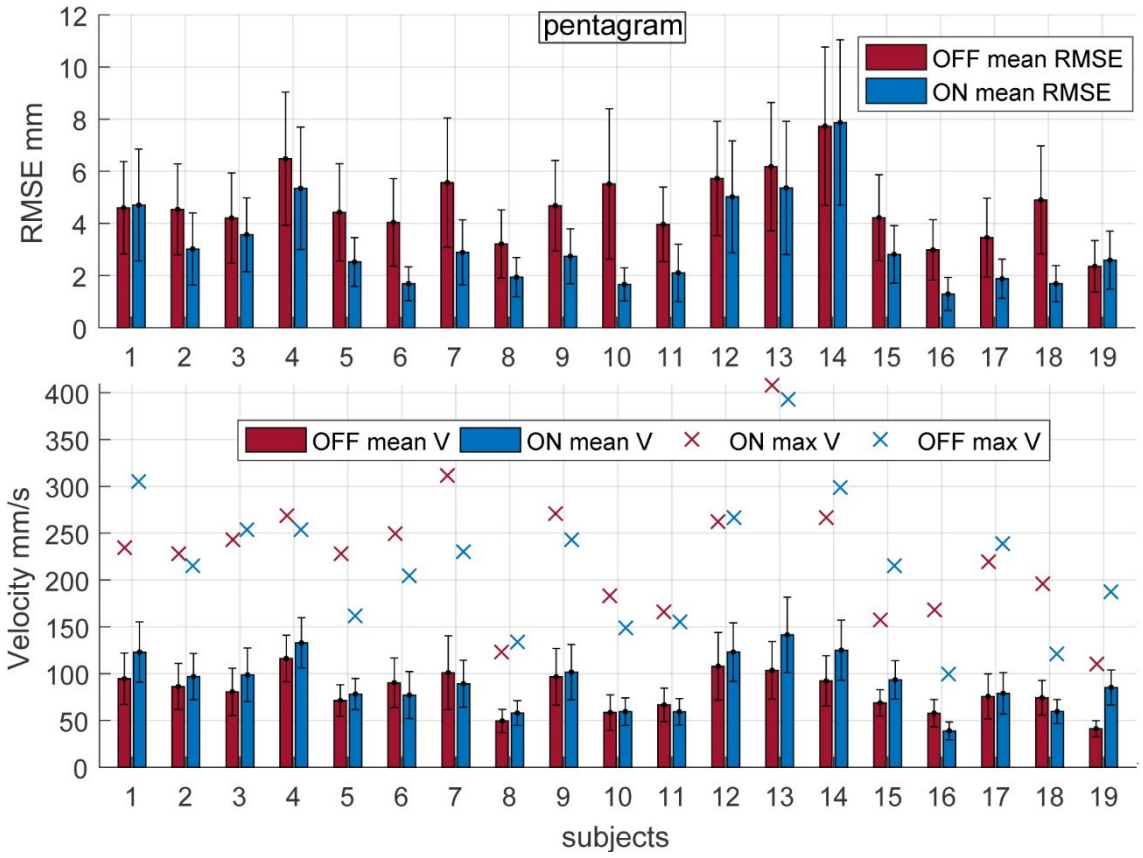

Figure 6.11: Mean root mean square error, mean velocity and maximum velocity results for 5 repetitions of the pentagram trajectory by subjects 1-19 in guidance off and on modes. The guidance off mode was utilized first. The variability of the mean RMSE and mean velocity is shown as standard deviation.

subjects 20-38 indicate that the subjects using the robot in the guidance on mode could achieve higher movement speed and accuracy (subjects 20, 21, 22, 25-37), or just higher accuracy (all subjects, excluding subject 27).

6.7.3 Results for Square Trajectory

Figure 6.13 presents sample XY plots of subject 14 (guidance off first) and subject 26 (guidance on first) results for 5 repetitions of the square trajectory. The difference between the guidance off and on mode is visible in the plots.

Figure 6.14 presents results for RMSE, mean velocity and maximum velocity for square trajectory for subjects 1 to 19 for both guidance off and on modes. It can be seen that the RMSE for the guidance on mode part of the experiment is lower than the RMSE for the guidance off part for most of the subjects, apart from the subjects 1, 4, 12, 13, 14 and 19 which showed lower RMSE for the guidance off mode when compared to guidance on mode. However, it was recorded that for the subjects 2, 6, 7, 16, 17 and 18 mean velocity of movement was higher in the guidance on mode when compared to the guidance off mode, which could cause the higher RMSE values. In the case of the majority of the subjects the recorded mean velocity was higher for the guidance on mode, however subjects 6, 7, 11, 16, 17 and 18 showed a different trend, in their case mean velocities for the guidance off mode movement were higher than the mean velocities for the guidance on mode part of the experiment. But, for the subjects 6, 7, 11, 16, 17 and 18 the RMSE recorded for the guidance on mode were lower when compared to the guidance off mode. It was recorded that the maximum measured velocity of movement for both guidance off and on mode could reach over 300 mm/s. The RMSE and velocity results for the square trajectory and subjects 1-19 indicate that the subjects using the robot in the guidance on mode could achieve higher movement speed and accuracy (subjects 3, 5, 8-11), or just higher accuracy (subjects 2, 3, 5-11, 15-18).

Figure 6.15 presents results for RMSE, mean velocity and maximum velocity for square trajectory for subjects 20 to 38 for both guidance on and off modes. It can be seen that the RMSE for the guidance on mode part of the experiment is lower than the RMSE for the guidance off part for most of the subjects, apart from subjects 21, 25, 27 and 28 which showed lower RMSE for the guidance off mode when compared to guidance on mode. Though, it was recorded that for the subjects 21, 25, 27 and 28 the mean recorded velocity of movement was higher in the guidance on mode when compared to the guidance

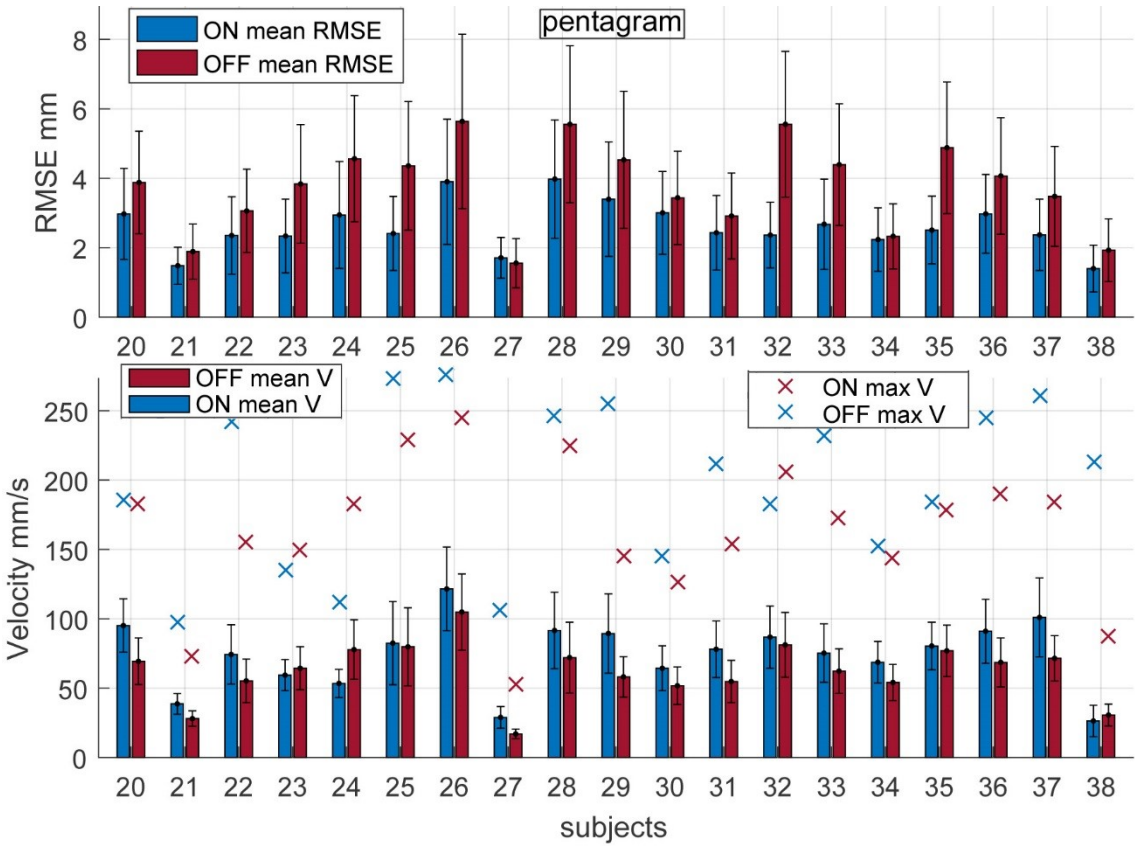

Figure 6.12: Mean root mean square error, mean velocity and maximum velocity results for 5 repetitions of the pentagram trajectory by subjects 20-38 in guidance on and off modes. The guidance on mode was utilized first. The variability of the mean RMSE and mean velocity is shown as standard deviation.

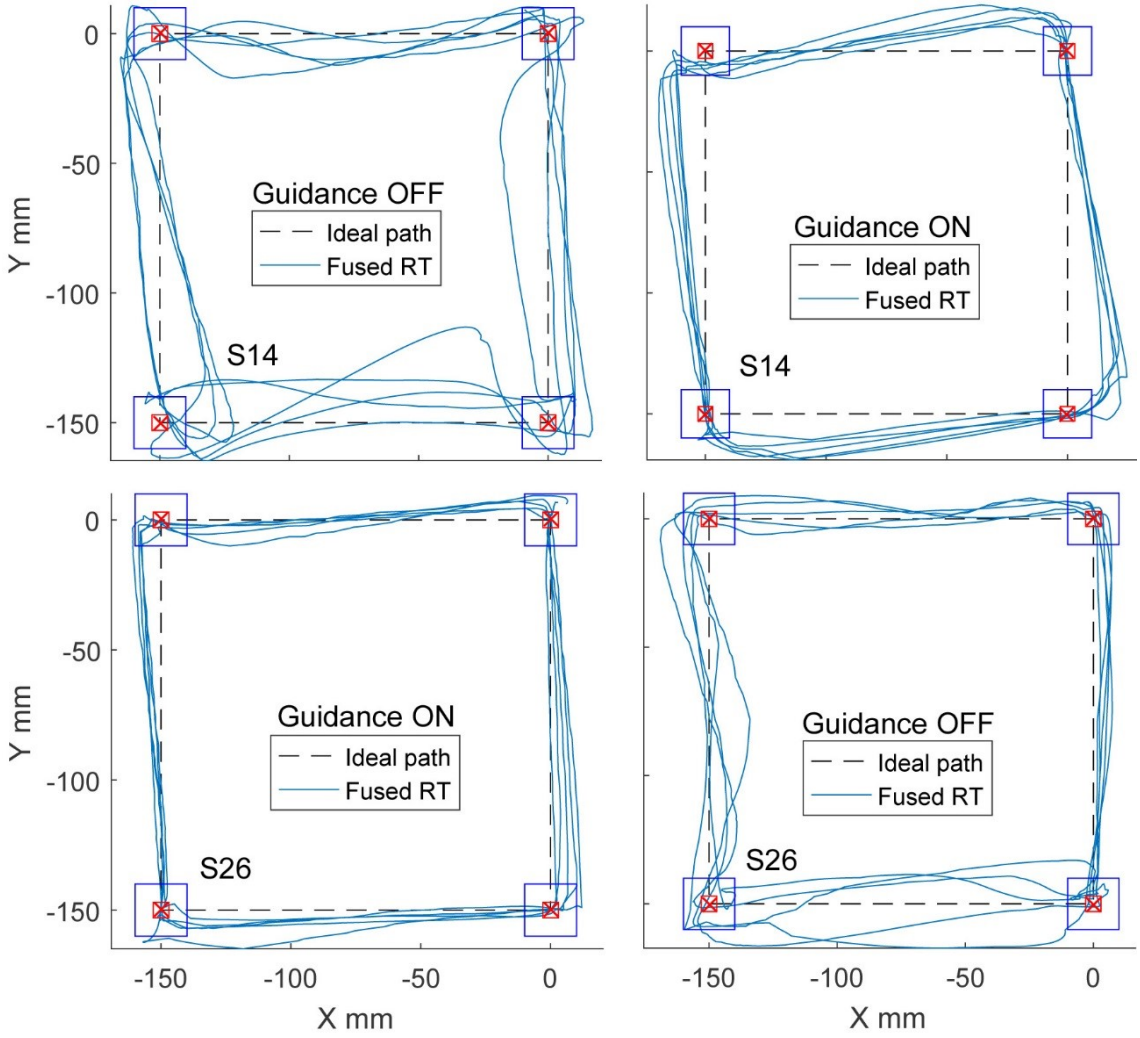

Figure 6.13: Results for 5 repetitions of the square trajectory in guidance off and on modes for subject 14 and guidance on and off modes for subject 26.

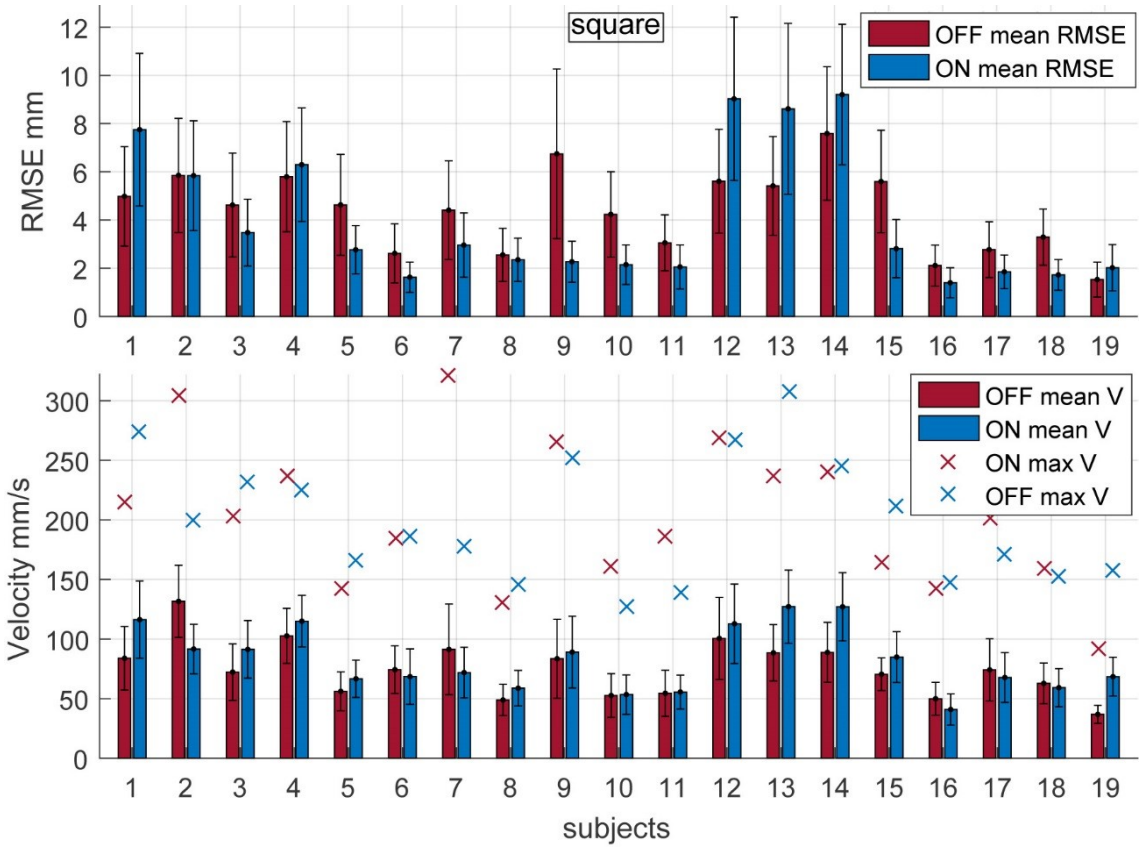

Figure 6.14: Mean root mean square error, mean velocity and maximum velocity results for 5 repetitions of the square trajectory by subjects 1-19 in guidance off and on modes. The guidance off mode was utilized first. The variability of the mean RMSE and mean velocity is shown as standard deviation.

off mode, which could cause the higher RMSE value. In the case of all the subjects the recorded mean velocity was higher for the guidance on mode. It was recorded that the maximum measured velocity of movement for guidance off mode could reach close to 230 mm/s and for the guidance on mode 280 mm/s. The RMSE and velocity results for the square trajectory and subjects 20-38 indicate that the subjects using the robot in the guidance on mode could achieve higher movement speed and accuracy (subjects 20, 21-24, 26, 29-38).

6.7.4 Results for Circle Trajectory with Visual Feedback

Figure 6.16 presents sample XY plots of subject 13 (guidance off first) and subject 31 (guidance on first) results for 5 repetitions of the circle_v_f trajectory (circle trajectory with visual feedback on). The difference between the guidance off and on mode is visible in the plots.

Figure 6.17 presents results for RMSE, mean velocity and maximum velocity for circle_v_f trajectory for subjects 1 to 19 for both guidance off and on modes. It can be seen that the RMSE for the guidance on mode part of the experiment is lower than the RMSE for the guidance off part for most of the subjects, apart from the subject 10 which showed lower RMSE for the guidance off mode when compared to guidance on mode. Though, it was recorded for the subject 10 that the mean velocity of movement was higher in the guidance on mode when compared to the guidance off mode, which could cause the higher RMSE value. In the case of the majority of the subjects the recorded mean velocity was higher for the guidance on mode, however the subjects 2, 6, 7, 11 and 16 showed a different trend, in their case mean velocities for the guidance off mode movement were higher than the mean velocities for the guidance on mode part of the experiment. Though, for the subjects 2, 6, 7, 11 and 16 the RMSE recorded for the guidance on mode were lower when compared to the guidance off mode. It was recorded that the maximum measured velocity of movement for both guidance off and on mode could reach approximately 190 mm/s and 200 mm/s respectively. The RMSE and velocity results for the circle_v_f trajectory and subjects 1-19 indicate that the subjects using the robot in the guidance on mode could achieve higher movement speed and accuracy (subjects 1, 3-5, 8-9, 12-15, 17-19), or just higher accuracy (all subjects, excluding subject 10).

Figure 6.18 presents results for RMSE, mean velocity and maximum velocity for circle_v_f trajectory for subjects 20 to 38 for both guidance on and off modes. It can be

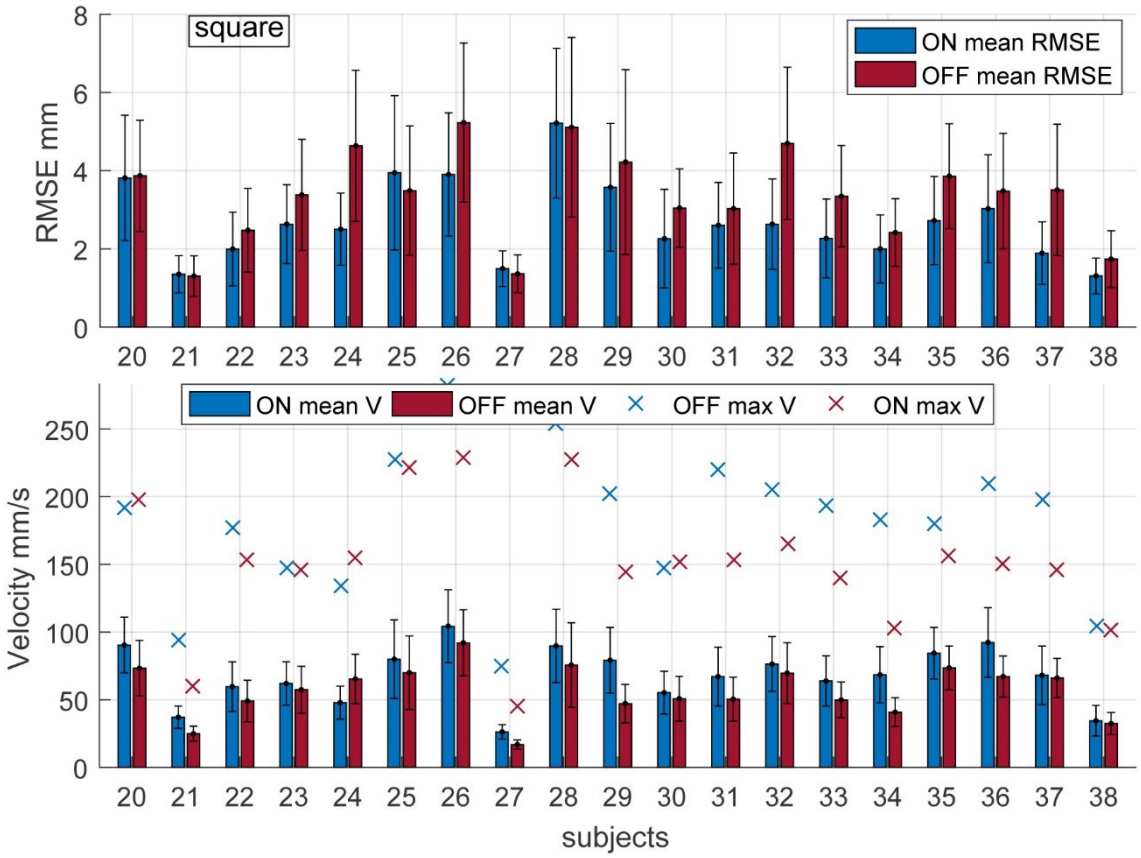

Figure 6.15: Mean root mean square error, mean velocity and maximum velocity results for 5 repetitions of the square trajectory by subjects 20-38 in guidance on and off modes. The guidance on mode was utilized first. The variability of the mean RMSE and mean velocity is shown as standard deviation.

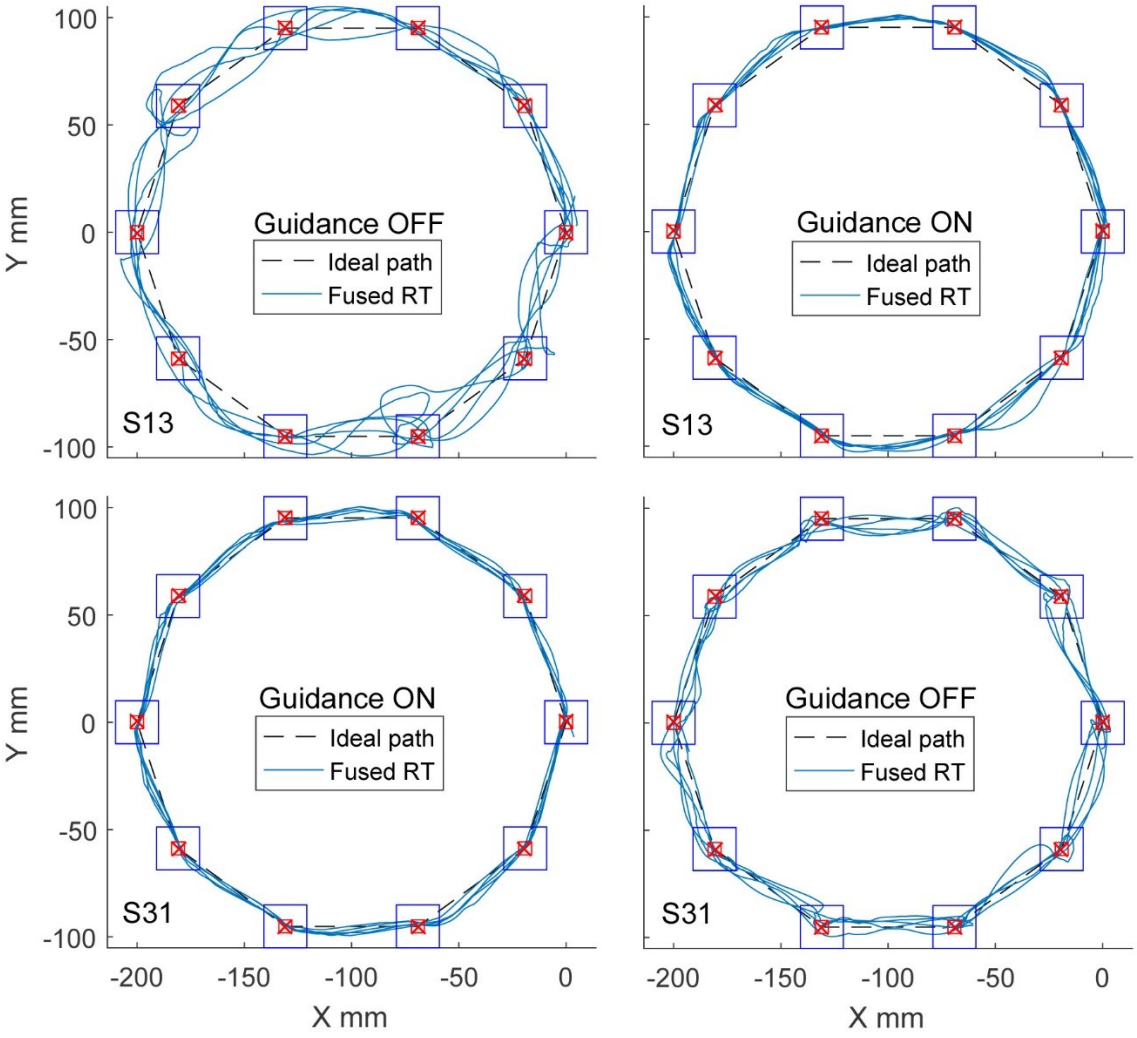

Figure 6.16: Results for 5 repetitions of the circle_v_f trajectory in guidance off and on modes for subject 13 and guidance on and off modes for subject 31.

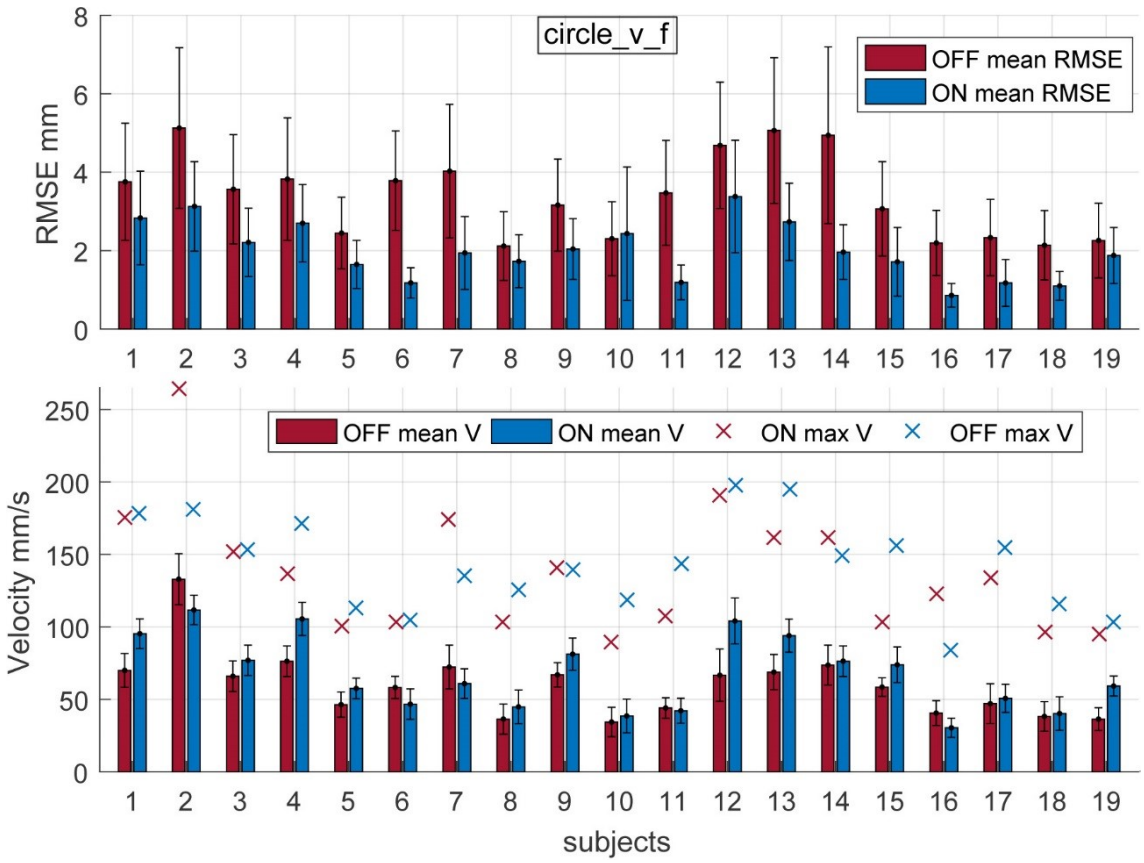

Figure 6.17: Mean root mean square error, mean velocity and maximum velocity results for 5 repetitions of the circle_v_f trajectory by subjects 1-19 in guidance off and on modes. The guidance off mode was utilized first. The variability of the mean RMSE and mean velocity is shown as standard deviation.

seen that the RMSE for the guidance on mode part of the experiment is lower than the RMSE for the guidance off part for all the subjects. In the case of most of the subjects the recorded mean velocity was higher for the guidance on mode, though subjects 23, 28 and 32 showed a different trend, in their case mean velocities for the guidance off mode movement were higher than the mean velocities for the guidance on mode part of the experiment. However, for the subjects 23, 28 and 32 the RMSEs recorded for the guidance on mode were lower when compared to the guidance off mode. It was recorded that the maximum measured velocity of movement for guidance off mode could reach approximately 170 mm/s and for the guidance on mode 230 mm/s. The RMSE and velocity results for the circle_v_f trajectory and subjects 20-38 indicate that the subjects using the robot in the guidance on mode could achieve higher movement speed and accuracy (subjects 20-22, 24-27, 29-31, 33-38), or just higher accuracy (all subjects).

6.7.5 Results for Circle Trajectory Without Visual Feedback

The circle_n_v_f trajectory was the last trajectory utilized in both guidance off and guidance on part of the experiment. After finishing movement on the circle_v_f trajectory, subjects were asked to perform the same trajectory (circle) but this time with the computer monitor switched off. Figure 6.19 presents sample XY plots of subject 13 (guidance off first) and subject 31 (guidance on first) results for 5 repetitions of the circle_n_v_f trajectory (circle trajectory with no visual feedback). The difference between the guidance off and on mode is clearly visible in the plots. While the guidance module was on, the subjects 16 and 25 were still able to follow the circle trajectory. While the guidance was off subjects tried to perform the circular motion based on what they memorised when they performed movements on the same trajectory with the computer screen switched on.

Figure 6.20 presents results for mean RMSE, mean velocity and maximum velocity for circle_n_v_f trajectory for subjects 1 to 19 for both guidance off and on modes. When the subjects cannot see the screen the advantage of the guidance on mode is very clear. As it was expected, subjects were not able to stay on the trajectory and hit the targets when the screen was switched off and the robot was in the guidance mode. Not all of the guidance on mode results were successful, but most of the subjects managed to stay on the correct trajectory and move through all of the targets (subjects 1, 3-17, 19). The variability of the mean RMSE and mean velocity is shown as standard deviation.vvvvv.

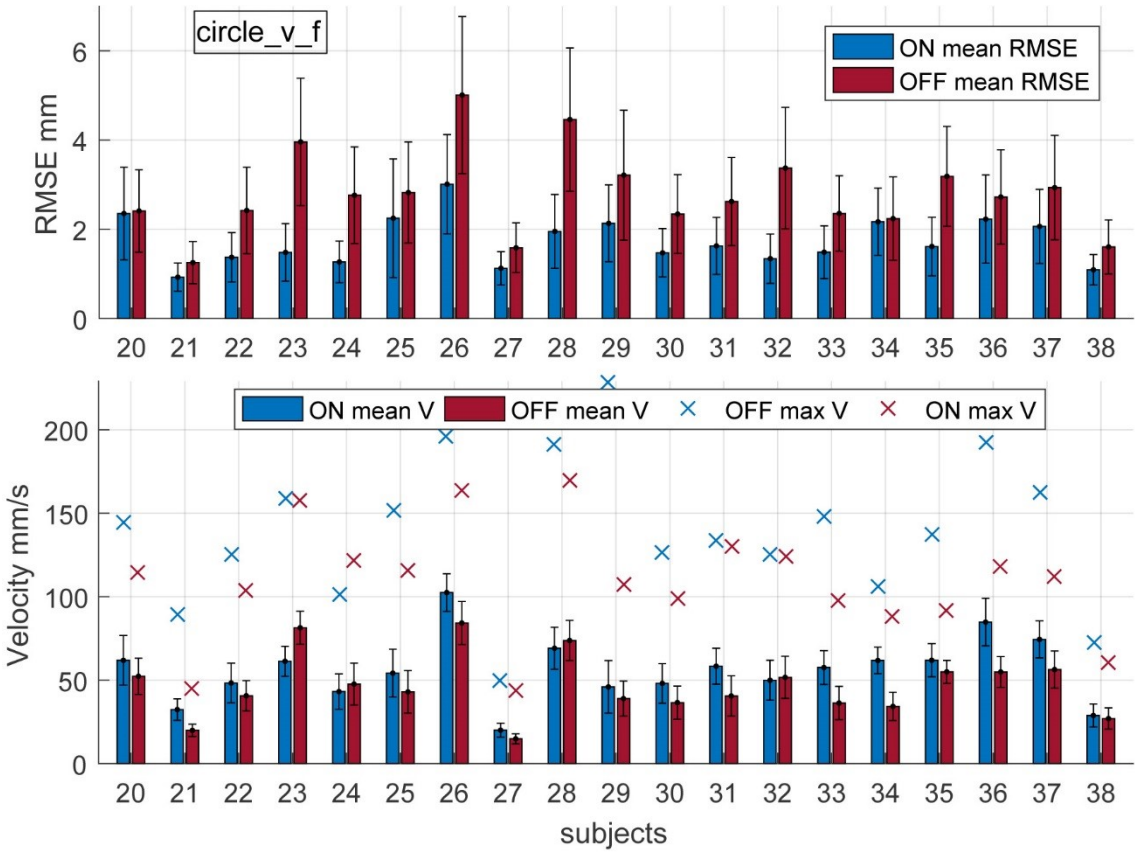

Figure 6.18: Mean root mean square error, mean velocity and maximum velocity results for 5 repetitions of the circle_v_f trajectory by subjects 20-38 in guidance on and off modes. The guidance on mode was utilized first. The variability of the mean RMSE and mean velocity is shown as standard deviation.

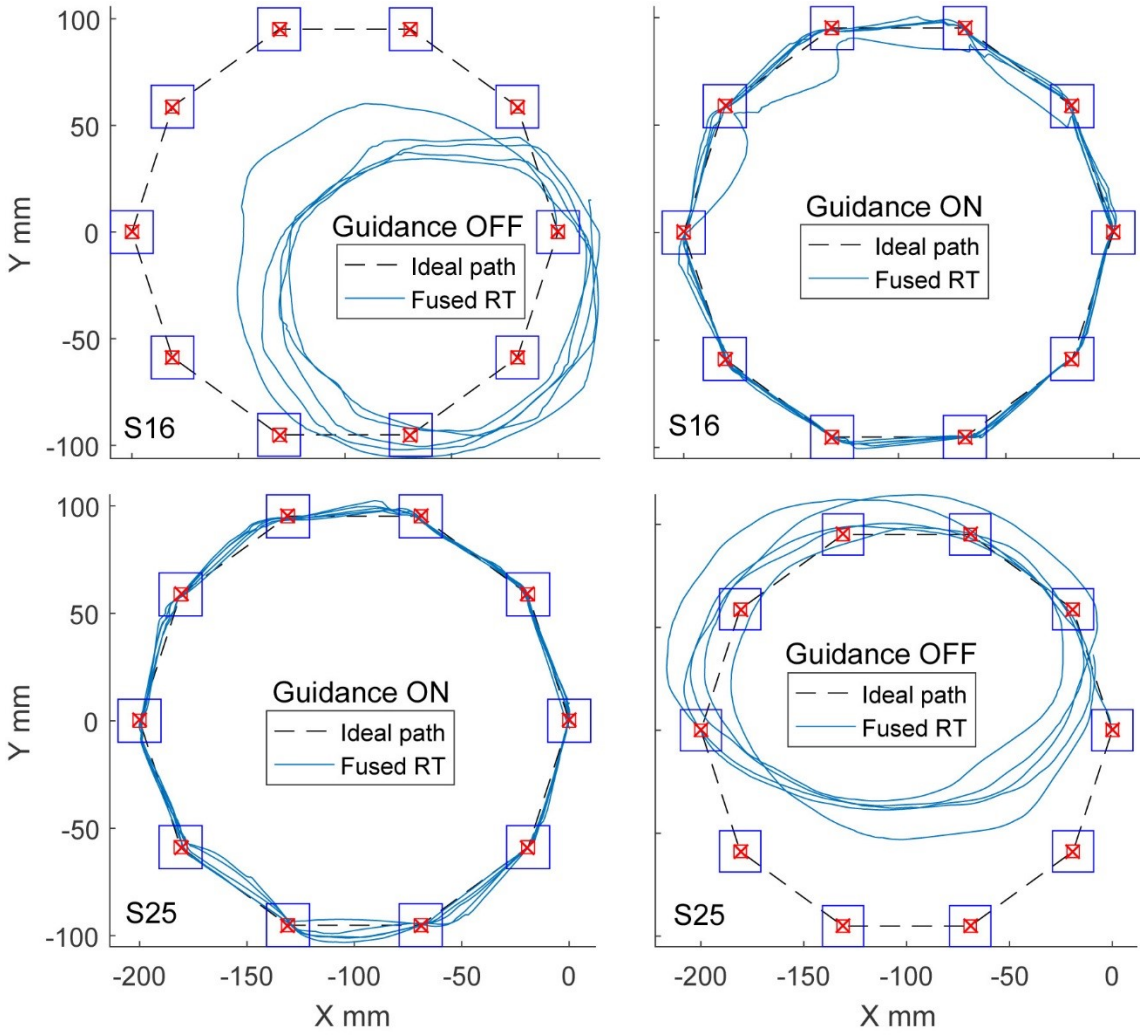

Figure 6.19: Results for 5 repetitions of the circle_n_v_f (no visual feedback) trajectory in guidance off and on modes for subject 16, and guidance on and off modes for subject 25. After subjects moved the robot on the circle trajectory with the computer screen switched on, they were asked to perform the same movement with the screen switched off.

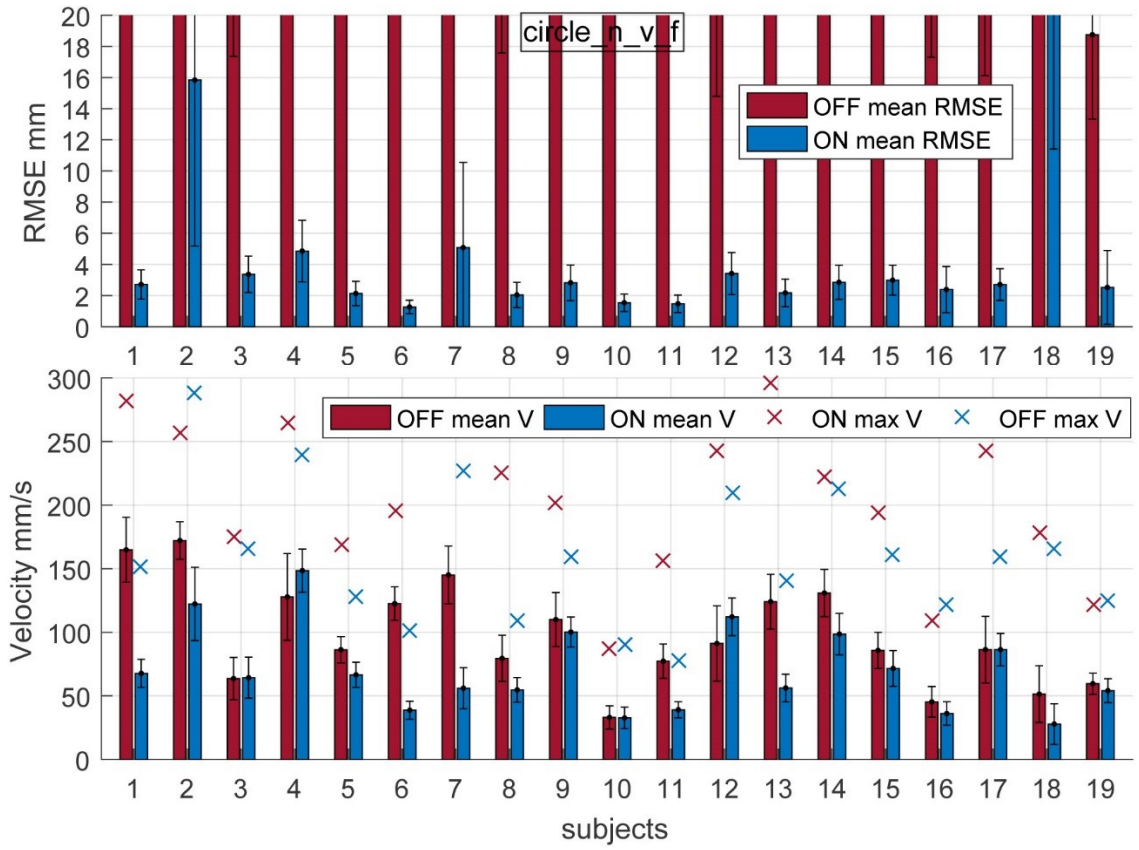

Figure 6.20: Mean root mean square error, mean velocity and maximum velocity results for 5 repetitions of the circle_n_v_f (no visual feedback) trajectory by subjects 1-19 in guidance off and on modes. The guidance off mode was utilized first. The variability of the RMSE and mean velocity is shown as standard deviation.

Figure 6.21 presents results for mean RMSE, mean velocity and maximum velocity for circle_n_v_f trajectory for subjects 20 to 38 for both guidance off and on modes. The results presented here show similar trends to the results presented in Figure 6.20. Most of the subjects could stay on the circle trajectory when the guidance mode was on, even though the screen was switched off. In the guidance off mode the subjects were not able to complete the task when the screen was switched off even though they were doing the same exercise with the screen switched on earlier. The variability of the mean RMSE and mean velocity is shown as standard deviation..

6.8 Movement Performance Analysis

Visual inspection of the results presented in experimental results section suggests that the guidance module was effective at improving tracking performance in comparison to the unguided system. Further analysis was conducted to confirm this using objective performance metrics. All of the trajectories are included in the analysis, however the results for the circle trajectory without visual feedback (circle_n_v_f) are excluded. The purpose of asking the subjects to follow the circle trajectory without the visual feedback was to show that subjects are able to follow the trajectory even if they cannot see the position of the robot and target on the screen. For the majority of the subject this was confirmed. The analysis of the results focuses only on the results for trajectories where the visual feedback was available, therefore the following trajectories from the experimental section are included: sin4, sin16, pentagram, square and circle_v_f (visual feedback).

The experimental results suggest some correlation between the root mean square error (RMSE) and mean velocity. To investigate this, the RMSE results for all the trajectories and guidance off and on mode (with visual feedback) were plotted versus mean velocity as it is shown in Figure 6.22. A linear fit (trend line) for both guidance off and on were plotted using the "polyfit" function in MATLAB. The trend lines for both guidance off and on modes confirm that when the robot was moving faster (greater mean velocity) the movement was less accurate (greater RMSE), which was expected. It can also be noticed that the trend lines have similar gradients but a noticeable difference in the y-intercepts. The intercept for the guidance on trend line is smaller than the intercept for the guidance off trend line. The trend lines indicate that the robot used by a subject in the guidance on mode could have greater movement velocity when compared to the robot

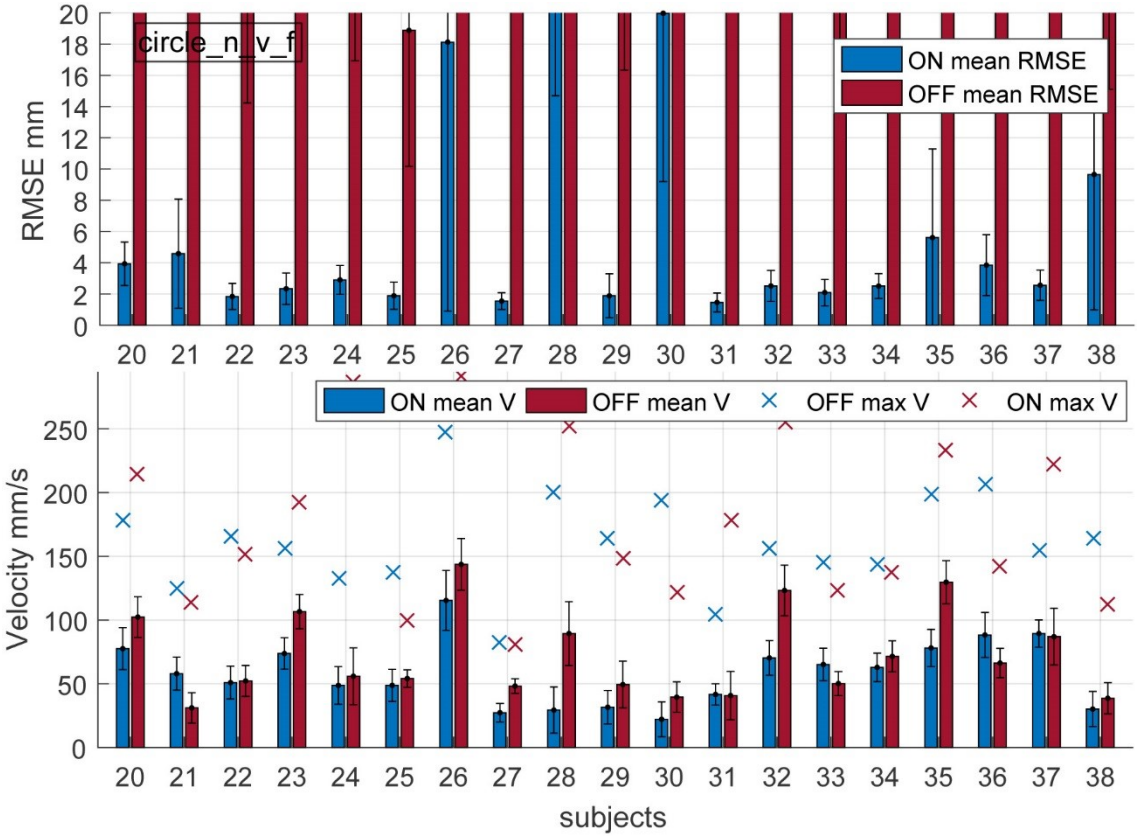

Figure 6.21: Mean root mean square error, mean velocity and maximum velocity results for 5 repetitions of the circle_n_v_f (no visual feedback) trajectory by subjects 20-38 in guidance on and off modes. The guidance on mode was utilized first. The variability of the mean RMSE and mean velocity is shown as standard deviation.

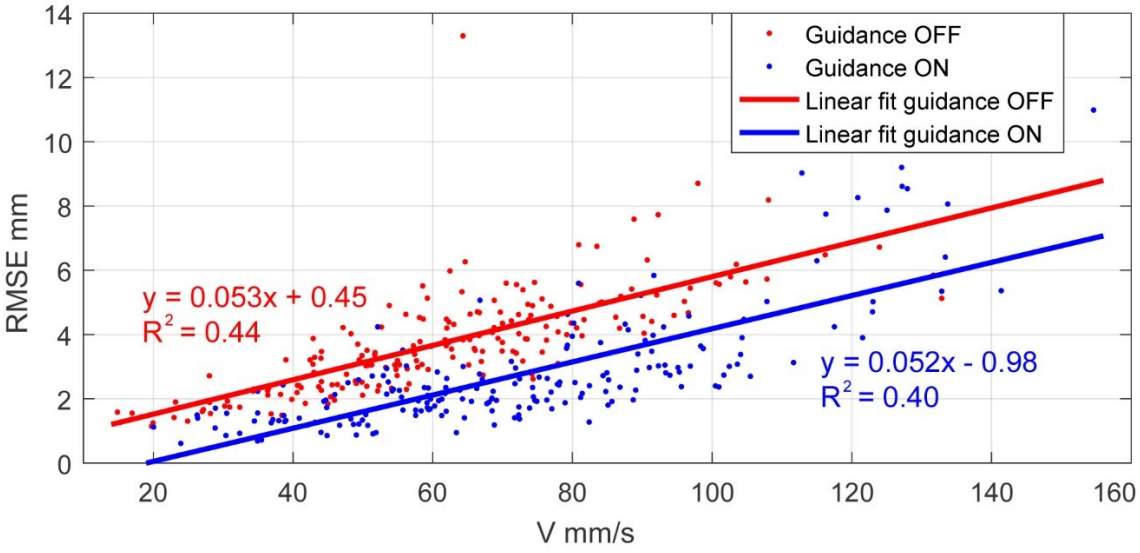

Figure 6.22: Dependence between mean RMSE (root mean square error) and mean velocity for sin4, sin16, pentagram, square and circle_v_f results for guidance on and off modes with trend lines.

in the guidance off mode while still maintaining the same accuracy (RMSE). Or when the velocity of movement is the same for the robot in guidance on and off mode the trend lines indicate that the movement in the guidance on mode was more accurate (lower RMSE) when compared to the guidance off mode. It is important to mention that the trend lines do not accurately describe all of the results.

Two other correlations which were suggested by the experimental results are the correlation between RMSE and the distance between the target points and between mean velocity and distance between target points. Results presented in Figure 6.23 show two plots, the plot on the left presents the correlation between RMSE and distance between target points and the plot on the right shows dependence between velocity and distance between target points. The RMSE and velocity results were averaged for all 38 subjects and sin4, sin 16, pentagram, square and circle_v_f trajectories. Figure 6.23 indicates that when the distance between target points increases, the accuracy of movement decreases (RMSE increases). The pentagram trajectory (190 mm target separation) showed lower mean RMSE for all 38 subjects than square and sin4 for both guidance off and on mode.

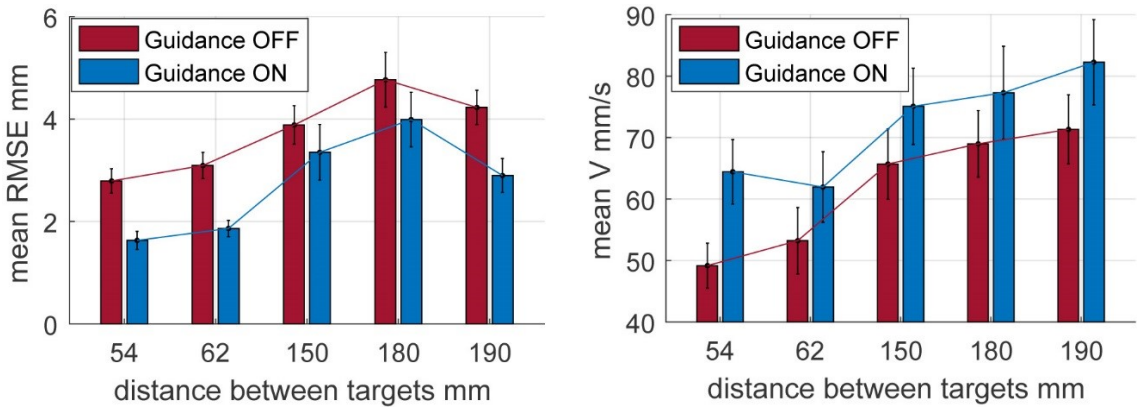

Figure 6.23: Plots presenting the relationship between mean RMSE and distance between target points (left) and velocity and distance between target points (right). Confidence intervals represent standard deviation.

Velocity and distance between target points plot shows similar trends, as the distance between target points increases the velocity of movement increases too.

During the experiments, subjects 1-19 performed the first part of the experiment in the guidance off mode and the second part in the guidance on mode. Subjects 20-38 did exactly opposite thing, first used the robot in the guidance on mode and then once again in the guidance off mode. Results presented in Figure 6.24 were plotted to investigate if there is any noticeable difference between the performance of subjects 1-19 and subjects 20-38. The results indicate that there are differences and the same trend applies to all trajectories. First, for both groups the averaged velocity across all subjects in each group is greater for the guidance on mode than for the guidance off mode. Secondly, the RMSE averaged across all subjects in each group is smaller for the guidance on mode than for the guidance off mode. What is different for both groups is that subjects 1-19 which started the exercise in the guidance off mode had greater average velocity than subjects 20-38 for every single trajectory, for both guidance off and on modes. Also for every single trajectory and both guidance off and on mode the average RMSE for the subjects 20-38 was lower than for subjects 1-19.

Figure 6.25 presents maximum velocity results averaged for each trajectory. The results suggest that the maximum velocities recorded for guidance on mode are greater than for

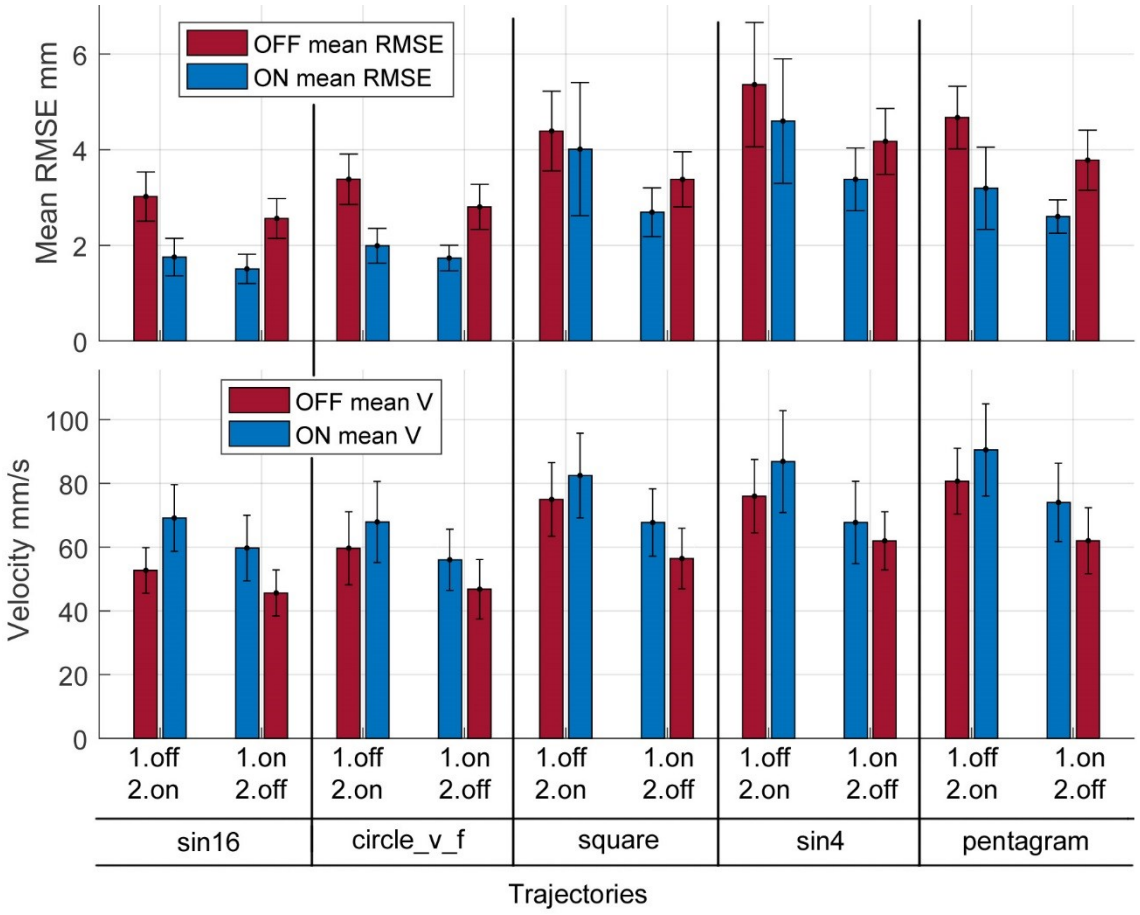

Figure 6.24: Mean RMSE and mean velocity plotted separately for subjects 1-19 (1.off 2.on) and subjects 20-38 (1.on 2.off) for each trajectory. Confidence intervals represent standard deviation.

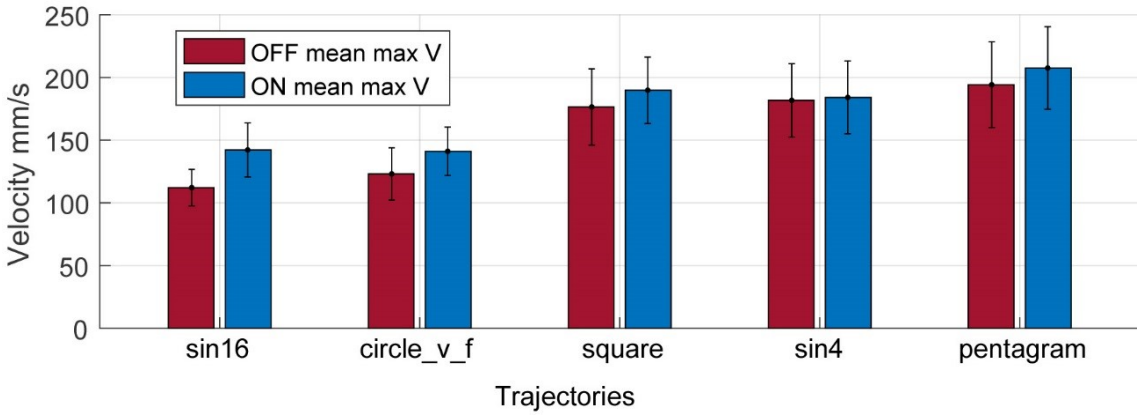

Figure 6.25: Maximum velocity results averaged for all 38 subjects for each trajectory. Confidence intervals represent standard deviation.

the guidance off mode for each trajectory. Also, the results indicate that for trajectories with greater distance between target points the maximum recorded velocity is greater.

6.9 Statistical Power of the User Testing

The user testing presented in this chapter was a pilot trial, therefore statistical power was calculated after the trial was concluded. The tool used for power calculation was an experiment power and sample size calculator (powerandsamplesize.com, 2018) which is useful for experiments comparing difference between the means of two groups. The power was calculated based on the results presented in Figure 6.24 to check the statistical significance of the difference between mean root mean square error (RMSE) with (on) and without (off) the presence of the guidance module. The number of samples was 38 (equal to the total number of participants) and the alpha level was set to 0.05. The calculated experiment statistical power was 96.7% for mean RMSE, which suggest that the study was powerful. Additionally, the statistical power was calculated for the mean velocity measurements also presented in Figure 6.24 to check the statistical significance of the difference between mean velocity with (on) and without (off) the presence of the guidance module for all 38 users. The calculated statistical power was 68.9% for velocity, which suggest that the experiment was slightly underpowered. In order to achieve 90%

power, in the investigation of the difference between the mean velocity with and without the guidance, the number of participants would have to be increased to 71.

6.10 Discussion - User Testing

User testing was successfully conducted without any interruptions that could affect the quality of the results. All the subjects were healthy adults which during the experiments used the prototype in the guidance off and on mode. The robot is designed for post-stroke arm rehabilitation and the presented results and conclusions could be different if a clinical trial with subjects with arm impairment was conducted. During the trial, all 38 recruited subjects used their non-dominant arms to move the robot, as this was predicted to show results trends which were closer to those that an impaired subject would have had.

The subjects found the robot very intuitive and easy to use. Generally, the subjects needed around a minute to familiarise themselves with the operation of the robot. Also, the difference between the guidance on and off mode was obvious to the subjects, generally they found the guidance on mode more intuitive to use than the guidance off mode. The robot was connected to a computer via a USB cable. A power cable was also connected to the robot. The cables could have some effect on the performance of the subjects, but this can be compared to the effect that a USB cable of a wired computer mouse has on its use.

Before the experiment, five main experimental questions were formulated and these can now be answered.

1. What is the difference of participants' point-to-point movement accuracy when the guidance module is used and when it is not? The results indicate that when the robot is used in the guidance on mode, the accuracy (lower RMSE) of point-to-point movements is greater than the accuracy of movements in the guidance off mode (Figure 6.22).

2. What is the movement velocity when the guidance module is used and when it is not used? The results indicate that the velocity of movement is greater when the guidance module is on, as compared to the guidance off mode movement velocity (Figure 6.22).

3. Does the guidance module make it easier to move the rehab robot to targets? The results indicate that the guidance on mode makes it easier for the subjects to move the robot between target points. Recorded movements with the guidance on mode are faster and more accurate (Figure 6.22).

4. How does the user testing compare to the experiment presented in Chapter 5? While comparing the user testing results for the sin4 trajectory results in the guidance testing in Chapter 5 it can be noticed that the user testing results are more accurate in terms of the measured RMSE. For example, the subjects 1-19 moved the robot along the target on the sin4 trajectory at the velocity of approximately 90 mm/s and had RMSE equal to approximately 4 mm. In the guidance testing for sin4 a comparable RMSE was recorded for experiment 5 where the velocity of movement was 50 mm/s. For the sin16 trajectory results the subjects 1-38 are comparable with the experiment 11 in the guidance testing, in both case the RMSE is less than 2 mm. Overall, the comparison of the user testing and the guidance testing results indicates that the guidance testing conducted in Chapter 5 accurately represented user performance for the sin16 trajectory and for the sin4 trajectory better accuracy was recorded in the user testing (as compared to the guidance testing). However, for the sin4 trajectory the velocity of movement was higher during the user testing than in the guidance experiment 5 and the accuracy was the same. This can be explained by the fact that the trajectories recorded in the user testing are a combination of user input and the performance of the guidance module. In the guidance experiment the recorded trajectories are the output of the performance of only the guidance module.

5. Is the robot safe to use? The robot is deemed to be safe to use, no concerns regarding the participants safety were observed during the testing.

6. Is the performance of the robot repeatable? The performance of the robot was repeatable during the performed user testing. No problems regarding the stability and functionality of the robot were observed.

7. What are the recommendations for future development of the robot? The current prototype of the robot performed well in user testing, however some changes could be recommended. First, it is predicted that increasing the maximum rpm of the

guidance module motor would have a positive effect on the performance of the guidance module. Secondly, the guidance algorithm could be modified to account for the distance between the robot and the target point, the robot's velocity and the position of the next target.

During the user testing experiments subjects 1-19 did the experiment in the guidance off mode first and the guidance on mode later. Subjects 20-38 did the experiment in a reverse order, first in the guidance on and then in the guidance off mode. The results presented in Figure 6.24 (on off) indicate that there is a noticeable difference between the performance of subjects 1-19 and 20-38 what was not expected. The subjects 1-19 (1.off 2.on) for every single trajectory (sin4, sin 16, pentagram, square and circle_v_f) were moving the robot faster than the subjects 20-38 (1.on 2.off) in both guidance off and on modes. Because of faster movement speed the RMSE reported for subjects 1-19 is also higher than the RMSE for subjects 20-38. These suggest that the faster movement velocity reported for subjects 1-19 is corelated with the order in which the experiment was performed.

Figure 6.23 (distance between target points) indicates that the velocity of movement for averaged results for all 38 subjects increases as the distance between the target points on the trajectory increases. Similar correlation is noticeable for RMSE and distance between the target points, which results from the faster movement velocity. The shape and complexity of the trajectory can also affect the RMSE which would partially explain the lower mean RMSE for the pentagram than the mean RMSE for the square and sin4 trajectories. The maximum velocity results presented in Figure 6.25 (average max velocity per trajectory) show that the fastest peak movement velocities were reported for the pentagram trajectory. The results indicate that the peak velocities increase with the distance between targets in a trajectory. Also, the peak velocities reported for the guidance on mode are higher than for the guidance off mode for every single trajectory.

During the experiments, all subjects could see on the screen (apart from the no visual feedback circle_n_v_f) a solid blue line outlining the shape which they had to follow. It is predicted that if they could not see that line, the difference between the guidance on and off mode would have been more prominent. The results for the circle trajectory which was followed by the subjects with the screen switched off (circle_n_v_f) was not utilized in the results analysis. The results analysis was performed only for the results which were

collected when the screen was switched on and subjects could see the trajectory, a target point and the position of the robot. However, even without further analysis the results presented for the circle_n_v_f indicate that the majority of the subjects were able to follow targets on the circle trajectory even if the screen was switched off.

6.11 Summary - User Testing

The developed prototype of the rehabilitation robot was evaluated in user testing with 38 healthy adult subjects. During the experiments all subjects used the robot with their non-dominant hands. Each subject took part in the experiment separately and the experiment was divided into two parts in which the robot was used in guidance off or on mode. The results indicate that in the guidance on mode the majority of the subjects could perform faster and at the same time more accurate movements. It is predicted that if the device was tested with subjects suffering arm impairment, the difference between the guidance on and off mode would have been more prominent. The developed rehabilitation robot was clearly capable of applying a passive force of sufficient magnitude and in the right direction to increase the accuracy of able-bodied adults trying to complete the tasks. It can be said that the system the guidance mechanism and the guidance algorithm works in real-world scenarios. The resistance to movement, both friction and inertia are sufficiently low that they do not appear to reduce the subjects' ability to move at speeds which represent normal reaching movements, which means the robot is light enough with sufficiently low friction to be moved by able bodied people without it unduly affecting their movement speed.

Chapter 7

Conclusions and Future Work

The mechanical design, position and orientation tracking system and inherently safe arm movement guidance system were described in this thesis. This chapter details the conclusions drawn from this study and outlines directions for future work.

7.1 Assessment of Research Objectives

In Chapter 1, four research objectives were defined. This section describes the extent to which these objectives were fulfilled during the study.

Develop the mechanical design of an inherently safe, upper-limb rehabilitation robot

This objective was addressed in Chapter 3. The mechanical design was developed and a prototype was manufactured. The prototype employs low rolling resistance variable-offset caster wheels and a dual-wheel COBOT unicycle module for inherently safe guidance. The user testing in Chapter 6 proved that the robot can be successfully used by adults through appropriate arm movement range to implement upper-limb rehabilitation therapy. Moreover, the robot mechanical design was evaluated to be robust and safe to use.

Develop a position tracking system for tracking arm movements and rehabilitation progress monitoring

This objective was addressed in Chapter 4. A hybrid position and orientation tracking system was developed for the robot prototype introduced in Chapter 3. The system estimates

the robot's position by fusing data from two sensors: a laser optical sensor and a webcam. The experimental results demonstrated that the developed fusion position tracking system can reliably track the robot's 2D position with greater accuracy than would be possible with the webcam or the optical sensor tracking systems on their own (Wojewoda *et al.*, 2016). Furthermore, in the second iteration of the system, the functionality of the system was expanded to orientation tracking and it was experimentally proven that the developed hybrid position tracking system can track the 2D position and orientation with greater accuracy than the webcam or optical sensors alone. Moreover, experiments also confirm that the developed system is capable of tracking recovery trends during rehabilitation therapy (Wojewoda *et al.*, 2017).

Develop an inherently safe guidance system to guide patients' arm movements

This objective was addressed in Chapter 5. An inherently safe guidance system capable of creating 2D virtual constrains was developed. The system is based on a dual-wheel COBOT unicycle module actuated with a stepper motor and it was validated in an experiment investigating the precision and stability of guidance.

Test the performance of the developed rehabilitation system during training

This objective was addressed in chapter 6. The performance of the developed rehabilitation device was investigated during a pilot randomized trial involving 38 healthy adults. The results confirmed that the performance of the robot is stable and repeatable during training. Moreover, it was noticed that the guidance system has a positive effect on the speed and precision of the arm movements.

7.2 Conclusions

The work presented in this thesis provides insight into the development of an inherently-safe, portable, table-top rehabilitation robot and its subsystems. The developed device met the requirements necessary for extensive evaluation in experiments and trials with healthy participants, however design modifications and improvements are needed to prepare the device for clinical testing with stroke patients. The conducted user testing with healthy participants using their nondominant arms indicated that the performance of the

robot is repeatable, stable, and has a positive influence on the speed and precision of reaching and retrieving arm movements. It is highly recommended that the robot is tested in a randomized clinical trial with moderate or mild stroke survivors able to perform voluntary arm movements, but needing to improve the range, speed and precision of arm movements.

There are two main contributions to the field of upper-limb robotic rehabilitation described in this thesis:

Hybrid Position and Orientation Tracking System for Table-Top Upper-Limb Rehabilitation Robot

The position tracking system developed in this thesis is the first of its kind - a 2D movement tracking system fusing data from a webcam and optical sensors to track the position and orientation with greater accuracy than would be possible with the webcam or optical sensors alone. The results also confirm that the developed system is capable of tracking recovery trends during rehabilitation therapy. Moreover, it is more accurate than the state-of-the-art position tracking system utilized in table-top rehabilitation robots. This movements tracking system could be successfully implemented in a wide range of table-top rehabilitation robots as it is not limited to the robot design presented in this thesis.

Two publications covering the developed tracking system were presented at IEEE international conferences in Chengdu and London:

- Wojewoda, K.K., Culmer, P.R., Jackson, A.E. and Levesley, M.C., 2016, June. Position tracking of a passive rehabilitation robot. In Cyber Technology in Automation, Control, and Intelligent Systems (CYBER), 2016 IEEE International Conference on (pp. 1-6). IEEE.

- Wojewoda, K.K., Culmer, P.R., Gallagher, J.F., Jackson, A.E. and Levesley, M.C., 2017, July. Hybrid position and orientation tracking for a passive rehabilitation table-top robot. In Rehabilitation Robotics (ICORR), 2017 International Conference on (pp. 702-707). IEEE.

Inherently Safe Guidance System for a Table-Top Upper-Limb Rehabilitation Robot

The inherently safe guidance system developed in this thesis is the first of its kind implementation of a COBOT unicycle mechanism in a table-top rehabilitation robot. The guidance mechanism is inherently safe as it is not able to generate an active force that would act on the patient's arm. It was designed to create 2D virtual constrains which should help guide arm movements in the desired direction. The conducted user trial indicated that the guidance system can increase precision and speed of arm movements. The work regarding the guidance system has not been published to date, however it is planned to be published in the near future.

7.3 Limitations of the Work

Not all of the specified product requirements for the developed inherently-safe arm rehabilitation robot were met in this thesis. Four sets of product requirements were derived in Chapter 3:

7.3.1 Safety Requirements

There is one safety requirement which was not addressed in this thesis: safety requirement (e): "The device SHALL incorporate a solution preventing it from falling off a table edge during training while attached to a patient's arm". During the conducted user testing the robot was not fixed in any way to the participants' arms, therefore a fall prevention solution was not needed. However, it is highly recommended that a fall prevention solution is implemented in a future iteration of the robot as it is necessary to conduct clinical trials with stroke patients.

7.3.2 Usability Requirements

One of the usability requirements were not met. The usability requirement (c): "The device setup and takedown time SHALL be less than 2 minutes" was not investigated in this thesis, as the used porotype is an early design iteration and this should be investigated in the next design iteration.

7.3.3 Functionality Requirements

Five of the functionality requirements were partially met or were not met:

(b) The device MAY provide variable resistance (braking)

A variable resistance mechanism generating extra resistance to oppose patients' arm movements was not implemented in the design. Such a mechanism might be beneficial for patients trying to improve arm strength. Implementing such a mechanism should be considered in the next iteration of the robot's design.

(f) The device SHALL monitor patients' therapy progress

This requirement was partially met, as it was proven that the developed hybrid position tracking system can detect trends in arm rehabilitation therapy. However, the robot lacks real-time therapy monitoring, which should be implemented in the next iteration of the robot's design.

(g) The device is RECOMMENDED to have an on-board rechargeable battery enabling 10 hours of continuous use

The developed robot was powered from an external power supply, but it is recommended that an onboard battery is implemented in the future design.

(h) The device SHALL support a virtual user interface with interactive games

This requirement was partially met, as an interactive user interface was developed for the user testing (Chapter 6). However, the system would benefit if custom games were designed to maximise patients' attention during training.

(i) The device is RECOMMENDED to support wireless connectivity to avoid wires that could potentially interrupt training

This requirement was not met as the robot was connected to a PC with a USB cable. It is assumed that the device would be easier to use if it was wireless. It is recommended that the next generation of the robot is completely wireless.

7.3.4 Clinical Requirements

The clinical requirements were not met in this thesis. However, work presented in chapters 4, 5 and 6 indicates that the developed system has the potential to meet them.

(a)The device SHALL be suitable for functional reach movement training for patients after stroke suffering mild upper-limb hemiparesis

In order to validate this requirement a randomised clinical trial involving participants suffering mild upper-limb hemiparesis is required.

(b)The device SHALL be suitable for functional upper-limb reach movement training for improving patients after stroke which are able to move their upper-limbs independently

Similarly, as the requirement above, this requirement could only be validated in a randomised clinical trial involving participants suffering mild upper-limb hemiparesis.

(c)The device SHALL focus on rehabilitation training targeting upper-limb deficiencies after stroke such as: reduced range of movement, reduced movement speed and reduced movement precision

The robot presented in this thesis is designed to utilise a large workspace in order to support rehabilitation exercises aimed at increasing the arm range of movement. Moreover, the aim of the guidance mechanism is to enable patients to perform more precise and faster arm movements in the desired direction. However, as is the case with the previous two clinical requirements, this requirement could only be fully validated in a randomised clinical trial with after stroke patients suffering mild upper-limb hemiparesis.

7.4 Future Work

This research has provided a starting point for research into inherently-safe table-top rehabilitation robots based on the COBOT unicycle mechanism. A great deal of additional research can be performed. This section summarizes which aspects of the developed systems would benefit from further development and investigation to optimise performance and prepare the system for clinical trials.

7.4.1 Mechanical Design

The two most significant aspects of the design limiting the use of the current prototype in clinical trials are the lack of full-length forearm support and the lack of a design feature preventing the possibility of the robot falling off a table edge. The full arm support orthosis design could be based on the orthosis design found in ArmAsist. The main requirement for the orthosis is to provide firm vertical support of the forearm. Ensuring that the orthosis does not constrain elbow joint mobility and mounting the orthosis on the robot through a pivot (as was done for the ArmAssist) would enable a potential patient to freely perform planar movements with constant vertical arm support. The design feature preventing the robot from falling of a table edge can be achieved with a rubber band approximately 36 mm thick attached to the underside of the robot. With the rubber band employed in the design, if the robot was about to fall off a table edge and one of the caster wheels was off the table surface, the robot would tilt, but it would not slide off the table edge as the rubber band would prevent it. If problems with designing an on-board feature preventing the robot from falling off a table edge are encountered, a square frame with elevated edges creating a clear visible and physical barrier around the workspace can be implemented. The current design was developed prioritising robustness and quick manufacturing. However, future iterations of the design could focus more on aesthetic design and ergonomics. The design of the custom developed caster wheels could be modified to investigate larger offsets of the caster wheel axis from the centre of rotation of the caster module. It is predicted that for the current diameter of the caster wheels (25 mm) developing a new design allowing to set the offset between 12 and 30 mm would be sufficient.

7.4.2 Position and Orientation Tracking System

The position tracking system was extensively evaluated experimentally and its performance is sufficient for application in the developed inherently safe rehabilitation system. However, in the current design, the tracking system utilizes a webcam which must be mounted approximately 0.6 m above the workspace. This could be inconvenient - a tall and sturdy stand for mounting the webcam is required. However, the webcam tracking could be modified to get rid of the stand. This could be achieved by using two webcams instead of one. The webcams would have to be mounted on a short stand (20 - 30cm) placed next to the work space and positioned horizontally next to each other at an angle

creating an equilateral triangle between the webcams and a random point which is an equal distance from both webcams. However, if the webcam module is modified, the shape of the markers has to be modified too. The current version of the system utilizes two 40 mm diameter hemispherical markers which are optimized for tracking by the webcam mounted above the work space to compute the position and orientation of the robot. However, for the new configuration of the module the marker shapes would have to be changed to a sphere (a diameter of 40 mm should be sufficient) and, similarly to the current approach, two markers would have to be used. Overall, changing the configuration of the webcam module is predicted to have no significant effect on the general performance and accuracy of the tracking system. The only purpose would be to make the system more compact and easy to set up, as mounting the webcam above the workspace would not be needed. Finally, the position and orientation tracking would benefit from illuminating the webcam markers from the inside. This would be beneficial for the current configuration as well as the proposed new configuration utilizing two webcams. Illuminated webcam markers would make the tracking system less sensitive to dark light and changing light conditions.

7.4.3 Guidance System

Some problems with the guidance system were reported in experiment 12 in Chapter 5, however it is worth noting that apart from this experiment, which was not a complete failure, all the other experiments covered in Chapter 5 were completed successfully. Moreover, user testing experiments in Chapter 6 did not report any significant issues with the guidance system. However, it is predicted that some adjustments could be beneficial for improved performance and smoother operation. First, the 1.1 rev/s rotational velocity of the motor could be increased to improve the performance of the device when performing sharp angle turns at high velocities and improve overall robustness of the system. Figure 7.1 presents a simulation of the ideal performance of the guidance system at 200 mm/s and one repetition of the sin4 trajectory for two rotational speeds (1.1 and 5.0 rev/s) of the stepper motor. The difference between the plots is clear and in favour of 5 rev/s and according to the velocity measurements recorded in Chapter 6 movements, velocities of 200 mm/s or faster were common. The target hit-and-miss approach presented in Chapter 5 modelled the target hit zone as a 6 by 6mm square and the larger zone, used for a target miss detection, as a larger 12 by 12 mm square. Overall, no problems were detected

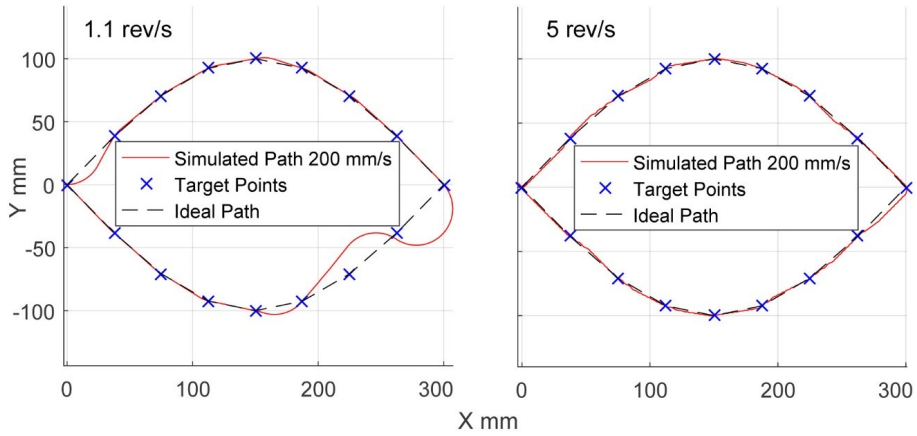

Figure 7.1: Simulation of the ideal performance of the guidance system at 200 mm/s and one repetition of the sin4 trajectory for two rotational speeds of the stepper motor (1.1 vs 5.0 rev/s).

because of the square shape of the zones, however, these are recommended to be changed to 6 and 12 mm diameter circles.

7.4.4 Clinical Trials

During the user testing conducted in this thesis all participants could see the current position of the robot, the position of a target they had to move to, and a line outlining the positions of all targets. It is hypothesised that this made the participants move the robot quicker, as they knew where all the targets were and as soon as a target was reached they knew exactly in which direction they had to move next. It is advised that the clinical trials in the future are performed without revealing the trajectory shape to subjects. It is predicted that if subjects do not see which trajectory they are following, the advantage of using the guidance system would be even more prominent than was reported in Chapter 6. During user testing, the subjects moved the robot at a velocity which was comfortable for them. There was no attempt to make the subjects move the robot faster or slower. It is advised that in the future, the effect of trying to influence the velocity of movement is investigated. The basic user interface prepared for user testing in Chapter 6 was used successfully. However, it is advised that a new, interactive user interface with custom designed games is developed to maximise subjects' attention by making the exercises

more engaging. It is recommended that a randomized clinical trial involving patients after stroke suffering mild hemiparesis is organized in the future in order to validate the clinical product requirements.

References

Amirabdollahian, F., Harwin, W. & Loureiro, R. (2007). Analysis of the fugl-meyer outcome measures assessing the effectiveness of robot-mediated stroke therapy. In *Rehabilitation Robotics, 2007. ICORR 2007. IEEE 10th International Conference on*, 729–735, IEEE. 42

Barnes, M.P. & Johnson, G.R. (2008). *Upper motor neurone syndrome and spasticity: clinical management and neurophysiology*. Cambridge University Press. 9, 10

Bill, G., Insurance, L., Insurance, T.I., Prescriptions, R., Prevention, C., Headstones, M., Certificates, M.P.M., Locator, N.G., Flags, B., Allowance, B. *et al.* (2011). Bilateral upper-limb rehabilitation after stroke using a movement-based game controller. 26, 27

Bradner, S. (1997). Key words for use in rfcs to indicate requirement levels. 69

Brookes, J., Kuznecovs, M., Kanakis, M., Grigals, A., Narvidas, M., Gallagher, J. & Levesley, M. (2017). Robots testing robots: Alan-arm, a humanoid arm for the testing of robotic rehabilitation systems. In *Rehabilitation Robotics (ICORR), 2017 International Conference on*, 676–681, IEEE. 114

Byl, N., Roderick, J., Mohamed, O., Hanny, M., Kotler, J., Smith, A., Tang, M. & Abrams, G. (2003). Effectiveness of sensory and motor rehabilitation of the upper limb following the principles of neuroplasticity: patients stable poststroke. *Neurorehabilitation and neural repair*, **17**, 176–191. 18

Cabral, N.L., Moro, C., Silva, G.R., Scola, R.H. & Werneck, L.C. (2003). Study comparing the stroke unit outcome and conventional ward treatment: a randomized study in joinville, brazil. *Arquivos de neuro-psiquiatria*, **61**, 188–193. 10

Casadio, M., Sanguineti, V., Morasso, P.G. & Arrichiello, V. (2006). Braccio di ferro: a new haptic workstation for neuromotor rehabilitation. *Technology and Health Care*, **14**, 123–142. xvi, 37, 38, 60

CCOHS (2008). What can workers do to reduce the discomfort of working in a standing position? http://www.ccohs.ca/oshanswers/ergonomics/standing/standing_basic.html, accessed: 2014-09-25. xvii, 60, 61

Chua, J.Y. (2006). Design of a wearable cobot. xvi, xvii, 57, 58, 59

Cincura, C., Pontes-Neto, O.M., Neville, I.S., Mendes, H.F., Menezes, D.F., Mariano, D.C., Pereira, I.F., Teixeira, L.A., Jesus, P.A., de Queiroz, D.C. *et al.* (2009). Validation of the national institutes of health stroke scale, modified rankin scale and barthel index in brazil: The role of cultural adaptation and structured interviewing. *Cerebrovasc Dis*, **27**, 119–122. 10

Coote, S., Murphy, B., Harwin, W. & Stokes, E. (2008). The effect of the gentle/s robot-mediated therapy system on arm function after stroke. *Clinical rehabilitation*, **22**, 395–405. 42

Culmer, P.R. (2007). *Development of a Cooperative Robot System to Aid Stroke Rehabilitation*. Ph.D. thesis, University of Leeds. 8, 9, 10, 17, 18

Culmer, P.R., Levesley, M.C., Mon-Williams, M. & Williams, J.H. (2009). A new tool for assessing human movement: the kinematic assessment tool. *Journal of neuroscience methods*, **184**, 184–192. 119

Daly, J.J., Hogan, N., Perepezko, E.M., Krebs, H.I., Rogers, J.M., Goyal, K.S., Dohring, M.E., Fredrickson, E., Nethery, J. & Ruff, R.L. (2005). Response to upper-limb robotics and functional neuromuscular stimulation following stroke. *Journal of rehabilitation research & development*, **42**. 54

Dietz, V., Nef, T. & Zev Rymer, W. (2012). *Neurorehabilitation Technology*. Springer. 33, 49

Directive, C. (1993). 93/42/eec of 14 june 1993 concerning medical devices. 61, 62, 70, 151

Dobkin, B.H. (2004). Strategies for stroke rehabilitation. *The Lancet Neurology*, **3**, 528–536. 2

Elmenreich, W. (2007). A review on system architectures for sensor fusion applications. *Software Technologies for Embedded and Ubiquitous Systems*, 547–559. 110

EPP (2006). Workstation design. http://www.ccohs.ca/oshanswers/ergonomics/standing/standing_basic.html, accessed: 2014-09-25. xvii, 60, 61

Fess, E., Gettle, K., Philips, C. & Robin, J. (2005). Hand and upper extremity splinting. 82

Feys, H., De Weerdt, W., Verbeke, G., Steck, G.C., Capiau, C., Kiekens, C., Dejaeger, E., Van Hoydonck, G., Vermeersch, G. & Cras, P. (2004). Early and repetitive stimulation of the arm can substantially improve the long-term outcome after stroke: a 5-year follow-up study of a randomized trial. *Stroke*, **35**, 924–929. 17

Fischer, U., Baumgartner, A., Arnold, M., Nedeltchev, K., Gralla, J., Marco De Marchis, G., Kappeler, L., Mono, M.L., Brekenfeld, C., Schroth, G. *et al.* (2010). What is a minor stroke? *Stroke*, **41**, 661–666. 8

Gallagher, J., Preston, N., Holt, R., Mon-Williams, M., Levesley, M. & Weightman, A. (2015). Assessment of upper limb movement with an autonomous robotic device in a school environment for children with cerebral palsy. In *Rehabilitation Robotics (ICORR), 2015 IEEE International Conference on*, 770–774, IEEE. 114

Gillen, G. (2010). *Stroke rehabilitation: a function-based approach*. Elsevier Health Sciences. 7

Gillespie, R.B., Colgate, J.E. & Peshkin, M.A. (2001). A general framework for cobot control. *Robotics and Automation, IEEE Transactions on*, **17**, 391–401. 56

Gladstone, D.J., Danells, C.J. & Black, S.E. (2002). The fugl-meyer assessment of motor recovery after stroke: a critical review of its measurement properties. *Neurorehabilitation and neural repair*, **16**, 232–240. xxv, 8, 12, 13, 14

He, J., Koeneman, E., Schultz, R., Huang, H., Wanberg, J., Herring, D., Sugar, T., Herman, R. & Koeneman, J. (2005). Design of a robotic upper extremity repetitive therapy device. In *Rehabilitation Robotics, 2005. ICORR 2005. 9th International Conference on*, 95–98, IEEE. xvi, 52

Herder, J. (2005). Development of a statically balanced arm support: Armon. In *Rehabilitation Robotics, 2005. ICORR 2005. 9th International Conference on*, 281–286, IEEE. 36

Herder, J.L., Vrijlandt, N., Antonides, T., Cloosterman, M., Mastenbroek, P.L. *et al.* (2006). Principle and design of a mobile arm support for people with muscular weakness. *Journal of rehabilitation research and development*, **43**, 591. 36

Hesse, S., Schulte-Tigges, G., Konrad, M., Bardeleben, A. & Werner, C. (2003). Robot-assisted arm trainer for the passive and active practice of bilateral forearm and wrist movements in hemiparetic subjects. *Archives of physical medicine and rehabilitation*, **84**, 915–920. xv, 30, 31

Hesse, S., Schmidt, H., Werner, C., Rybski, C., Puzich, U. & Bardeleben, A. (2007). A new mechanical arm trainer to intensify the upper limb rehabilitation of severely affected patients after stroke: design, concept and first case series. *Europa medicophysica*, **43**, 463–468. 31

Housman, S.J., Le, V., Rahman, T., Sanchez, R.J. & Reinkensmeyer, D.J. (2007). Arm-training with t-wrex after chronic stroke: preliminary results of a randomized controlled trial. In *Rehabilitation Robotics, 2007. ICORR 2007. IEEE 10th International Conference on*, 562–568, IEEE. 49

Housman, S.J., Scott, K.M. & Reinkensmeyer, D.J. (2009). A randomized controlled trial of gravity-supported, computer-enhanced arm exercise for individuals with severe hemiparesis. *Neurorehabilitation and neural repair*. 16, 20, 49

Howard, V.J., McClure, L.A., Meschia, J.F., Pulley, L., Orr, S.C. & Friday, G.H. (2006). High prevalence of stroke symptoms among persons without a diagnosis of stroke or transient ischemic attack in a general population: the reasons for geographic and racial differences in stroke (regards) study. *Archives of internal medicine*, **166**, 1952–1958. 8

Jackson, A., Levesley, M., Makower, S., Cozens, J. & Bhakta, B. (2013). Development of the ipam mkii system and description of a randomized control trial with acute stroke patients. In *IEEE... International Conference on Rehabilitation Robotics:[proceedings]*, vol. 2013, 6650407–6650407. xvi, 44, 45

Jahanshahloo, G.R., Lotfi, F.H. & Izadikhah, M. (2006). An algorithmic method to extend topsis for decision-making problems with interval data. *Applied mathematics and computation*, **175**, 1375–1384. xxv, 75, 76

Johnson, M., Van der Loos, H., Burgar, C. & Leifer, L. (1999). Driver's seat: simulation environment for arm therapy. In *Proceedings of the 6th International Conference on Rehabilitation Robotics (ICORR'99), Stanford, CA, US*. xvi, 39, 40

Johnson, M., Wisneski, K., Anderson, J., Nathan, D. & Smith, R. (2006). Development of adler: The activities of daily living exercise robot. In *Biomedical Robotics and Biomechatronics, 2006. BioRob 2006. The First IEEE/RAS-EMBS International Conference on*, 881–886, IEEE. 42

Kim, Y.S., Lee, J., Lee, S. & Kim, M. (2005). A force reflected exoskeleton-type masterarm for human-robot interaction. *Systems, Man and Cybernetics, Part A: Systems and Humans, IEEE Transactions on*, **35**, 198–212. xvi, 48, 49

Knecht, S., Hesse, S. & Oster, P. (2011). Rehabilitation after stroke. *Deutsches Ärzteblatt International*, **108**, 600. 15

Kowalczewski, J., Ravid, E. & Prochazka, A. (2011). Fully-automated test of upper-extremity function. In *Engineering in Medicine and Biology Society, EMBC, 2011 Annual International Conference of the IEEE*, 7332–7335, IEEE. 19, 33

Krakauer, J.W. (2006). Motor learning: its relevance to stroke recovery and neurorehabilitation. *Current opinion in neurology*, **19**, 84–90. 63

Krebs, H.I., Volpe, B.T., Williams, D., Celestino, J., Charles, S.K., Lynch, D. & Hogan, N. (2007). Robot-aided neurorehabilitation: a robot for wrist rehabilitation. *Neural Systems and Rehabilitation Engineering, IEEE Transactions on*, **15**, 327–335. 44

Kwakkel, G. & Meskers, C.G. (2014). Effects of robotic therapy of the arm after stroke. *The Lancet Neurology*, **13**, 132–133. 19, 51, 63, 126

Kwakkel, G., Wagenaar, R.C., Twisk, J.W., Lankhorst, G.J. & Koetsier, J.C. (1999). Intensity of leg and arm training after primary middle-cerebral-artery stroke: a randomised trial. *The Lancet*, **354**, 191–196. xv, 1, 16, 17

Kwakkel, G., Kollen, B.J. & Krebs, H.I. (2008). Effects of robot-assisted therapy on upper limb recovery after stroke: a systematic review. *Neurorehabilitation and neural repair*, **22**, 111–121. 18, 53, 54, 55

Langhorne, P., Bernhardt, J. & Kwakkel, G. (2011). Stroke rehabilitation. *The Lancet*, **377**, 1693–1702. 16

Lawrence, E.S., Coshall, C., Dundas, R., Stewart, J., Rudd, A.G., Howard, R. & Wolfe, C.D. (2001). Estimates of the prevalence of acute stroke impairments and disability in a multiethnic population. *Stroke*, **32**, 1279–1284. 8

Levin, M.F., Sveistrup, H. & Subramanian, S. (2010). Feedback and virtual environments for motor learning and rehabilitation. *Schedae*, **1**, 19–36. 16, 17

Lo, A.C., Guarino, P.D., Richards, L.G., Haselkorn, J.K., Wittenberg, G.F., Federman, D.G., Ringer, R.J., Wagner, T.H., Krebs, H.I., Volpe, B.T. *et al.* (2010). Robot-assisted therapy for long-term upper-limb impairment after stroke. *New England Journal of Medicine*, **362**, 1772–1783. 1, 8, 54, 55

Loureiro, R.C., Harwin, W.S., Nagai, K. & Johnson, M. (2011). Advances in upper limb stroke rehabilitation: a technology push. *Medical & biological engineering & computing*, **49**, 1103–1118. 2, 18, 19, 20, 42, 46, 53, 54, 55, 62, 63

Lum, P., Burgar, C.G., Van der Loos, M., Shor, P., Majmundar, M. & Yap, R. (2005). The mime robotic system for upper-limb neuro-rehabilitation: results from a clinical trial in subacute stroke. In *Rehabilitation Robotics, 2005. ICORR 2005. 9th International Conference on*, 511–514, IEEE. xvi, 44, 45

Luo, D., Schauer, T., Roth, M. & Raisch, J. (2012). Position and orientation control of an omni-directional mobile rehabilitation robot. In *Control Applications (CCA), 2012 IEEE International Conference on*, 50–56, IEEE. 26, 80, 93, 111, 125

Masory, O. & Sanroma, O. (2013). Upper-limbs rehabilitation devices part ii-passive devices. In *RESNA ANNUAL CONFERENCE*, RESNA. 34

Montagner, A., Frisoli, A., Borelli, L., Procopio, C., Bergamasco, M., Carboncini, M.C. & Rossi, B. (2007). A pilot clinical study on robotic assisted rehabilitation in vr with an arm exoskeleton device. In *Virtual Rehabilitation, 2007*, 57–64, IEEE. xvi, 51

Morse, A. & General, A. (2010). Progress in improving stroke care. 1

Nef, T. & Riener, R. (2005). Armin-design of a novel arm rehabilitation robot. In *Rehabilitation Robotics, 2005. ICORR 2005. 9th International Conference on*, 57–60, IEEE. 16, 19, 47, 50

Nef, T., Mihelj, M., Colombo, G. & Riener, R. (2006). Armin-robot for rehabilitation of the upper extremities. In *Robotics and Automation, 2006. ICRA 2006. Proceedings 2006 IEEE International Conference on*, 3152–3157, IEEE. 51

Nef, T., Mihelj, M. & Riener, R. (2007). Armin: a robot for patient-cooperative arm therapy. *Medical & biological engineering & computing*, **45**, 887–900. xvi, 51

Nicosevici, T., Garcia, R., Carreras, M. & Villanueva, M. (2004). A review of sensor fusion techniques for underwater vehicle navigation. In *OCEANS'04. MTTS/IEEE TECHNO-OCEAN'04*, vol. 3, 1600–1605, IEEE. 110

NINDS (2018). Nih stroke scale. https://www.ninds.nih.gov/sites/default/files/NIH_Stroke_Scale_Booklet.pdf, accessed: 2018-12-30. 10

Norouzi-Gheidari, N., Archambault, P.S. & Fung, J. (2012). Effects of robot-assisted therapy on stroke rehabilitation in upper limbs: systematic review and meta-analysis of the literature. *J Rehabil Res Dev*, **49**, 479–496. 1, 2

Organization, W.H. *et al.* (2011). World report on disability 2011. xv, 14, 15

Peattie, A., Korevaar, A., Wilson, J., Sandilands, B., Chen, X. & King, M. (2009). Automated variable resistance system for upper limb rehabilitation. *Robotics and Automation*. 24, 80, 92, 125

Perry, J.C., Zabaleta, H., Belloso, A., Rodríguez-de Pablo, C., Cavallaro, F.I. & Keller, T. (2012). Armassist: development of a functional prototype for at-home telerehabilitation of post-stroke arm impairment. In *Biomedical Robotics and Biomechatronics (BioRob), 2012 4th IEEE RAS & EMBS International Conference on*, 1561–1566, IEEE. 22, 23, 70, 80, 92, 93, 122, 125

Peshkin, M. & Colgate, J.E. (1999). Cobots. *Industrial Robot: An International Journal*, **26**, 335–341. 57

Peshkin, M.A., Colgate, J.E., Wannasuphoprasit, W., Moore, C.A., Gillespie, R.B. & Akella, P. (2001). Cobot architecture. *Robotics and Automation, IEEE Transactions on*, **17**, 377–390. xvi, xvii, 56, 57, 58, 59

powerandsamplesize.com (2018). Calculate sample size needed to compare 2 means: 2-sample, 1-sided. http://powerandsamplesize.com/Calculators/Compare-2-Means/2-Sample-1-Sided, accessed: 2018-12-30. 189

Reinkensmeyer, D.J., Dewald, J.P. & Rymer, W.Z. (1999). Guidance-based quantification of arm impairment following brain injury: a pilot study. *Rehabilitation Engineering, IEEE Transactions on*, **7**, 1–11. xv, 35, 36

Reinkensmeyer, D.J., Kahn, L.E., Averbuch, M., McKenna-Cole, A., Schmit, B.D. & Rymer, W.Z. (2000). Understanding and treating arm movement impairment after chronic brain injury: progress with the arm guide. *Journal of rehabilitation research and development*, **37**, 653–662. 36

Riener, R., Nef, T. & Colombo, G. (2005). Robot-aided neurorehabilitation of the upper extremities. *Medical and Biological Engineering and Computing*, **43**, 2–10. 20, 43

Rohrer, B., Fasoli, S., Krebs, H.I., Hughes, R., Volpe, B., Frontera, W.R., Stein, J. & Hogan, N. (2002). Movement smoothness changes during stroke recovery. *The Journal of Neuroscience*, **22**, 8297–8304. 94, 99

Rosamond, W.D., Gorton, R.A., Hinn, A.R., Hohenhaus, S.M. & Morris, D.L. (1998). Rapid response to stroke symptoms: the delay in accessing stroke healthcare (dash) study. *Academic Emergency Medicine*, **5**, 45–51. 7

Sacco, R.L., Kasner, S.E., Broderick, J.P., Caplan, L.R., Culebras, A., Elkind, M.S., George, M.G., Hamdan, A.D., Higashida, R.T., Hoh, B.L. *et al.* (2013). An updated definition of stroke for the 21st century a statement for healthcare professionals from the american heart association/american stroke association. *Stroke*, **44**, 2064–2089. 7

Sanchez Jr, R., Wolbrecht, E., Smith, R., Liu, J., Rao, S., Cramer, S., Rahman, T., Bobrow, J. & Reinkensmeyer, D. (2005). A pneumatic robot for retraining arm movement after stroke: Rationale and mechanical design. In *Rehabilitation Robotics, 2005. ICORR 2005. 9th International Conference on*, 500–504, IEEE. xvi, 52

Shah, S., Vanclay, F. & Cooper, B. (1989). Improving the sensitivity of the barthel index for stroke rehabilitation. *Journal of clinical epidemiology*, **42**, 703–709. xxv, 10, 11, 12

Stienen, A.H., Hekman, E.E., Van der Helm, F.C., Prange, G.B., Jannink, M.J., Aalsma, A.M. & Van der Kooij, H. (2007a). Dampace: dynamic force-coordination trainer for the upper extremities. In *Rehabilitation Robotics, 2007. ICORR 2007. IEEE 10th International Conference on*, 820–826, IEEE. 47

Stienen, A.H., Hekman, E.E., Van der Helm, F.C., Prange, G.B., Jannink, M.J., Aalsma, A.M. & Van der Kooij, H. (2007b). Freebal: dedicated gravity compensation for the upper extremities. In *Rehabilitation Robotics, 2007. ICORR 2007. IEEE 10th International Conference on*, 804–808, IEEE. 39, 40

Stienen, A.H., Hekman, E.E., Prange, G.B., Jannink, M.J., Aalsma, A.M., van der Helm, F.C. & van der Kooij, H. (2009a). Dampace: Design of an exoskeleton for force-coordination training in upper-extremity rehabilitation. *Journal of Medical Devices*, **3**, 031003. 47

Stienen, A.H., Hekman, E.E., Prange, G.B., Jannink, M.J., van der Helm, F.C. & van der Kooij, H. (2009b). Freebal: design of a dedicated weight-support system for upper-extremity rehabilitation. *Journal of Medical Devices*, **3**, 041009. 40

Stienen, A.H.A. (2009). *Development of novel devices for upper-extremity rehabilitation*. University of Twente. 43

Sukal, T.M., Ellis, M.D. & Dewald, J.P. (2005). Dynamic characterization of upper limb discoordination following hemiparetic stroke. In *Rehabilitation Robotics, 2005. ICORR 2005. 9th International Conference on*, 519–521, IEEE. 42

Tomić, T.J.D., Savić, A.M., Vidaković, A.S., Rodić, S.Z., Isaković, M.S., Rodríguez-de Pablo, C., Keller, T. & Konstantinović, L.M. (2017). Armassist robotic system versus matched conventional therapy for poststroke upper limb rehabilitation: a randomized clinical trial. *BioMed research international*, **2017**. 56

Toth, A., Fazekas, G., Arz, G., Jurak, M. & Horvath, M. (2005). Passive robotic movement therapy of the spastic hemiparetic arm with reharob: report of the first clinical test and the follow-up system improvement. In *Rehabilitation Robotics, 2005. ICORR 2005. 9th International Conference on*, 127–130, IEEE. xvi, 44, 45

van Delden, A., Peper, C.L.E., Kwakkel, G. & Beek, P.J. (2012). A systematic review of bilateral upper limb training devices for poststroke rehabilitation. *Stroke research and treatment*, **2012**. 28, 29, 31, 32

van Delden, A.L.E., Peper, C.L.E., Harlaar, J., Daffertshofer, A., Zijp, N.I., Nienhuys, K., Koppe, P., Kwakkel, G. & Beek, P.J. (2009). Comparing unilateral and bilateral upper limb training: the ultra-stroke program design. *BMC neurology*, **9**, 57. 29

Veerbeek, J.M., Langbroek-Amersfoort, A.C., Van Wegen, E.E., Meskers, C.G. & Kwakkel, G. (2017). Effects of robot-assisted therapy for the upper limb after stroke: a systematic review and meta-analysis. *Neurorehabilitation and neural repair*, **31**, 107–121. 53, 55, 62, 63

Wannasuphoprasit, W. (1999). Cobots: Collaborative robots. *ProQuest Dissertations and Theses*, 1–13. 57

Wannasuphoprasit, W., Gillespie, R.B., Colgate, J.E. & Peshkin, M.A. (1997). Cobot control. In *Robotics and Automation, 1997. Proceedings., 1997 IEEE International Conference on*, vol. 4, 3571–3576, IEEE. 56

Welch, G. & Bishop, G. (1995). An introduction to the kalman filter. university of north carolina, department of computer science. Tech. rep., TR 95-041. 97

Wojewoda, K., Culmer, P., Gallagher, J., Jackson, A. & Levesley, M. (2017). Hybrid position and orientation tracking for a passive rehabilitation table-top robot. In *Rehabilitation Robotics (ICORR), 2017 International Conference on*, 702–707, IEEE. 196

Wojewoda, K.K., Culmer, P.R., Jackson, A.E. & Levesley, M.C. (2016). Position tracking of a passive rehabilitation robot. In *Cyber Technology in Automation, Control, and Intelligent Systems (CYBER), 2016 IEEE International Conference on*, 1–6, IEEE. 116, 119, 121, 196

Wong, C.K., Jordan, K. & King, M. (2011). Robotic arm skate for stroke rehabilitation. In *Rehabilitation Robotics (ICORR), 2011 IEEE International Conference on*, 1–6, IEEE. 25, 80, 93, 125

Zabaleta, H., Valencia, D., Perry, J., Veneman, J. & Keller, T. (2011). Absolute position calculation for a desktop mobile rehabilitation robot based on three optical mouse sensors. In *Engineering in Medicine and Biology Society, EMBC, 2011 Annual International Conference of the IEEE*, 2069–2072, IEEE. 92